STUDIES AIMED AT UNDERSTANDING HOW PHOSPHORYLATION AND MIRNAS CONTRIBUTE TO THE CIRCADIAN CLOCK MECHANISM IN *DROSOPHILA*

by

EVRIM YILDIRIM

A dissertation submitted to the

Graduate School-New Brunswick

Rutgers, The State University of New Jersey

and The Graduate School of Biomedical Sciences

In partial fulfillment of the requirements

For the degree of

Doctor of Philosophy

Graduate Program in Biochemistry

Written under the direction of

Professor Isaac Edery

And approved by

_____

_____

_____

_____

New Brunswick, New Jersey

OCTOBER, 2014

ABSTRACT OF THE DISSERTATION

STUDIES AIMED AT UNDERSTANDING HOW PHOSPHORYLATION AND MIRNAS CONTRIBUTE TO THE CIRCADIAN CLOCK MECHANISM IN *DROSOPHILA*

By EVRIM YILDIRIM

Dissertation Director:

Dr. Isaac Edery

Circadian (≅24 hr) rhythms in physiology and behavior are driven by endogenous cellular clocks that can be synchronized (entrained) by environmental cues, most notably the daily light-dark and temperature cycles. Circadian timing mechanisms in a wide variety of organisms are based on a small set of species-specific clock genes that participate in negative transcriptional feedback loops intertwined with post-transcriptional and post-translational regulatory schemes that ultimately drive cyclical gene expression.

Phosphorylation is the most pervasive post-translational modification of clock proteins and is central to setting the pace of the clock. PERIOD (PER), the main repressor in animal clocks, is progressively phosphorylated during its life cycle, which has potent effects on its stability and nuclear localization. In this thesis I used *D. melanogaster* as an animal model system and identified a new role for PER phosphorylation in entraining to light-dark and temperature cycles. Prior work showed that the light-mediated degradation of TIMELESS (TIM), a key partner of PER, is critical for photic entrainment. My studies have significantly revised this model with the demonstration that the light-mediated

degradation of TIM leads to an increase in the phosphorylation of two nearby sites on PER (S826/828), and that blocking phosphorylation at these sites causes altered entrainment, revealing a surprising new role for PER in circadian responses to environmental cues.

In related work I contributed to studies that identified phosphorylation sites on the central circadian transcription factor termed CLOCK (CLK), and showed that these modifications are also involved in entrainment. Together, these studies reveal that phosphorylation of PER and CLK is not only critical for setting the pace of the clock but also its ability to interpret external time cues.

In another study I found that the miRNA *bantam* (*ban*) regulates *Clk* through three target sites on its 3' UTR. Flies harboring mutations in *ban* target sites on *Clk* show weaker circadian rhythms and less CLK protein staining specifically in the s-LNvs, the key circadian pacemaker cells. These findings show that *ban* imparts robustness to circadian rhythms by adjusting CLK levels in master pacemaker neurons, and suggest a non-conventional mode-of-operation for *ban* on *Clk* expression.

Acknowledgement

I would like to thank following people for their support during the time I spent for my Ph.D.

To Isaac Edery for supporting me during these long years and for his help in preparation of this thesis.

To Drs. Richard W. Padgett, William J. Belden and Samuel I. Gunderson for serving in my dissertation committee and for their advises.

To my current and previous lab mates; Rudra Dubey, Chaya Dharia, Gabe Villegas, Weihuan Cao, Yong Yang and Zhichao Zhang; for scientific discussions and for their understanding.

To many laboratories in Waksman Institute, Nelson building and CABM; and also to *Drosophila* community for sharing materials, protocols, and equipment.

And finally, to my family; my father Devrim, my mother Firkat, and sister Eylem; for their encouragement and infectious optimism.

Table of contents

List of figures

List of tables

Chapter 1. Introduction

Overview of Circadian Rhythms

A diverse range of organisms, from single celled bacteria to plants and humans, evolved internal time keeping mechanisms, called circadian clocks (circa=about; dian=day) that enable them to adapt to daily changes in the environment, mainly light/dark and temperature cycles (reviewed in [1]). These endogenous clocks not only help organisms perform biological activities at advantageous times of the day, but also provide the means to anticipate and hence better prepare for environmental transitions, such as sunrise.

Circadian clocks are cell-based oscillators that have a period of about 24 hours, and persist or 'free-run' even in the absence of environmental cues. These rhythms are entrained (synchronized) to local time by zeitgebers (time-giver in German, or synchronizer) such as the daily cycles in light intensity, ambient temperature and to a lesser extent, food availability or social cues. The entrainment process occurs on a daily basis, slightly advancing or delaying endogenous clocks so that they keep alignment with the 24 hr solar day. In addition, the phase of circadian clocks is also adjusted throughout the year as the day length and temperature changes between seasons in temperate climates, enabling the clock to also function in seasonal adaptation, such as flowering in plants. Even though temperature can alter the phase of the rhythms; the period length of the internal oscillations is temperature compensated and remains relatively constant over a wide range of physiological temperatures; contrary to typical biochemical reactions whose rates are increased with increasing temperature. In summary, circadian rhythms are defined by the following properties; 1) endogenous periods of approximately 24 hr, 2) persist in constant environmental conditions, 3) synchronized to local time by environmental cues, especially daily light/dark cycles, and 4) exhibit an ill-defined property

termed temperature compensation that allows them to operate over a wide temperature range. The circadian timing system is typically represented as having three parts that are interconnected; an *input* pathway that can receive and transmit environmental cues to an intracellular *clock* mechanism that transmits temporal information to many different downstream *output* pathways ([1]).

Many behavioral and metabolic processes are regulated by circadian rhythms. In humans the level of plasma cortisol, melatonin and insulin show daily oscillations in levels (reviewed in [2]); body temperature cycles and probably entrains peripheral clocks [3]. However the most prominent rhythm is the sleep-wake cycle even though many graduate students may not have realized it during their studies. In animals, the wake-sleep cycle is driven by a 'master clock' in the brain, whereas all the other clocks (even those in other parts of the brain) are considered peripheral clocks. The disruption of circadian rhythms, either by mutation or by conflict with the local time due to trans-meridian flight or work-shift schedules, may result in serious health implications, including sleep disorders, depression, digestive problems, lower mental acumen, increased risk to many diseases such as diabetes and cancer [2].

To decipher the interaction of circadian rhythms with many physiological systems, it is essential to dissect the molecular mechanisms underlying circadian clocks. Many lines of evidence gathered from a wide range of model organisms indicate that clock mechanisms share similar features. In general, circadian clocks are based on a small set of species-specific 'clock' genes, whose RNA and protein products participate in multiple interacting transcriptional-translational feedback loops that ultimately drive cyclical gene expression, which underlies many of the physiological and behavioral rhythms observed (reviewed in [4]). Essentially, positive acting transcription factors drive the expression of negative regulators that after a time-delay feedback to inhibit the transcription factors until the negative factors are eliminated, enabling the next round of gene expression. Post-

transcriptional regulatory pathways, especially time-of-day-specific phosphorylation of clock proteins plays a key role in the time-delay and regulating the timing and duration of when the negative regulators function, resulting in oscillatory transcription factor activity and hence cyclical gene expression.

My work mainly focused on how the post-transcriptional pathways of protein phosphorylation and miRNAs contribute to the clock mechanism using *Drosophila melanogaster* as a model organism. The first clock gene, termed *period* (*dper*) was discovered in *D. melanogaster* ([5]) and this species has been at the forefront of trying to understand the molecular underpinnings for circadian rhythm generation. Importantly, the clock genes and mechanism in *D. melanogaster* are very similar to that operating in animals, including humans. As such, below I will focus on describing the clock mechanism in *D. melanogaster* with an emphasis on phosphorylation and miRNAs.

Molecular clock in *Drosophila melanogaster*

The molecular architecture of circadian clocks is remarkably similar between evolutionary distant species, and based on genes repressing their own expression through negative feedback loops. Transcription factors involved in these circuits relay the time-of-day information to downstream clock controlled genes and orchestrate circadian gene expression. Overlaying posttranscriptional and posttranslational modifications of core clock factors stabilizes the network and ensures a near 24 hour period for the oscillatory process.

In *Drosophila*, the basic-helix-loop-helix transcription factors CLOCK (dCLK) and CYCLE (CYC) heterodimerize and bind to the E-box regions (usually CACGTG) in target promoters including their repressor's, *period* (*dper*) and *timeless* (*tim*), driving their expression in the middle of the day (summarized in Figure 1.1) (reviewed in [6]). The newly synthesized dPER and TIM proteins slowly accumulate and dimerize in the cytoplasm

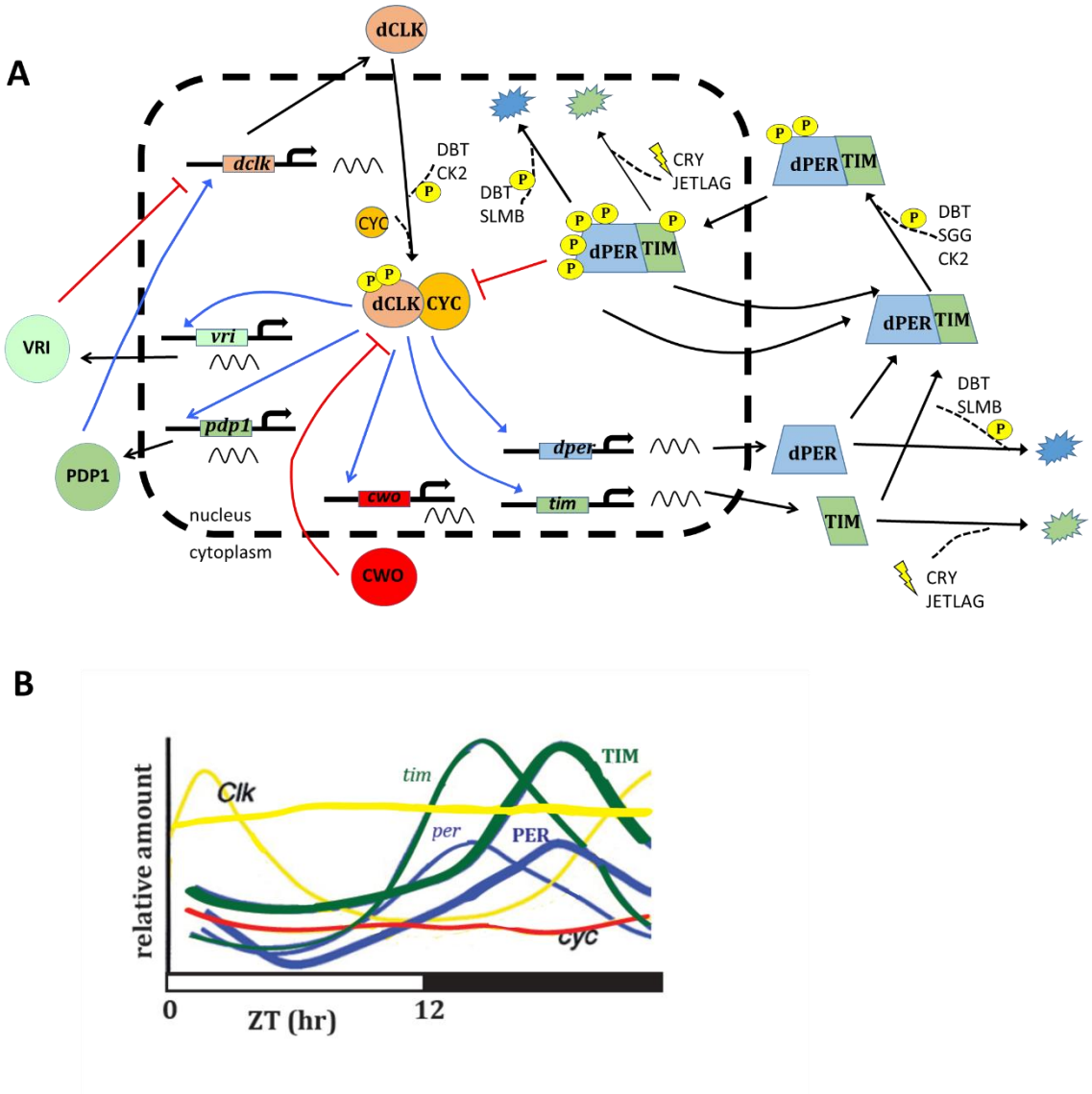

Figure 1.1. Overview of the multiple feedback loops underlying the *Drosophila* circadian clock and daily abundance cycles of clock mRNAs and proteins.

A, Model of the *Drosophila* circadian circuit involving three feedback loops and overlaying posttranslational modifications. Blue arrows marks transcriptional activation, red lines ending in bars show inhibitory effects. **P** in yellow circles denote phosphorylation, and squiggly lines indicate rhythmic transcription. Lighting symbol represents light exposure, and degradation. **B,** Daily oscillating levels of core clock mRNA and proteins

Figure legend of figure 1.1 continued

(modified from [4]). Note the delay in the accumulation of dPER and TIM proteins relative to their mRNA profile.

before entering the nucleus in the middle of the night; imposing a critical time-delay between their activation and repression.

Once in nucleus the dPER/TIM complex inhibits the transcriptional activity of dCLK-CYC, thus repressing their own expression. The mode of repression is two-fold [7]. First, in the on-DNA repression, dPER-TIM physically interacts with dCLK-CYC that is still on the promoter and displaces the transcription complex from the chromatin. Then, in the off-DNA repression phase dPER remains bound to dCLK, preventing re-initiation of transcription. The circadian clock inhibitory domain (CCID) at the C-terminus of dPER directly interacts with dCLK [8]. TIM may reposition dPER and aid in dCLK-binding, because the removal of the latter half of the CCID of dPER does not abolish the dPER/dCLK complex formation in the presence of TIM [9]. While binding of the dPER-TIM dimer to dCLK-CYC is important for repression it is not sufficient; current evidence strongly indicates that dPER acts as a scaffold to seed a large multi-subunit repressor complex on dCLK-CYC, regulating the activity and half-life of that complex [10].

The circadian clock is reset daily by light and in *Drosophila* light information is processed mainly by the cell-autonomous blue light receptor termed CRYPTOCHROME (CRY) [11]. Light activates CRY, which increases its affinity for binding TIM probably by a conformational change, and also makes CRY more prone to degradation [12]. The interaction of TIM and CRY poises TIM for rapid degradation probably by phosphorylation of key residues. Both CRY and TIM are targeted to the 26S proteasome by the E3 ligase JETLAG (JET) [13],[14]. The specific isoforms of TIM and the effective concentration of CRY and TIM determine the sequential degradation of both proteins [14]. CRY also mediates temperature responses through dPER/TIM/CRY complex [15], and acts as a transcriptional repressor in peripheral tissues [16]. Without TIM, dPER is unstable and is degraded in a similar manner by the proteasome pathway through binding to the F-box protein SUPERNUMERARY LIMBS (SLMB) [17]. The loss of dPER relives the repression

of dCLK-CYC, and the transcription cycle begins again. As will be discussed in more detail below, phosphorylation plays a key role in regulating the timing of dPER degradation.

In a second loop dCLK-CYC drives the expression of a second set of transcription activator *Par domain protein 1* (*pdp1*) and repressor *vrille* (*vri*), which regulate *dClk* and *cry* expression among other genes [18]. PDP1 accumulation is delayed relative to VRI, resulting in rhythmic transcription of target genes in anti-phase of *dper* and *tim*. The physiological significance of rhythmic *dClk* expression is not clear, because dCLK protein levels remain relatively constant though-out a day, and anti-phase *dClk* expression does not affect the rhythmicity [19]. However, mutations in *pdp1* results in attenuation of circadian rhythmicity especially in aged flies [20]. *Cyc* RNA and protein are expressed constantly trough the day [21] [22] [23].

Yet in another feedback loop, dCLK-CYC activates a repressor, *clockwork orange* (*cwo*), which bind to E-boxes and represses basal E-box activity in addition dCLK mediated transactivation including its own expression [24]. However, loss of function mutants have lower amplitude RNA rhythms of core clock genes and high *cwo* RNA, implying *cwo* might also activate or repress its own and other clock gene's transcription in a time of day specific manner [25]. Figure 1.1 summarizes the feedback loops in the *Drosophila melanogaster* circadian clock and resulting RNA and protein rhythms of core clock factors.

Posttranslational regulation with an emphasis on phosphorylation of dPER

Even though transcriptional negative feedback loops constitute a major part of the circadian machinery, there are instances where circadian rhythms in molecular oscillations can be generated without any transcription. The most fascinating example is from cyanobacteria: for example, the KaiC daily phosphorylation rhythm can be reconstituted *in vitro* by supplying KaiA, which enhances KaiC autophosphorylation, and KaiB which

attenuates the effect of KaiA [26]. In human red blood cells [27] and in unicellular alga *Ostreococcus tauri* [28], peroxiredoxins, highly conserved antioxidant proteins, undergo temperature compensated circadian redox cycles in the absence of transcription. Both peroxiredoxin and cyanobacterial KaiB are members of the thioredoxin-like superfamily, and it is an intriguing possibility that this posttranslational clock might be the remains of a proto-clock. In these cases posttranslational modifications are the main biochemical oscillations.

While the above-mentioned examples demonstrate that cyclical gene expression is not required for circadian molecular rhythms, posttranslational modifications usually function in concert with transcriptional pathways to generate the oscillatory mechanisms driving circadian clocks. In *Drosophila* circadian pacemakers, posttranslational modifications regulate numerous aspects of clock protein function and metabolism; including, timing of degradation and nuclear translocation, DNA-binding, potency of transcription and repression, and interaction with other core clock proteins. Core clock proteins are glycosylated, acetylated, sumoylated and phosphorylated in a phase-specific and usually reversible manner. Those modifications in some cases compete with each other for the same sites (reviewed [29], [30], [31] [32]).

My work focused mainly on dPER phosphorylation, which will be explained here in more detail. dPER of *Drosophila*, is the main negative regulator in the clock mechanism and is the key factor setting the speed of the clock. Likewise, FREQUENCY (FRQ) in *Neurospora* and mammalian PER2 (mPER2) have similar functions as dPER in *Drosophila*. A shared characteristic of these negative regulators is that they undergo progressive phosphorylation during their daily life cycle that are inextricably linked to clock progression [33]. Features of the phosphorylation program, such as hierarchical phosphorylation and modular phospho-sites are shared between all three proteins. Many phospho-sites were mapped by mass spectrometry for dPER [34], FRQ [35] and mPER2

[36]. While it is tempting to assign each phospho-event a specific function, phosphorylation of different modules in distant parts of a protein might collectively induce a confirmational change to a more open structure, which is prone to further modifications or to degradation, as in the case of FRQ [37] and probably dPER [38]. Yet in other cases mutations of single phospho-sites have clear and profound effects on dPER metabolism, the circadian period and/or phase ([39], [34], [40], [38], [41]).

dper (and *tim*) mRNA undergoes daily cycles in levels and begins to accumulate during the mid-day, peaking in the early night. However, newly synthesized dPER first appears as a non/hypo-phosphorylated species in early night. Part of the delay between *dper* mRNA accumulation and that of its cognate protein is because phosphorylation of dPER by the kinase DOUBLETIME (DBT; *Drosophila* homolog of mammalian casein kinase Iδ/ε; CKIδ/ε) targets it for rapid degradation by the proteasome. As dPER protein levels begin to accumulate it interacts with TIM, which seems to prevent phosphorylation at least some of the sites on dPER protecting it from subsequent degradation [17]. As mentioned above, the levels of TIM are low during the day because it is photosensitive. Thus, after sunset, there is an increase of TIM protein which interacts with dPER and this association enhances the nuclear entry of both. After nuclear translocation, dPER continues to undergo progressive phosphorylation such that hyper-phosphorylated isoforms appear in the early day and targeted for rapid degradation. The rapid decline in dPER levels during the early day requires phosphorylation at Ser47 by DBT, which is a key site in creating a binding site for SLMB, which targets it to the proteasome [34]. Altering S47 to Ala lengthens circadian periods (~30h) even though dPER is still hyper-phosphorylated, while changing S47 to the phospho-mimic Asp speeds up the clock (~21h). Numerous phospho-clusters that operate in a hierarchical manner regulate the timing of S47 phosphorylation, ensuring it occurs in the early day. Most notably, the ‘Per-short’ phospho-cluster regulates the timing of S47 phosphorylation by creating a delay-

circuit for DBT activity at S47. In the Per-short module, the NEMO/NLK kinase phosphorylates S596 of dPER stimulating progressive phosphorylation of nearby sites (S589, S585) by DBT, which slows down the ability of DBT to phosphorylate S47 [38]. Recently, phosphorylation of T610/S613 cluster was shown to have epistatic effects to the Per-short domain [41]. Although it is not yet clear if that cluster acts through S596 or in parallel, given the proximity of both modules it will not be surprising if both modules cooperate, setting the speed of the clock (Figure 1.2 A).

Not all phospho-sites are involved in the regulation of dPER's half-life. Phosphorylation of S661 by an unknown kinase early in dPER's life-cycle primes phosphorylation of S657 by GLYCOGEN SYNTHASE KINASE 3B/SHAGGY (SGG) [40]. Mutating of S661 to Ala abolishes S657 phosphorylation and increases the circadian period by ~2 hours. The lengthening of the period can be explained by a ~2 hour delay of dPER nuclear entry. Phosphorylation of several N-terminal sites (S149, S151 and S153) by CASEIN KINASE 2 (CK2) also delays the nuclear translocation and subsequently lengthens the period [39]. Suppression of CK2 activity has more severe effect on the period than altering the N-terminal sites, therefore its likely CK2 has more targets on dPER and/or other core clock proteins, most probably on dCLK [42] and TIM [43] [44]. p90 RIBOSOMAL S6 KINASE (S6KII) is another kinase that can influence the stability and repression potential of dPER, probably by interacting with and regulating CK2 activity [45]. Similar to CK2, DBT is also involved in dPER nuclear translocation by delaying nuclear entry [46]. Both DBT and CK2 potentiate dPER transcriptional repressor activity in tissue culture cells [47].

It should be noted that none of the kinases above show circadian oscillation in abundance either in RNA or protein levels from whole head extracts. However, recent evidence from single cells RNA-seq experiments suggest at least some kinases have rhythmic expression patterns in key pacemaker neurons [48]. Phase-specific

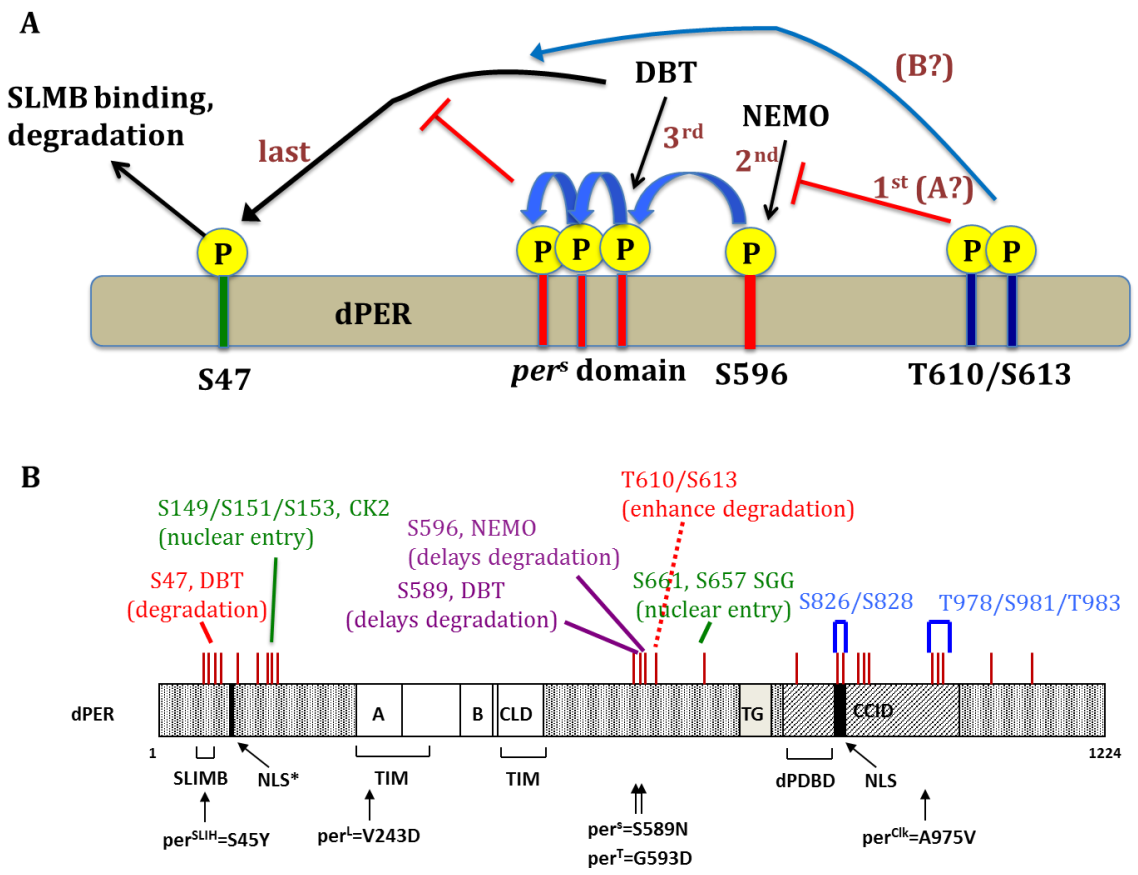

Figure 1.2. Phosphorylation of dPER regulates different aspects of dPER metabolism.

A, Model representing how phosphorylation near *per*^{S} domain regulates the pace of the clock. In scenario (A), the phosphorylation of T610/S613 might repress the phosphorylation of S596 by NEMO, which stimulates the DBT-dependent phosphorylation of S589, S585 and T583. Phosphorylation of this cluster somehow delays the phosphorylation of S47 and subsequent SLMB binding and degradation. In scenario (B), the phosphorylation of T610/S613 might enhance the DBT-dependent phosphorylation of S47 and act in parallel to *per*^{S} domain in adjusting the speed of the clock. **B,** Schematic diagram of dPER open reading frame showing the distribution of phosphorylation sites identified through mass spectrometry in relation to identified/suspected functional domains

Figure legend of figure 1.2 continued

and residues altered in known *per* mutants (modified from [34]). Functional domains are represented as follows; Two putative nuclear localization signals (NLS; aa 71-79 and 813-840) are shown as vertical black lines [8]. PAS domain (aa 238-512), including PAS-A and -B repeats are shown as a white box [74]. Cytoplasmic localization domain (CLD; aa 452-512) located within the PAS domain [78]. dCLK-CYC inhibitory domain (CCID; aa 764-1034) is shown as a hatched white box [8]. The TG (Thr-Gly) repeat region is shown as a dark gray box labeled “TG”. Regions that bind known interaction partners, including DBT (dPDBD; [75], [76], TIM [77]; [78], and SLIMB [34] are marked by brackets. Characterized phospho-sites with relevant kinases and function are shown above the diagram. The function of phospho-sites in blue are examined in this thesis.

phosphorylation can arise from activities of phosphatases as well. Protein phosphatase 2A (PP2A) regulates the degree of phosphorylation of dPER in cell culture and *in vivo*. Two regulatory subunits of PP2A, *twins* (*tws*) and *widerborst* (*wdb*) are expressed rhythmically in fly heads, and their overexpression alters the circadian period [49]. PP1A, on the other hand affects the stability of dPER, probably acting through TIM [50]. Thus, the phosphorylation program of dPER is very complex involving numerous kinases, phosphatases and phosphorylation sites that regulate numerous aspects of dPER function, including its stability and nuclear entry.

In addition to dPER, dCLK also shows oscillations in phospho-isoforms and is phosphorylated by DBT, which is likely seeded on dCLK by interactions via the dPER/TIM repressor complex [10] and CK2 [42]. While less is known about how phosphorylation regulates dCLK, several lines of evidence indicate that it modulates its transactivation potential and stability [10,42].

Although phosphorylation is the best studied and almost certainly most critical post-translational modification in animal clock mechanisms, O-GlcNAcylation is a newly described circadian modification, with the first described example being dPER in *Drosophila* [51]. O-GlcNAcylation contributes to the timing of dPER nuclear entry and stability, and might attenuate or compete with phosphorylation on some sites on dPER. The balance between kinases with phosphatases and competing modifications creates a complex phosphorylation program for dPER that sets the speed of the clock. Phosphorylation of dPER is relevant to human health, because mutations of a key phospho-site S662 on mPER2 is associated with familial advance sleep syndrome (FASPS) causing early sleep times and early awakening [52]. Mapped phospho-sites on *Drosophila* PER with respective kinases and mutant phenotypes are summarized in Figure 1.2B.

Neural circuitry underlying circadian pacemakers in *Drosophila melanogaster* brains

Like most diurnal animals, *D. melanogaster* exhibits two major activity peaks centered on sunrise (‘morning’ bout) and sunset (‘evening’ bout) that are separated by a mid-day ‘siesta’. The bimodal activity rhythm of *Drosophila melanogaster* clock-controlled and is generated by a network of ~150 neurons in the brain of adult flies. Distinct subsets of these neurons drive different parts of the behavior at different times of day or under different environmental conditions. They are classified into subgroups according to their locations and function in the brain and include the small and large lateral neurons (s-LNv, l-LNv), dorsal lateral neurons (LNd), three groups of dorsal neurons (DN1, DN2, DN3) and lateral posterior neurons (LPN) (Figure 1.3) (reviewed in [53]).

The s-LNvs are termed morning (M) cells because of their importance in morning anticipation whereby flies begin to become active prior to sunrise. LNvs express the neuropeptide PIGMENT DISPERSING FACTOR (PDF) and send projections to other circadian groups, mainly DN1’s [54], [55]. s-LNvs are sufficient and necessary to drive the activity rhythms in constant darkness conditions (DD) and are therefore considered the ‘master’ clock cells. The ablation of s-LNv’s or the loss of PDF causes dampening of rhythms in DD and disappearance of morning anticipation [56]. The mode of action of PDF involves the activation of cyclic AMP synthesis in target circadian neurons [57] and subsequent stabilization of dPER [58]. This way, LNv’s communicate and adjust the pace of PDF responding neurons.

The so-called evening (E) cells consisting of LNd’s and DN’s, underlie the evening anticipation. E cells drive the behavior rhythm in the presence of light [59]. According to the length of the day (photoperiod), M or E cells act as the dominant clock and determines the phase of the behavior. During long winter nights, M cells run the circadian network,

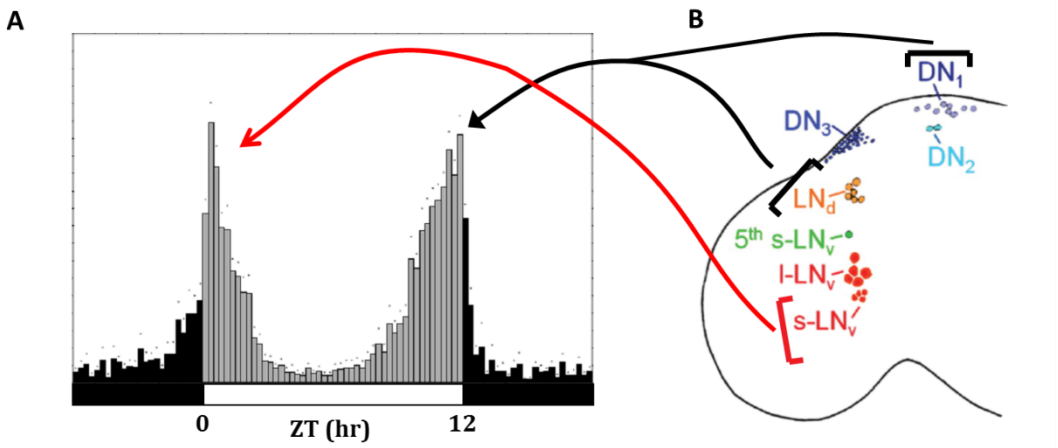

Figure 1.3. Groups of circadian pacemaker neurons in the *Drosophila* brain drive different aspects of behavior.

B, PDF-expressing ventro lateral neurons (LNvs) are shown in red, three dorsal neuron groups (DNs) in blue, lateral dorsal neurons in orange and non-PDF positive small-LNv in green. **A,** Small LNvs drive the morning activity and LNds together with DN1s underlie the evening activity (modified from [79]).

and during long summer days, E cells are more dominant; this may form the basis of seasonal adaptation [59].

Very recent evidence has challenged the dual oscillator model (i.e., strict morning and evening clocks). By changing the pace of specific clocks with overexpressing circadian relevant kinases (such as DBT and SGG) in small subsets of circadian neurons, it was shown that there exists at least three functional oscillators in E cells [60]. Each of these independent clocks is coupled to some but not all oscillators by different neuropeptides. Similar complexity is found in the master clock in mammals, which resides in the suprachaismatic nucleus (SCN) in the brain (reviewed in [61]). Thus, the overall daily rhythm in wake-sleep is an emergent property of the neural logic based on interactions between many individual clock cells. However, it appears that the core clock mechanism is the same, if not identical, in each clock cell.

Brief overview of miRNAs

Micro RNAs (miRNAs) are short (~22 nt) non-coding RNAs that regulate gene expression in a target specific manner by translational repression, mRNA destabilization or both. It is estimated that 1-2% of the genes in diverse species encode miRNAs; currently, there are 256 mature miRNA sequences in *Drosophila melanogaster* miRNA database (www.mirbase.org, version 21, Jun 2014). Most of the genome might be under miRNA mediated regulation with 60% of protein coding genes predicted to be targeted computationally by miRNAs [62], [63]).

miRNAs find their target mRNA owing to *cis*-acting binding sites mostly on the 3' untranslated regions (UTR). Most metazoan miRNAs have only partial complementarity to their target and the specificity of interaction is dictated by the 6-8bp ‘seed’ region on the 5’ end of the miRNA (Figure 1.4). Although the 3’ portion of miRNAs usually does not match well with the target mRNA, the 3’ pairing might compensate a mismatch or bulge in

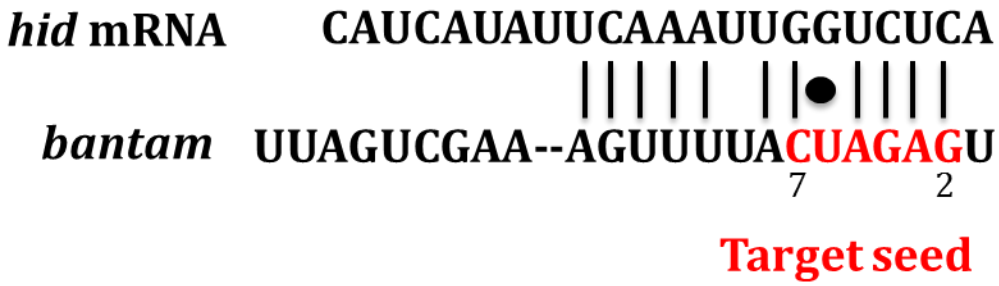

Figure 1.4. An example of miRNA target recognition.

Complementary base-pairing between a site on the *hid* 3' UTR and *bantam* miRNA [80]. Residues in red on the *bantam* miRNA are the 'seed' region for target recognition. Vertical dashes represent Watson-Crick base pairing, and black circle denotes wobble base pairing.

the seed region. The miRNA-mRNA pair is loaded onto a RNA induced silencing complex and targeted for deadenylation and decapping (reviewed in [63]).

miRNAs can act as on/off switches regulating target gene expression by repressing it in a complete and reversible manner. However most miRNA-mRNA interactions result in only subtle decreases (less then 2 fold) in protein levels. Knockdown of many miRNAs in worms and some in flies resulted in no or subtle phenotypes under lab conditions [64], [65]. Together, these observations led to the view that most miRNA mediated regulation reinforces and confers robustness to systems by micromanaging protein levels. miRNAs might buffer the systems against internal or external perturbations and smooth the response to environmental transitions (reviewed in [66], [67]). Therefore, it is not surprising that miRNAs are implicated both in core circadian mechanism and in its output. Many miRNAs are expressed rhythmically [68], [69], [70]. Rhythms in activity [71] and feeding [72] are at least partially regulated by miRNAs in *Drosophila*. In mammalian clocks, miRNAs are involved in modulation of light input and circadian period [70]. Finally the miRNA *bantam* was characterized as a regulator of *Drosophila dClk,* imparting robustness to the circadian clock [73], (Yildirim, Chapter 4 and 5, manuscript still in preparation).

Overview of thesis

The work presented in my thesis involves findings on a new phospho-cluster in dPER that is photosensitive and regulates entrainment (Chapter 2). This work is in the process of being submitted for publication. Chapters 3 describes recently published work that I contributed to and is related to dCLOCK phosphorylation, showing a specific role in entraining to daily temperature but not light/dark cycles. In addition, I present work I did on identifying *bantam* miRNA sites on *dClk* and the functional consequences thereof (Chapter 4), work that unfortunately has yet to be published because a manuscript with

similar data was published while our paper was under review. Nonetheless, additional findings described in Chapter 5 will be added to this manuscript and submitted in the near future. Results in Chapter 5 further support a surprising role for *ban* miRNA in upregulating dCLK proteins levels in key brain pacemaker neurons. I also include two addendum sections that summarize several key findings that are still in progress but will form the basis of manuscripts; these are; 1) addendum 1, showing that *ban* sites on *dClk* affect longevity, and 2) addendum 2, identifying a novel phospho-cluster in the vicinity of the previously identified per^{Clk} mutation that regulates clock speed. Finally, Chapter 6 provides a summary of my thesis work. Thus, work described in this thesis identifies novel roles for dPER and dCLK phosphorylation in entrainment and suggest a non-conventional mechanism for miRNA function in controlling dCLK levels.

Chapter 2: Identification of light-sensitive phosphorylation sites on PERIOD that regulate entrainment of the *Drosophila* circadian clock

(Evrim Yildirim, Joanna Chiu and Isaac Edery, manuscript in preparation)

INTRODUCTION

A wide variety of life forms exhibit circadian (~24 hr) rhythms in metabolism, physiology and behavior, which are governed by cellular 'clocks' based on the expression of species or tissue-specific sets of 'clock' genes (reviewed in [1]). A biologically relevant feature of circadian clocks is that they can be synchronized (entrained) to local time by external time cues, most notably the daily light-dark and temperature cycles. As a result, organisms can perform activities at biologically advantageous times and anticipate environmental changes. In general, clock mechanisms are biochemical oscillators built on interlocked loops of transcriptional negative feedback and protein degradation, wherein a 'master' clock transcription factor drives expression of one or more key repressor proteins that after a time-delay feedback to inhibit the transcription factor until the repressor(s) decline in abundance, enabling another round of gene expression [4]. Studies based on a wide range of model systems indicate that the daily changes in the levels of the key clock feedback repressor(s) is driven by complex temporal phosphorylation programs that dictate the pace of the clock [29, 30, 32, 81]. In animals, PERIOD (PER) proteins are the central components of the negative arm of the clock mechanism and behave as the primary 'phospho-timer' regulating clock speed [29, 30]. A major effect of phosphorylation on regulating clock pace is via evoking temporal changes in the stability of PER proteins, which yields daily cycles in their levels that are inextricably

linked to clock progression. Studies in *Drosophila melanogaster* have been instrumental in our understanding of clock mechanisms in general and mammalian ones in particular.

The *D. melanogaster* intracellular clock mechanism is comprised of inter-locked transcriptional feedback loops with overlaying posttranslational regulatory circuits (reviewed in, [6]). Prominent players in the first or 'major' loop are PER (herein referred to as *Drosophila* PER, dPER), TIMELESS (TIM), CLOCK (dCLK) and CYCLE (CYC; homolog of mammalian BMAL1). dCLK and CYC are transcription factors of the basic-helix-loop-helix (bHLH)/PAS (Per-Arnt-Sim) superfamily, that heterodimerize to stimulate the daily transcription of *dper* and *tim*, in addition to other clock and downstream genes. dPER plays a pivotal role in driving cyclical gene expression by undergoing daily translocation from the cytoplasm to the nucleus where it functions as a critical nexus in the phase-specific inhibition of dCLK-CYC transcriptional activity. Kinases are key players controlling when in a daily cycle dPER engages in autoinhibition by regulating its stability, timing of nuclear entry, duration in the nucleus and possibly repressor potency (reviewed in, [30]).

Newly synthesized dPER is first observed as non/hypo-phosphorylated variants in the cytoplasm that after a time-delay enters the nucleus and undergoes progressive increases in phosphorylation until it reaches a hyper-phosphorylated state in the early morning, which triggers its degradation. Much progress has been made in understanding the role of phosphorylation in regulating dPER's daily life-cycle. During the mid-day, *dper* and *tim* mRNA levels begin to rise but dPER and TIM protein levels remain low during the day. The instability of dPER is mainly due to phosphorylation by the DOUBLETIME (DBT; *Drosophila* homolog of CK1δ/ε) kinase [82, 83], whereas TIM is degraded in a light-mediated pathway that involves the circadian photoreceptor CRYPTOCHROME (CRY) (reviewed in, [84]). After nightfall, TIM levels increase and this enhances interaction with dPER, which protects dPER against DBT-mediated degradation. In addition, the

interaction of dPER and TIM promotes the translocation of both (in addition to dPER-bound DBT) from the cytoplasm to the nucleus, an event that occurs around mid-night [78, 85, 86]. In the nucleus, dPER acts as a scaffold to seed ill-defined repressor complexes that block dCLK-CYC-mediated transcription [87, 88]. As TIM levels begin to drop in the late night/early morning, dPER becomes hyper-phosphorylated and is recognized by the F-box protein β-TrCP (termed SLIMB in *Drosophila*), which targets dPER for rapid degradation via the proteasome [17, 89]. Rapid decline in the nuclear levels of dPER relieves autoinhibition and enables another round of circadian gene expression. Although DBT is the main kinase underlying the progressive phosphorylation of dPER and temporal changes in its stability, other kinases such as CK2 [43, 90], GSK-3β (SHAGGY; SGG in *Drosophila*) [91] and NEMO [38, 92], and protein phosphatases (such as PP1 and PP2A) [49, 50] regulate dPER metabolism and function.

Using mass spectrometry we and others identified over 30 phospho-sites on dPER [34, 38, 40, 41, 93]. Intriguingly, many of these sites are organized in phospho-clusters that appear to have different functions and are phosphorylated in an ordered or hierarchical manner. To date, all of the phospho-sites that have been characterized appear to have primary effects on either dPER stability and/or timing of nuclear translocation. Herein, we identify a phospho-cluster that does not affect dPER stability or timing of nuclear entry but rather reveals a surprising novel function for dPER phosphorylation in entrainment. The phospho-sites (Ser826/828) are phosphorylated by DBT, enhanced by light and attenuated by TIM. Flies where phosphorylation at these phospho-sites is prevented cannot properly synchronize to daily light-dark and temperature cycles, suggesting phosphorylation of dPER at specific sites is a key conduit in how the clock responds to environmental cues.

MATERIALS AND METHODS

Generation of transgenic flies

To generate transgenic flies carrying *dper* mutations, we used the previously characterized vector that contains a 13.2kb *dper* genomic fragment tagged with an HA epitope and multiple histidine residues (10XHis) at the carboxyl terminal (13.2*per*$^{+}$-HAHis) [94]. A XbaI–BamHI subfragment of this vector including sequences encoding amino acids 1–870 of dPER was subcloned into pGEM7 vector (Promega); and the resulting plasmid was used as the template for site-directed mutagenesis using the QuickChange Site-Directed Mutagenesis kit (Stratagene). Desired mutated *dper* regions were confirmed by DNA sequencing and used to replace the corresponding fragment in the 13.2*per*$^{+}$-HAHis plasmid. Transgenic flies were generated by Genetics Services Inc. (Sudbury, MA, USA) using standard P element-mediated transformation techniques and *w*^{1118}*per*$^{+}$ (referred to as either *wper*$^{+}$ or *w*) embryos as hosts. For each construct, several independent germ-line transformants in the *wper*$^{+}$ background were obtained, yielding a wildtype version (*wper*$^{+}$;p{*dper*-HAHis}); herein more simply referred to as p{*dper*}), and several mutant versions; p{*dper*(S826A)}; p{*dper*(S828A)}; p{*dper*(S826D)}; p{*dper*(S828D)}; p{*dper*(S826A/S828A)}; p{*dper*(S826D/S828D)}; p{*dper*(K822A/R823A/K825A/K837A)}, which herein is simplified as p{*dper*(NLS-2mut)}; and p{*dper*(NLS-2mut/S826A/S828A)}. The transgenes were crossed into a *wper*^{01} background, thus the only functional copy of *dper* is expressed from the transgene. p{*dper*(ΔDBD)} flies [which contains a deletion in the corresponding DBT binding domain (Δaa 755-809) on *dper*] were previously generated and described in [75] *w*;;*cry*^{01} flies which are null mutants for the circadian light receptor cryptochrome (*cry*) were generated and characterized in [95]. All flies were routinely reared at room temperature (22-25^{o}C) and maintained in vials or bottles containing standard agar-cornmeal-sugar-yeast-tegosept media.

Behavioral assays

Locomotor activity was continuously monitored and recorded in either 15- or 30-minute bins by placing individual adult male flies in glass tubes and using the Drosophila Activity Monitoring system from Trikinetics (Waltham, MA) as previously described [96]. Briefly, 3-7 day old male flies were kept in incubators at the indicated temperature (18°, 25° or 29°C) and entrained for at least five daily light-dark cycles (LD). For the light/dark cycles, flies were exposed to one of several regimes that differed in day length (photoperiod); namely, the standard condition of 12hr light:12hr dark (12:12LD), a shorter (9:15LD), or longer (15:9LD) photoperiod. In all cases, zeitgeber time (ZT) 0 is defined as the start of the light period. Cool white fluorescent light (~2000 lux) was used during LD and the temperature did not vary by more than 0.5°C between the light and dark periods. After the LD cycles, flies were kept at the same temperature for at least 7 days in constant dark conditions (DD) to determine free-running period. In addition, some flies were subjected to a daily temperature cycle (TC) in constant dark conditions. Temperature cycles were 12 hr at 24°C followed by 12 hr of 29°C [12:12TC; where ZT0 is the beginning of the warm phase] for at least 5 days and subsequently kept at 24°C for 7 days. Data analysis was done on a Macintosh computer with the FaasX software (kindly provided by F. Rouyer, CNRS, Gif-sur-Yvette, France). Rhythmic flies were defined by *Chi*-square periodogram analysis with the following settings; power ≥ 10, width ≥ 2. Values for individual flies were pooled to obtain an average value for each independent line analyzed. For each construct, locomotor activity rhythms were measured from at least two independent lines in the *wper*^{01} genetic background, which are representative of behavioral results obtained with other independent transgenic lines (data not shown).

To measure acute circadian responses to light stimulation, we used the standard method of an anchored phase response curve (PRC) protocol as previously described

[97], [98]. Briefly, adult male flies were entrained five days to 12:12LD cycles at 25°C. Every 2 hr beginning at ZT13 of the last LD cycle, one group of flies was exposed to a 10 min light-pulse (white light, 100 lux) and returned to complete darkness for at least 7 days; a control group of flies was not exposed to light treatment. The resulting shift in the phase of the locomotor activity rhythm was measured by comparing the phases of light-pulsed flies to the control untreated group on the second and third day of DD. The offset of evening activity (defined as 75% of the evening activity peak) was used as the phase marker and phases determined using the Brandeis Rhythm Package software.

Plasmids for S2 cell expression

Most of the plasmids used in this study were described previously: pAct-*per*-V5/His [17], pAct-*per*(513-1224)-V5/His, pAct-*per*(513-1224)-V5/His (K822A/R823A) and pAct-*per*(513-1224)-V5/His (K822A/R823A + SV40NLS) [8], pAct-3xFlag-6xHis-*per*-6xmyc [34], pMT-*dbt*-V5/His [17], pMT-*sgg*-V5/His [40], pMT-*CK2α* and pMT-CK2*β*-V5/His [10], pMT-*nemo*-HA [38], pMT-*Clk*-V5/His [10], pAct-E-box-luc [87], and pAct-ren.luc is a gift from Dr. Padgett [99]. To generate *dper* containing point-mutations (e.g., S826A, S828A, S826/828A), we used the previously described pAct-*per*-V5/His vector [17] and pAct-*per*(514-1224)-V5/His [8], in combination with the QuickChange Site-Directed Mutagenesis kit (Stratagene). Final constructs were confirmed by sequencing prior to use.

S2 cell culture-based assays

S2 cells and *Drosophila* Expression System (DES) expression medium were obtained from Invitrogen, and transient transfections were performed using effectene (Qiagen) according to the instructions of the manufacturer. For each transient transfection, 0.8 μg of different *dper* or *tim* containing plasmids and 0.2 μg of pMT vectors expressing kinases or empty control pMT-V5/His plasmids were used. Induction of pMT driven

kinases were achieved by adding 500 μM $CuSO_4$ to the culture media 24 h after transfection. Cells were collected at the indicated times after induction. When indicated, the proteasome inhibitor MG132 (50 μM; Sigma) and cycloheximide (10 μg/ml; Sigma) were added to the media 18 h after *dbt* induction, and cells were collected 4 h later. For stability assay in the absence of *de novo* protein synthesis, cycloheximide (10 μg/ml; Sigma) was added to the media 18 h after *dbt* induction and cells were collected at the indicated times.

To measure dCLK-mediated transactivation in tissue culture, we used the standard approach of E-box-mediated transcription of a *luciferase* (*luc*) reporter in combination with the Dual-Glo luciferase assay system (Promega) as described in [76]. Briefly, $1x10^6$ S2 cells in 1ml of S2 cell media supplemented with 10% bovine serum were seeded on 12-well plates. One day after seeding, cells were transfected with 2 ng of a pMT-*Clk* vector either alone or mixed with 1.5 or 10 ng of *dper* expressing pAct-based plasmids, in addition to 10 ng pAc-E-box-luc [87] and 25 ng pAct-ren.luc. An empty pAct-V5/His vector was used to balance the total amount of plasmids transfected into each well. One day after transfection, *dClk* expression was induced by adding 500 μM $CuSO_4$ (final) to the media, after another day luminescence from fire fly and renilla luciferase were measured from 75 μl of cell suspension using protocols supplied by the manufacturer (Promega).

Generation of dPER anti-pS826/pS828 phospho-specific antibody

Affinity-purified dPER anti-pS826/pS828 antibodies were generated by Proteintech Group, Inc. (USA). Briefly, two rabbits were immunized with a 16 aa peptide [amino acid 820-835; GIKRGGpSHpSWEGEANK (pS826/pS828), in which p indicates phosphate, and numbering is based on the full-length dPER sequence] that was conjugated to the carrier keyhole limpet hemocyanin. Antisera were affinity purified on a resin containing the pS826/p828 peptide, yielding anti-pS826/p828 Rb1 and Rb2

antibodies. In this study only the Rb2 antibody was used, as it has higher affinity. ELISA tests using peptides that are non-phosphorylated (S826/S828), singly phosphorylated (pS826/S828, S826/pS828) or doubly phosphorylated (pS826/pS828) showed that the anti-pS26/pS828 antibody recognizes only the doubly phosphorylated version (Figure S2.1 D).

Immunoblotting

To prepare cell-free extracts for immunoblotting of proteins in cultured S2 cells, the cells were harvested, washed in PBS, and homogenized using EB2 solution (20mM Hepes pH 7.5, 100mM KCl, 5% glycerol, 5mM EDTA, 1mM DTT, 0.1% Triton X-100, 25mM NaF, 0.5mM PMSF) supplemented with complete EDTA-free protease inhibitor cocktail (Roche) [34]. Extracts from fly heads were prepared as previously described [9]. Briefly, flies were collected by freezing at the indicated times in LD or DD, and total fly head extracts prepared by homogenizing in modified RIPA buffer (50 mM Tris-HCl pH 7.5, 150 mM NaCl, 1% NP40, 0.25% sodium deoxycholate, 0.5 mM PMSF), with the addition of complete EDTA-free protease inhibitor cocktail and PhosStop (Roche) [9]. Extracts were resolved using either 6% or 4-15% SDS-polyacrylamide gels to detect dPER and other proteins as indicated in figure legends. Primary antibodies were used at the following dilutions: rat anti-HA (3F10; Roche), 1:1000; rat anti-TIM R3 [100], 1:2000; mouse anti-TUBULIN (Sigma), 1:7000; mouse anti-V5 (Invitrogen), 1:5000; and mouse anti-c-MYC 9E10 (Sigma) 1:5000. Appropriate HRP-conjugated IgG secondary antibodies were used at a 1:2000 dilution (GE Healthcare).

Immunoprecipitation and phosphatase treatment

To examine phosphorylation of dPER on S826/828 with the anti-pS826/pS828 antibody, we first purified dPER by subjecting extracts to immunoprecipitation (IP), as

described in [34]. Briefly, extracts from S2 cells or ~800 fly heads, were prepared using EB2 buffer (20mM Hepes pH 7.5, 100mM KCl, 5% glycerol, 5mM EDTA, 1mM DTT, 0.1% Triton X-100, 25mM NaF, 0.5mM PMSF) supplemented with complete EDTA-free protease inhibitor cocktail (Roche) or modified RIPA (50 mM Tris-HCl pH 7.5, 150 mM NaCl, 1% NP40, 0.25% sodium deoxycholate, 0.5 mM PMSF) respectively, with the addition of a protease inhibitor cocktail and PhosStop (Roche). About 20 µl of extracts were kept for input analysis and to the rest of extracts, 30 µl of anti-V5 agarose (Sigma) or anti-HA agarose (Sigma) resins were added depending on the epitope tag on *dper*; followed by incubation with gentle rotation at 4°C for 4 hr. For experiments involving *w;;cry*^{01} flies, extracts were incubated with 3 µl of anti-dPER antibody (GP-73) [100] followed by 1 hr incubation with GammaBind Plus Separose beads (GE Healthcare). Beads were collected and washed for 10 min with the lysis buffer, then resuspended in 30 µl of 1X SDS-PAGE sample buffer and incubated for 5 min at 100°C. The resulting supernatants were resolved by immunoblotting using either 6% or 4-15% SDS-polyacrylamide gels for full length dPER or truncated dPER (513-1224), respectively. To detect phosphorylated S826/S828, immunoblots were incubated with rabbit anti-pS826/pS828 phospho-specific antibodies at 1:1000-2000 dilution. For input analysis, extracts were resolved using 4-15% SDS-polyacrylamide gels unless otherwise stated.

For phosphatase treatment, immune complexes bound to anti-HA or anti-V5 agarose beads (see above) were washed twice with modified-RIPA followed by another was in λ-protein phosphatase (λ-PP) buffer (NEB). Immune complexes then were resuspended in 40 µl λ-PP buffer, and one aliquot treated with λ-PP (NEB) for 30 min at 30°C, whereas another aliquot was mock-treated in the absence of λ-PP. Immune complexes were resuspended in 1x SDS sample buffer and directly analyzed by immunoblotting as described above.

Confocal imaging of adult brains

Whole mounts of adult brains were prepared and imaged as described previously [51] with the following modifications. Briefly, adult flies were collected at the indicated times during a daily LD cycle and fixed for 3 hr in 4% paraformaldehyde with 0.1% Triton X-100 at room temperature (RT) in darkness. After fixation, brains were dissected in cold PBS and washed twice with PBT solution (PBS containing 0.5% Triton X-100). Brains were incubated in blocking solution (PBT with 10% goat serum) for 1 hr at RT, and then overnight at 4^{o}C with the addition of primary antibodies at the following final dilutions: anti-dPER [25], 1:200; and anti-PDF C7 [101], 1:200. Subsequently, brains were washed three times with PBT and then incubated overnight in blocking solution with the secondary antibodies Alexa Fluor 488-conjugated anti-rabbit IgG (Invitrogen) or Alexa Fluor 594-conjugated anti-mouse IgG (Invitrogen), both at a final dilution of 1:200 dilution. After several washes with PBT, brains were transferred onto slides and mounted with Vectashield (Vector Laboratories) on a coverslip. Confocal images were obtained with a Leica SP2 confocal microscope and processed with LCS Lite software.

Measuring *dper* mRNA levels

The relative levels of *dper* mRNA in fly head extracts were measured by semi-quantitative RT-PCR as described previously [102]. Briefly, ~100 adult flies were entrained in the respective LD regime (i.e., 12:12LD or 9:15LD) for four days and collected during the last day at the indicated times by freezing. For each time point, heads were isolated and total RNA extracted using TriReagent (Sigma) per manufacturers' instruction. Approximately 1 µg of total RNA was reverse-transcribed using the ThermoScript RT-PCR kit (Invitrogen) in the presence of oligo-dT_{20} as a primer. To amplify *dper* and the non-cycling control mRNA encoding the cap binding protein 20 (*cbp20*), 2 µl aliquot of the reaction was further processed by PCR using the *dper*-specific primers P7197 and P6869,

and *cbp20* specific primers CBP236 and CBP594, respectively, as previously described [102].

RESULTS

Phosphorylation of two Ser residues in a putative NLS on dPER occurs in the late night/early morning and is mediated by DBT

Among the phospho-sites we identified on dPER expressed in cultured *Drosophila* S2 cells using mass spectrometry were Ser826 and Ser828 [34], whereas a more recent study using similar methodology further supports phosphorylation at Ser826 [41]. We were initially prompted to investigate the role of dPER phosphorylation at Ser826/828 because these sites are embedded in a sequence that has signature motifs of a bipartite NLS (Figure 2.1A), and more importantly was shown to function in this capacity when evaluated in *Drosophila* S2 cells [8]. Moreover, Ser826/828 and the surrounding putative NLS sequences are highly conserved in *Drosophila* (Figure S2.1A). In keeping with the nomenclature of a recent study we refer to this putative dPER NLS as NLS-2 [41].

To better study phosphorylation of Ser826/828 we sought to generate phospho-specific antibodies, a strategy we previously used successfully to examine the *in vivo* phosphorylation of dPER at other phospho-sites [34, 38, 40]. Due to the closeness of Ser826 and Ser828 we were concerned that antibodies only recognizing a single phospho-site might not detect the doubly phosphorylated version *in vivo*, and thus used a doubly phosphorylated peptide (pS826/pS828) as immunogen (see Materials and Methods). Enzyme-linked immunosorbent assay (ELISA) showed that the anti-dPER-pS826/pS828 antibody used here mainly recognizes the doubly phosphorylated peptide (Figure S2.1D).

To determine if our phospho-specific antibody recognizes dPER *in vivo*, we used previously described transgenic flies that are otherwise wildtype except carry a copy of *dper* modified with an HA epitope tag to facilitate purification of dPER (termed p{*dper*})

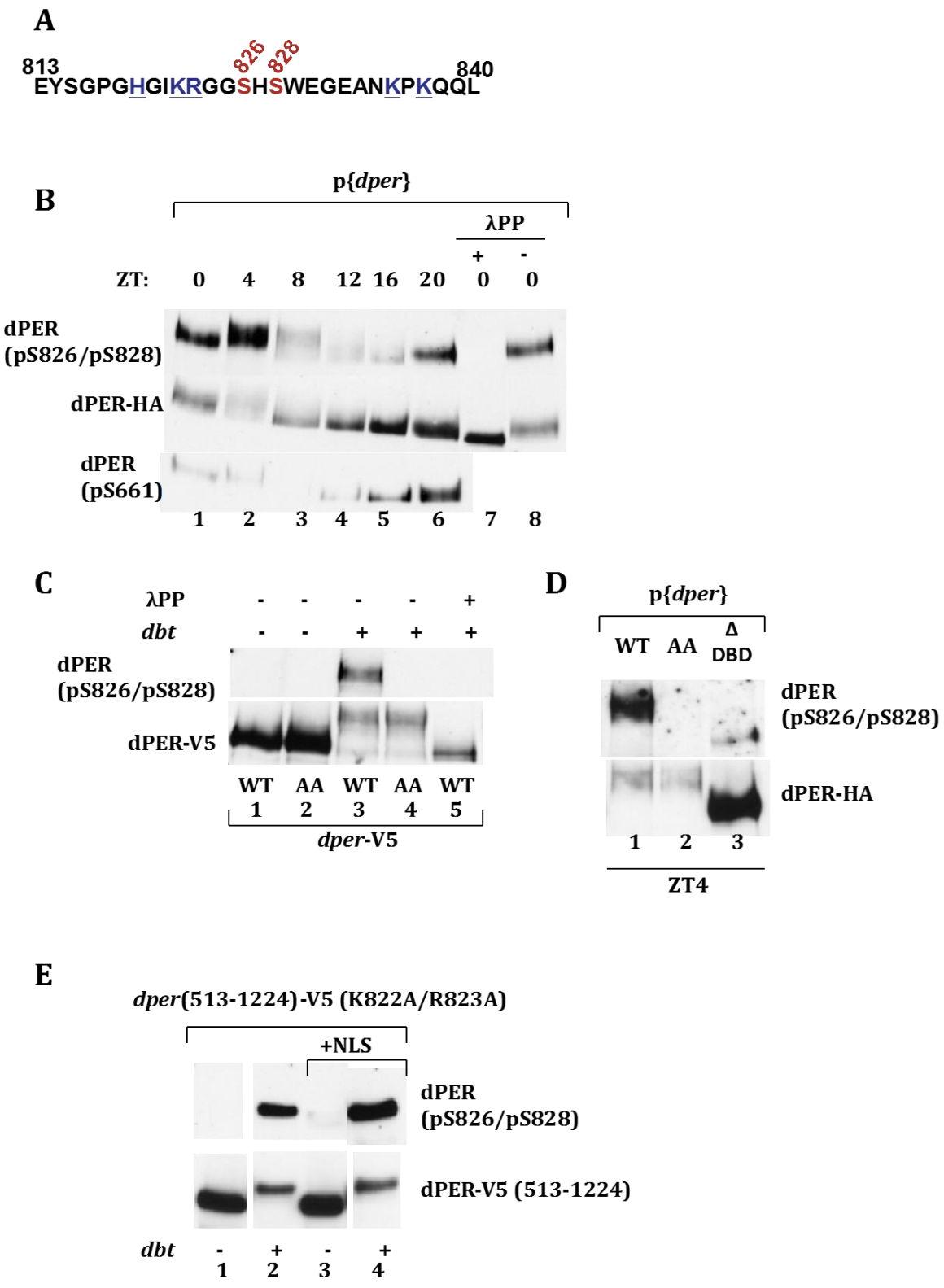

Figure 2.1. Late night/early morning phosphorylation of Ser826 and Ser828 in the NLS-2 region of dPER.

Figure legend of figure 2.1 continued

A, The sequence of dPER between residues 813-840, displaying S826/S828 in red, and basic residues of a previously characterized bipartite nuclear localization signal (NLS) in blue and underlined. ***B,*** Adult flies were collected at the indicated times (ZT) and head extracts prepared. dPER-HA was immunoprecipitated (IP) with anti-HA beads; for ZT0 the sample was divided in two and treated in the presence (+) or absence (-) of lamda phosphatase (λPP). Recovered immune complexes were resolved by 6% SDS-PAGE and blotted in the presence of anti-HA to measure total dPER levels or dPER phospho-specific antibodies (pS826/pS828 or p661) (left of panels). ***C*****,** S2 cells were transiently transfected with pAct-*dper*-V5/His (WT) or pAct-*dper*-(S826A/S828A)-V5/His (AA) in the presence or absence of pMT-*dbt*-V5/His. Cells were harvested 18 hr post-*dbt* induction, extracts subjected to IP using anti-V5 beads and the sample in lane 5 was further treated with λPP. Immune complexes were resolved by 6% SDS-PAGE and immunoblots incubated with anti-V5 or anti-pS826/pS828 antibodies. ***D*****,** Flies from the indicated genotypes (top) were collected at ZT4 and head extracts prepared followed by IP with anti-HA beads and immunoblotting with anti-pS826/pS828 or anti-HA antibodies (right of panels). ***E*****,** Lysates from S2 cells expressing pAct-*dper*(513-1224)-V5/His (K822A/R823A) or pAct-*per*(513-1224)-V5/His (K822A/R823A + SV40NLS) in the presence or absence of pMT-*dbt*-V5/His were prepared and immunoprecipitated with anti-V5 beads. Recovered immune complexes were resolved by 4-15% SDS gradient gels and blotted with anti-pS826/pS828 or anti-V5 antibodies (right of panels). Results shown are typical of multiple independent experiments.

[40, 75]. Flies were entrained (synchronized) under standard conditions of 12 hr light/12 hr dark cycles [12:12LD; where zeitgeber time 0 (ZT0)] at 25ºC, collected at different times in the day and head extracts prepared. Subsequently, dPER was immunoprecipitated followed by immunoblotting in the presences of anti-dPER-pS826/pS828 antibodies. Strong staining was observed at several times throughout a daily cycle but not when extracts were first treated with phosphatase, verifying the phospho-specificity of our anti-dPER-pS826/pS828 antibody (Figure 2.1B, top panel, compare lanes 7 and 8). When we probed for total dPER levels, we observed the expected wild type pattern whereby dPER is first detected as a newly synthesized hypophosphorylated species (fastest migrating species) at ~ZT8, undergoes progressive increases in phosphorylation, peaks in abundance at ~ZT20 and attains the most highly phosphorylated isoforms around ZT4, concomitant with rapid decreases in levels (Figure 2.1B, middle panel) [33]. Intriguingly, significant phosphorylation of S826/828 was first observed at ZT20, with peak values at ZT4, despite the fact that total levels of dPER begin to rapidly decline during the early day (Figure 2.1B, middle panel). This staining pattern is very different from that obtained for a dPER phosphorylation site (S661) we previously showed affects the timing of dPER nuclear entry, which is readily observed at ZT16 and essentially follows the daily changes in total dPER levels (e.g., Figure 2.1B, bottom panel) [40].

Several lines of evidence using cultured S2 cells and flies indicate that Ser826 and Ser828 are phosphorylated by DBT, consistent with our earlier results using mass spectrometry [34]. In prior work we showed that although some endogenous kinases can phosphorylate dPER at several sites in S2 cells, the co-expression of *dbt* with recombinant *dper* evokes the slow conversion of hypo-phosphorylated dPER to hyper-phosphorylated variants that are recognized by SLIMB for rapid degradation by the proteasome, recapitulating the main features of the dPER phosphorylation program observed in flies [17]. Phosphorylation of S826/828 was detected when *dbt* was co-expressed with *dper*

in S2 cells but not in the absence of recombinant *dbt* (Figs. 2.1C and S2.1B, compare lanes 1 and 2). We tested several clock-relevant kinases but only *dbt* resulted in significant phosphorylation of Ser826/828 (Figure S2.1E). In flies, efficient phosphorylation of dPER by DBT requires the DBT binding domain (DBD) on dPER and removal of this region (dPER(ΔDBD)) results in flies that produce very stable dPER with little changes in abundance or phosphorylation throughout a daily cycle [75]. As was the case when we used other dPER phospho-specific antibodies to sites that are phosphorylated by DBT [34, 38], when probed with the anti-dPER-pS826/pS828 antibody, there was little signal with dPER(ΔDBD) compared to dPER even though the levels of dPER(ΔDBD) are much higher then those of dPER (Figure 2.1D, lanes 1 and 3). Together, these results strongly suggest that DBT directly phosphorylates Ser826 and Ser828 on dPER.

The specificity of the anti-dPER-pS826/p828 antibody was further confirmed by showing a lack of signal when probing S2 cells extracts containing a dPER mutant version where S826 and S828 were replaced by Ala residues [dPER(S826A/S828A)] (Figure S2.1B, lanes 1 and 2). Likewise, as will be described in more detail below, dPER was not recognized by the anti-pS826/pS828 antibody in transgenic flies bearing a *dper* modified with S826A/S828A (Figs. 2.1D, lanes 1 and 2; S2.1C, lanes 1 and 4). We also tested singly mutated versions of *dper* (S826A or S828A) produced in S2 cells or flies and did not detect staining with the anti-dPER-pS826/pS828 antibody (Figs. S2.1B, S2.1C), consistent with the specificity of the phospho-specific antibody (Figure S2.1D). Attempts to raise singly phosphorylated phospho-specific antibodies (i.e., pS826 or pS828) were not successful and therefore we do not know if blocking phosphorylation at one site affects phosphorylation at the neighboring site.

Numerous lines of evidence indicate that dPER enters the nucleus of key pacemaker neurons in the brain between ZT19-20 [85]. However, as noted above the majority of Ser826/828 phosphorylation occurs in the late night/early morning, subsequent to nuclear translocation (Figure 2.1B). To test if phosphorylation of Ser826/828 can occur in the cytoplasm, nucleus or both we used a previously described mutant fragment of dPER [dPER(513-1224/K822A/R823A)-V5] that spans from amino acid 513 till the C-terminus of dPER [dPER(513-1224)] and includes mutations that abrogate the NLS function of the NLS-2 sequence (i.e., K822A/R823A) in S2 cells [8]. Furthermore, they showed that while dPER(513-1224/K822A/R823A) is exclusively located in the cytoplasm of S2 cells, a version that includes a strong heterologous NLS resides in the nucleus [8]. When we co-expressed *dbt,* both versions of the dPER fragment (i.e., with and without the heterologous NLS) showed strong phosphorylation of Ser826/828, indicating that these phospho-sites can be phosphorylated, at least in S2 cells, in both the cytoplasm and nucleus (Figure 2.1E). We consistently observed slightly greater staining of Ser826/828 phosphorylation when the dPER fragment was mostly located in the nucleus, although the reasons for this are not presently clear.

Blocking phosphorylation at Ser826/828 shortens behavioral rhythms by about 1 hour with little effect on the *dper* protein and mRNA cycles

To study the physiological role of phosphorylation at Ser826/828 in circadian timing we generated a series of transgenic flies that produce HA epitope tagged versions of dPER that have Ser to Ala replacements to block phosphorylation at S826, S828 or both; i.e., dPER(S828A), dPER(S828A) and dPER(S826A/S828A). In addition, we also generated versions where each or both of the phosphorylated residues were replaced with Asp, as a potential phospho-mimetic [dPER(S826D), dPER(S828D), dPER(S826D/S828D)]. The effects of the different transgenes were examined in the *per*-

null *wper*^{0} [5], whereby the only functional copy of *dper* is provided by the transgene. At least two independent lines of each genotype were analyzed. Flies were kept at 25^{o}C and entrained for 4 days in 12:12LD followed by 7 days in DD (constant dark) to determine their free-running period. As previously shown, *wper*^{0} flies expressing the wild type *dper* transgene with an HA tag (p{*dper*}) exhibit strong rhythms with ~24 hr periods (Figure 2.5 and Tables 2.1, S2.1 and S2.2) [75, 103].

The p{*dper*(S826A/S828A)} flies [referred to as *wper*^{0}; *per*$^+$-HA(S826A/S828A) in the Tables to better identify the genotypes] manifest robust activity rhythms that are 1 hr shorter compared to the wild type control (Table 2.1). The singly Ser to Ala replacements [p{*dper*(S826A} and p{*dper*(S828A}] also showed shorter rhythms but of slightly less magnitude change compared to the doubly mutated version (Table S2.1), suggesting similar circadian functions for both phospho-sites. Mutant versions of dPER where S826, S828 or both were replaced by Asp residues did not lead to changes in the periodicity of behavioral rhythms (Tables 2.1 and S2.1), which could imply that the introduced negative charges do not act as phospho-mimetics or that constitutive phosphorylation at these sites does not affect clock speed. In any event, our results indicate that while phosphorylation at S826/828 modulates behavioral periods the effects are mild. For example, some dPER phospho-site mutants can shorter or lengthen behavioral periods by over 6 hr [38, 41].

Because p{*dper*(S826A/S828A)} flies yielded the most significant changes in behavioral periods we focused on these flies to examine the molecular status of the clock by tracking the daily rhythms in *dper* protein and mRNA levels. The dPER(S826A/S828A) protein exhibited daily rhythms in abundance and phosphorylation that are indistinguishable from that observed in control wild type transgenics (Figs. 2.2A and B), although a 1 hr difference would be difficult to detect using immunoblotting. Similar results were also obtained in S2 cells whereby the kinetics of DBT-mediated progressive phosphorylation and degradation of hyper-phosphorylated isoforms of dPER was similar

Table 2.1: Locomotor activity rhythms for mutant *dper* transgenics and controls[a]

Genotype[b]	Period (hr ±SEM)	Power[c]	Rhythmicity (%)[d]	Total flies[e]
wper^{0}; *per*$^{+}$-HA (S826A/S828A) (1M)	22.3±0.06	145.2	96.8	32
wper^{0}; *per*$^{+}$-HA (S826A/S828A) (2M)	22.4±0.11	92.2	100	12
wper^{0}; *per*$^{+}$-HA (S826D/S828D) (2M)	23.9±0.13	90.8	95.8	25
wper^{0}; *per*$^{+}$-HA (S826D/S828D) (4F)	23.8±0.06	117.9	96.9	32
wper^{0}; *per*$^{+}$-HA (NLS-2mut) (1M)	25.5±0.13	79	70.6	29
wper^{0}; *per*$^{+}$-HA (NLS-2mut) (1F)	25.1±0.1	95.2	100	24
wper^{0}; *per*$^{+}$-HA (1M)	23.5±0.05	139.3	100	30
wper^{0}; *per*$^{+}$-HA (2M)	23.4±0.07	125.2	100	32

[a] Young male flies were maintained at 25^{o}C and exposed to 5 days of 12:12 LD cycles followed by 7 days of DD

[b] Independent transgenic lines are designated by the numbers in parenthesis

[c] Power is a measure of the strength or amplitude of the rhythm in arbitrary units

[d] Percentage of flies showing locomotor rhythms with a power value of ≥10 and a width value of ≥2

[e] Total number of flies that survived until the end of the experimental period

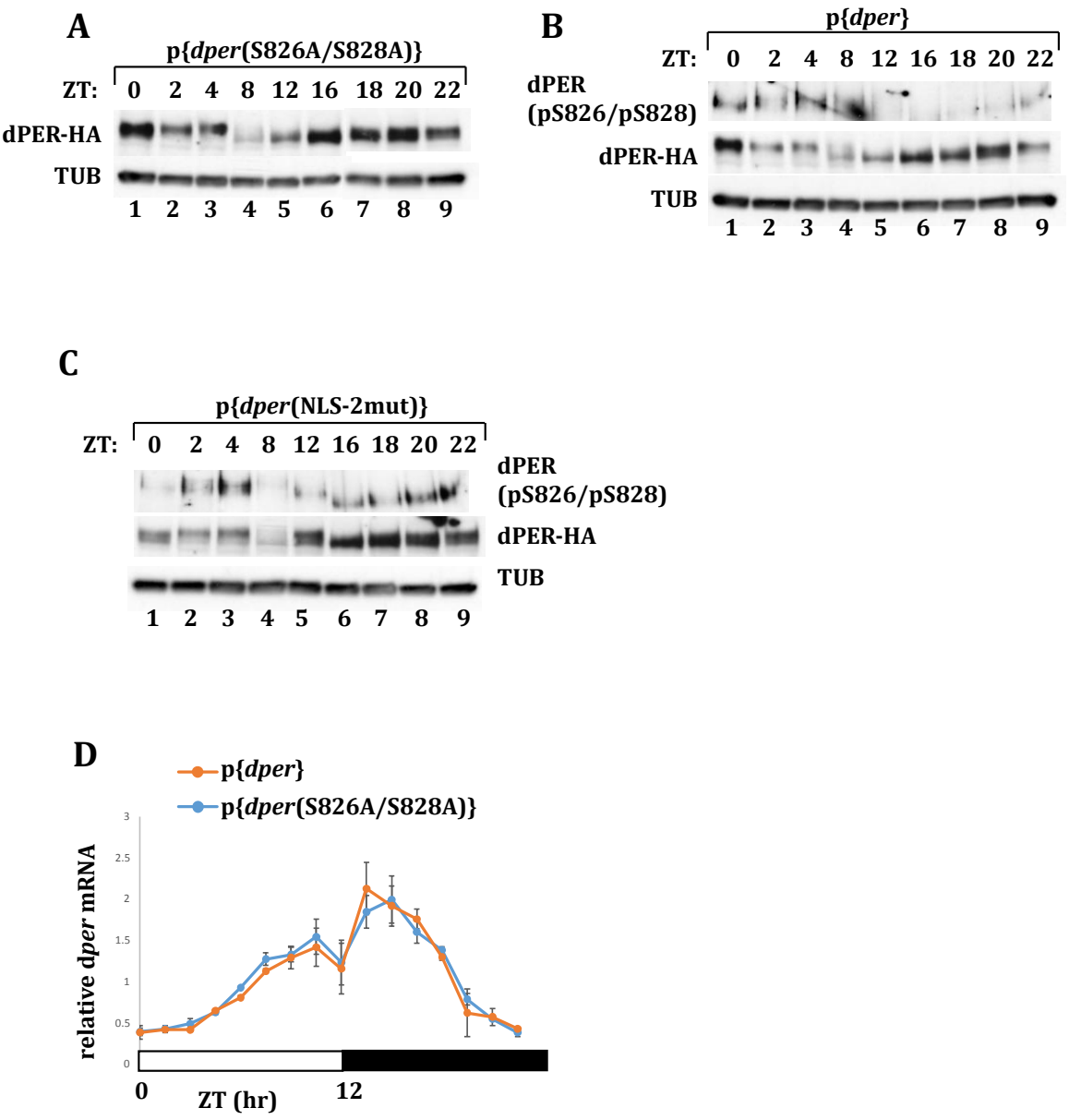

Figure 2.2. Transgenic flies harboring mutations at S826/S828 or NLS-2 region on dPER display similar daily profiles of *dper* protein and mRNA oscillations compared to wild type controls.

A, B, C, Adult flies from p{*dper*(S826A/S828A)} (A), p{*dper*} (B), p{*dper*(NLS-2mut)} (C), were collected at the indicated times in LD. Head extracts were either directly resolved by 4-15% SDS-polyacrylamide gels and blotted in the presence of anti-HA or anti-Tubulin

Figure legend of figure 2.2 continued

antibodies (A), or first subjected to IP with anti-HA beads (B, C) followed by the analysis of immune complexes by resolving on either 6% SDS-PAGE and immunoblotted with anti-pS826/pS828 antibody or by 4-15% gradient gels and immunoblotted with anti-HA or anti-tubulin antibodies. ***D*****,** Daily *dper* mRNA cycling from head extracts of p{*dper*}, p{*dper*(S826A/S828A)} flies. Data from at least two independent experiments were pooled to get the average profiles shown (for each value, SEM is shown).

for dPER(S826A/S828A) and wild type dPER (Figure S2.2A). In addition, dPER and dPER(S826A/S828A) have virtually identical stabilities when measured in S2 cells in the presence of cycloheximide to block *de novo* protein synthesis (Figs. S2.2B and C). Together, our results indicate that phosphorylation at Ser826 and Ser828 have little to no effects on dPER stability or its overall global phosphorylation program. These findings are starkly different from other characterized phospho-sites on dPER that are phosphorylated by DBT which have significant effects on stability, temporal phosphorylation or both [34, 38, 40, 41, 93].

A recent study using mass spectrometry and phosphatase inhibitors to identify phosphorylation sites on dPER expressed in S2 cells investigated a different but somewhat overlapping *dper* mutant (T808/S815/S826) and did not find effects on behavioral periods (they did not include S828, which might explain the smaller effects on behavioral periods) [41]. In addition, when they tested mutants in these phospho-sites in S2 cells, they did not observe effects on stability or hyper-phosphorylation. However, they did note that a dPER-S826A mutant has significantly less repressor function when evaluated by the standard S2 cell assay of dCLK-mediated transcription of a *per-luciferase* (*per-luc*) reporter. Likewise, we obtained a similar result when we used the smaller dPER(513-1224) fragment (Figure 2.1E) in combination with the S826A/S828A mutations. dPER(513-1224/S826A/S828A) is about 20-30% less efficient in repressing dCLK-mediated transcription but greater inhibition is observed with the mutant version containing a heterologous NLS [dPER(513-1224/S826A/S828A)-NLS], suggesting phosphorylation at Ser826 and/or Ser828 promotes nuclear localization and hence dPER repressor function (Figure S2.2D). However, analysis of the *dper* mRNA daily rhythm using 1.5 hr time points showed nearly identical curves for p{*dper*} and p{*dper*(S826A/S828A)} flies (Figure 2.2D), suggesting that *in vivo* phosphorylation of S826/S828 has minimal effects on the timing of dPER nuclear entry (or its repressor potential). Taken together, our results

and those of Garbe et al. (2013) indicate that although phospho-sites in around the vicinity of the NLS-2 region can affect the nuclear localization of dPER in S2 cells, they have little effect on dPER stability, temporal phosphorylation and repressor function, raising suspicion that these phospho-sites do not affect dPER nuclear translocation in flies.

Mutations that block phosphorylation at Ser826/828 and impair the NLS function of NLS-2 do not affect timing of dPER nuclear entry

To test if phosphorylation of S826/828 modulates dPER nuclear localization *in vivo* we focused on the small ventro-lateral neurons (s-LNvs), which are key pacemaker neurons in the adult brain that drive circadian behavior (reviewed in, [53]). The majority of s-LNvs express the circadian relevant neuropeptide pigment dispersing factor (PDF), which can be used as a convenient cytoplasmic marker for these cells. In agreement with other studies, wild type dPER transitions from mostly cytoplasmic at ZT18 (characterized by 'doughnut' staining of dPER), followed by mixed cytoplasmic/nuclear at ZT19/20 to predominately nuclear by ZT21 (characterized by punctate staining of dPER) (Figs. 2.3A and B) [85, 104]. Our results clearly indicate that the nuclear entry time of dPER is indistinguishable in p{*dper*(S826A/S828A)} flies compared to their wildtype counterparts (Figs. 2.3A and B).

Based on these results we wondered if NLS-2 actually contributes to the nuclear localization of dPER in flies. To this end, we generated transgenic flies expressing a *dper* mutant with the same alterations in consensus basic residues that were previously shown to impair the nuclear localization function of NLS-2 in S2 cells (i.e., K822A/R823A/K825A/K837A; herein referred to as NLS-2mut) [8]. Flies expressing *dper*(NLS-2mut) manifest robust behavioral rhythms that are 2 hr longer (Tables 2.1 and S2.1). The dPER(NLS-2mut) protein undergoes daily cycles in abundance and phosphorylation that are similar to but not identical with those observed for wild type dPER

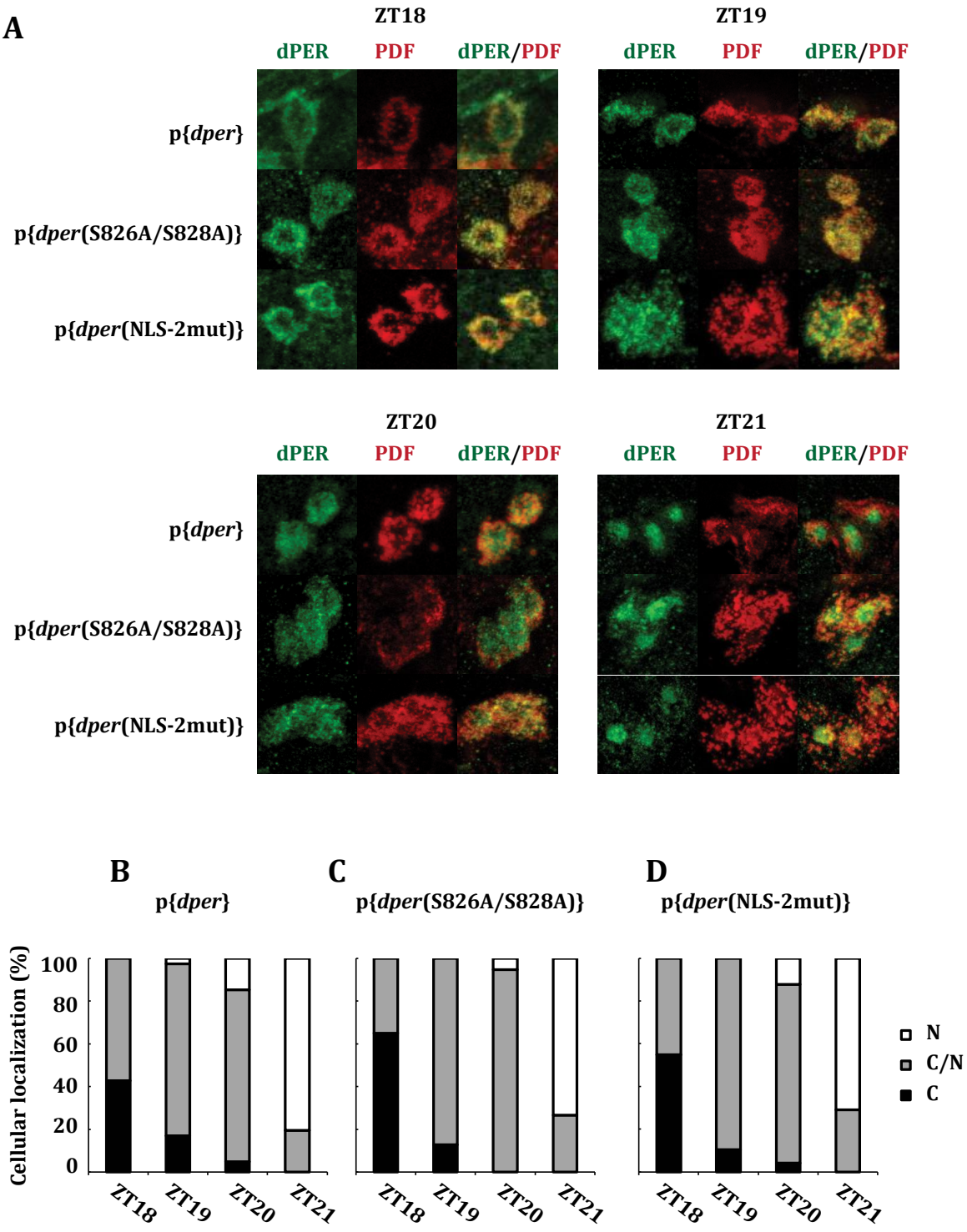

Figure 2.3. Mutations at S826/S828 or NLS-2 do not affect the timing of dPER nuclear entry in key brain pacemaker neurons.

Figure legends of figure 2.3 continued

A*,** Adult flies expressing wild type or mutant *dper* versions (indicated at left of panels) were collected at the indicated times in LD (top of panels) and isolated brains processed for whole mount immunohistochemistry. Representative images of s-LNvs from each genoytype are shown. dPER staining is shown in green, whereas PDF, which serves as a cytoplasmic marker for s-LNvs, is shown in red. ***B, C, D, For each genotype the subcellular localization was determined for ~30 s-LNvs from ~10 brains in two independent experiments.

(Figure 2.2, compare panels B and C). Similar to results obtained in S2 cells, phosphorylation of Ser828/828 can occur when 'inactivating' NLS-2 activity (Figs. 2.1E and 2.2C, top panel). However, phosphorylation of S826/828 occurs earlier in a daily cycle in p{*dper*(NLS-2mut)} flies; e.g., phosphorylation is clearly visible at ZT16 (Figure 2.2C, lane 6), suggesting that impairing the 'activity' of NLS-2 enhances S826/828 phosphorylation. These results and those based on the Ser to Ala replacements, raise the possibility that higher than normal levels of S826/S828 phosphorylation lengthens behavioral rhythms, whereas reductions are associated with faster rhythms. However, when we combined phospho-site mutants in S826, S828 or both with the NLS-2mut, the resulting flies had behavioral periods 2 hr longer then wild type controls and identical to that of the NLS-2mut (Table S2.1), suggesting that the NLS-2 region might have functions independent from and/or downstream to phosphorylation at Ser826/828. Future work will be required to better understand the possible interaction between the phosphorylated state at Ser826/828 and the function of NLS-2.

Surprisingly, dPER(NLS-2mut) shows the same timing of nuclear entry in the s-LNvs as wild type dPER and dPER(S826A/S828A) (Figure 2.3). Thus, despite the 3 hr difference in behavioral periods between p{*dper*(S826A/S828A)} and p{*dper*(NLS-2mut)} flies, the nuclear entry time of dPER is the same (Figure 2.3B). Although we did not perform an extensive study of other circadian pacemaker neurons in the brain, we did not detect differences in the temporal pattern of dPER nuclear accumulation in other clock cells when comparing p{*dper*}, p{*dper*(S826A/S828A)}, or p{*dper*(NLS-2mut)} flies (data not shown). While we cannot rule out the possibility that NLS-2 functions as a *bona-fide* dPER NLS in flies, at best it plays a minimal role in determining when dPER translocates to the nucleus. Indeed, an earlier report provided evidence for a functional NLS in the N-terminus of dPER [86], suggesting multiple and possibly redundant nuclear localization signals in dPER. Therefore, while blocking phosphorylation at Ser826/828 or altering

NLS-2 function leads to modest changes in the lengths of behavioral periods, the molecular underpinnings are not related to changes in dPER nuclear entry and currently remain elusive.

Phosphorylation of Ser826/828 is enhanced by light and attenuated by TIM

While the combined behavioral and molecular analysis might suggest that phosphorylation of S826 and S828 have minimal effects on the circadian timing system we were intrigued by the kinetics of phosphorylation at these sites in flies. Because phosphorylation of S826/828 peaks in the early morning (Figs. 2.1B and 2.2B), this raised the possibility that it is stimulated by light. To test this idea we entrained wild type p{*dper*} flies to several days of LD and to one group we advanced the timing of lights-on by 2 hr to ZT22. Remarkably, the staining intensity of phosphorylation at S826/828 rapidly increased in the presence of premature exposure to nocturnal light (Figure 2.4A, compare lanes 3 and 2, and 5 and 4). That the clock mechanism correctly responded to the premature start of the light phase was verified by measuring TIM levels, which is rapidly degraded by photic stimulation (Figure 2.4A, e.g., compare lanes 2 and 3).

We further analyzed the photosensitivity of S826/828 phosphorylation by using flies whereby CRY function is abolished (cry^{01}) [95, 105]. CRY is the main circadian photoreceptor in *Drosophila* and in cry^{01} mutants TIM is not degraded in the presence of light (e.g., Figure 2.4B) and circadian photosensitivity is strongly attenuated [95, 105]. Remarkably, even in the presence of light there was little to no phosphorylation of S826/828 in cry^{01} flies (Figs. 2.4B and C). Other dPER phospho-sites that we analyzed using phospho-specific antibodies did not show rapid light-mediated increases in staining intensities (data not shown), revealing that the phospho-occupancy at S826/828 is specifically responsive to photic signals. Because light triggers the rapid degradation of TIM and TIM is a key binding partner of dPER, we used S2 cells to test if TIM might

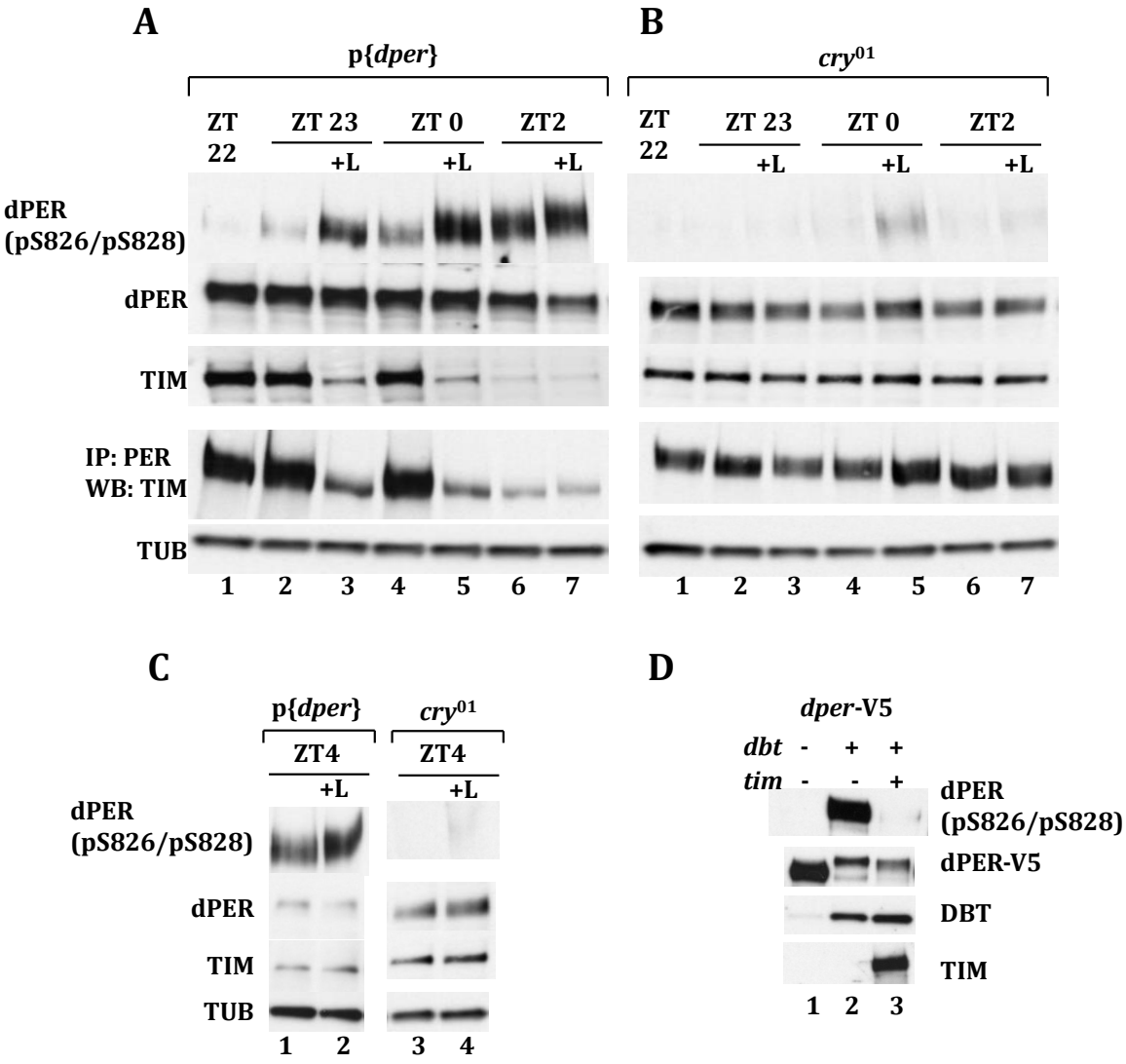

Figure 2.4. Phosphorylation of S826/S828 is enhanced by light, dependent on CRY and blocked by TIM.

Wild type control adult flies (A-C) or *cry*^{01} mutant flies (B-C) were entrained to 4 days of 12:12LD. During the last dark phase of LD, the lights-on time was advanced by 2 hr to ZT22 for one group of flies (+L), whereas lights-on remained at ZT24 for the other group. Flies were collected at the indicated times in LD (relative to the control group with lights-on at ZT24), head extracts prepared and a small amount saved for direct analysis by 4-15% SDS-PAGE followed by immunoblotting with anti-dPER, anti-TIM or anti-TUB

Figure legends of figure 2.4 continued

antibodies. To detect phosphorylation at S826/S828 using the anti-pS826/pS828 antibodies, the rest of the extracts were first subjected to IP with anti-dPER GP-73 antibody in the presence of sepharose beads, and immune complexes recovered. The immune complexes were split and resolved by 6% SDS-PAGE. One part was analyzed by immunoblotting in the presence of anti-pS826/p828 antibodies, whereas another part in the presence of anti-TIM antibodies (panel A, IP: PER, WB: TIM). ***D*****,** S2 cells expressing pAct-*dper*-V5/His with (+) or without (-) pAct-*tim*-HA and pMT-*dbt*-V5/His were treated for 4 hours with the proteasome inhibitor MG132 and the protein synthesis inhibitor cycloheximide after 18 hours of *dbt* induction. Extracts were immunoprecipitated with anti-V5 beads and analyzed by immunoblotting in the presence of anti-pS826/pS828 antibody (6% gels) or anti-TIM, anti-V5 or anti-DBT antibody (4-15% gradient gels).

attenuate phosphorylation of dPER at S826/828. Indeed, in the presence of TIM there was little phosphorylation of S826/828 by DBT (Figure 2.4D). Although earlier studies showed that TIM can slow down the DBT-mediated hyper-phosphorylation of dPER, it does not block it [106, 107], further demonstrating that S826/828 are particularly sensitive to regulation by TIM. Our results identify phospho-sites on dPER that are highly responsive to photic cues and strongly suggest that the binding of TIM to dPER protects S826/828 from phosphorylation by DBT.

Preventing phosphorylation at Ser826/828 impairs proper entrainment of behavioral rhythms to daily light-dark and temperature cycles

Because of TIM's light sensitivity and its role in photic entrainment we wondered if flies expressing the dPER(S826/828A) mutant have defects in entrainment. Under standard 12hr:12hr light/dark cycles, wild type *D. melanogaster* exhibit two main clock-controlled bouts of activity, a 'morning' peak centered on ZT0 and an 'evening' peak centered on ZT12 that begin to rise in activity levels prior to the light/dark transitions (Figure 2.5A) (reviewed in, [96]). In addition to the anticipatory morning and evening activity peaks, *D. melanogaster* routinely exhibit transient increases in activity at the light/dark transitions, termed 'startle' or masking responses. Finally, the bimodal pattern of activity continues in constant dark conditions whereby the evening peak persists and the morning peak becomes less apparent (Figure 2.5A).

To investigate if blocking phosphorylation at S826/828 or mutations in NLS-2 affect photic entrainment we measured the activity profiles of flies exposed to several days of LD. To enhance detection of possible entrainment defects we used the standard 12:12LD cycle in addition to a short (9:15LD) and long (15:9LD) photoperiod. The alignment of the morning and evening activity peaks relative to lights-on and lights-off changes as a function of photoperiod [108]. Under the short photoperiod, the timing of evening activity

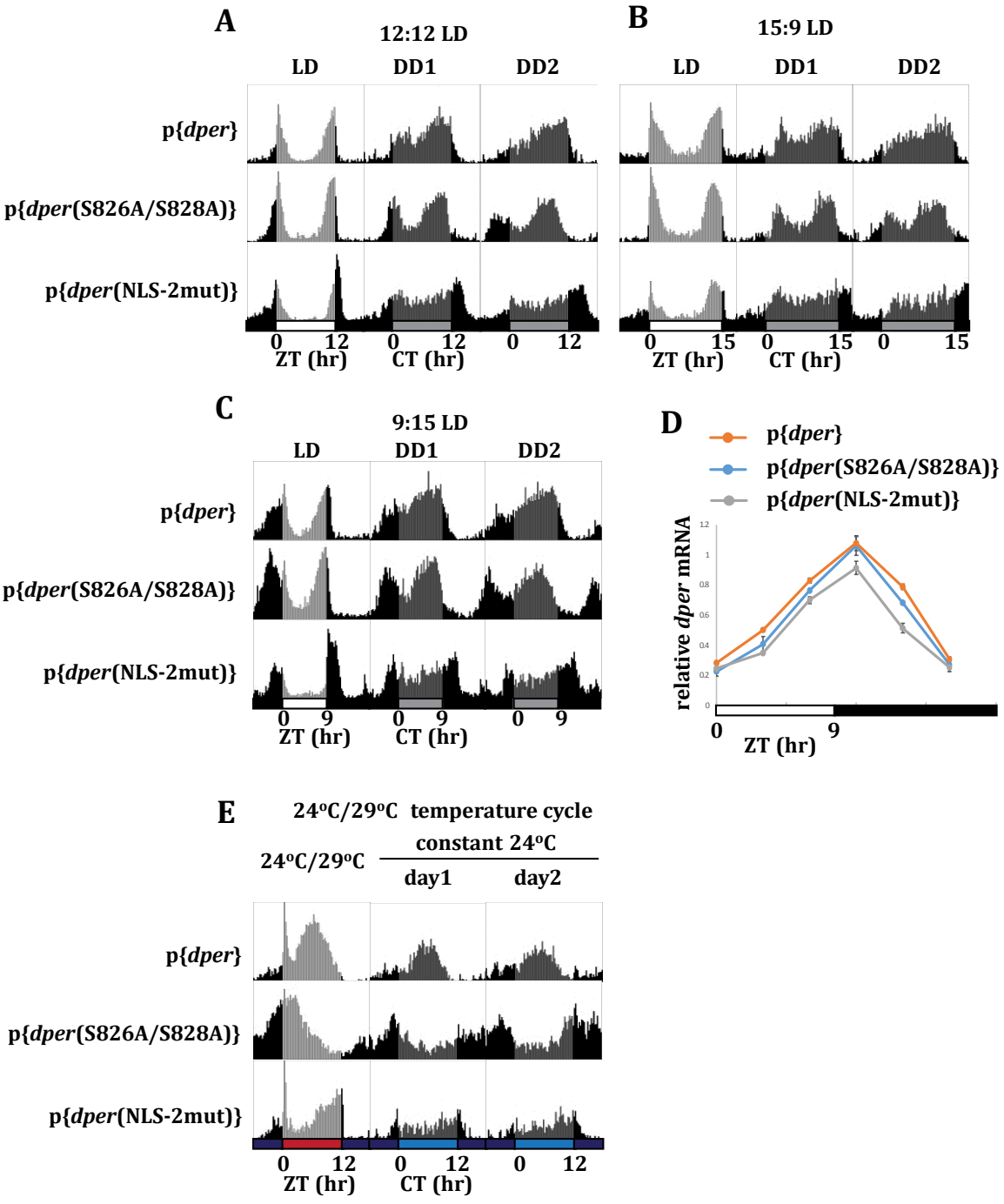

Figure 2.5. Blocking phosphorylation of S826/S828 or mutating NLS-2 lead to circadian entrainment defects to both photic and thermal cues.

A-D, Transgenic adult flies carrying wild type or mutant versions of *dper* (as indicated) were exposed to 5 days of LD cycles at the indicated photoperiod (i.e., 12:12, 15:9 or 9:15) (A-D) followed by 7 days in complete darkness (DD). ***E,*** Transgenic adult flies carrying

Figure legend of figure 2.5 continued

wild type or mutant versions of *dper* (as indicated) were exposed to 5 days of a temperature cycle in constant darkness followed by 7 days at 24^{o}C. Activity histograms are shown for the last entrainment cycle and the next 2 days in free-running conditions (A, B, C, E). Shown are the daily levels of *dper* mRNA from the indicated transgenic lines collected during the last LD cycle following entrained to 9:15LD.

in p{*dper*(S826A/S828A)} flies was similar to that of wild type controls but the morning activity is about 1 hr earlier. This is quite unusual because *dper* mutants that shorten behavioral rhythms show a much stronger effect on the timing of the evening bout, causing it to occur earlier, with less effect on the morning peak (e.g., [38, 103, 109-112]). During a long photoperiod we could not detect the start of the morning peak (as it likely begins after the light-on startle response) but the timing of the evening activity bout was again similar between p{*dper*} and p{*dper*(S826A/S828A)} flies (Figure 2.5B).

Abnormal activity patterns were also observed for the p{*dper*(NLS-2mut)} flies. Due to the longer periods we expected that the timing of the evening peak would be later for p{*dper*(NLS-2mut)} flies, which is was under the shorter photoperiods (9:15 and 12:12). However, in the long photoperiod the timing of the evening activity bout was almost identical to that of the wild type control and p{*dper*(S826A/S828A)} flies (Figs. 2.5A-C). The period lengths of the three genotypes following entrainment to the short and long photoperiods were similar to those at the standard photoperiod (Table S2.1). Clearly, the results are complex because unusual daily activity patterns for p{*dper*(S826A/S828A)} and p{*dper*(NLS-2mut)} flies are only readily observed under certain photoperiods. While future work will be required to better understand the photoperiod effect, our results indicate that phosphorylation of Ser826/828 and NLS-2 are required for normal adaptation of behavioral rhythms to daily light/dark cycles, defects that cannot be easily explained by changes in behavioral periods.

Remarkably, although p{*dper*}, p{*dper*(S826A/S828A)} and p{*dper*(NLS-2mut)} flies have periods that differ over a range of 3 hr and exhibit very different entraining patterns in 9:15LD (Figure 2.5C), their *dper* mRNA cycles are essentially identical (Figure 2.5D). This result is similar to the more extensive molecular studies performed under 12:12LD (Figure 2.2D), further reinforcing the notion that mutations in the S826/828 phospho-sites or NLS-2 have little effect on the core clock mechanism despite their effects

on circadian periodicity and entrainment. To the best of our knowledge, *dper* mutants that cause changes in behavioral periods always exhibit some alterations in the daily profiles of *dper* protein and/or mRNA.

We wondered if entrainment defects might be more easily detected using daily temperature cycles, which are weaker entraining agents compared to light/dark cycles. To this end we exposed flies to a standard temperature cycle of 5 cycles of 12 hr at 24ºC/12 at 29ºC (TC) followed by constant temperature (24ºC) in complete darkness. During TC, wild type flies exhibit a major 'evening' peak around the middle of the day with a smaller morning component around ZT0 (start of the warm phase), whereby the major activity bout continues in constant temperature conditions (Figure 2.5E) (e.g., [113]). In stark contrast, p{*dper*(S826A/S828A)} flies manifest one major activity bout centered around ZT0, peaking about 6 hr earlier compared to the wild type control. This dramatically advanced activity pattern continued in constant temperature conditions demonstrating the abnormal phasing is not an altered reaction to changes in temperature but a severe entrainment defect. The *dper*(NLS-2mut) also showed a very different distribution of activity in TC with a very delayed rise in activity prior to the transition from the thermo-phase to the cryo-phase (Figure 2.5E). The free-running periods of all three genotypes following TC were similar to those observed following LD (Table S2.1), indicating that the differences in the lengths of behavioral periods are stable features of the circadian timing system in these flies. Thus, the 3 hr difference in behavioral periods between p{*dper*(S826A/S828A)} and p{*dper*(NLS-2mut)} flies cannot explain the nearly 10 hr difference in the phases of their major activity bout in TC, indicating that entrainment defects are not limited to photic signals.

To further explore defects in entrainment we used the classic approach of measuring shifts in the phase of circadian behaviors elicited by exposure to short light pulses in the dark. Light pulses in the early night lead to phase delays in the circadian

timing system, whereas the same treatment in the late night result in phase advances, yielding a phase response curve (PRC) [114]. Intriguingly, although blocking phosphorylation at S826/828 did not affect the light-PRC, the magnitude of phase shifts in the NLS-2mut flies was strongly attenuated (Figure S2.3), and remarkably reminiscent of *cry* mutant flies [105]. Together, our results indicate that a specific region of dPER that includes phosphorylation of S826/828 and NLS-2 is critical for the ability of the circadian timing system to respond to photic and thermal cues, revealing an unprecedented non-speed control role for dPER in entrainment.

DISCUSSION

Time-of-day specific phosphorylation of one or more key clock proteins lies at the biochemical heart of the timing mechanism underlying circadian rhythms [29, 30, 32, 81]. In animals, a complex phosphorylation program drives daily cycles in the levels of PER proteins that are central to setting clock speed. This posttranslational regulatory mechanism intertwines with cyclical gene expression because PER proteins interact with central clock transcription factors in the nucleus to seed repressor complexes. By regulating PER stability and cytoplasmic-nuclear localization, phosphorylation plays a key role in restricting the duration and timing of when PER proteins engage in transcriptional repression. Indeed, many of the phosphorylation sites that have been mapped on PER proteins have been ascribed to primary effects on stability and/or sub-cellular localization, with some possibly related to repressor potency [34, 38, 40, 41, 93]. We now provide evidence for a novel function for PER phosphorylation in entrainment to daily light-dark and temperature cycles that remarkably does not appear to involve significant changes in the clockworks. Our findings suggest a model whereby factors that trigger TIM degradation (most notably light) stimulate phosphorylation of Ser826/828 by DBT, an event that is somehow part of the entrainment mechanism that ensures the proper

alignment of behavioral rhythms with local time. Moreover, although we did not detect a role in nuclear entry for the putative NLS that contains Ser826/828, this region strongly modulates circadian photosensitivity. Together, our findings identify a region on dPER that is exquisitely sensitive to photic signals and reveal a surprisingly major role for PER proteins in circadian responses to environmental cues.

To date, all the phospho-sites that we tested in flies using phospho-specific antibodies have verified that the phosphorylation events occurring in *Drosophila* S2 culture cells using recombinant dPER also occurs in flies [34, 38, 40]. Indeed, using phospho-specific antibodies that recognize the doubly phosphorylated pS826/pS828, we confirmed that Ser826/828 residues are phosphorylated *in vivo* (Figs. 2.1, 2.2, S2.1 and S2.2). Moreover, these studies identify DBT as the kinase most likely directly phosphorylating Ser826, Ser828 or both (Figs. 2.1 and S2.1). DBT is the major kinase driving daily cycles in dPER abundance and its slow conversion from newly synthesized non/hypo-phosphorylated isoforms in the cytoplasm during the early night to hyper-phosphorylated variants in the nucleus during the early day that are rapidly targeted for degradation, which initiates another round of dCLK-CYC-mediated transcription. Many of the phospho-sites and/or phospho-clusters that regulate dPER levels lead to large effects on the speed of the clock [34, 38, 40, 41, 93]. However, although p{*dper*(S826/828A)} flies exhibit shorter periods in behavioral rhythms, the effects are modest and in the range of approximately 1 hr. An earlier report that analyzed a different but somewhat overlapping *dper* mutant (T808/S815/S826) did not find effects on behavioral periods [41]. The modest changes we found on behavioral periods are consistent with the little to no effects of the dPER(S826/828A) mutant on 1) stability/levels in S2.2, 2) temporal changes in dPER phosphorylation and levels in flies, and 3) daily cycles in *dper* mRNA levels. Thus, although S826/828 are phosphorylated by DBT and this kinase has a major effect on

dPER stability, our findings identify DBT-dependent sites that play at best a minimal role in regulating dPER levels.

Less expected perhaps, was the finding that phosphorylation at S826/828 does not modulate the timing of dPER nuclear entry in key pacemaker neurons (Figure 2.3). Prior work has shown that DBT can influence the accumulation of dPER in the nucleus, however this is likely a consequence of primary effects on stability [101]. Nonetheless, phospho-sites on dPER have been found that appear to have primary effects on regulating the timing of when it translocates to the nucleus, which normally happens in the mid-night between ZT19-20 for the s-LNvs, the key circadian pacemaker neurons in the brain driving activity rhythms [39, 40]. These include CK2 and SGG dependent sites, although none of these regions have recognizable NLS or nuclear export signal (NES). In contrast, prior work showed that NLS-2 functions in S2 cells and that mutations in consensus sequences abolishes this function [8]. Because we did not observe any effects of Ser826/828 on dPER nuclear translocation (Figure 2.3), we evaluated the same NLS mutations in flies, which yielded 2 hr longer periods but no effects on the timing of dPER nuclear entry even when compared to the Ser826/828 flies that have 3 hr shorter periods (Figure 2.3 and Table 2.1). Thus, although we cannot rule out if this putative NLS is functional in this capacity, it is unlikely to have a major contribution on timing when dPER enters the nucleus.

The kinetics of phosphorylation at S826/828 is also consistent with a role subsequent to dPER nuclear entry. Phosphorylation atS826/828 is first detected at approximately ZT20 and peaks around ZT4, even though total dPER levels are very low during the early day (Figs. 2.1 and 2.2). This time-course seemed to parallel the daily decline in TIM levels, which is enhanced by light. Indeed, we show that nocturnal light, which advances the degradation of TIM, is accompanied by rapid and sustained increases in the levels of S826/828 phosphorylation but not in the cry^0 mutant (Figure 2.4).

Moreover, using S2 cells we show that phosphorylation at S826/828 is blocked by TIM (Figure 2.4D). Because the rapid degradation of TIM is the initial clock-relevant photic response we wondered if phosphorylation of S826/828 affects entrainment to daily light-dark cycles. Thus, we subjected p{*dper*(S826A/S828A} flies to a range of photoperiods and observed that the morning or evening bouts of activity are earlier compared to wildtype controls, which at first glance is generally consistent with the shorter free-running period. However, to our knowledge all clock-gene mutants, especially those of *dper*, with robust but short period behavioral rhythms exhibit earlier evening bouts of activity with more modest effects on the timing of the morning component (e.g., [38, 103, 109-112]). This is in sharp contrast with the behavior of p{*dper*(S826A/S828A)} flies in the shorter photoperiods, especially 9:15LD, where the morning activity was significantly earlier yet no shift in the onset of evening activity (Figure 2.5C). De-synchrony between the morning and evening bouts of activity strongly suggests that, at least under certain LD conditions, phosphorylation at Ser826/828 is required for proper alignment of behavioral rhythms to local time.

That phosphorylation of S826/828 on dPER is important for proper entrainment is further supported by studies using daily temperature cycles (Figure 2.5E). The activity profile for p{*dper*(S826A/S828A)} flies is dramatically different, manifesting one major activity bout that is centered around the cold-to-warm transition at ZT0 and occurs about 6 hr earlier compared to the widltype controls. This very advanced pattern continues under constant temperature conditions following TC indicating that it is not a reaction to changes in temperature but rather a defect in entrainment. These results indicate that phosphorylation at Ser826/828 is not only required for photic entrainment but also for correctly interpreting thermal cues.

Defects in entrainment were also observed in the p{*dper*(NLS-2mut)} flies. A surprising result was that the evening activity bout occurred about slightly earlier

compared to the wildtype controls under the long photoperiod, despite the 2 hr longer period for the mutant (Figure 2.5C). At shorter photoperiods the evening peak was delayed for p{*dper*(NLS-2mut)} flies, which would be the expected result for a long period mutant. However, the nuclear entry time of dPER in the key pacemaker cells driving clock speed was similar and unaffected in p{*dper*(NLS-2mut)} and p{*dper*(S826A/S828A)} flies, demanding an explanation beyond clock speed. In addition, the peak of activity in TC is about 10 hr different between p{*dper*(NLS-2mut)} and p{*dper*(S826A/S828A)} flies, which cannot be easily reconciled with their 2.5 hr difference in free-running periods. Moreover, despite the substantial differences in free-running periods and daily activity patterns for p{*dper*(S826A/S828A} and p{*dper*(NLS-2mut)} flies under the short photoperiod (Figure 2.5C), their *dper* mRNA cycles were identical (Figure 2.5D), further supporting a novel role for *dper* function that is not linked to modulating the pace of the clock. Because a combination of the NLS-2 and the S826/828A mutations results in flies with long periods equal to those of the NLS-2 mutant, it is possible that the readout from the phospho-occupancy of S826/828 is mediated via the NLS module.

Besides entrainment to daily light-dark and temperature cycles, the dPER(NLS-2mut) revealed a strong defect in circadian responses to acute photic cues (Figure S2.3). Remarkably, the p{*dper*(NLS-2mut)} exhibits a very attenuated PRC, suggesting highly impaired circadian photosensitivity. Indeed, the light PRC for p{*dper*(NLS-2mut)} flies is highly reminiscent of that obtained with *cry* mutants that are largely circadian blind for light [105]. Although the light-PRC for p{*dper*(S826/828A)} flies was similar to that of wildtype flies, it is possible that sub-saturating light-pulses will show a defect. In any event, our results reveal an unprecedented role for dPER via specific phosphorylation sites and surrounding sequences on entrainment to environmental signals. Although the mechanism is not clear, our studies suggest that rapid changes in TIM levels by external modalities such as photic signals leads to changes in the phospho-occupancy of S826/828

that might function together with surrounding sequences in NLS-2, contributing to proper phase alignment of behavioral rhythms to local time, suggesting that the Ser826/828 phospho-sites and NLS-2 function in concert as a dedicated ‘entrainment module’. Because we did not find significant effects of this module on the intracellular clock mechanism, it might operate at the pacemaker cellular network level that is critical for generating behavioral rhythms [53]. Thus, PER is not only critical for setting the speed of the clock but also for interpreting environmental signals, revealing a surprisingly complex multi-tasking circadian workhorse that operates via distinct functional modules, many of which seem to incorporate time-of-day-specific phosphorylation events as regulatory features.

Contributions: J. Chiu identified potential phospho sites on PER in a previous study (Chiu, 2008). All the experiments presented here were performed by Evrim Yildirim.

SUPPLEMENTARY TABLES AND FIGURES FOR CHAPTER 2

Table S2.1: Behavioral rhythms for mutant *dper* transgenics and controls[a]

Genotype[b]	Period (hr ±SEM)	Power[c]	Rhythmicity (%)[d]	Total flies[e]
wper^0; *per*$^+$-HA (S826A) (1M)	23.6±0.09	119.3	96.8	32
wper^0; *per*$^+$-HA (S826A) (2M)	22.9±0.09	98.4	78.1	32
wper^0; *per*$^+$-HA (S826A) (4M)	22.7±0.1	105.2	95.8	32
wper^0; *per*$^+$-HA (S826A) (6M)	22.9±0.05	139.7	87.5	32
***wper*^{0}; *per*$^+$-HA (826A) average**	**23.0±0.08**			
wper^0; *per*$^+$-HA (826D) (1M)	23.3±0.15	104	87.1	32
wper^0; *per*$^+$-HA (826D) (2M)	23.9±0.22	140.3	100	13
wper^0; *per*$^+$-HA (826D) (5M)	23.3±0.07	111.9	93.5	32
***wper*^{0}; *per*$^+$-HA (826D) average**	**23.5±0.16**			
wper^0; *per*$^+$-HA (S828A) (1M)	22.6±0.1	87.3	87.5	32
wper^0; *per*$^+$-HA (S828A) (4M)	22.9±0.31	92.2	83.3	32
wper^0; *per*$^+$-HA (S828A) (5M)	22.7±0.14	116.5	89.7	32
wper^0; *per*$^+$-HA (S828A) (7M)	22.4±0.05		93.5	32
***wper*^{0}; *per*$^+$-HA (S828A) average**	**22.6±0.18**			
wper^0; *per*$^+$-HA (S828D) (1M)	23.2±0.08	147.8	100	32
wper^0; *per*$^+$-HA (S828D) (3M)	23.2±0.09	145.8	96.9	32
wper^0; *per*$^+$-HA (S828D) (4M)	23.8±0.2	55.8	57.1	32
wper^0; *per*$^+$-HA (S828D) (5F)	24.8±0.1	116.8	100	32
***wper*^{0}; *per*$^+$-HA (S828A) average**	**23.7±.0.13**			
wper^0; *per*$^+$-HA (NLS-2mut /S826A/S828A) (2F)/-[f]	-	-	Arrhythmic	16
wper^0; *per*$^+$-HA (NLS-2mut /S826A/S828A) (2M)/-[f]	25.4±0.18	92.5	100	16
wper^0; *per*$^+$-HA (NLS-2mut /S826A/S828A) (4F)/-[f]	25.7±0.89	48.9	23.8	21
wper^0; *per*$^+$-HA (NLS-2mut /S826A/S828A) (1M)/-[f]	25.4±0.05	132.2	100	23
wper^0; *per*$^+$-HA (NLS-2mut /S826A/S828A) (1F)/-[f]	25.5±0.07	139.3	100	21
wper^0; *per*$^+$-HA (NLS-2mut) (1F)/-[f]	25.4±0.06	139.3	100	32
wper^0; *per*$^+$-HA (S826A/S828A) (1M)/-[f]	23.1±0.05	167.4	96.8	31
wper^0; *per*$^+$-HA (1M)/-[f]	24.3±0.13	139.5	100	27

[a] Young male flies were maintained at 25^{o}C and exposed to 5 days of 12:12 LD cycles followed by 7 days of DD

[b] Independent transgenic lines are designated by the numbers in parenthesis

[c] Power is a measure of the strength or amplitude of the rhythm in arbitrary units

[d] Percentage of flies showing locomotor rhythms with a power value of ≥10 and a width value of ≥2

[e] Total number of flies that survived until the end of the experimental period

[f] Flies carry only one copy of the transgene

Table S2.2: Locomotor activity rhythms for mutant *dper* transgenics and controls exposed to different photoperiods or temperature cycles as shown in Figure 5.

Genotype[a]	Photoperiod[b] or T-cycle[c]	Period (hr ±SEM)	Power[d]	Rhythmicity (%)[e]	Total flies[f]
wper^{0}; *per*$^{+}$-HA (1M)	9:15 LD	23.5±0.06	146.7	100	26
wper^{0}; *per*$^{+}$-HA (S826A/S828A) (1M)	9:15 LD	22.3±0.07	114.5	90	30
wper^{0}; *per*$^{+}$-HA (NLS-2mut) (1F)	9:15 LD	24.9±0.11	97.9	100	29
wper^{0}; *per*$^{+}$-HA (1M)	15:9 LD	23.3±0.06	125.8	100	28
wper^{0}; *per*$^{+}$-HA (S826A/S828A) (1M)	15:9 LD	22.6±0.41	109.7	87.5	31
wper^{0}; *per*$^{+}$-HA (NLS-2mut) (1F)	15:9 LD	25.2±0.09	93.9	87.1	31
wper^{0}; *per*$^{+}$-HA (1M)	24^{o}/29^{o}C	23.3±0.16	77.4	93.5	30
wper^{0}; *per*$^{+}$-HA (S826A/S828A) (1M)	24^{o}/29^{o}C	22.1±0.07	83.2	87.5	24
wper^{0}; *per*$^{+}$-HA (NLS-2mut) (1F)	24^{o}/29^{o}C	24.4±0.08	41.9	50	26

[a] Independent transgenic lines are designated by the numbers in parenthesis
[b] Young male flies were maintained at 25^{o}C and exposed to 5 days of indicated LD cycles followed by 7 days of DD
[c] Young male flies were exposed to 5 days of 12 hr 24^{o}C and 12 hr 29^{o}C temperature cycles followed by 7 days of constant 24^{o}C
[d] Power is a measure of the strength or amplitude of the rhythm in arbitrary units
[e] Percentage of flies showing locomotor rhythms with a power value of ≥10 and a width value of ≥2
[f] Total number of flies that survived until the end of the experimental period

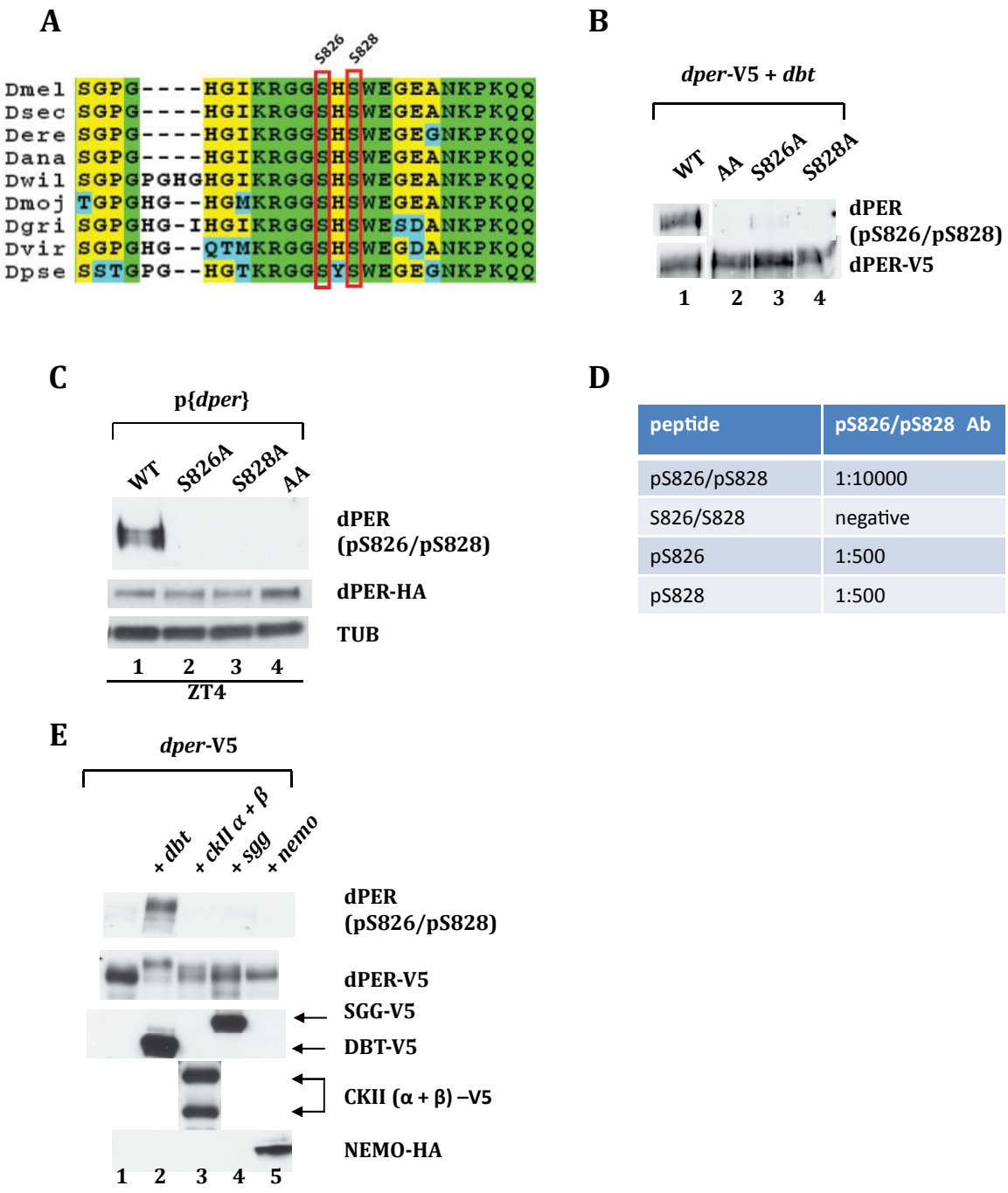

peptide	pS826/pS828 Ab
pS826/pS828	1:10000
S826/S828	negative
pS826	1:500
pS828	1:500

Figure S2.1. Characterization of a phospho-specific antibody that recognizes phosphor-sites S826 and S828 on dPER.

A, The NLS-2 region, including Ser826 and Ser828 are conserved in *Drosophila*. ***B,*** S2 cells were co-transfected with pMT-*dbt* and pAct-driven versions of *dper*-V5; wildtype, (WT); *dper*(S826A/S826A), (AA); *dper*(S826A), S826A; and *dper(*S828A), S828A. After

Figure legend of figure S2.1 continued

inducing *dbt* for 24 hr, cell extracts were either directly probed by immunoblotting for total dPER levels using anti-V5 antibodies, or subjected to immunprecipitation (IP) with anti-V5 antibody resins followed by immunoblotting in the presence of phospho-specific anti-pS826/pS828 antibodies. ***C,*** Transgenic adult flies of the indicated genotype (top panel) were collected at ZT4, head extracts prepared and a small portion immunoblotted in the presence of anti-HA antibody to detect total dPER levels (dPER-HA) or anti-tubulin antibodies as a loading control. The majority of the head extract was subjected to IP using anti-HA antibody resins and immunoblotted in the presence of phospho-specific anti-pS826/pS828 antibodies. ***D,*** Results of ELISA using a peptide that differed in phosphorylation at Ser826 and Ser828 of dPER. ***E,*** S2 cells were transfected with *dper*-V5 alone (lane 1) or co-transfected different pMT-versions of plasmids encoding clock relevant kinases (lanes 2-6, top of panels). After 24 hr post-induction, a small portion of the extract was directly analyzed by immunoblotting in the presence of anti-V5 or anti-HA antibodies to detect total dPER levels (dPER-V5), or the recombinant kinases. The rest of the extract was immunoprecipitated to recover dPER and immunoblotted in the presence of anti-pS826/pS828 antibody.

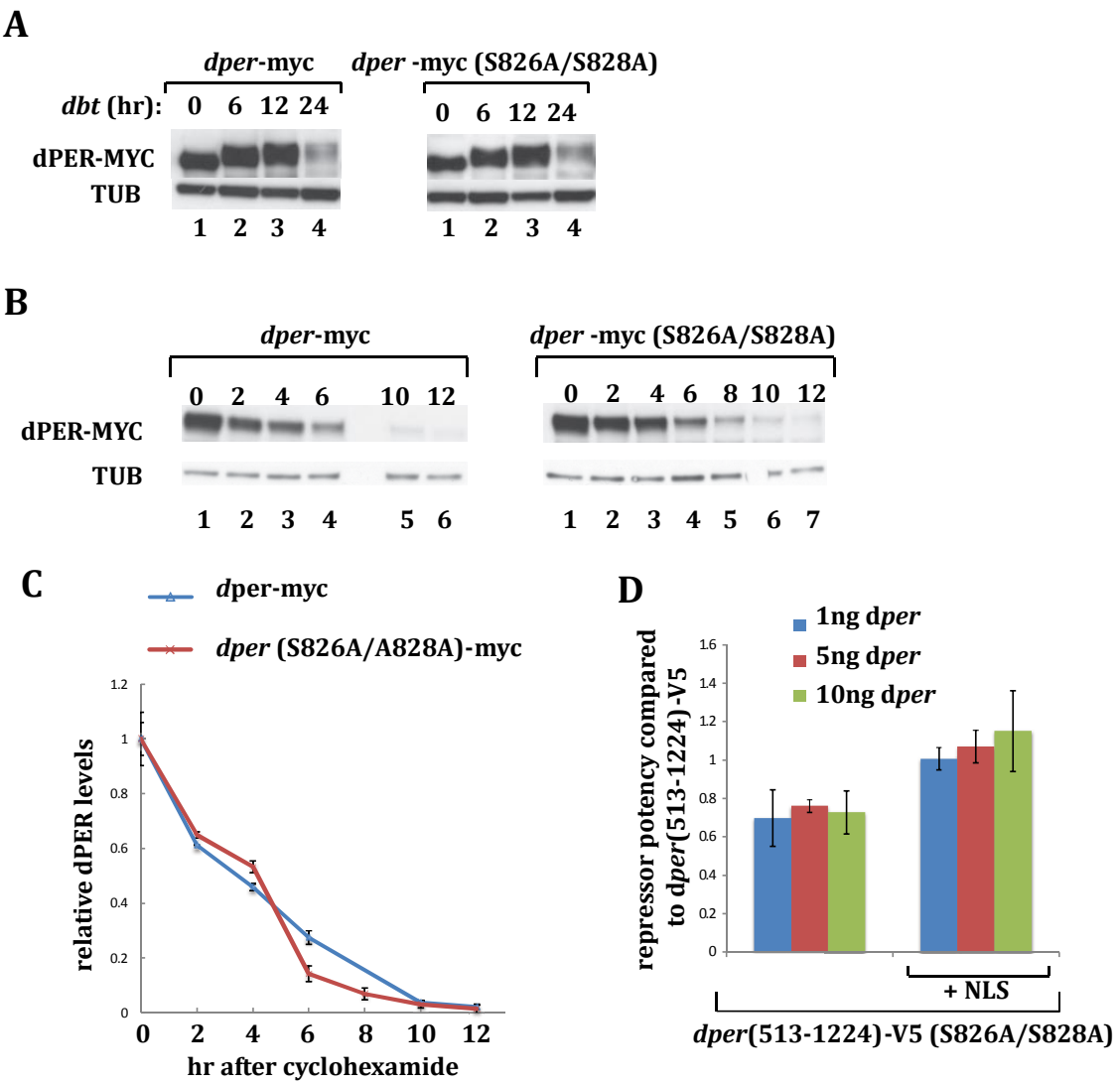

Figure S2.2. Blocking phosphorylation at S826/S828 has little to no effect on dPER stability but has modest effects on its repressor activity as measured in S2 cells.

A-C, Different versions of recombinant *dper-myc* plasmids were used to transfect S2 cells either with (A) or without (B, C) pMT-*dbt*. (A) Cells were harvested at the indicated times post-*dbt* induction and cell extracts probed by immunoblotting in the presence of anti-MYC antibodies (dPER-MYC) or anti-tubulin (TUB) antibodies. (B) S2 cells were treated with cycloheximide, collected at the indicated times (top, hr) and extracts subjected to immunoblotting the presence of either anti-MYC (dPER-MYC) or anti-tubulin (TUB) antibodies. (C) Quantification of dPER levels from several independent cycloheximide

Figure legend of figure S2.2 continued

experiments, as shown in panel B. D, dPER(S826A/S828A) is a weaker repressor of CLK-mediated transcription when assayed in S2 cells. Values shown were obtained by pooling results from several independent experiments.

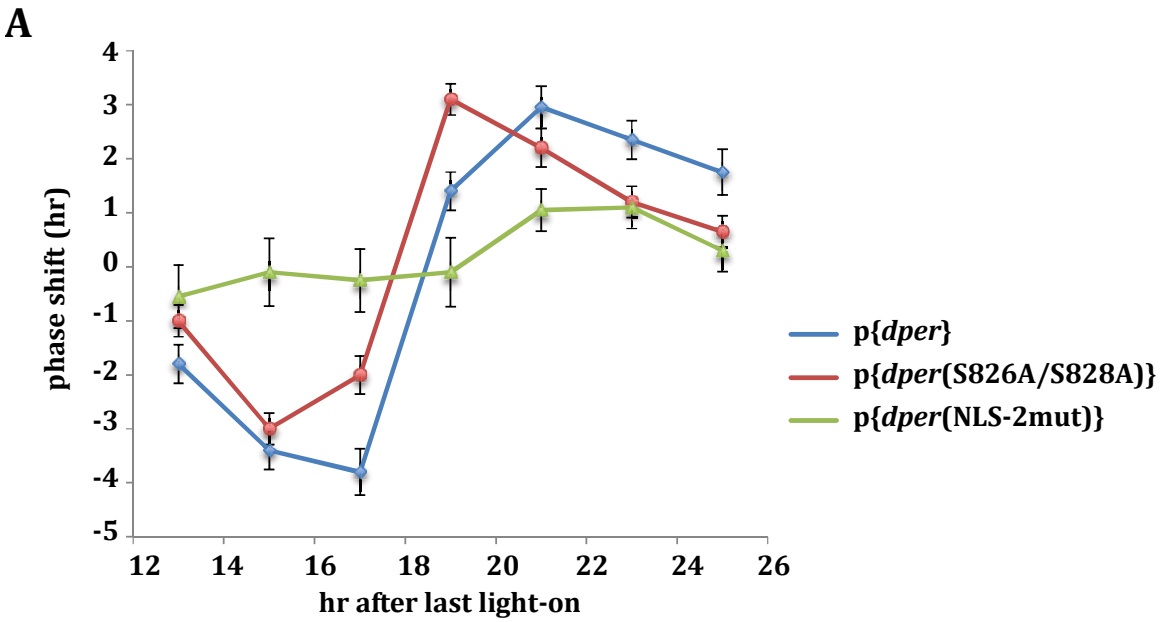

Figure S2.3. Highly attenuated light-PRC for flies expressing a dPER NLS-2 region. The indicated genotypes were entrained to 4 days of 12:12LD and on the last dark phase of LD, the lights were kept in constant darkness. Beginning in the last dark phase of LD different groups of flies were exposed to a short light-pulse at the indicated time; another group served as non-treated controls. For each genotype, shown are the differences in the phase of the daily activity rhythm between flies that were treated with light and control untreated flies. Advances are shown as positive numbers, whereas delays are shown as negative numbers. Values shown were obtained by pooling results from several independent experiments.

Chapter 3: Phosphorylation of a central clock transcription factor is required for thermal but not photic entrainment

(Euna Lee, Eun Hee Jeong, Hyun-Jeong Jeong, Evrim Yildirim, Jens T. Vanselow, Fanny Ng, Yixiao Liu, Guruswamy Mahesh, Achim Kramer, Paul E. Hardin, Isaac Edery, Eun Young Kim*; Plos Genetics*, 2014, 10(8))

INTRODUCTION

A large variety of life forms manifest circadian (≅24 hr) rhythms in behavior and physiology that are driven by endogenous cellular clocks or pacemakers [115, 116]. Perhaps the most biologically relevant property of circadian clocks is that they can be synchronized (entrained) to local time by external time cues, a feature that endows organisms with the ability to anticipate environmental changes and hence perform activities at optimal times during the day. The main environmental synchronizing agents of circadian clocks in nature are the daily cycles in light/dark and ambient temperature. In general, photic cues are the most potent synchronizing agent for organisms, whereas thermal entrainment is less powerful [117, 118]. Work in the last 20 years using a variety of model organisms has revealed that the molecular logic underlying circadian clock mechanisms is highly conserved [116]. Circadian clocks are based on intracellular mechanisms that involve a core transcriptional translational feedback loop (TTFL) composed of central clock proteins that drive daily oscillations in their own gene expression as well as downstream clock-controlled genes (ccgs). Daily oscillations in the transcript levels of ccgs ultimately drive many of the rhythmic behaviors and physiologies manifested by organisms.

The rate-limiting component of the main TTFL in *Drosophila* is the basic-helix-loop-helix (bHLH) PAS domain containing transcription factor termed dCLOCK (*Drosophila*

CLOCK; dCLK) [23], which forms a heterodimer with CYCLE (CYC), another bHLH-PAS containing clock transcription factor [119]. The dCLK-CYC heterodimer binds to E box DNA elements inducing the expression of the clock genes *period* (*per*) and *timeless* (*tim*), in addition to other clock genes and ccgs. Subsequently, the PER and TIM proteins interact in the cytoplasm and after a time-delay translocate to the nucleus where they function with other factors to inhibit the transcriptional activity of dCLK-CYC. Eventually, the levels of PER and TIM decline in the nucleus, facilitating another round of dCLK-CYC-mediated transcription. In a "secondary" stabilizing TTFL, the dCLK-CYC heterodimer induces the expression of *PAR domain protein 1ε* (*pdp1ε*) and *vrille* (*vri*), whose protein products (i.e., PDP1ε and VRI) in turn activate and repress the expression of *dClk*, respectively, leading to daily cycles in *dClk* mRNA levels [18, 120]. Mammalian clocks also use a CLOCK-based transcription factor in their main TTFL, which involves a heterodimer comprised of mCLOCK (mammalian CLOCK; mCLK) and BMAL1 (homolog of CYC) that governs rhythmic expression of the negative regulators *Per*1-3, in addition to other clock genes and ccgs [121].

Although TTFLs constitute a major molecular framework for the oscillatory behavior of cellular clocks, posttranslational modifications of clock proteins are central to maintain proper timekeeping functions by regulating clock protein stability, sub-cellular localization and activity [29, 30, 32, 122, 123]. A well studied example of clock protein phosphorylation is the progressive phosphorylation of PER, which has a critical role in setting the pace of the clock and controlling temporal changes in dCLK-CYC-mediated transcription by regulating PER stability, timing of nuclear entry and how long it persists in the nucleus [17, 34, 38, 41, 83, 89, 93, 101]. Newly synthesized PER is present as non-to-hypo-phosphorylated isoforms in the late day/early night and undergoes progressive increases in the extent of phosphorylation, culminating in the appearance of mostly or exclusively hyper-phosphorylated isoforms in the late night/early day that are recognized

for rapid degradation by the 26S proteasome [30]. Numerous PER-relevant kinases have been identified, with DOUBLETIME [DBT; homolog of vertebrate casein kinase Iδ/ε (CKIδ/ε)] [82, 83] operating as the major kinase regulating temporal changes in the stability of PER. Other kinases include SHAGGY [SGG; homolog of vertebrate glycogen synthase kinase 3β (GSK3β)] [91], casein kinase 2 (CK2) [43, 90] and NEMO [38, 92].

dCLK also undergoes circadian changes in phosphorylation state, but in a manner different from that of PER [10, 124]. dCLK is present in a mostly intermediate phosphorylated state throughout the day, converting to largely hyper-phosphorylated isoforms in the late night/early day. DBT stably interacts with PER throughout most of its daily life-cycle and this association likely facilitates the ability of DBT to regulate dCLK [10, 75, 124, 125]. Although the role(s) of dCLK phosphorylation is not clear it appears that hyper-phosphorylated isoforms have decreased stability and possibly reduced transcriptional activity [10, 124, 125]. In addition to DBT, several kinases such as protein kinase A (PKA), CaMKII, MAPK, and NMO have been implicated in regulating the activity and/or levels of dCLK [92, 126]. More recently CK2 was reported to act directly on dCLK, stabilizing it while reducing its activity [42]. The mammalian CLOCK protein also manifests circadian oscillations in phosphorylation *in vivo* [127, 128], which is triggered by hetero-dimeric complex formation with BMAL1 [127, 128]. Mass spectrometric analysis of purified mCLK from the mouse liver identified Ser38, Ser42, and Ser427 as sites phosphorylated *in vivo* [129]. Ser38 and Ser42 are located in the bHLH region and phosphorylation of those residues down-regulates transcriptional activity of mCLK via decreasing binding activity to E box element [129]. Phosphorylation of Ser427 is reported as being dependent on GSK-3β activity and relevant for degradation of mCLK [130]. PKG and PKC have been implicated as mCLK kinases regulating phase resetting [131, 132]. Despite these advances using several animal model systems, it is still unclear how CLOCK

phosphorylation impacts the function of circadian timing systems at the organismal level.

In this study, we used a simplified *Drosophila* S2 cell culture system in combination with mass spectrometry to map phosphorylation sites on dCLK. Our results indicate that dCLK is highly phosphorylated (at least 14 phospho-sites). In S2 cells, mutated versions of dCLK where all the mapped Ser/Thr sites were switched to Ala (herein referred to as dCLK-15A) manifested increased E box dependent transcriptional activity without affecting interactions with other core clock partners such as CYC and PER. In flies, dCLK-15A protein is exclusively hypo-phosphorylated suggesting that we identified, at the very least, a major portion of the total phosphorylation sites found on dCLK in flies. Expression of dCLK-15A rescues the arrhythmicity of *Clk*^{out} flies yet with an approximately 1.5 hr shorter period. Consistent with a role in regulating protein stability, the levels of dCLK15A are substantially higher compared to the control situation, which along with increases in transcriptional activity likely explains the faster pace of the clock. The daily peak levels in *per*/*tim* mRNA and protein reached higher values in dCLK-15A expressing flies, further supporting the notion that dCLK levels are normally rate-limiting in the clock mechanism. Surprisingly, the clock-controlled daily activity rhythm in dCLK-15A mutant flies fail to maintain synchrony with daily temperature cycles, although there is no defect in aligning to light/dark cycles. Together, our findings indicate that in animal systems, the post-translational modification of a master circadian transcription factor plays a critical role in setting the pace of the clock and regulating circadian entrainment.

MATERIALS AND METHODS

Plasmids for tissue culture

The pMT-*dClk*-V5, pMT-HA-*dClk*-V5, pMT-HA-*dClk,* pAct-*per,* pAct-*per*-V5 and pMT-*dbt*-V5 plasmids were described previously [10, 17, 75]. pMT-*dClk*15A-V5 and pMT-*dClk*16A-V5 were generated by serially changing codons for Ser to those of Ala by using

a Quick Change site-directed mutagenesis kit (Stratagene). All final constructs were verified by DNA sequencing.

Identification of dCLK phosphorylation sites by mass spectrometry

Hygromycin-resistant stable Schneider 2 (S2) cell lines expressing pMT-HA-*dClk*-V5 were established for dCLK purification. *dClk* expression was induced by adding 500μM $CuSO_4$ to the medium and cells were harvested 24 hr post-induction. 200ml of culture ($3X10^6$ cells/ml) was used and harvested cells were lysed using modified-RIPA buffer (50mM Tris-HCl [pH7.5], 150 mM NaCl, 1% NP-40, 0.25% Sodium deoxycholate) with the addition of a protease inhibitor cocktail (Roche) containing 1 mM EDTA, 25 mM NaF, and 1 mM Na_2VO_3. To extracts, anti-V5 antibody (Invitrogen) was added and incubated overnight with gentle rotation at 4°C followed by the addition of Dynabeads Protein A (Invitrogen) with a further overnight incubation. Beads were collected using DynalMPC. dCLK was eluted with modified Laemmli buffer (150mM Tris-HCl [pH 6.8], 6mM EDTA, 3% SDS, 30% Glycerol) supplemented with 50mM reducing agent TCEP (Calbiochem) at 65°C for 20min. Alkylation was performed by adding 0.5M IAA (iodoacetamide) for 20min at room temperature in the dark. The eluate was resolved using 8% SDS-PAGE, and all the detectable dCLK bands of differing electrophoretic mobility excised (which under the conditions used was mainly the 'intermediate' phosphorylated band), subjected to protease digestion and analyzed by mass spectrometry. Mass spectrometry was performed as described in Schlosser et al. 2005. Data analysis was performed as described previously [133].

Luciferase assay

S2 cells were obtained from Invitrogen and transfected using effectene following the manufacturer's protocol (Qiagen). *Luciferase* (*luc*) reporter assay was performed as described previously [8, 10]. Briefly, S2 cells were placed in 24-well plates and co-tranfected with 0 – 100ng pMT-*dClk*-V5 and pMT-*dClk*-16A-V5 along with 10 ng of perEluc, 30 ng of pAct-*β-gal*-V5/His as indicated. PER mediated repression of dCLK dependent transactivation was measured by transfecting 0 - 20 ng of pAct-*dper* together with 2ng of pMT-*dClk*-V5 or pMT-*dClk*-16A-V5. One day after transfection, *dClk* expression was induced with 500 μM $CuSO_4$ (final in the media), and after another day cells were washed in phosphate buffered saline (PBS), followed by lysis in 300 μl of Reporter Lysis Buffer (Promega). Aliquots of cell extracts were assayed for β-galactosidase and luciferase activities using the Luciferase Assay System and protocols supplied by the manufacturer (Promega).

Transgenic flies

Clk^{out} flies were generated in one of our laboratories (P.E.H.) as follows: 5.2kb deletion of *dClk* exon 1 and upstream sequences was generated by FLP-mediated recombination between FRT sites in the pBac Clk[f06808] and pBac Clk [f03095] [134, 135]. Flippase (FLP)-induced recombination was induced by a daily 1 h heat-shock at 37°C given to hsFLP;;f06808/f03095 larvae and pupae. Three recombinants were recovered, and each produced a deletion rather than a duplication of intervening *dClk* sequences. The remaining pBac insert was excised via pBac transposase induced transposition resulting in white-eyed flies harboring the deletion [136]. A DNA fragment containing the deleted sequences was amplified using primers situated upstream of the f03095 insertion site (5' CGGAATATTGGACAACAAACAG 3') and downstream of the

f06808 insertion site (5'CAGCAGTGGAATCTTAATACAG 3'), and sequenced to confirm the endpoints of the deletion. This new *dClk* deletion allele was named *Clk*^{out}.

To generate transgenic flies that produce wild-type dCLK tagged with V5 at the C-terminus, *dClk*-containing P[acman] transgene was generated using recombineering-mediated gap repair [137]. To prepare the P[acman] vector, homology arms were amplified from genomic DNA with primers clkLA-f (ATGTGGCGCGCCGCCCCAAAAATCCATAAATGCT) and clkLA-r (GTGTTGGATCCAGGGGTGTTATAGAGAGGGACA) for the left arm and clkRA-f (GTGTGGATCCGCAGAGTGAAACCTGTGCAA) and clkRA-r (ATATATGTGCGGCCGCTCCCGGTTATGAGTTTTTCG) for the right arm via PCR, and cloned as AscI-BamHI and BamHI-NotI fragments into AscI and NotI digested attB-P[acman]-ApR vector (modified to remove the SphI site) to form attB-P[acman]ClkLARA. Recombination-competent SW102 cells harboring BAC clone RP98 5K6 (BACPAC Resource Center, Oakland, Ca, USA), which contains the *dClk* genomic region, were transformed with the attB-P[acman]ClkLARA vector (linearized with BamHI). Recombinants containing 15.5kb of genomic sequence beginning ~8kb upstream of the *dClk* translation start and ending ~2.5kb downstream of the *dClk* stop codon were verified by PCR and sequencing and termed attB-P[acman]-*Clk.* To introduce a V5 epitope tag at the C-terminus of the *dClk* open reading frame (ORF), a 3' genomic fragment of *dClk* (from 351bp upstream to 1580bp downstream of the translation stop) was cloned into pGEM-T vector (Promega, Madison, WI). Sequences encoding V5 were introduced in-frame immediately upstream of the *dClk* stop codon using the Quickchange site directed mutagenesis kit (Stratagene, La Jolla, CA) to create pGEM-T-*dClk*3'V5. The 3' *dClk* genomic fragment in attB-P[acman]- *dClk* was swapped with the 3' fragment in pGEM-T-*dClk*3'V5 using SphI and NotI to form attB-P[acman]- *dClk*V5. This transgene was

inserted into the VK00018 attP site on chromosome 2 via PhiC31-mediated transgenesis [137, 138].

Transformation vector containing a genomic *dClk* wherein the codons for the 15 identified phospho-serine were switched to those for alanine was generated in multiple stages as follows: A genomic *dClk* sub-fragment from NheI to SphI site was isolated from P[acman]-*dClk*-V5 and subcloned into pSP72 vector where the multi-cloning sites were mutagenized to introduce a NheI site, and named this plasmid as pSP72-*dClk*(NheI/SphI). Next, we obtained a *dClk* sub-fragment spanning from the NcoI to SphI sites by restriction digestion of pSP72-*dClk*(NheI/SphI), subcloned the released fragment into pSP72 where the multi-cloning sites were mutagenized to introduce a NcoI site, and named this plasmid as pSP72-*dClk*(NcoI/SphI). We performed serial site directed mutagenesis with pSP72-*dClk*(NcoI/SphI) and finally made pSP72-*dClk*(NCoI/SphI)-S11A wherein codons for the serine residues at amino acids 209, 210, 211, 444, 450, 487, 504, 611, 645, 859, 902 on dCLK were all switched to those for alanine residues [(GenBank accession number NP_001014576)]. We purified the *dClk*(NCoI/SphI)-S11A insert by restriction enzyme digestion of pSP72-*dClk*(NCoI/SphI)-S11A and replaced the wild-type *dClk*(NcoI/SphI) insert, generating pSP72-*dClk*(NheI/SphI)-S11A. Next, a more 3' genomic *dClk* sub-fragment from the SphI to NotI sites was subcloned into pSP72 vector where the multi-cloning sites were mutagenized to include NotI and NheI sites, and named this plasmid as pSP72-*dClk*(SphI/NotI). We performed serial site directed mutagenesis with pSP72-*dClk*(SphI/NotI) and made pSP72-*dClk*(SphI/NotI)-S4A wherein codons for the serine residues at amino acids 924, 934, 938, 1018 were switched to those for alanine. Finally, the genomic *dClk*(SphI/NotI)-S4A fragment was ligated with pSP72-*dClk*(NheI/SphI)-S11A generating pSP72-*dClk*(NheI/NotI)-S15A, and then *dClk*(NheI/NotI)-S15A fragment was switched with wild-type *dClk*(NheI/NotI) fragment in pacman-*dClk*-V5 plasmid yielding P[acman]-*dClk*-15A-V5. Transgenic flies were generated by BestGene Inc. (CA, USA).

P[acman]-*dClk*-15A-V5 transformation vector was injected into flies carrying the VK00018 attP docking site on the second chromosome for site-specific integration [137]. Two independent germ-line transformants bearing the *dClk*-15A-V5 transgene in a wild-type background were obtained and then crossed into a Clk^{out} genetic background to yield *dClk*-15A-V5;Clk^{out}.

Behavioral assays

The locomotor activities of individual flies were measured as previously described using the Drosophila Activity Monitoring system from Trikinetics (Waltham, MA). Young adult flies were used for the analysis and exposed to 4 days of 12 h light followed by 12 h dark [where zeitgeber time 0 (ZT0) is defined as the time when the light phase begins] at 25°C and subsequently kept in constant dark conditions (DD) for 7 days. Temperature entrainment (temperature cycle, TC) was performed in constant dark condition and in some cases, in the presence of constant light (>2000lux). Temperature cycles were 12h of 24°C (cryo phase) followed by 12h of 29°C (thermal phase) (where ZT0 is defined as the time when the cryo phase begins) for 4 days and subsequently kept at 24°C for 7 days. The locomotor activity data for each individual fly was analyzed using the FaasX software (Fly Activity Analysis Suite for MacOSX), which was generously provided by F. Rouyer (CNRS, France). Periods were calculated for each individual fly using *chi*-square periodogram analysis and pooled to obtain a group average for each independent transgenic line or genotype. Power is a quantification of the relative strength of the rhythm during DD. Individual flies with a power ≥10 and a 'width' value of 2 or more (denotes number of peaks in 30-min increments above the periodogram 95% confidence line) were considered rhythmic. Actogram represents the locomotor activity data throughout the experimental period. Vertical bars in the actogram represent absolute activity levels for

each 30 min intervals averaged for each given genotypes of flies. The strength of this measurement can be manipulated by using the function called hash density, which represent the number of times fly need to make beam crossing to be registered as one vertical bar. The hash density of the actogram was varied for better comparison depending on the activity levels of given genotypes of flies.

Immunoblotting and immunoprecipitation

Protein extracts from S2 cells were prepared as previously described [75]. Briefly, the cells were lysed using modified-RIPA buffer (50mM Tris-HCl [pH7.5], 150 mM NaCl, 1% NP-40, 0.25% Sodium deoxycholate) with the addition of protease inhibitor cocktail (GeneDEPOT) and phosphatase inhibitor cocktail (GeneDEPOT). For detection of dCLK recombinant protein, extracts were obtained using RIPA buffer 25mM Tris-HCl [pH 7.5], 50mM NaCl, 0.5% Sodium deoxycholate, 0.5% NP40, 0.1% SDS) and were sonicated briefly as previously described [10]. Flies were collected by freezing at the indicated times in light-dark (LD) or temperature cycles (TC) and total fly head extracts prepared using modified-RIPA buffer or RIPA buffer with sonication (for dCLK). Extracts were resolved by 5% polyacrylamide gels or by 3-8% Tris-acetate Criterion gel (Bio-Rad) in some case for dCLK, transferred to PVDF membrane (Immobilon-P, Millipore), and immunoblots were treated with chemiluminescence (ECL, Thermo). Primary antibodies were used at the following dilutions; anti-V5 (Invitrogen), 1:5000; anti-HA (12CA5, Roche), 1:2000; anti-OGT (H-300, Santa Cruz), 1:3000; anti-PER, (Rb1) 1:3000; anti-TIM (TR3), 1:3000; anti-dCLK (GP208) 1:3000. Quantification of band intensity was performed using image J software.

For immunoprecipitation, cell extracts from S2 cells were prepared and 3 μl of anti-HA (12CA5) or anti-V5 antibody was added depending on the target protein sought, and incubated for overnight at 4°C with gentle rotation. The next day, 20μl of Gammabind-

sephase bead (GE healthcare) was added with a further incubation of 3 hr at 4°C. The immune complexes were eluted with 1X SDS-PAGE sample buffer. For λ- phosphatase treatment, the purified immune complexes were resuspended in λ protein phosphatase buffer (50mM Tris-HCl [pH7.5], 0.1mM EDTA, 5mM DTT, 0.01% Triton X-100, 2mM $MnCl_2$, and 0.1mg/ml bovine serum albumin) , divided into two equal aliquots. One aliquot of bead was treated with 200 units of λ protein phosphatase (NEB) and no addition was made to the other aliquot. Both aliquots were incubated for 30min at 30°C with occasional shaking, and immune complexes analyzed by immunoblotting.

Quantitative Real time RT-PCR

Total RNA was isolated from frozen heads using QIAzol lysis reagent (QIAGEN). 1μg of total RNA was reverse transcribed with oligo-dT primer using Prime Script reverse transcriptase (TAKARA) and real-time PCR was performed in Corbett Rotor Gene 6000 (Corbett Life Science) using Quantitect SYBR Green PCR kit (Qiagen). Primer sequences used here are as follows; *dper* forward: 5′-GACCGAATCCCTGCTCAATA-3′; *dper* reverse: 5′-GTGTCATTGGCGGACTTCTT-3′; *tim* forward: 5′-CCCTTATACCCGAGGTGGAT-3′; *tim* reverse: 5′-TGATCGAGTTGCAGTGCTTC-3′; *dClk* forward: 5′-CAGCCGCAATTCAATCAGTA-3′; *dClk* reverse: 5′-GCAACTGTGAGTGGCTCTGA-3′. We also included primers for the noncycling mRNA coding for CBP20 as previously described , and sequences are as follows; *cbp*20 forward: 5′-GTCTGATTCGTGTGGACTGG-3′; *cbp*20 reverse: 5′-CAACAGTTTGCCATAACCCC-3′. Results were analyzed with software associated with Rotor Gene 6000, and relative mRNA levels were quantitated using the $2^{-\Delta\Delta Ct}$ method.

RESULTS

Identification of dCLK phosphorylation sites in cultured *Drosophila* cells

As an initial attempt to better understand the role(s) of dCLK phosphorylation we sought to map phosphorylation sites using recombinant protein production in cultured *Drosophila* S2 cells. This simplified cell culture system was successfully used to identify physiologically relevant phosphorylation sites on *Drosophila* PER [34, 38, 40, 41]. Prior work showed that production of recombinant dCLK in S2 cells leads to significant shifts in electrophoretic mobility that are due to phosphorylation [10]. Thus, we established S2 cell lines stably expressing HA-*dClk*-V5 under the inducible metallothionein promoter (pMT). Total cell lysates were subjected to immunoprecipitation with anti-V5 antibody, followed by multi-protease digestion, titansphere nanocolumn phosphopeptide enrichment, and tandem mass spectrometry, as previously described [34, 133]. We identified 14 phosphorylation sites on dCLK, all of which are at Ser residues, with the possible exception of Tyr607 (Table 3.1). Many of the identified phosphorylation sites are in the C-terminal half of dCLK, which contains several Q-rich regions that might function in transcriptional activation (Figure 3.1A). Phosphorylation was also detected at sites close to the N- and C-terminus of the dCLK protein. Interestingly, no phosphorylation sites were found in any of the known functional domains of dCLK; e.g. bHLH, PAS domains and Q-rich regions (Figure 3.1A and Table 3.1).

In preliminary studies we individually mutated each of the identified phosphorylated Ser residues to Ala residues but did not see major effects on dCLK electrophoretic mobility, except for the S859A mutant version of dCLK, which manifested slightly faster electrophoretic mobility. (Figure S3.1A and B). The transcriptional activities of most single site mutants were somewhat increased ($\leq$ 2 fold), except for the S924A mutant version of dCLK, which manifested a slight but reproducible decrease (Figure S3.1C). Overall, our initial studies in S2 cells were not able to identify whether certain individual phospho-sites

Table 3.1. Identification of phosphorylation sites on dCLK produced in *Drosophila* S2 cells

dCLK[a]
S5[b]
[S209,S210,S211][c]
S444
S450
S487
S504
[Y607,S611][c]
S645
S859
S902
S924
S934
S938
S1018

[a]Stable cell line expressing *dClk* under the control of pMT-inducible promoter.
[b]Amino acids are numbered according to sequence of dCLK (amino acids 1-1027), GenBank accession number NP_001014576.
[c]Only one site in the bracket is phosphorylated.

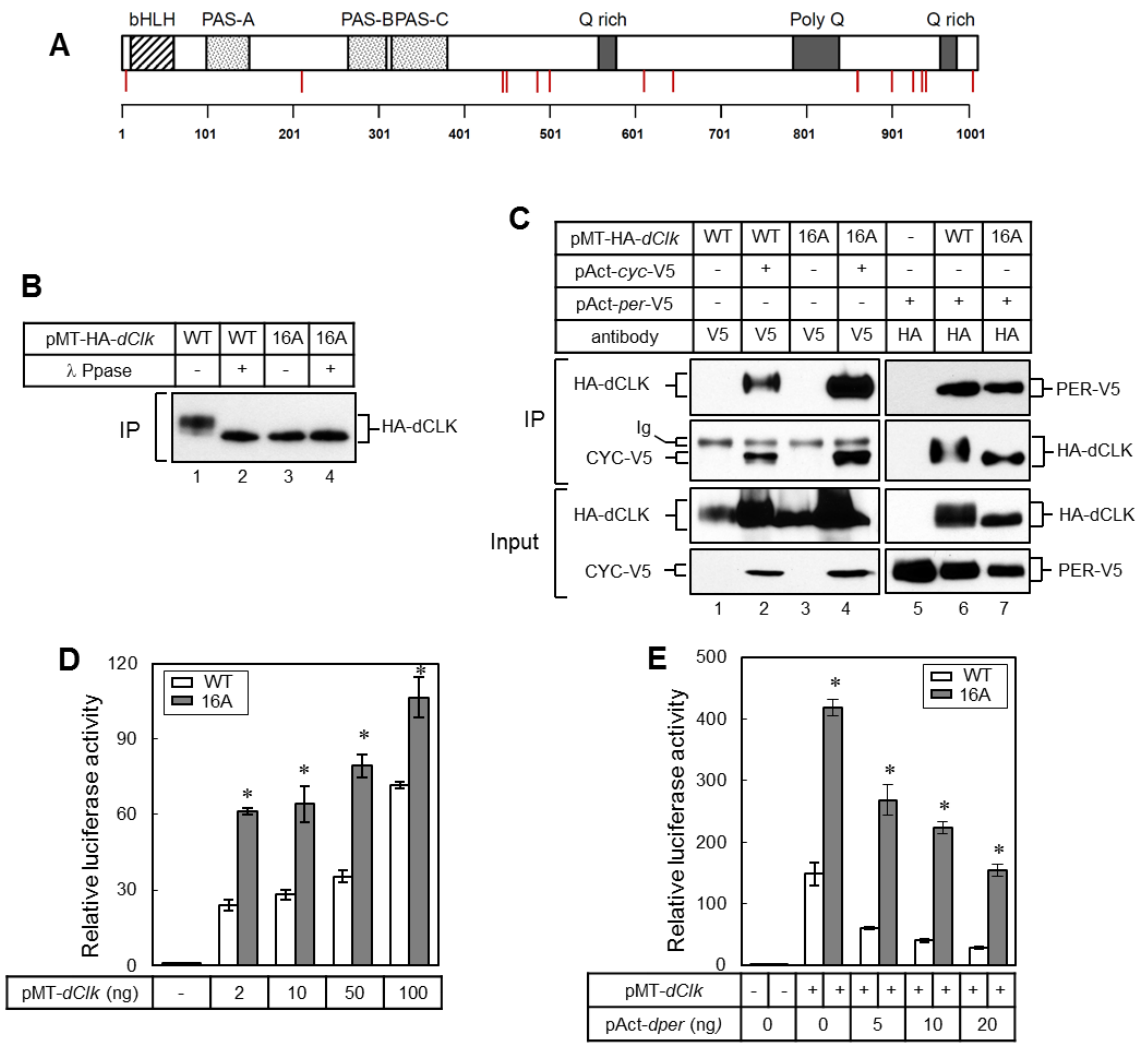

Figure 3.1. Blocking phosphorylation at multiple phospho-sites on dCLK prevents global phosphorylation but does not impair several key clock-relevant activities.

(A) Schematic diagram of dCLK protein. Phosphorylation sites on dCLK identified in this study are indicated as red vertical lines. Horizontal line at bottom indicates relative positions of amino acid residues. (B, C) S2 cells were transiently transfected with 500ng of pMT-HA-*dClk* (WT) or pMT-HA-*dClk*-16A (16A), either singly or in combination with 500ng of pAct-*cyc*-V5 or pAct-*per*-V5 as indicated. Expression of dCLK was induced 24hr after transfection by adding 500μM $CuSO_4$ to the medium. Cells were harvested 24hr after

Figure legend of figure 3.1 continued

induction, and protein extracts were first subjected to immunoprecipitation using anti-HA (12CA5) antibody (B), the anti-epitope tag antibodies (V5 or HA) as indicated on top of the blots (C). Immune complexes were directly analyzed by immunoblotting (C) or further incubated in the absence (-) or presence (+) of λ phosphatase followed by immunoblotting (B). (D, E) S2 cells were transiently co-transfected either singly with pMT-*dClk*-V5 (WT) and pMT-*dClk*-16A-V5 (16A) (D), or in combination with increasing amount of pAct-*per* (E). Shown are the average values from three independent experiments for relative E box dependent luciferase activity in the absence (-) or presence (+) of pMT-*dClk*-V5. *$p < 0.05$; error bars denote SEM.

are particularly significant in regulating dCLK metabolism or activity. While ongoing work is aimed at better understanding the roles of individual phospho-sites, in this study we focused on more global aspects of dCLK phosphorylation by generating a mutant version wherein all the Ser phospho-acceptor sites identified by mass spectrometry were switched to Ala. Since the mass spectrometry data did not unambiguously identify which Ser among amino acids 209-211 is phosphorylated, we switched all 3 Ser to Ala. In addition, although Tyr 607 or Ser 611 is phosphorylated, to focus on Ser phosphorylation, we only mutated Ser 611 to an Ala. By using site-directed mutagenesis, we serially mutated the aforementioned 16 Ser to Ala (dCLK-16A). The electrophoretic mobility of dCLK-16A is indistinguishable from that of λ-phosphatase treated wild-type dCLK and was not altered by λ-phosphatase treatment (Figure 3.1B), indicating that we mapped most, if not all, the sites on dCLK phosphorylated by endogenous kinases in S2 cells.

dCLK-16A interacts with either CYC or PER proteins to a similar extent as that observed for the wild-type version (dCLK-WT), demonstrating that dCLK-16A is not grossly misfolded (Figure 3.1C). In addition, our findings suggest that the phosphorylated state of dCLK is not a major signal regulating interactions with core clock partners. Consistent with prior work, we observed increases in non/hypo-phosphorylated isoforms of dCLK when dPER is co-expressed (Figure 3.1C, compare lane 1 and 6) [75]. With regards to transcriptional activity, dCLK-16A is more potent compared to dCLK-WT in stimulating E-box dependent transcription (Figure 3.1D), while still maintaining its sensitivity to inhibition by PER (Figure 3.1E). Earlier findings showed that hyper-phosphorylated dCLK is less stable and that DBT might contribute to this instability, although the exact role of DBT is not clear [10, 124, 125]. We compared the stabilities of dCLK-16A and dCLK-WT under a variety of conditions, including overexpressing DBT, but did not detect a significant difference (Figure S3.2A and B), suggesting we did not map one or more phosphorylation sites critical for regulating dCLK stability and/or the pathway

for dCLK degradation in S2 cells is not identical to that in flies (see below). Taken together, the results obtained using well-established S2 cell based assays indicate that dCLK-16A retains key clock-relevant biochemical functions and suggest that global phosphorylation of dCLK reduces its transactivation potential.

Flies expressing dCLK-15A display behavioral rhythms with short periods

To investigate whether the dCLK phosphorylation sites we identified play a physiological role in the *Drosophila* circadian timing system, we first evaluated the ability of a novel wildtype *dClk* transgene to rescue behavioral rhythms in the arrhythmic Clk^{out} genetic background (herein, termed as p{*dClk*-WT};Clk^{out}). Clk^{out} is a newly described arrhythmic null mutant that does not produce dCLK protein (Mahesh et al., submitted). The transgene was constructed with a 13.9 kb genomic fragment that contains the *dClk* gene, which we modified by introducing a V5 epitope tag at the C-terminus of the *dClk* open reading frame for enhanced protein surveillance. Flies were exposed to standard entraining conditions of 12hr light:12hr dark cycles [LD; where zeitgeber time 0 (ZT0) is defined as lights-on] at 25^{o}C, followed by several days in constant dark conditions (DD) to measure free-running behavioral periods. In the behavioral analysis, p{*dClk*-WT};Clk^{out} flies manifested robust locomotor activity rhythms with normal ~24 hr periods (Table 3.2, Mahesh et al., submitted), indicating that the circadian clock system functions properly in these flies.

Next, we sought to generate transgenic flies harboring a dCLK-16A version of the *dClk* rescue transgene. However, because of technical difficulties in generating a version that also included replacing Ser5 with Ala, we made a *dClk* version wherein the other 15 Ser residues were switched to Ala, termed *dClk*-15A. In S2 cells, dCLK-15A behaves similar to dCLK-16A, including no observable effect of phosphatase treatment on electrophoretic mobility and enhanced E-box dependent transcriptional activity (Figure S3.3). Although phosphorylation of Ser5 might affect dCLK function in a manner that is

Table 3.2. Behavioral analysis of p{*dClk*-15A}; *Clk*^{out} flies following light/dark entrainment[a]

Genotype	Temp (°C)	#[b]	Tau ± S.E.M. (h)	Rhythmicity (%)[c]	Power[d]
p{*dClk*-WT}, A;*Clk*^{out}	18	30	24.0 ± 0.08	66.7	39.8
p{*dClk*-15A}, 2M; *Clk*^{out}	18	28	22.2 ± 0.09	71.4	47.8
p{*dClk*-15A}, 6M; *Clk*^{out}	18	42	22.1 ± 0.12	33.3	43.0
Clk^{out}	25	19	AR	AR	AR
p{*dClk*-WT}, A;*Clk*^{out}	25	63	24.0 ± 0.08	87.3	114.7
p{*dClk*-15A}, 2M; *Clk*^{out}	25	39	22.3 ± 0.07	61.5	67.4
p{*dClk*-15A}, 6M; *Clk*^{out}	25	42	22.7 ± 0.08	73.8	67.2
p{*dClk*-WT}, A;+/+	25	29	23.0 ± 0.07	48.3	62.8
p{*dClk*-WT}, A;*Clk*^{out}	29	30	24.1 ± 0.05	83.3	113.5
p{*dClk*-15A}, 2M; *Clk*^{out}	29	24	22.5 ± 0.5	12.5	86.4
p{*dClk*-15A}, 6M; *Clk*^{out}	29	14	22.3 ± 0.12	35.7	51

[a] Flies were kept at indicated temperatures (18°C, 25°C, 29°C) and exposed to 4 days of 12:12 LD followed by 7 days of DD.

[b] Total number of flies that survived until the end of the testing period.

[c] Percentage of flies with activity rhythms having a power value of ≥ 10 and a width value of ≥ 2.

[d] Measure of the strength or amplitude of the rhythm.

not revealed in the S2 cell based assays we used, the CLK-15A protein contains the majority of phosphorylation sites and should address if global phosphorylation of dCLK plays an important role in the circadian timing system. Two independent lines of transgenic flies harboring the *dClk*-15A transgene were obtained and circadian behavior was monitored in the Clk^{out} genetic background (referred to as p{*dClk*-15A}, 2M; Clk^{out} and p{*dClk*-15A}, 6M; Clk^{out}). In sharp contrast to flies harboring the control version of *dClk*, the two independent lines of p{*dClk*-15A};Clk^{out} flies manifested generally weaker behavioral rhythms that are approximately 1.5hr shorter compared to their wild-type counterparts (Table 3.2).

Under standard conditions of LD at 25^{o}C, *D. melanogaster* exhibits a bimodal distribution of activity with a “morning” and “evening” bout of activity centered around ZT0 and ZT12, respectively. Although p{*dClk*-15A};Clk^{out} flies manifest the typical bimodal distribution of locomotor activity, the onset of both the morning and evening bouts of activity were earlier (Figure 3.2, compare panels B and C to A), consistent with the shorter free-running periods. The Clk^{out} flies only showed a “startle” response to the lights-on transition but no rhythmic behavior (Figure 3.2E). In constant dark conditions, the downswing in evening activity is clearly earlier in p{*dClk*-15A};Clk^{out} flies, in agreement with the shorter free-running period (Table 3.2, Figure 3.2 and S3.4). We also examined the locomotor behavior of flies harboring the *dClk*-WT transgene in a wild-type genetic background, resulting in flies with four copies of the *dClk* gene (herein referred to as p{*dClk*-WT};+/+). The circadian period was shortened to approximately 23hr (Table 3.2 and Figure 3.2D), which is well correlated with previous reports demonstrating that increasing the copy number of *dClk* shortens the circadian period of behavioral rhythms [139, 140].

A hallmark property of circadian rhythms is that the period length is very constant over a wide range of physiologically relevant temperatures, termed temperature

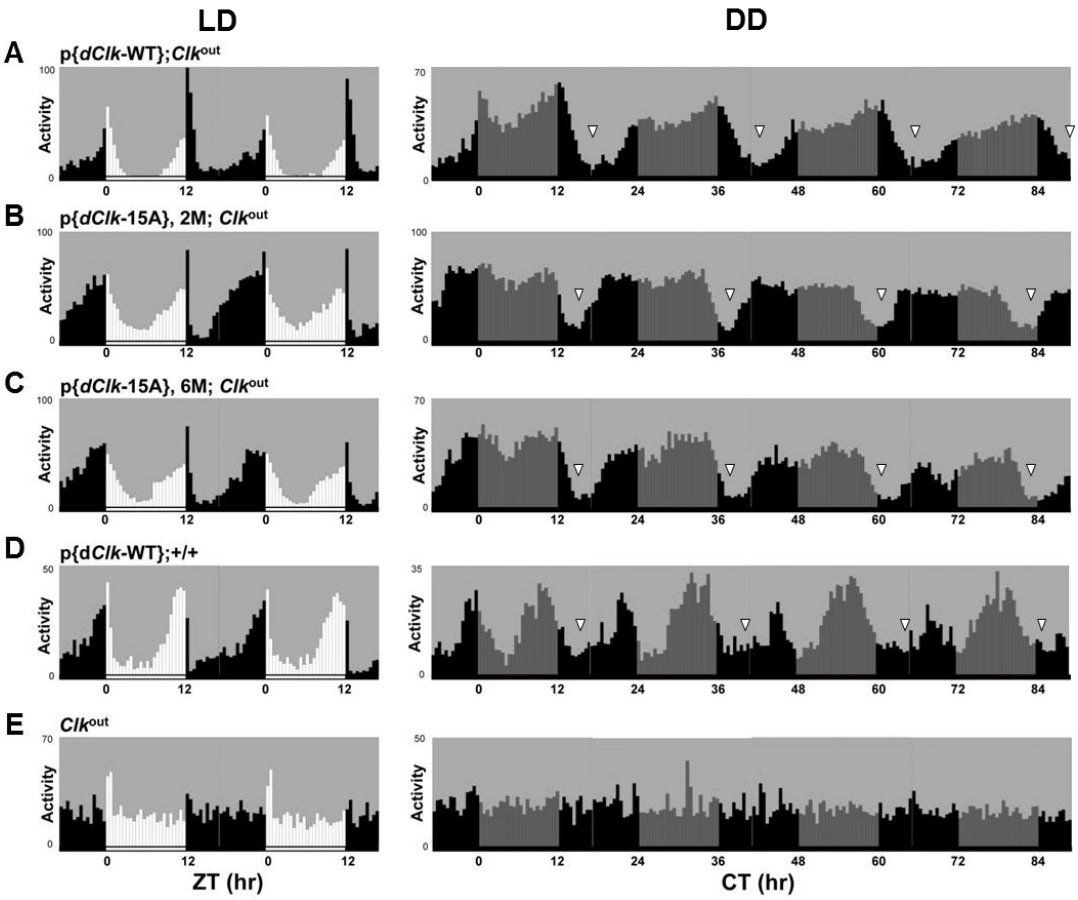

Figure 3.2. The p{*dClk*-15A};*Clk*^{out} flies manifest short period behavioral rhythms. (A - E) Each panel represents the average activity of male flies for a given genotype during the third and forth day of 12hr light:12hr dark entrainment (LD) followed by 4 days of constant darkness (DD). White vertical bars represent locomotor activity during light phase and black vertical bars represent locomotor activity during dark phase in LD. Gray vertical bars represent locomotor activity during the subjective light phase in DD. White horizontal bars and black horizontal bars below each panel indicate 12 hr periods of lights-on and lights-off, respectively. Arrowheads indicate the times in a daily cycle when trough levels of activity were attained following the evening bout of activity. Standard error of the mean is indicated as dots above each bars.

compensation [141]. To investigate whether phosphorylation of dCLK might have a role in temperature compensation, we analyzed behavioral rhythms at three standard temperatures (i.e., 18^{o}, 25^{o} and 29^{o}C). Although we noted a decrease in rhythmicity for *dClk*-15A;*Clk*^{out} flies at 29^{o}C, the periods were quite similar over the temperature range tested (Table 3.2), suggesting that global phosphorylation of dCLK does not play a major role in temperature compensation.

dCLK-15A is exclusively hypo-phosphorylated and very abundant in flies

We examined the temporal profiles of dCLK protein by analyzing head extracts prepared from p{*dClk*-WT};*Clk*^{out} and p{d*Clk*-15A};*Clk*^{out} flies in LD conditions (Figure 3.3A and C). dCLK-WT protein undergoes daily changes in phosphorylation that are consistent with earlier results probing endogenously produced dCLK; namely, hypo- to medium-phosphorylated isoforms present during the mid-day/early night (e.g., ZT 8 to ZT 16) and mostly hyper-phosphorylated isoforms present in the late night/early day (e.g., ZT20 to ZT4) (Figure 3.3A) [10, 124]. However, the mobility of dCLK-15A was similar throughout a daily cycle (Figure 3.3A), and co-migrated with λ phosphatase treated dCLK-WT (Figure 3.3B). Thus, similar to results in S2 cells, dCLK-15A exhibits little to no phosphorylation *in vivo*, suggesting that the phospho-sites we identified by mass spectrometry comprise, at the very least, a major portion of the total phosphorylation sites found on dCLK in flies (it is also possible that one or more of the phospho-sites we mutated are required for phosphorylation at other sites, but this would still result in a mainly hypo-phosphorylated dCLK protein). Intriguingly, the levels of dCLK-15A were substantially higher compared to dCLK-WT throughout a daily cycle. Quantification of immunoblots indicated that the average daily levels of dCLK-15A are about 2.5 times more than those of dCLK-WT (Figure 3.3C).

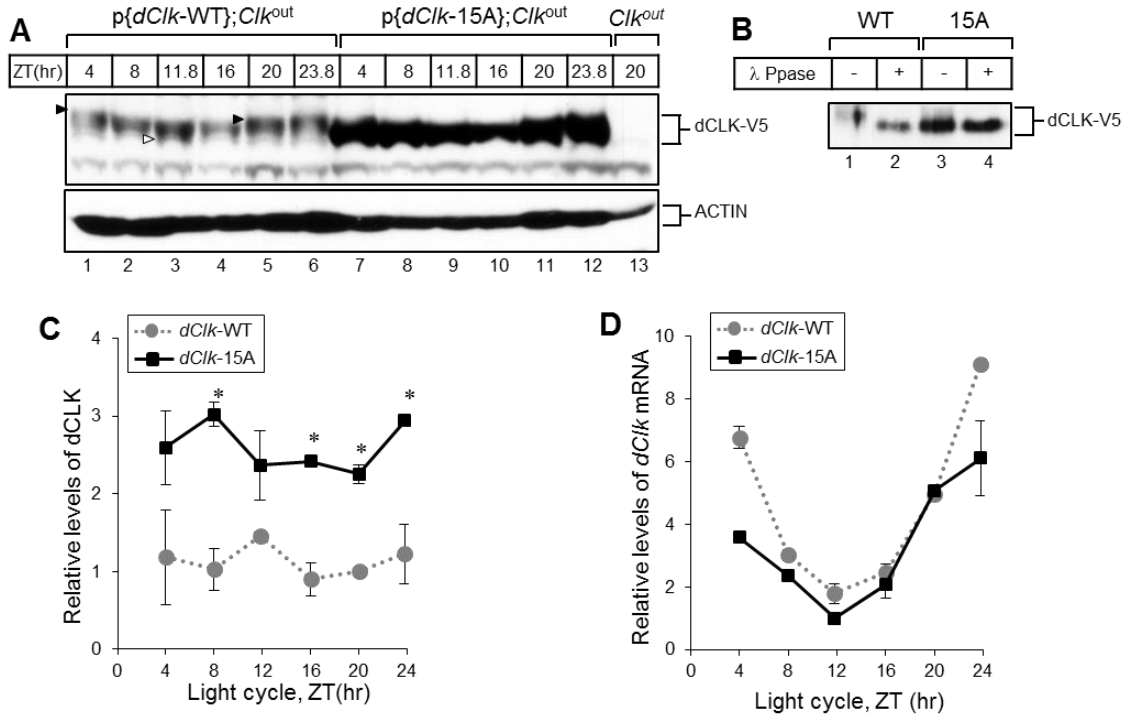

Figure 3.3. The levels of dCLK are substantially higher and hypo-phosphorylated at all times of the day in p{*dClk*-15A};*Clk*^{out} flies.

(A-C) Adult flies of the indicated genotype were collected at different times of day (ZT), head extracts prepared and directly analyzed for immunoblotting (A) or processed for immunoprecipitation with anti-V5 Ab (B). β-Actin (ACTIN) served as a loading control. Immune complexes were further incubated in the absence (-) or presence (+) of λ phosphatase and immunoblotted with anti-V5 antibody, as indicated (B). Filled arrowheads denote hyper-phosphorylated isoforms of dCLK and open arrowhead denotes hypo-phosphorylated isoforms of dCLK (A). (C) Relative levels of dCLK were determined by measuring staining intensities using image J software. Shown are the average values from three independent experiments. (D) Total RNA was extracted from fly heads, and quantitative real-time RT-PCR was performed to measure the relative levels of *dClk* transcripts. Shown are the average values from three independent experiments using p{*dClk*-15A}, 6M;*Clk*^{out} flies. Error bars denote SEM.

To examine whether the high levels of dCLK-15A proteins results from elevated mRNA abundance, we measured *dClk* transcript levels. As reported previously, although the overall daily abundance of dCLK-WT protein is essentially constant throughout a daily cycle, *dClk*-WT mRNA levels oscillate with peak amounts attained during the late night-to-early day and reaching trough values around ZT12 [19, 94]. The daily oscillation in *dClk*-15A mRNA abundance is similar to the wild-type situation and even seemed to have lower peak levels (Figure 3.3D). These results indicate that in general global phosphorylation of dCLK decreases its stability *in vivo*, consistent with prior findings using S2 cells [10, 124].

To further examine the status of the clockworks, we measured the daily profiles in *per* and *tim* transcripts and protein levels. Both *per* and *tim* mRNA levels in p{*dClk*-15A};*Clk*^{out} flies were reproducibly higher, especially during the daily upswing that occurs between ZT4 – 12 (Figure 3.4A and B). These result further support the notion that dCLK levels are normally rate-limiting for circadian transcription and suggest that despite the increased abundance of dCLK-15A there is sufficient PER to engage in normal repression of dCLK-15A/CYC activity. Indeed, PER protein levels were reproducibly higher in p{*dClk*-15A};*Clk*^{out} flies (Figure 3.4C and D), consistent with the increased transcript levels. In p{*dClk*-15A};*Clk*^{out} flies, TIM protein levels were slightly but reproducibly increased (Figure 3.4E and F). The increased daily upswing in *tim* mRNA levels in p{*dClk*-15A};*Clk*^{out} flies might have a smaller effect on overall TIM protein levels because light induces the rapid degradation of TIM [84], possibly limiting the ability of TIM to accumulate during the early night prior to the start of transcriptional feedback repression. Taken together, we show that the stability of dCLK in flies is strongly increased by blocking phosphorylation at one or more sites. Moreover, augmenting the total abundance of dCLK accelerates the daily accumulation of *per*/*tim* transcripts and increases their peak levels, indicative of higher overall dCLK-CYC-mediated transcription. In addition, increased *in vivo* transcriptional

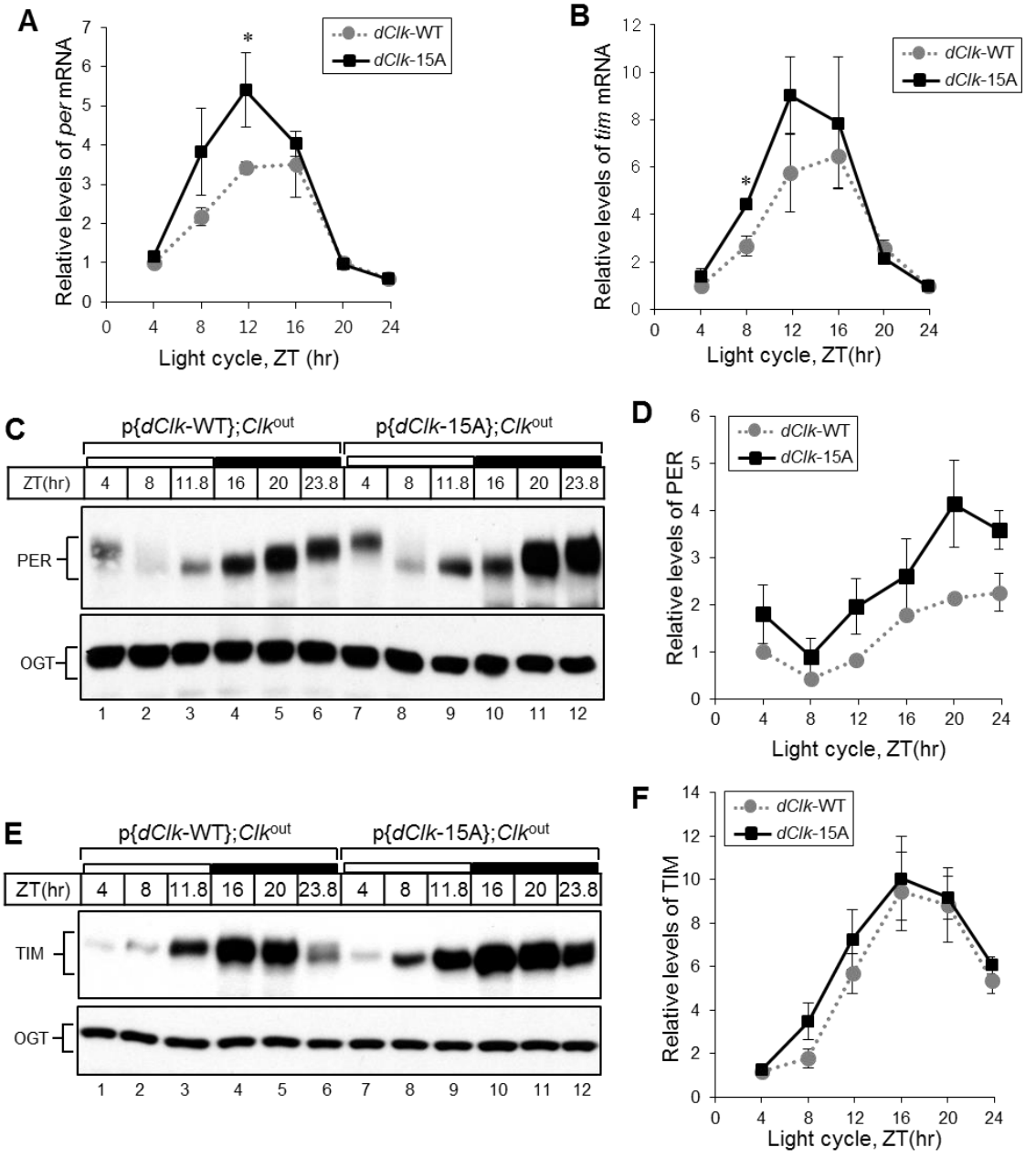

Figure 3.4. Higher amplitude rhythms of *per* mRNA and protein in p{*dClk*-15A};*Clk*^{out} flies.

Adult flies of the indicated genotype were collected at the indicated times (ZT) during a day and total RNA (A, B) or protein extracts (C to F) prepared. (A, B) Quantitative real-time RT-PCR was performed to measure the relative levels of *per* (A) or *tim* (B) transcripts. Shown are the average values from three independent experiments. (C to F)

Figure legend of figure 3.4 continued

Immunoblotting was performed using anti-PER (Rb1) or anti-TIM (TR3) Ab. *O*-GlcNAc transferase (OGT) served as a loading control. Relative levels of PER and TIM proteins were determined by measuring band intensities of immunoblot using image J software (D, F). Shown are the average values from three independent experiments using p{*dClk*-15A}, 6M;*Clk*^{out} flies. *p < 0.05; error bars denote SEM.

activity of dCLK-15A may also contribute to higher dCLK-CYC-mediated transcription, as is the case in S2 cells (Figure 3.1D). These results demonstrate that dCLK phosphorylation plays a key role in setting the amplitudes of the *per* mRNA and protein rhythms, molecular oscillations that are central to the primary TTFL and circadian speed control in *Drosophila* [34, 142]

Flies expressing dCLK-15A manifest a defect in behavioral synchronization to daily temperature cycles

Besides light-dark cycles, daily changes in temperature can also synchronize (entrain) circadian rhythms in a wide variety or organisms [143]. Prior work showed that *D. melanogaster* can entrain to daily cycles of alternating 12hr 'warm'/12 hr 'cold' cycles that differ by as little as 2-3 ^{o}C [112, 113, 144]. To determine if flies expressing dCLK-15A have a defect in entraining to temperature cycle, flies were kept in constant darkness, exposed to 12hr:12hr temperature cycles of 24°C:29°C (TC) and locomotor activity rhythms analyzed (Table 3.3 and Figure 3.5). The daily distribution of activity in p{*dClk*-15A};*Clk*^{out} flies is strikingly different compared to the wild-type control. As previously observed for wildtype strains of *D. melanogaster* entrained to daily temperature cycles [112, 113, 144], p{*dClk*-WT};*Clk*^{out} flies exhibit the classic "anticipatory" rise in activity just prior to the low-to-high and high-to-low temperature transitions, similar to what is observed in light-dark cycles around ZT0 and ZT12 (Figure 3.5 and S3.5; there is a "startle" response at the transition from low-to-high temperature that is also observed in *Clk*^{out} flies, analogous to the transient burst in activity at lights-on in a LD cycle). In sharp contrast, during the beginning of the temperature entrainment regime although p{*dClk*-15A};*Clk*^{out} flies also manifest two activity peaks, they occur much earlier at around the middle of the warm- and cryo-phases (Figure 3.5B).

Table 3.3. Behavioral analysis of p{*dClk*-15A}; *Clk*^{out} flies following temperature cycles[a]

Genotype	Number[b]	Tau ± S.E.M. (h)	Rhythmicity (%)[c]	Power[d]
p{*dClk*-WT}, A;*Clk*^{out}	38	23.7± 0.12	73.7	122.9
p{*dClk*-15A}, 2M; *Clk*^{out}	8	21.9±0.13	50	83.4
p{*dClk*-15A}, 6M; *Clk*^{out}	14	22.0±0.27	35.7	69.5
p{*dClk*-WT}, A;+/+	37	23.1±0.67	59.5	72.2

[a] Flies were kept in constant darkness and exposed to 12hr:12hr temperature cycles of 24°C:29°C for 9 days and followed by 7 days of constant 24°C.

[b] Total number of flies that survived until the end of the testing period.

[c] Percentage of flies with activity rhythms having a power value of ≥ 10 and a width value of ≥ 2.

[d] Measure of the strength or amplitude of the rhythm.

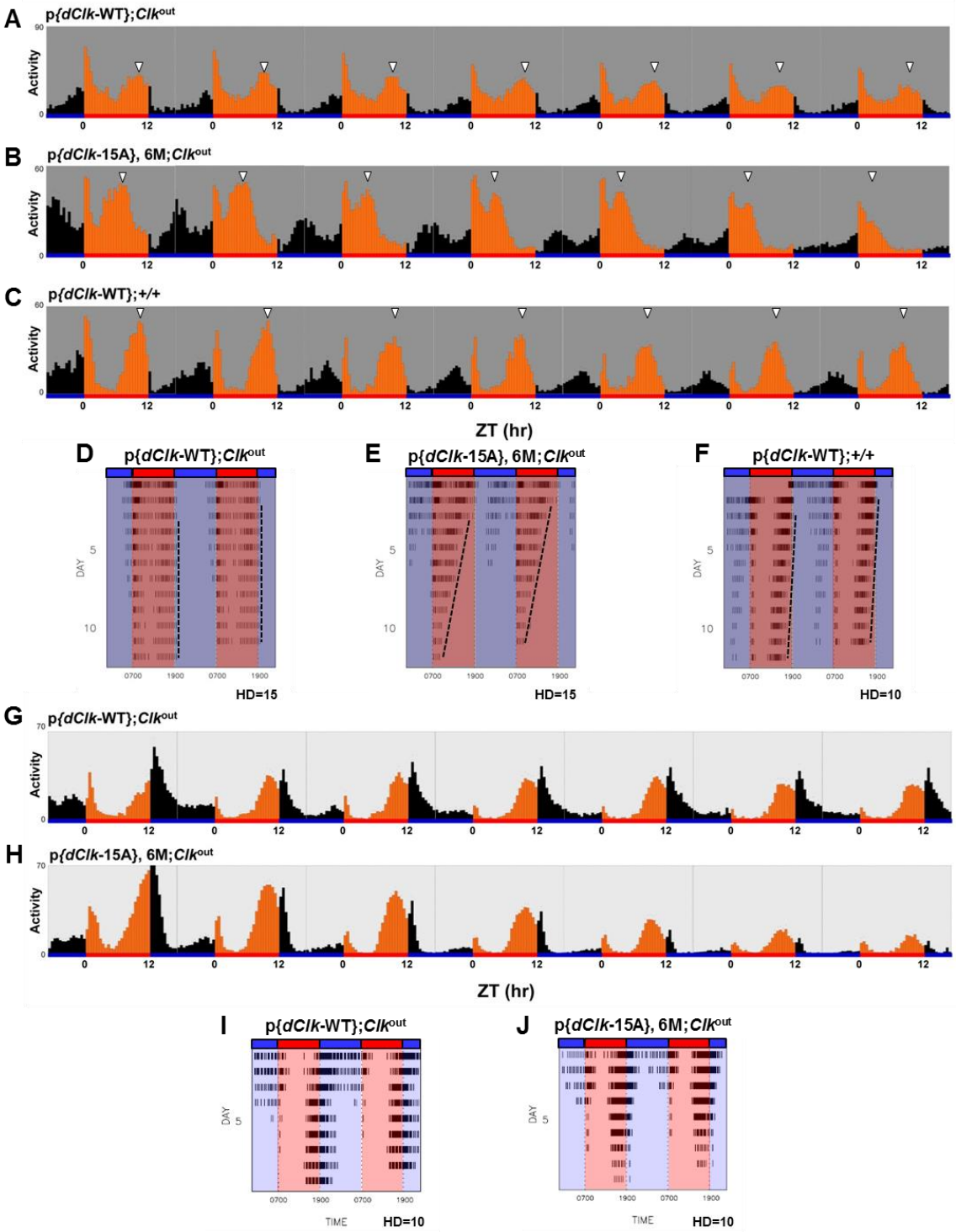

Figure 3.5. Impaired behavioral entrainment of p{*dClk*-15A};*Clk*^{out} flies in daily temperature cycles.

Adult male files of the indicated genotype were entrained in 12h:12h temperature cycles of 24°C:29°C in the absence (A-F) or presence (G-J) of constant light. (A-C, G, H) Each

Figure legend of figure 3.5 continued

panel represents the daily average activity beginning on the third day of TC followed by 7 consecutive days. Orange vertical bars represent locomotor activities during the thermo phase and black vertical bars represent locomotor activities during the cryo phase. Red and blue horizontal bars indicate thermo- and cryo-phases, respectively. (D-F, I, J) Red and blue shades indicate thermo-and cryo-phases, respectively. The vertical black bars on each row of the actogram depict fly activity (measured in 30 min intervals). HD, hash density of the actogram (for example, HD=10 signifies that 10 activity events are required to produce a hash mark). To better visualize rhythmic behavior, each row of an actogram was double plotted. To better visualize the progressive advancement of the main activity bout in p{*dClk*-15A};Clk^{out} flies, a vertical line was drawn across the activity offsets.

Interestingly, while the timing of the “startle” response at the transition from low-to-high temperature remained constant in p{*dClk*-15A};*Clk*^{out} flies, the timing of the major activity peak occurring during the mid-warm phase appeared to progressively advance on subsequent days in TC (Figure 3.5B). Analysis of individual activity records also confirmed this trend (Figure 3.5E). The abnormal behavioral pattern under temperature cycles for p{*dClk*-15A};*Clk*^{out} flies was also observed when flies were exposed to a temperature cycle after first treating them with constant light for 6 days to abolish the circadian timing system (Figure S3.6). Thus, the defective entrainment of p{*dClk*-15A};*Clk*^{out} flies to TC is not dependent on the status of the clock at the time that the temperature entrainment was initiated. Furthermore, although the main activity bout in p{*dClk*-15A};*Clk*^{out} flies advanced on subsequent days during TC, the rate of advancement was clearly greater during free-running conditions following TC (Figure S3.5), suggesting partial entrainment during TC. Following entrainment to TC, the free-running period of dCLK-15A producing flies is about 1.5hr shorter compared to the wild type dCLK-WT control (Table 3.3 and Figure S3.5). The faster running clock in p{*dClk*-15A};*Clk*^{out} flies during free-running conditions after exposure to TC is consistent with results obtained following entrainment to LD (Table 3.2). Thus, it appears that when exposed to daily temperature cycles p{*dClk*-15A};*Clk*^{out} flies can adopt some alignment with the entraining conditions, albeit without a normal phase relationship, but that this entrainment is weak and the flies partially free-run at their shorter endogenous periods, leading to progressive advances in their behavioral rhythm relative to the 24hr entraining regime. Although not as dramatic, the timing of the warm-phase activity bout in p{*dClk*-WT};+/+ flies also advanced during TC (Figure 3.5F), whereas this was not the case for p{*dClk*-WT};*Clk*^{out} flies (Figure 3.5D). In addition, the clock in p{*dClk*-WT};+/+ runs about 1hr faster than the control situation, strongly suggesting that augmenting dCLK levels (Figure S3.7) impairs the ability of the circadian timing system to entrain to daily temperature cycles.

Temperature cycles can entrain behavioral rhythms in *Drosophila* exposed to constant light (LL) despite the fact that LL normally abolishes circadian rhythms [144-146]. Intriguingly, constant light exposure rescues the ability of the p{*dClk*-15A};*Clk*^{out} flies to maintain a more stable 24-hr phase relationship with the temperature cycle (Figure 3.5, panels G-J), further supporting the notion that entrainment to temperature but not light is specifically impaired in these flies. Taken together, these data suggest that in the absence of light, the dCLK phosphorylation program is required for the proper entrainment of behavioral rhythms to daily temperature cycles and reveal an unanticipated role for a central clock transcription factor in modality-specific entrainment.

Molecular oscillations in p{*dClk-15A*};*Clk*^{out} flies differ from those in control flies after prolonged exposure to temperature cycles

In p{*dClk*-WT};*Clk*^{out} flies, hypo/intermediate-phosphorylated dCLK isoforms are present throughout the thermo phase in TC (Figure 3.6A, lane 2 and 3), while hyper-phosphorylated dCLK isoforms are only observed during the latter half of the cryo phase (Figure 3.6A, lane 5 and 6). This temporal pattern in dCLK phosphorylation is similar to that observed in LD cycles and is consistent with prior work showing that the circadian clock mechanism in *Drosophila* can be synchronized by daily temperature cycles [113, 144]. As expected and similar to results using LD cycles, dCLK-15A attains higher overall daily levels and does not exhibit significant phosphorylation in p{*dClk*-15A};*Clk*^{out} flies exposed to temperature cycles (Figure 3.6A).

Since p{*dClk*-15A};*Clk*^{out} flies display altered entrainment to TC cycles that becomes progressively more abnormal with prolonged duration, we tested whether the molecular clock might also exhibit a more defective status with increasing time by measuring the levels of the *tim* mRNA at both early (e.g., day 3) and later (e.g., day 6) days of exposure to TC. We chose *tim* mRNA levels as a surrogate marker for clock

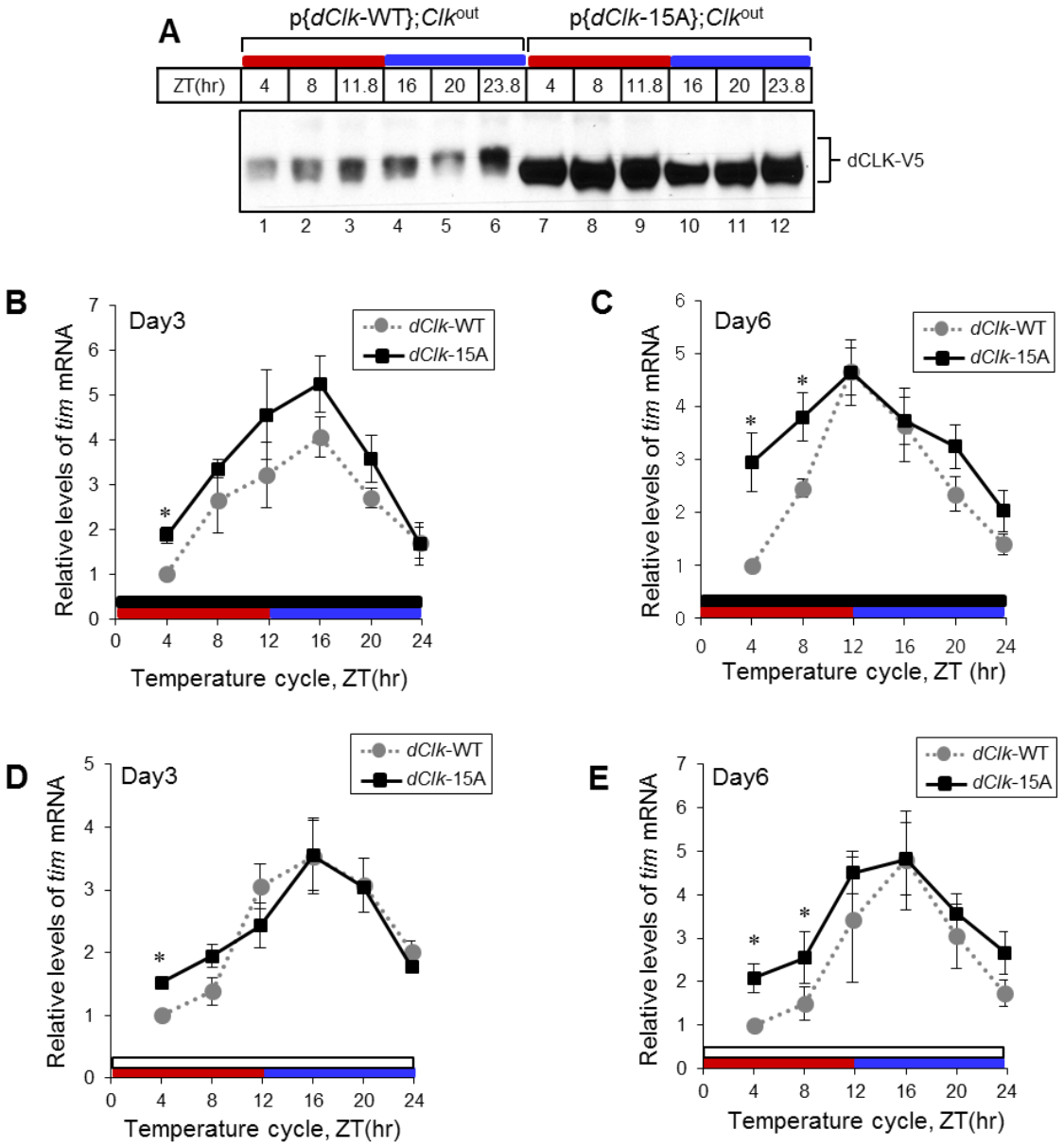

Figure 3.6. Molecular rhythms in p{*dClk*-15A};*Clk*^{out} flies show increased alterations after prolonged entrainment to temperature cycles.

Adult flies of the indicated genotype were entrained in 12hr:12hr of 24°C:29°C temperature cycle in the absence (A-C) or presence of light (D, E). During the third (A, B, D) and sixth day (C, E) of TC, flies were collected and protein (A) or RNA (B-E) was extracted from fly heads. Protein extracts were analyzed by immunoblotting using anti-V5 Ab to probe dCLK. Quantitative real-time RT-PCR was performed to measure the relative levels of *tim*

Figure legend of figure 3.6 continued

mRNA. Shown are the average values from three independent experiments using p{*dClk*-15A}, 6M;*Clk*^{out} flies. *p < 0.05; error bars denote SEM. Red horizontal bars represent thermo phase, blue horizontal bars represent cryo phase, black horizontal bars represents constant dark conditions, and white horizontal bars represents constant light conditions.

dynamics because it normally has a robust high amplitude rhythm (Figure 3.4A, B; [147]), facilitating measuring changes in molecular oscillations over the course of several days. Although the daily average levels in *tim* mRNA were higher in p{*dClk*-15A};*Clk*^{out} flies on day three of TC compared to the wild-type situation (Figure 3.6B), consistent with findings in LD (Figure 3.4B), both genotypes showed similar and robust cycling patterns. However, by day six of TC, the *tim* mRNA oscillation pattern in p{*dClk*-15A};*Clk*^{out} flies became significantly different from that observed for p{*dClk*-WT};*Clk*^{out} flies (Figure 3.6C). Most notably, while *tim* mRNA cycling still manifested high-amplitude cycling in p{*dClk*-WT};*Clk*^{out} flies on day six of TC, *tim* mRNA levels during the upswing phase were significantly higher in p{*dClk*-15A};*Clk*^{out} flies, resulting in an abnormal cycling pattern. Although we did not establish a causal relationship between the observed loss in normal *tim* mRNA cycling and the defective behavioral entrainment in p{*dClk*-15A};*Clk*^{out} flies during TC, the results clearly show that prolonged exposure to TC is not only associated with increasingly altered phasing of rhythms at the behavioral level (Figure 3.5) but also at the molecular level.

As with behavioral rhythms prior work showed that circadian molecular cycles can be synchronized to TC in the presence of constant light [144, 145]. In agreement with the observation that constant light exposure enabled p{*dClk*-15A};*Clk*^{out} flies to more robustly synchronize to temperature cycles (Figure 3.5), daily rhythms in the levels of *tim* mRNA for both genotypes were quite similar even after six days in constant light during TC (Figure 3.6D and E), indicating the clock in p{*dClk*-15A};*Clk*^{out} flies is functioning in a more wild-type manner under these conditions. Taken together, while this molecular analysis is of limited scope, it suggests that constant light exposure facilitates the ability of p{*dClk*-15A};*Clk*^{out} flies to entrain to TC by enhancing normal clock function.

DISCUSSION

Phosphorylation of clock proteins plays diverse roles in circadian oscillatory mechanisms by regulating numerous aspects of clock protein metabolism/activity, including time-of-day dependent changes in stability, transcriptional activity and subcellular localization [29, 30, 122]. Although dCLK, the master transcription factor in the *Drosophila* circadian clock [140, 148], undergoes daily changes in phosphorylation, the physiological role of dCLK phosphorylation was not clear. As a means to address this issue, we first identified phosphorylation sites on dCLK purified from cultured *Drosophila* S2 cells (Table 3.1 and Figure 3.1A). To examine the *in vivo* significance of dCLK phosphorylation, we generated transgenic flies expressing dCLK-15A wherein 15 serine residues that were identified as sites (or possible sites) of phosphorylation were switched to alanine, and examined circadian behavior in a Clk^{out} genetic background. Our results indicate that global phosphorylation of dCLK is an important aspect of setting clock speed by regulating the daily levels and/or activity of dCLK. This is consistent with earlier work suggesting dCLK is the rate-limiting component in the central transcriptional/translational feedback loop (TTFL) in the *Drosophila* clock mechanism, and that increasing the levels of dCLK lead to shorter behavioral periods [23, 139, 140]. A surprising finding is that entrainment to daily temperature cycles but not light-dark cycles are highly dependent on dCLK phosphorylation. These results suggest a novel role for phosphorylation in circadian timing systems; namely, the effective strength of an entraining cue can be modulated by adjusting the dynamics of the TTFL via controlling the levels/activity of a master circadian transcription factor (see below).

In this study, we show that dCLK undergoes multi-site phosphorylation. Among the phospho-sites identified, seven serine residues are situated immediately N-terminal to a proline, indicating a major role for the CMGC group of kinases. Indeed, studies using cultured S2 cells suggested that dCLK is a potential target of several distinct CMGC

kinases [126]. More recent work also identified the pro-directed kinase NEMO as a dCLK-relevant kinase [92]. Ongoing work is aimed at identifying the kinases responsible for targeting the different phospho-sites on dCLK. It should be noted that in this study we mapped phosphorylation sites on dCLK expressed in S2 cells, which when resolved by SDS-polyacrylamide gel electrophoresis is mainly observed as two major electrophoretic mobility bands corresponding to non/hypo-phosphorylated isoforms and an 'intermediate' more highly phosphorylated slower migrating species [10]. Although DBT is endogenously expressed in S2 cells, the addition of exogenous DBT and/or the inhibition of protein phosphatases leads to the detection of hyper-phosphorylated isoforms of dCLK in S2 cells [10]. Thus, it is likely that we did not identify all the phospho-sites on dCLK. However, we cannot rule out the possibility that there were minor levels of hyper-phosphorylated dCLK in our preparations that were above the detection limit for phospho-site mapping by mass spectrometry. Irrespective, the phospho-sites that we identified in S2 cultured cells make a clear contribution to the daily dCLK phosphorylation program in flies and contribute to the circadian timing system.

Elimination of phosphorylation sites from dCLK (dCLK-15A) leads to significant increases in the overall daily levels of dCLK in flies, which is well correlated with previous reports in S2 cells showing that hyper-phosphorylated dCLK is sensitive to degradation [10, 124]. In general, global phosphorylation appears to reduce the stabilities of clock proteins by generating one or more phospho-degrons that are recognized by E3 ubiquitin ligases, which ultimately leads to the accelerated degradation of the phosphorylated isoforms via the proteasome pathway [32]. The E3 ligase termed CTRIP appears to directly regulate the levels of dCLK (and possibly PER), although the role of dCLK phosphorylation in this mechanism, if any, is not clear [149]. When assayed in S2 cells the stability of dCLK-16A was similar to that of dCLK-WT (e.g., Figure 3.1 and Figure S3.2). Because differences in transcript levels cannot explain the significantly higher levels of

dCLK-15A in flies compared to dCLK-WT (Figure 3), it is almost certain that dCLK-15A is a more stable protein in clock cells. Thus, it appears that S2 cells do not fully recapitulate the *in vivo* role of phosphorylation on dCLK degradation. If we did miss mapping some sites on hyper-phosphorylated dCLK that are critical for regulating stability it is possible that these sites can still be phosphorylated on dCLK-15A expressed in S2 cells but not in flies. For example, hyper-phosphorylation of dCLK might depend on prior phosphorylation at one or more of the 15 phospho-sites we identified, and this dependency might be more strict in flies compared to the S2 cell over-expression system. Hierarchical phosphorylation has been demonstrated for other clock proteins, such as *Drosophila* PER and mammalian CLK [38, 40, 130]. Future work will be required to determine if there are other phospho-sites besides those we identified that regulate dCLK stability in flies.

Besides regulating the stability of core clock transcription factors, phosphorylation modulates trans-activation potential [129, 130, 150-153]. dCLK-15A expressed in S2 cells exhibited normal binding to CYC (and PER) but exhibits more potent transcriptional activity, at least in the context of a simple E-box driven expression (Figure 3.1D). Consistent with this, the levels of *per* and *tim* mRNAs in p{*dClk*-15A};*Clk*^{out} flies are higher compared to the control situation (Figure 3.4A, B). Of course, phosphorylation also affects the levels of dCLK-15A in flies, so at this stage it is not possible to determine how much the increased *per*/*tim* transcript levels are due to changes in the levels or activity of dCLK-15A. Nonetheless, our results strongly suggest that in wild-type flies the levels and/or activity of dCLK act in a rate-limiting fashion during the daily accumulation phase of *per/tim* transcripts and possibly other targets. In addition, the phospho-sites that we identified do not seem to be play a major determinant in feedback repression by PER and associated factors. Strong repression was observed in S2 cells for the dCLK-15A version (Figure 3.1E) and the normal daily downswing in *per*/*tim* levels occurred in p{*dClk*-15A};*Clk*^{out} flies

(Figure 3.4A and B). However, it is possible that we missed some phospho-sites that more specifically regulate the transcriptional activity of dCLK.

At the behavioral level, p{*dClk*-15A};*Clk*^{out} flies exhibit short period rhythms, consistent with prior work showing that increasing the dosage of *dClk* quickens the pace of the clock [139, 140]. In light-dark cycles, p{*dClk*-15A};*Clk*^{out} flies maintain a stable phase relationship with the entraining environment, displaying the typical anticipatory bimodal activity pattern (Figure 3.2). Moreover, in a daily light-dark cycle the timing of the morning and especially evening peak of activity is shifted in flies with different endogenous periods, appearing earlier in fast clocks and later in slow clocks [112]. Indeed, the p{*dClk*-15A};*Clk*^{out} flies follows this trend as the evening (and morning) bout of activity in LD is earlier compared to control flies (Figure 3.2). Together, these results indicate that although global phosphorylation of dCLK is an important determinant in setting clock speed, it plays little to no role in photic entrainment.

Surprisingly, the elimination of phosphorylation sites on dCLK strongly influences circadian behavior in daily temperature cycles (Figure 3.5). Temperature cycles with amplitudes of only 2° to 3°C robustly synchronizes circadian rhythms in *Drosophila* and other organisms [112, 144, 154-158]. When exposed to temperature cycles of 24°C/29°C, control p{*dClk*-WT};*Clk*^{out} flies manifested the typical bimodal activity pattern with bouts of activity anticipating the two temperature transition points, similar to that occurring during entrainment to LD cycles (Figure 3.5A and S3.5A). However, even during the first days in TC, p{*dClk*-15A};*Clk*^{out} flies already exhibit a very abnormal phase alignment with 'morning' and 'evening' bouts of activity that occur much earlier, around the middle of the cryo- and thermal-phases, respectively (Figure 3.5B and S3.5B, C). The advanced timing of the morning and evening bouts of activity is much earlier than would be expected based solely on the 1.5 hr shorter circadian period in p{*dClk*-15A};*Clk*^{out} flies (Table 3.3). That

entrainment to TC is highly defective in p{*dClk*-15A};*Clk*^{out} flies is even more dramatically underscored by the progressive advances in the evening component of activity on subsequent days (Figure 3.5). Although not as apparent, flies with increased dosage of *dClk* (p{*dClk*-WT};+/+ flies) also showed progressively earlier evening activity bouts in thermal cycles (Figure 3.5C and F) but not LD cycles, further suggesting that increased levels/activity of dCLK are causally linked to the inability of maintaining a stable phase relationship with TC. Because the timing of the evening activity in both p{*dClk*-15A};*Clk*^{out} and p{*dClk*-WT};+/+ flies occurs progressively earlier during TC, our results strongly suggest that these flies are only weakly synchronized to TC and are partially free-running at their faster endogenous periods.

In trying to determine why p{*dClk*-15A};*Clk*^{out} flies might exhibit a defect in temperature entrainment but not photic entrainment, it is important to note that several lines of evidence support the notion that light is a more potent synchronizer of the clock in *D. melanogaster* compared to temperature entrainment, including the use of out-of-phase light/dark and temperature cycles [118]. In addition, lowering the levels/function of the key photic entrainment photoreceptor CRYPTOCHROME (CRY) increases the ability to synchronize to TC [159], suggesting the dominance of light input under normal conditions. Also, it takes many more days to shift the phase of the clock via TC compared to LD cycles [113]. The overall strength of light in *D. melanogaster* entrainment is not surprising given the ability of light pulses to evoke the rapid degradation of TIM and the great sensitivity of *Drosophila* CRY/TIM to light [160].

Indeed, constant light rescues the ability of TC to stably entrain behavioral rhythms in p{*dClk*-15A};*Clk*^{out} (Figure 3.5, G-J), presumably by maintaining the clock in a more normal state (Figure 3.6). Intriguingly, prior work showed a similar pattern for the classic *per*^{S} and *per*^{L} mutants that display short (19 hr) and long (29 hr) endogenous rhythms, respectively [158]. That is, while wild-type flies entrain to TC in DD or LL, but *per*^{S} and

per^{L} flies only entrain to TC in LL [158]. This suggests that alterations in the PER protein rhythm might preferentially disrupt thermal entrainment. In the case of p{*dClk*-15A};*Clk*^{out} flies the amplitude of the PER abundance cycle is increased reaching higher peak values (Figure 3.4). Clocks with higher amplitudes are more resistant to entrainment by weak zeitgebers [161-163]. Relevant to this discussion, reducing CLOCK activity in mice decreased the amplitude of the circadian pacemaker and *per* gene expression, enhancing the ability to evoke phase shifts in behavioral rhythms [164, 165]. Thus, a simple model for our results is that the increased *per* mRNA and protein rhythms in p{*dClk*-15A};*Clk*^{out} flies leads to an increase in pacemaker amplitude minimizing their ability to synchronize to weaker entraining signals such as TC. However, it should be noted that higher amplitude rhythms of cycling mRNAs are highly suggestive but not definitive proof of an increase in oscillator strength. A standard approach to infer the relative amplitude of a clock is to increase the strength of the entraining signal, which should enhance its entrainment potential [161, 162, 166].

Although a change in the amplitude of the clock in p{*dClk*-15A};*Clk*^{out} flies offers a plausible explanation for the preferential defect in temperature entrainment, there are other possibilities. For example, CRY-positive clock cells are more important for entraining to LD cycles, whereas CRY-negative clock cells are more important for TC entrainment [118]. Thus, dCLK-15A could have preferential effects in CRY-negative cells to lessen their contribution, impairing TC entrainment. Another more speculative idea is that the phosphorylation of dCLK can act as a thermal sensor, although this would be specific to temperature entrainment as temperature compensation appears normal in the p{*dClk*-15A};*Clk*^{out} flies (Table 3.2). Clearly, future studies will be required to better address the mechanism underlying the impaired synchronization of p{*dClk*-15A};*Clk*^{out} flies to temperature cycles. However, our findings reveal that phosphorylation of a key rate-limiting circadian transcription factor is critical for entrainment to daily temperature

cycles. Indeed, the CLOCK protein in zebrafish [157] was shown to be regulated by temperature, suggesting a universal role for CLOCK in the adaptation of animal circadian clocks to thermal cues.

Contributions: Evrim Yildirim created the *Clk* transgenic construct and supplied this construct and wild type transgenic flies for this study. Fanny Ng, Yixiao Liu, Guruswamy Mahesh in Paul Hardin's lab created the Clk^{out} flies. Jens T. Vanselow in Achim Kramer's lab did the mass spectrometry experiments to identify phospho sites on CLK. Euna Lee, Eun Hee Jeong, Hyun-Jeong Jeong in Eun Young Kim's lab performed the experiments presented in this chapter.

SUPPLEMENTARY FIGURES FOR CHAPTER 3

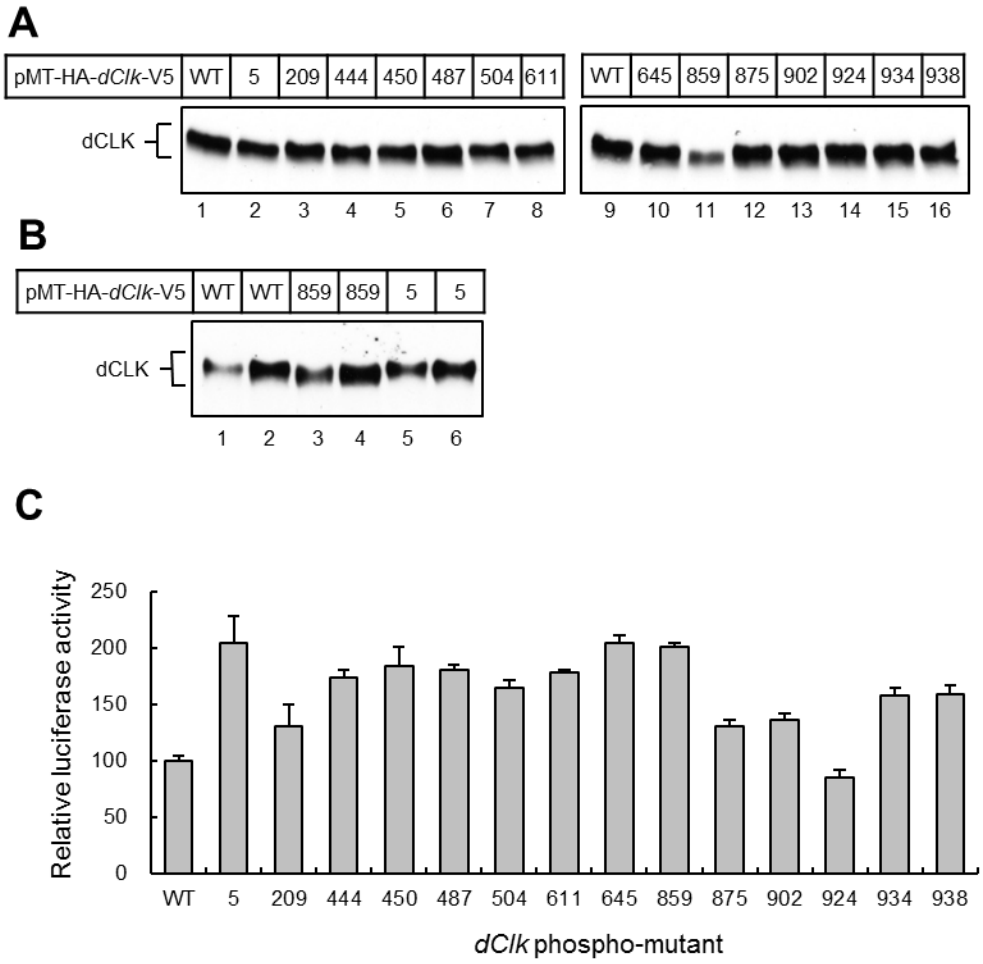

Figure S3.1. Analysis of CLK phosphorylation site mutants for electrophoretic mobility and transcriptional activity in S2 cells.

(A, B) S2 cells were transiently transfected with 500ng of wild-type (WT) or serine to alanine mutated version of pMT-HA-*dClk*-V5. Mutated sites are indicated on the top. Expression of dCLK was induced 24hr after transfection by adding 500μM $CuSO_4$ to the medium. Cells were harvested 24hr after induction, and protein extracts were subjected to western blot analysis. dCLK was visualized with anti-V5 Ab. Please note that the decrease in the levels of dCLK S859A (A) was not reproducible as shown in (B). (C) Shown are the average values for relative E box dependent luciferase activity in the

Figure legend of figure S3.1 continued

presence of 2ng of wild-type (WT) or serine to alanine mutated version of pMT-HA-*dClk*-V5. dCLK-S875A was included as randomly chosen serine to alanine mutant.

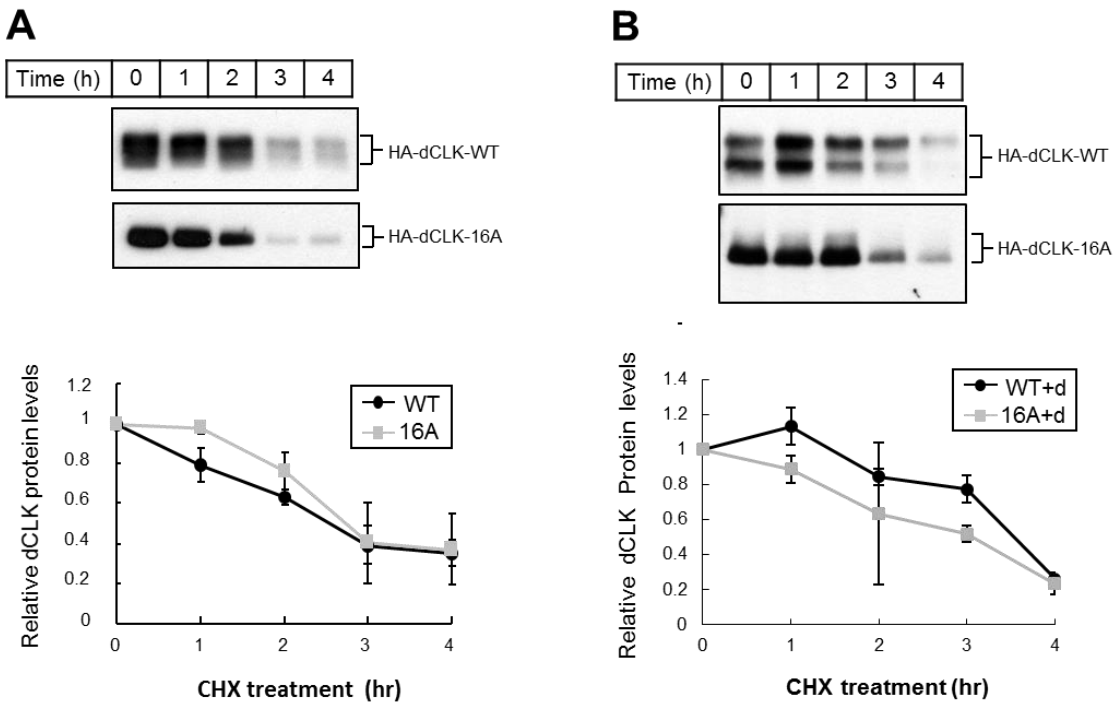

Figure S3.2. Stability of dCLK-WT and dCLK-16A protein in S2 cells.

(A, B) S2 cells were transiently transfected with 300ng of pMT-HA-*dClk* (WT) or pMT-HA-*dClk*-15A (15A) singly (A) or in combination with 600ng of pMT-*dbt*-V5 (B). Expression of dCLK and DBT was induced 24hr after transfection by adding 500μM $CuSO_4$ to the medium. 24hrs post induction, 10μg/ml of cycloheximide (CHX) was treated to inhibit translation. Cells were harvested at the indicated time points and protein extracts were subjected to immunoblotting. dCLK was visualized with anti-HA (3F10) antibody. Shown are the representative blots for each analysis and relative levels of dCLK proteins were determined by measuring band intensities of immunoblot using image J software.

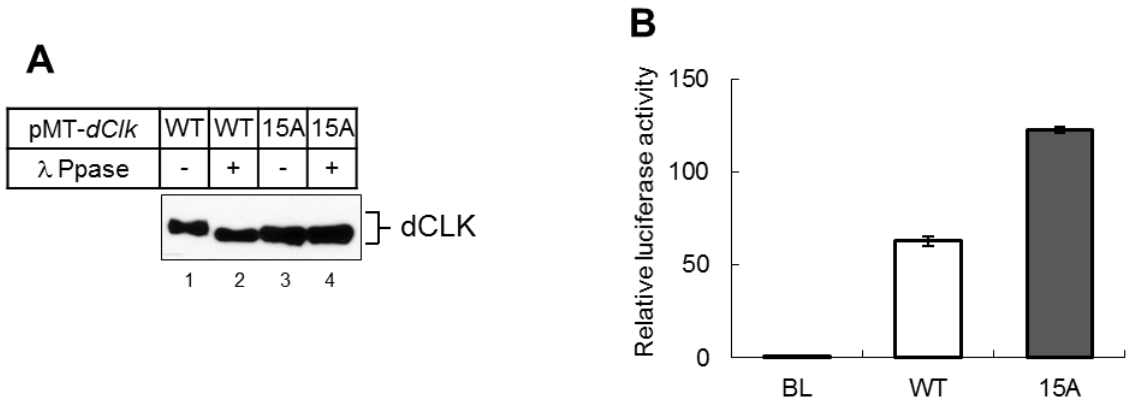

Figure S3.3. dCLK-15A manifests similar alterations as dCLK-16A compared to dCLK-WT in terms of stability and transcriptional activity in S2 cells.

(A) S2 cells were transiently transfected with 500ng of pMT-HA-*dClk* (WT) or pMT-HA-*dClk*-15A (15A). Expression of dCLK was induced 24hr after transfection by adding 500μM $CuSO_4$ to the medium. Cells were harvested 24hr after induction and protein extracts were first subjected to immunoprecipitation using anti-HA (12CA5) antibody and immune complexes were incubated in the absence (-) or presence (+) of λ phosphatase followed by immunoblotting. (B) Shown are the average values from three independent experiments for relative E box dependent luciferase activity in the absence (BL) or presence of pMT-*dClk*-V5 (WT) or pMT-*dClk*-15A (15A).

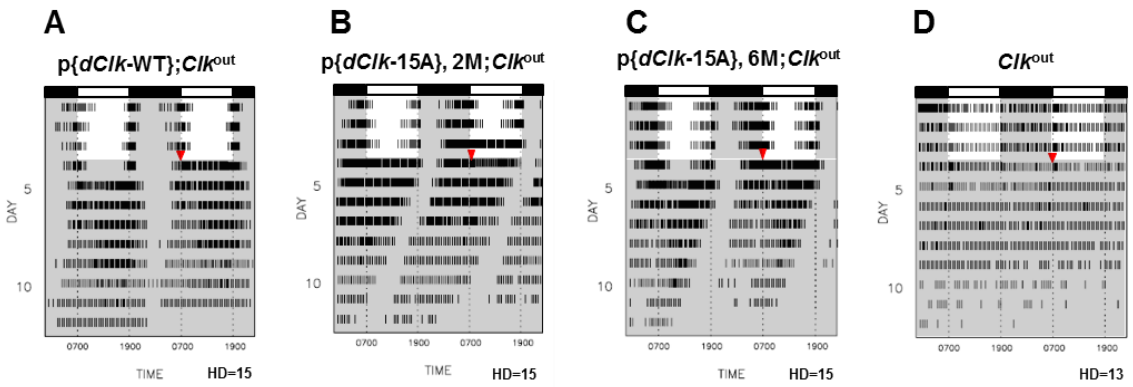

Figure S3.4. Representative daily locomotor activity patterns of p{*dClk*-WT};*Clk*^{out} and p{*dClk*-15A};*Clk*^{out} flies in light/dark cycles.

(A – D) Adult flies of the indicated genotype (as indicated, top of panels) were entrained with 12hr:12hr light:dark cycles for 4 days followed by 8 days in DD. Black and white bar on top of each actogram indicates when lights were off and on, respectively. Red arrowhead indicates when DD starts. The vertical black bars on each row of the actogram depict the activity of the fly (measured in 30 min intervals). To better visualize rhythmic behavior, each day's worth of activity recordings was double plotted. HD, hash density of the actogram.

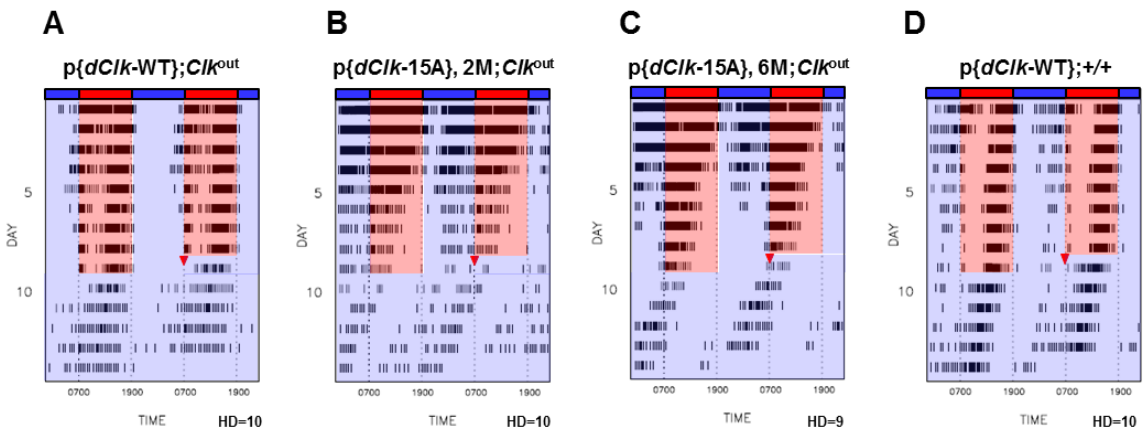

Figure S3.5. Representative daily locomotor activities of p{*dClk*-WT};*Clk*^{out} and p{*dClk*-15A};*Clk*^{out} flies in temperature cycles in the absence of light.

(A – D) Adult male files for a given genotype (as indicated, top of panels) were entrained in 12hr:12hr temperature cycles of 24 °C:29 °C for 9 days and maintained at 24 °C for 7 days in the absence light. The vertical black bars on each line of the actogram depict fly activity (measured in 30 min intervals). Each day's worth of activity recordings was double plotted to better visualize rhythmic behavior. Red horizontal bars and blue horizontal bars below each panel indicated thermo- or cryo-phases, respectively. The results clearly indicate that the offset in evening activity occurs progressively earlier in p{*dClk*-15A};*Clk*^{out} flies even during TC. HD, hash density of the actogram.

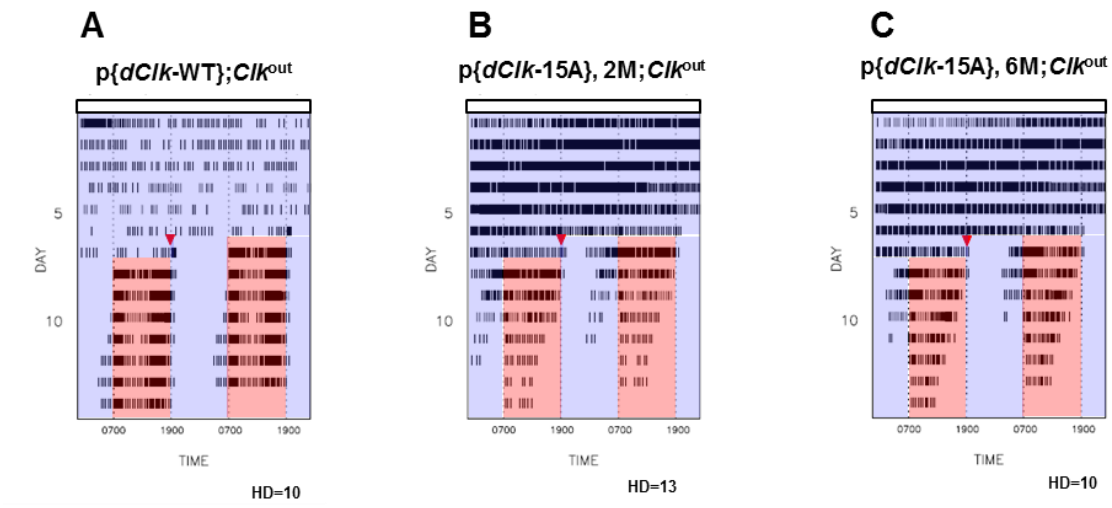

Figure S3.6. Representative daily locomotor activities of p{*dClk*-WT};*Clk*^{out} and p{*dClk*-15A};*Clk*^{out} flies in temperature cycles after exposure to constant light.

(A – C) Adult male files for a given genotype (as indicated, top of panels) were exposed to constant light for 6 days and then entrained in 12hr:12hr temperature cycles of 24 °C:29 °C for 7 days in the absence light. The red arrowhead indicates when the lights were turned off. The vertical black bars on each line of the actogram depict fly activity (measured in 30 min intervals). Each day's worth of activity recordings was double plotted to better visualize rhythmic behavior. Flies became arrhythmic shortly after exposure to constant light. The results clearly indicate that the offset in evening activity occurs progressively earlier in p{*dClk*-15A};*Clk*^{out} flies during TC. HD, hash density of the actogram.

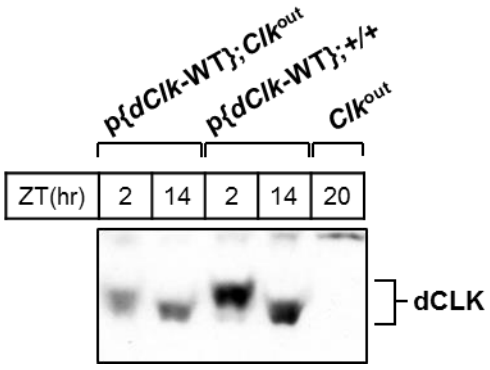

Figure S3.7. dCLK protein levels and phosphorylation in p{*dClk*-WT};*Clk*^{out} and p{*dClk*-WT};+/+ flies.

Adult flies of a given genotype (indicated at the top of panels) were collected at the indicated time in LD (ZT) and protein extracts analyzed by immunoblotting using the anti-dCLK antibody (gp208). Note that the levels of dCLK are higher in p{*dClk*-WT};+/+ flies.

Chapter 4: *bantam* miRNA imparts robustness to circadian rhythms by increasing CLOCK levels in key pacemaker neurons

(Yildirim, Houl, Liu, Ng, Yu, Mahesh, Hardin & Edery, as originally submitted, to be combined with Chapter 5 for a manuscript)

INTRODUCTION

By means of endogenous circadian (approx. 24 hr) "clocks" or pacemakers that can be synchronized to daily and seasonal changes in external time cues (zeitgebers), most notably visible light and ambient temperature, life forms anticipate environmental transitions, perform activities at biologically advantageous times during the day and undergo characteristic seasonal responses (reviewed in [1]). In general, circadian pacemakers are cell-autonomous entities based on a small number of species or tissue specific clock genes, whose RNA and protein products participate in interconnected positively and negatively acting transcriptional-translational feedback loops [4]. As a result of the design principles inherent in these autoregulatory molecular loops, the RNA and protein products from one or more of the core clock genes manifest daily rhythms in abundance that are central to normal clock progression. Posttranslational regulatory schemes, most notably time-of-day specific differences in phosphorylation, govern daily changes in clock protein abundance, key aspects determining the pace and phase of the clock (recently reviewed in, [29, 30]).

Recent findings implicate an additional layer of post-transcriptional regulation with the discovery that microRNAs (miRNAs) regulate clock mechanisms [70]. In addition, a growing list of miRNAs undergo daily oscillations in abundance [68, 70, 167-169]. While a role for miRNAs might not be surprising based on the estimate that a substantial fraction of mRNAs are potential targets for regulation by miRNAs, their roles in circadian systems

are not well understood. miRNAs are short (~22 nt) non-coding RNAs that inhibit mRNA translation and/or stability (recently reviewed in, [63, 170]). The biogenesis of miRNAs involves several maturation steps whereby a primary transcript (pri-miRNA) is cleaved to a smaller hairpin-containing pre-miRNA (~60-70 nt) and finally the mature single-stranded miRNA is assembled into an active RNA-induced silencing complex (RISC) where they are bound by a member of the argonaute (Ago) family. In metazoans, target recognition is thought to be based largely on base-pairing between binding sites located primarily within the 3' UTRs of mRNAs and the "seed" sequence at the 5' end of the miRNA (usually nucleotides 2-7 or 8) (reviewed in [63, 170]). An emerging realization is that miRNAs appear to fine-tune gene expression and can add robustness to gene expression networks and biological systems [171-173], properties that would appear extremely relevant to the highly dynamic systems underlying circadian rhythmicity.

We recently showed that several miRNAs in *Drosophila melanogaster* exhibit daily oscillations in levels [68]. Studies using *D. melanogaster* as a model system have led to many seminal insights into mechanisms underlying circadian clocks, especially those operating in animals [6, 30]. The general framework of the clock in *Drosophila* is usually depicted as two interconnected transcriptional feedback loops. In the "main" circuit, the transcription factors CLOCK (CLK) and CYCLE (CYC) heterodimerize and bind E-box containing DNA elements to drive expression of *period* (*per*) and *timeless* (*tim*). PER and TIM proteins enter the nucleus around the middle of the night where PER promotes repression of CLK-CYC-mediated transcription by presumably binding CLK and acting to seed an inhibitory complex. The timing and duration of PER-dependent transcriptional repression is modulated by a complex web of phosphorylation programs that drive daily changes in the subcellular localization and stability of PER. This PER-dependent phase-specific inhibition of CLK-CYC-mediated transcription generates cyclical gene expression of not only several core clock genes, such as *per* and *tim*, but also downstream output

genes, contributing to circadian rhythms in cellular, physiological and behavioral phenomena. A second transcriptional autoregulatory loop generates oscillations in *Clk* mRNA levels that are antiphase to those of *per*/*tim* transcripts, although CLK protein levels are relatively constant throughout a daily cycle [10, 124, 174]. Thus, CLK plays a central role in the intertwined circadian transcriptional loops and is thought to be a limiting factor in the core clock mechanism [19, 23, 175]. A similar mechanism whereby PER proteins are critical factors in regulating daily cycles in the transcriptional activity of a CLOCK-BMAL1 (homolog of CYC) complex is also observed in the mammalian clockworks [29].

Using a *Drosophila* cell culture system we show that the 3' untranslated region (UTR) of *Clk* contains at least two binding sites for the *bantam* (*ban*) miRNA. We generated a novel *Clk* null mutant as a basis for assaying the function of *Clk* transgenes and show that *ban* sites on the *Clk* 3' UTR function in a combinatorial manner to increase the amplitude of behavioral rhythms. Surprisingly, the levels of CLK protein in the key pacemaker neurons required for driving circadian behavioral rhythms exhibit dramatic reductions in flies with mutated *ban* sites on *Clk*. We suggest that *ban*, a miRNA initially shown to have strong biological effects on growth and development [80, 176], also plays a significant role in the core clockworks of *Drosophila* but apparently in a non-conventional manner by up-regulating CLK protein levels in a key sub-group of pacemaker cells.

MATERIALS AND METHODS

Fly strains used in this study

The following fly strains were used in this study and were previously described: *yw*;;UAS-*bantam* [80], *timGAL4* [11], *tim*(UAS)*GAL4* [177], *pdfGAL4* [178], *cryGAL4*(39) [179], *C929GAL4* [180], *gmrGAL4*, UAS-miR-7 [181], UAS-miR9a(#3) [65]; $ban^{\Delta 1}$, ban^{L1170} and *EP(3)3622* [176]. w^{1118} and *yw* mutants are part of our laboratory collection.

yw;PBac{y^{+}-attp-9A}VK00018 and *yw;*P{CaryP}attP40 were previously described [137, 182, 183] and obtained from the Bloomington Stock Center (Indiana, USA).

Clk^{out} deletion mutant generation and analysis

A deletion within *Clk* was generated by recombination between FRT sites from pBac{WH}Clk[f06808], which inserted 64bp into the first exon of *Clk*, and pBac{WH}Clk[f03095], which is inserted 5334bp upstream of exon 1 [120]. Flippase (FLP)-induced recombination was induced by a daily 1 hr heatshock at 37^{o}C given to hsFLP;;f06808/f03095 larvae and pupae. Three recombinants were recovered based on a lighter orange eye color due to loss of one pBac element, and each produced a deletion rather than a duplication of intervening *Clk* sequences. The remaining pBac insert in each recombinant strain was excised by crossing recombinants to to *w*;CyO, P{Tub-pBac\T}2/*wg*$^{Sp-1}$;+/6B flies, which express pBac transposase. The resulting *w*;CyO, P{TubpBac\T}2/*wg*$^{Sp-1}$;*Clk*-out/6B flies were then crossed to *w*;;TM2/TM6B, and white eyed progeny lacking the remaining pBac element were selected. The deleted region from all three *Clk* deletion strains was amplified with a primer upstream of f03095 (5' CGGAATATTGGACAACAAACAG 3') and downstream of f06808 (5'C AGCAGTGGAATCTTAATACAG 3') and sequenced. In each case, the deletion removed sequences between the initial pBac insertion sites. Three lines of evidence demonstrate that this *Clk* deletion is a null mutant. First, this deletion is behaviourally arrhythmic as a homozygote (Table 4.2) or in heterozygous form over either *Clk*^{Jrk} or a deletion that removes *Clk* and flanking genes (data not shown). Second, *Clk* mRNA is undetectable by qPCR in flies homozygous for the *Clk* deletion (data not shown). Third, in flies homozygous for the *Clk* deletion, CLK protein is not detectable on immunoblots (data not shown) or by immunostaining (Figure 4.3). We refer to this new *Clk* deletion allele as *Clk*^{out}.

Monitoring locomotor activity

Locomotor activity was continuously monitored and recorded in 5-min bins by placing individual adult male flies (3-7 days old) in glass tubes and using a Trikinetics (Waltham, MA, USA) system, as previously described [184]. Briefly, throughout the testing period flies were maintained at the indicated temperature and photoperiod [LD; where zeitgeber time 0 (ZT0) is defined as lights-on] for 5 days, followed by 6 days of constant dark conditions. Data analysis was done with the FaasX software (kindly provided by M. Boudinot, and F. Rouyer, CNRS, France). The histograms (eductions) showing the distribution of locomotor activity through a 24 hr period (e.g., see Figure S4.2) were obtained using the 'eduction' option of the FaasX software. The last 3 days worth of LD data were averaged for each fly, and data pooled to generate the group averages shown. A correction was applied to neutralize "startle responses" (i.e., increased bout of fly activity following the light-to-dark and dark-to-light environmental transitions. Free-running periods and power (amplitude or strength of the rhythm) were obtained using the *Chi*-square periodogram module available within the FaasX program using activity data collected in 30 min bins during the 6 consecutive days in DD. Flies with values for power $\geq$10, width $\geq$2, and periods between 20-30 hr were designated rhythmic. Values for individual flies were pooled to obtain an average value for each genotype.

Tissue culture constructs and measuring Luc activity

The pAc-*luc* (firefly *luciferase* gene under the actin 5C promoter; pAc), pAc-*bantam* (276bp fragment containing sequences for the *ban* miRNA and stem-loop structure fused downstream of pAc promoter) and '*bantam* sensor' (two fully complementary *ban* miRNA sites placed downstream of the pAc promoter) were previously described [99]. In addition, we mutated the pAc-*bantam* construct at the second and third positions on the seed region

to generate, pAc-ban(UU) (Figure 4.1C); this version also included complementary mutations in the hairpin). This was done by site-directed mutagenesis using the Quickchange site directed mutagenesis kit from Stratagene (La Jolla, CA, USA) in the presence of the following primers; ban(UU)-f1, ban(UU)-r1, ban(UU)-f2 and ban(UU)-r2. Plasmids containing *Clk* 3'UTR sequences were cloned into pAc-*luc* using the AscI and FseI restriction sites. To create pAc-*luc*-*Clk* 3' UTR fusion constructs the following primers were used; for the shorter *Clk* 3' UTR (Figure 4.1C), *AscI*-*clk*3'-f and *FseI*-*clk*3'-241-r; for the ~1.5kb *Clk* 3' UTR (*Clk*3'-*l*; Figure 4.2E), *AscI*-*clk*3'-f and *FseI*-*clk*-1580-r. Mutations in *ban* binding sites were generated by site-directed mutagenesis, resulting in the following constructs; *Clk*3'/ban(AA) for the short form (primers; ban1-f and ban1-r); and *Clk*3'-l/ban#1 (ban1-f and ban1-r), *Clk*3'-l/ban#2 (ban2-f and ban2-r) and *Clk*3'-l/ban#1-2 for the long form. All final constructs were verified by sequencing.

For luciferase assays, S2 cells were co-transfected with 0.5µg of pAc-*luc*-*Clk*3' (short or long versions of the *Clk* 3' UTR; see Figure 4.2) and 1µg of either pAc-*bantam* or an "empty" pAc plasmid. We also included 0.2µg of a plasmid expressing renilla *luciferease* as a transfection control. For each combination of plasmids, transfections were done in triplicate using Cellfectin reagent (Invitrogen, Carlsbad, CA, USA) according to manufacturer's instructions, and seeded in 6-well plates. After 2-3 days post-transfection, Luc activity was measured using the Dual-Glo *luciferase* assay system from Promega (Madison, WI, USA), according to manufacturer's instructions. The firefly Luc activity derived from the *luc*-*Clk* reporter genes was first normalized to renilla *luciferase* activity. For each *luc*-*Clk* reporter assayed, Luc activity levels in the absence of exogenously provided *ban* was normalized to 100 and values obtained in the presence of ectopic *ban* expressed relative to those obtained in its absence, as previously described [99].

Constructs for transgenic flies

To generate *Clk*-containing transformation vectors we used a recombineering mediated gap repair strategy that was previously described [137]. Homology arms were amplified using PCR from genomic DNA with primers *Clk*LA-f and *Clk*LA-r for the left arm; and *Clk*RA-f and *Clk*RA-r for the right arm. Right and left homology arms were cloned as AscI-BamHI and BamHI-NotI fragments into AscI and NotI digested *attB*-P[acman]-Ap^R-*SphI* by three way ligation to create *attB*-P[acman]*Clk*LARA. A BAC clone containing the *dClk* genomic region (RP98 5K6; obtained from the BACPAC Resource Center, Oakland, Ca, USA) was electroporated into SW102 cells [185]. Transformed cells were isolated on chlorampenicol-containing plates and verified by colony PCR using primers *Clk*LA-f and *Clk*LA-r. Subsequently, cells containing the BAC clone were grown at 32°C until OD_{600}=0.6 and heat shocked at 42°C for 15min to induce the recombination enzymes. The *attB*-P[acman]*Clk*LARA construct was linearized with BamHI and transformed into the BAC-containing cells by electroporation. Amplicilin resistant clones were identified by colony PCR for correct recombination events of both arms using the appropriate pairs of primers; MSC-F and c*lk*5'check-r, or *clk*3'check-f and MCS-R. The desired construct was further verified by sequencing with primers *clk*LAseq-f and RAseq-r. This construct, termed *attB*-P[acman]-*Clk*, contains genomic region beginning ~8kb before the translation start codon of *Clk* and ending ~2.5kb downstream of stop codon. Subsequently, we used site-directed mutagenesis (using the following primers; V5-f and V5-r) to introduce sequences encoding the V5 epitope tag just upstream of the translation stop codon, and in the process removed 1kb of the 3'-most genomic *Clk* region, resulting in the construct called *attB*-P[acman]-*Clk*V5 that ends at 1580bp beyond the translation stop signal (herein more simply identified as p{*Clk*WT}). This plasmid was also used as a template for introducing the *ban* binding site mutants analyzed here, which was accomplished by site

directed mutagenesis using primers *ban*1-f, *ban*1-r for the first *bantam* target site (ban#1) and *ban*2-f, *ban*2-r for ban#2 (Figure 4.1B and 4.2D).

The *Clk*-containing transformation vectors were injected into either *yw*;PBac{y$^+$-attp-9A}VK00018 or *yw;*P{CaryP}attp40 embryos by BestGene Inc. (Chino Hills, CA,USA) and Genetic Services (Cambridge, MA, USA), respectively. Multiple independent lines were obtained and crossed into the *Clk*^{out} genetic background such that the only functional copy of *Clk* is provided by the transgene. Although there were some variations in activity rhythms for independent lines of the same transgene when assayed in the *Clk*^{out} genetic background, the relative differences in the strengths of the activity rhythms between the different transgenes were observed for all lines independent of insertion site (Table 4.1 and data not shown). Thus, we routinely use flies with the same transgene interchangeably. For unclear reasons a few independent lines were not very healthy and we did not analyze them extensively.

RNA analysis

For RNA extraction, ~30 adult heads were homogenized using a motorized pestle in 200-300µl of TRI-reagent (Sigma) according to the manufacturer's instructions, and as described previously [102]. For 3' RACE (rapid amplification of cDNA ends) and poly(A) tail-length assay, the final RNA pellet was resuspended in RNAse free water and treated with RQ1 DNAse (Promega, Madison, WI, USA) for 45 min at 65^{o}C. For RNAse protection assays (RPA), the RNA pellet was resuspended in hybridization buffer (80% formamide, 100nM sodium citrate, 100nM sodium acetate, and 1mM EDTA).

3' RACE was done with the Generacer kit from Invitrogen (Carlsbad, CA, USA) according to manufacturer's instructions. To amplify the 3 'UTR of *Clk* cDNA, the primers *AscI-Clk*3'-f and Generacer3' provided with the kit were used.

To measure the length of the polyA tail, we used the Poly(A) tail length assay kit from USB (Cleveland, Ohio, USA) according to the manufacturer's instructions. To amplify the *Clk* poly(A) tail, primers *Clk*3'-133-f and *Clk*3'-962-f were used with the universal reverse primer supplied with the kit. These primers were chosen because they are ~100bp upstream of annotated 3' cleavage site and another suspected site ~1kb downstream of *Clk* translation stop signal (Figure 4.2).

RNAse protection assays were done essentially as previously described [22, 186]. Antisense probes for *Clk* 3' UTR were used to determine the relative abundance and cycling profiles of *Clk* transcripts and to check for the presence of "short" and "long" forms of the *Clk* 3' UTR (Figure 4.2). *Clk* probe1 contains *Clk* 3' UTR sequences between 100-345nt downstream of the stop codon, and *Clk* probe2 includes sequences between 472-634nt (Figure 4.2). The probes were generated by PCR with the following primers; *Clk* probe1, *Clk*3'-100-f and *Clk*3'345-r; *Clk* probe2, *Clk*3'472-f and *Clk*3'634-r. Subsequently, these PCR products were subcloned into pGEM-T vector (Promega, Madison, WI, USA). The vectors were linearized with EcoRI and T7 RNA polymerase (Applied Biosystems/Ambion, Austin, TX, USA) was used for *in vitro* transcription in the presence of α-^{32}P-UTP to create anti-sense radiolabeled probes. Protected bands were quantified with a PhosphorImager from Molecular Dynamics and values were normalized relative to those of RP49 transcripts, as previously described [186].

Immunostaining

Brains were dissected from flies collected at ZT1, dissected, fixed, immunostained with anti-CLK GP50, and imaged by confocal microscopy as described in Houl *et al*., 2008 [206].

RESULTS

Driving expression of *ban* in central pacemaker neurons yields longer behavioral rhythms

As an initial attempt to identify core clock genes that might be direct targets for regulation by miRNAs, we used the target prediction programs Pictar [187] and Targetscan [188] to search for potential mRNA-miRNA interactions. Recent findings measuring global changes in protein levels suggest that Pictar and Targetscan are the most reliable commonly used prediction programs to identify physiologically relevant targets [189]. We were intrigued by the observation that both programs predicted a putative binding region for the *bantam* (*ban*) miRNA within the *Clk* 3'UTR (Figure 4.1A), which is also conserved in other *Drosophila* species (Figure S4.1A). *Clk* plays a pivotal role in driving cyclical gene expression and is thought to the limiting component in the *Drosophila* clockworks [19, 23, 175], suggesting that even modest alterations in its regulation might lead to observable circadian phenotypes. *Ban* is one of the best-characterized miRNAs in *Drosophila* and has several biological functions, most notably in growth and development [80, 176, 190, 191] but also exhibits adult phenotypes in the central nervous system [192, 193]. In addition, *ban* miRNA expression is regulated by the *Wingless* (*Wnt*) signalling pathway [80, 194] and several members of this pathway also have roles in the *Drosophila* clock [30].

We first sought to determine if *ban* might have a circadian function by using the UAS/GAL4 binary system to drive its expression in brain pacemaker neurons underlying daily rhythms in activity. Transgenic flies bearing UAS-*ban* were crossed with a variety of *GAL4* driver lines. Progeny from the crosses were entrained (synchronized) for 4-5 days by exposing them to standard conditions of 12 hr light: 12 hr dark [12:12LD, where lights-on is defined as zeitgeber time (ZT) 0] at 25^{o}C and then maintained under constant dark conditions (DD) to measure clock-controlled free-running locomotor activity rhythms.

There are approximately 150 circadian clock neurons in the adult fly brain, bilaterally clustered into six groups of cells that function as a network to regulate daily rhythms in activity [53]. Ectopic expression of *ban* in all or most of the pacemaker neurons (i.e., *tim-GAL4* and *cry-GAL4*) but not the eyes (*gmr-GAL4*) significantly lengthens behavioural rhythms by 2-4 hr compared to the ~24 hr periods observed for control flies (Table 4.1 and Figure S4.2). In contrast, widespread expression of several other miRNAs (such as miR-7 and -9a) in the circadian cellular network had no noticeable effects on behavioral rhythms, arguing that the effects of *ban* on circadian periodicity cannot be accounted by general effects on the miRNA machinery resulting from forced expression of miRNAs in pacemaker neurons. In addition, although we cannot rule out non-specific effects from overexpressing a miRNA, recent findings based on genome-wide scale analysis suggest that even in cases where miRNAs are overexpressed they still exhibit high selectivity towards physiologically relevant targets [189, 195].

More restricted spatial expression in the ~20 brain neurons producing pigment dispersing factor (*pdf*) also lengthened behavioural periods but not to the extent observed with more widespread clock cell expression. A subset of these PDF-expressing cells, termed the small ventral lateral neurons (s-LNvs), are required for driving robust activity rhythms in free-running conditions [56, 178, 196]. Indeed, consistent with recent reports that the large LNvs (l-LNvs) function as part of a sensory-modulated arousal circuit but have little influence on the circadian system [197, 198], ectopic expression of *ban* in the l-LNvs as the only clock cells by using the *C929* driver [180] had no significant effect on period length (Table 4.1). Finally, ectopic expression of *ban* in pacemaker cells lengthened activity rhythms over a wide range of temperatures (Table S4.1 and data not shown). We did not observe any gross morphological defects or effects on the general health of flies with ectopic expression of *ban* (data not shown), indicating that the period-

Table 4.1: Locomotor activity rhythms for *bantam* overexpression lines, mutants and controls[a]

Genotype[b]	Period (hr ±SEM)	Power[c]	Rhythmicity (%)[d]	Total flies[e]
yw;;UAS-*bantam*	23.6±0.25	89.7	75.9	22
yw;*pdfGAL4*	24.6±0.1	81.1	64.5	20
pdfGAL4>UAS-*bantam*	25.2±0.09*	129.6	90.3	31
w;*tim*(UAS)*GAL4*	24.2±0.21	59.8	67.7	21
tim(UAS)*GAL4*>UAS-*bantam*	25.9±0.08*	129.7	96.3	27
yw;*timGAL4*/*cyo*	24±0.1	92.6	96.9	31
timGAL4>UAS-*bantam*	27.1±0.13*	102.5	100	32
w;*cryGAL4*(39)	24.9±0.63	40.5	32.3	31
cryGAL4(39)>UAS-*bantam*	26±0.08*	147	77.8	27
w;*gmrGAL4*	23.2±0.05	158.2	96.9	32
gmrGAL4>UAS-*bantam*	23.5±0.05	123.1	83.9	31
w;*C929GAL4*	24±0.58	47.8	33.3	9
C929GAL4>UAS-*bantam*	24.3±0.13	56.6	66.7	21
w;;UAS-miR-9a(#3)	23.5±0.07	142.1	93.8	32
tim(UAS)*GAL4*>UAS-miR-9a(#3)	24.2±0.11	188	100	6
w;;UASmiR-7/*TM6b*	24.1±0.1	117.5	89.3	28
tim(UAS)*GAL4*>UASmiR-7	24.3±0.24	102.3	87.5	32
w^{1118}	23.5±0.06	145.5	100	31
w;;$ban^{\Delta 1}$ /+	23.6±0.03	169.6	100	32
w;;ban^{L1170}/+	23.6±0.03	156.6	100	29
w;;*EP(3)3622*/+	23.5±0.04	158	100	32
w;;$ban^{\Delta 1}/ban^{L1170}$	23.3±0.07*	160.5	95.5	22
w;;$ban^{\Delta 1}$/*EP(3)3622*	23.3±0.05*	161.4	100	28

[a] Young male flies were maintained at 25°C and exposed to 5 days of 12:12 LD cycles followed by 6 days of DD.
[b] Independent transgenic lines are designated by the numbers in parenthesis.
[c] Power is a measure of the strength or amplitude of the rhythm in arbitrary units.
[d] Percentage of flies showing locomotor rhythms with a power value of ≥10 and a width value of ≥2
[e] Total number of flies that survived until the end of the experimental period.
* The periods of these crosses are statistically different (p-values<0.01) compared to both parental controls.

lengthening effects of increasing *ban* levels in pacemaker neurons is likely to be a direct effect on the clockworks.

We also measured activity rhythms in several hypomorphic *ban* alleles over a *ban* deletion ($ban^{\Delta 1}$) [80, 176] and noted that the flies exhibit small but significantly faster periods compared to appropriate heterozygous genetic controls (Table 4.1). These results suggest that *ban* levels are either not reduced to low enough levels in these mutants to evoke large changes in circadian periods and/or the circadian clock is more resistant to decreases in *ban* levels compared to increases. We could not evaluate adult locomotor activity rhythms in *ban* loss-of-function mutants as they are lethal [80, 176].

Despite the significant period-lengthening effects of driving the expression of *ban* in pacemaker neurons, there was little to no effect on the daily distribution of activity in 12:12LD cycles (Figure S4.2, panels A to M). In daily light/dark cycles, *D. melanogaster* exhibits two peaks of activity, a morning bout centred on ZT0 and an evening bout around ZT12 [199]. When exposed to daily light/dark cycles, the timing of the evening peak is usually later in flies with longer endogenous periods [199]. Because the timing of the morning and evening bouts of activity are not only regulated by the clock but also by light/dark cycles it is possible that the 12 hr photoperiod is overriding or “masking” the effects by which *ban* overexpression alters the endogenous period of the clock. Indeed, when *tim-GAL4>UAS-ban* flies were entrained to a shorter photoperiod (9:15LD) they exhibit a later evening peak compared to parental control flies (Figure S4.2, panels N to P). At present, it is not clear how light might attenuate the *ban*-mediated period-lengthening effects on the daily distribution of activity.

The *Clk* 3' UTR is longer than previously reported and contains multiple target sites for *ban*

As an initial attempt to evaluate the functionality of the predicted *ban* site on the *Clk* 3' UTR (Figure 4.1A), we assayed the ability of ectopically expressed *ban* to inhibit firefly *luciferase* (*luc*) reporter genes expressed in cultured *Drosophila* S2 cells [99]. The *Clk* 3' UTR was placed downstream of the *luc* open reading frame to generate *luc*-*Clk*3'. To better determine specificity, we mutated two bases in the putative *ban* site on *Clk* that are predicted to abrogate or attenuate base-pairing with the *ban* seed region, yielding the construct termed *luc*-*Clk*3'/ban(AA) (Figure 4.1B). We also evaluated the effects of an altered *ban* version with compensatory base-pair changes that are complementary to the *Clk*3'/ban(AA) mutant, termed [*ban*(UU)] (Figure 4.1B). As a control for *ban*-mediated repression of reporter activity, we used a previously described "*ban* sensor" that has a 3'UTR region containing two copies of sequences complementary to the entire mature *ban* miRNA [80, 99].

The presence of ectopic *ban* reduced expression of *luc*-*Clk*3' by ~40% but had no noticeable effect on *luc*-*Clk*3'/ban(AA) (Figure 4.1C). This amount of inhibition for a (presumably) single miRNA binding site is consistent with prior findings using a similar experimental platform [99] and is likely an underestimate as S2 cells are known to express endogenous *ban* (e.g., [200, 201]). The mutant form of *ban* [*ban*(UU)] lowered expression of *luc*-*Clk*3'/ban(AA) by ~40%, but there was no significant change in the expression of *luc*-*Clk*3', strongly suggesting that the *ban*-mediated inhibition is occurring via appropriate mRNA-miRNA base-pair interactions involving the seed region. Both the wildtype and mutant forms of *ban* inhibited the expression of the *ban* sensor by ~50%, not surprising given that the *ban* binding sites on this sensor are complementary to the entire mature miRNA. These results indicate that the *Clk* 3'UTR has a functional *ban* site situated within 141-163nt downstream of the translation stop signal (Figure 4.1A).

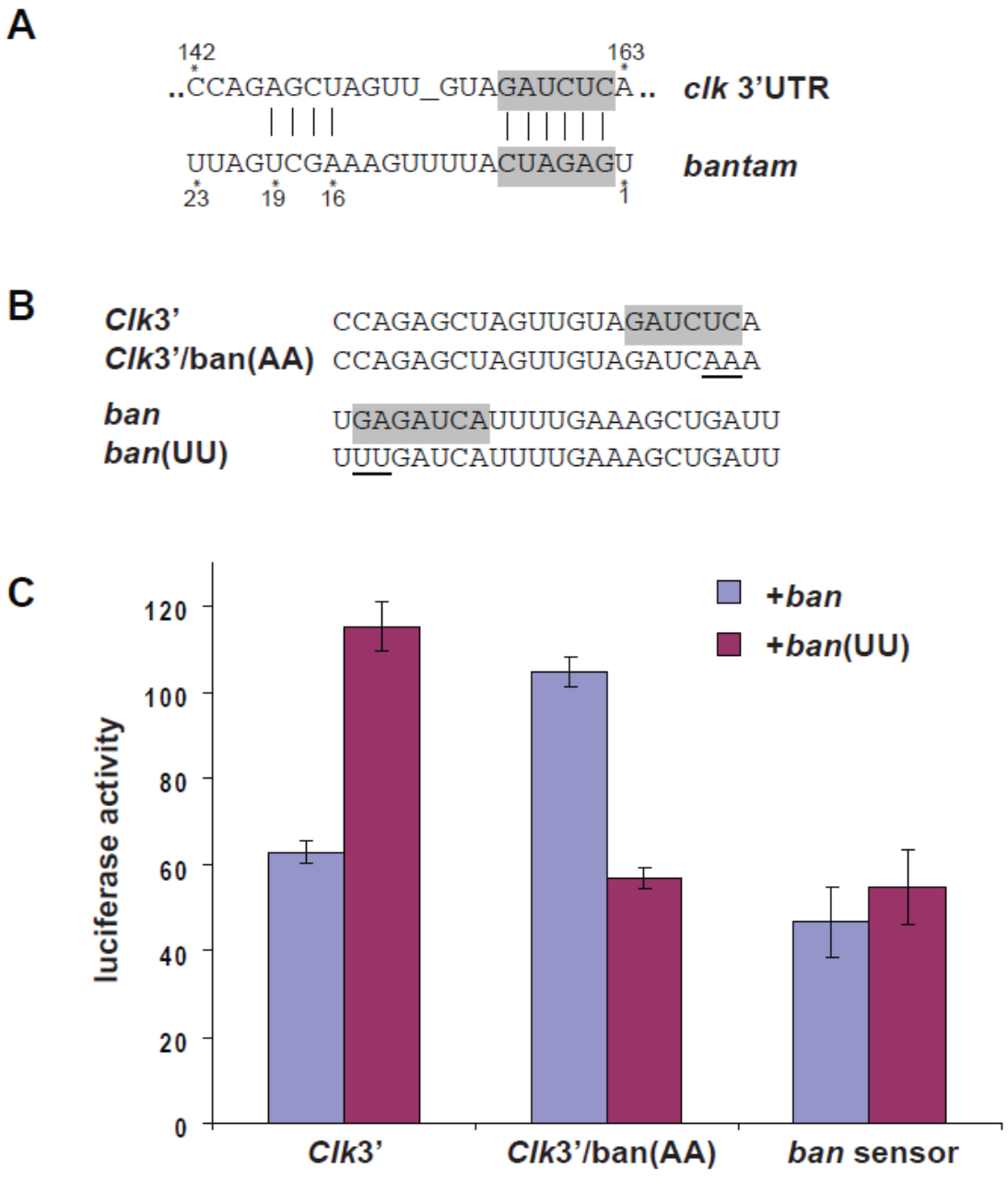

Figure 4.1. Identification of a *ban* binding site in the 3' UTR of *Clk*.

A. Alignment between the *ban* miRNA and a computationally predicted *ban* binding site in the annotated *Clk* 3' UTR. Shown in shade are the predicted base-pair interactions (small vertical line) with the region involving the seed (miRNA positions 2-7). Numbering of the *Clk* 3' UTR is relative to the translation stop codon. **B.** Shown are relevant sequences for

Figure legend of figure 4.1 continued

the mutant forms of the *luc*-*Clk*3' [*Clk*3'/ban(AA)] and *ban* miRNA [ban(UU)], aligned with the wild-type counterparts. The seed region of the *ban* miRNA and those potential target region on the *Clk* 3' UTR are shaded in the wild-type sequences, and the mutated bases are underlined. **C.** For each reporter construct, the Luc activity was set to 100 in the absence of exogenously expressed miRNAs, and shown are the normalized values obtained in the presence of exogenously expressed wild-type *ban* or mutant *ban*(UU) miRNAs. The *ban* sensor was used as a positive control. Luc activity levels were obtained from three independent experiments and the average values with the standard error shown.

However, there are several features of *Clk* 3' regions that made us wonder if we assayed the entire 3'UTR. For example, within the currently annotated *Clk* 3'UTR we did not observe a canonical polyadenylation/3'-cleavage signal (AAUAAA) (data not shown). Perhaps more disconcerting is that in the region where it is thought that the *Clk* 3'UTR ends is situated a stretch of 12 A residues (Figure 4.2A), which could serve as an internal priming region for oligo-dT-based reverse transcription, leading to characterization of an artifactually short 3' UTR. Indeed, the original molecular characterization of *Clk* was partly based on using available EST and cDNA clones [22, 87, 202]. This was of interest to us because we noted the presence of another putative *ban* binding region that extended across the presumed 3' cleavage site (Figure 4.2A). Cleavage at the annotated site (between positions 242 and 243) would remove a C residue predicted to base-pair with position 2 of the *ban* seed region and the A1 residue (at position 244), almost certainly eliminating the ability of *ban* to target this region. This putative second *ban* site in the *Clk* 3' UTR is more reminiscent of a so-called '3'-compensatory site', whereby base-pairing to the 3' portion of the miRNA can not only supplement a 7-8mer match, but it can also compensate for a single nucleotide bulge or mismatch in the seed [63] (Figure S4.1B). The first canonical polyadenlyation/3'-cleavage site in *Clk* 3' sequences is located between positions 1023-1028bp downstream of the translation stop codon (Figure 4.2A), suggesting the *Clk* 3'UTR is much longer than currently thought and hence potentially including multiple *ban* sites.

Indeed, several different strategies indicate that the *Clk* 3'UTR is actually ~1kb long and that the "short" form is an experimental artifact (Figure 4.2, B and C, and S4.3). For example, we observed two bands of ~0.3 and 1.1 kb when performing RACE (rapid amplification of cDNA ends) in the presence of oligo-dT as primer (Figure 4.2B). This was observed for RNA extracted from both flies and S2 cells that express a reporter construct containing a *Clk* fragment that encompasses ~1.5 kb downstream of the translation stop

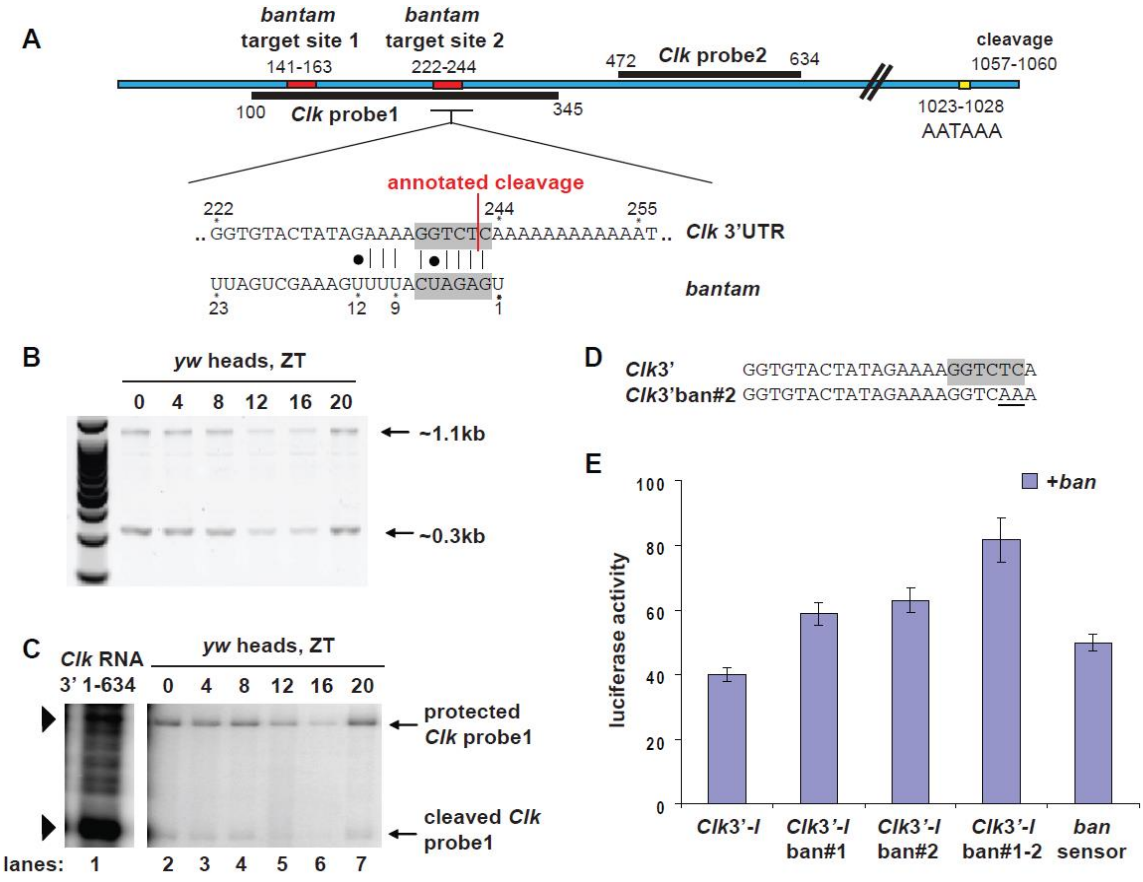

Figure 4.2. The *Clk* 3' UTR is significantly longer than the annotated version and contains at least one additional *ban* site.

A. Schematic representation of the *Clk* 3' UTR showing putative *ban* bindings sites (#1 and #2), putative poly(A)/3'-cleavage signal (AATAAA), and *Clk* probes used for RPA (*Clk* probe1 and *Clk* probe2). Numbering is from the translation stop signal. The region for the second *ban* site, including a 3' flanking stretch of 12 A residues, is enlarged and shows the predicted alignment between the *ban* miRNA and the target site; closed circle, possible G:U wobble; shade, seed region. **B.** Control *yw* flies were collected at the indicated times in 12:12LD and RNA extracted from heads. Results from 3' RACE indicate the presence of two major bands for the *Clk* 3' UTR that undergo daily cycles in levels. **C.** RPA was performed with either an *in vitro* transcribed RNA encompassing the first 634nt of the *Clk* 3' UTR (lane 1) or RNA isolated from fly heads (lanes 2-7) at the indicated time points in

Figure legend of figure 4.2 continued

12:12LD. Two major bands are observed for *in vitro* transcribed RNA (arrowheads) and fly RNA (arrows) when using *Clk* probe1. **D.** Sequences for *ban* site #2 on the *Clk* 3' UTR and the mutated version analyzed (*Clk*3'ban#2); the potential target region on the *Clk* 3' UTR is shaded in the wild-type sequence (*Clk*3'), and below is the counterpart sequence for altered version (*Clk*3'ban#2) showing the mutated bases (underlined). **E.** For each reporter construct, the Luc activity was set to 100 in the absence of exogenously expressed miRNA, and shown are the normalized values obtained in the presence of exogenously expressed wild-type *ban* miRNA. The *ban* sensor was used as a positive control. Luc activity levels were obtained from 2-6 independent experiments and the average values with the standard error shown.

signal (Figure 4.2B and data not shown). We sequenced multiple independent isolates of the long form and the results suggest 3' cleavage mainly occurs between positions 1057-1060 (Figure 4.2A). Importantly all these 3'-terminal *Clk* sequences were followed by a non-encoded polyA stretch (data not shown), indicative of mature transcripts. In addition, we collected flies at different times in a daily cycle, isolated RNA and performed RNAse protection assays (RPA) using a probe that spans the currently annotated cleavage site at position 242nt (*Clk* probe 1, Figure 4.2A). We routinely observed two bands; one consistent with cleavage at position 242nt and another consistent with an mRNA with a 3'UTR that extends beyond this region (Figure 4.2C). The levels of both the 'long' and 'short' forms cycle in phase with that previously reported for *Clk* mRNA using more internal probes [22]. Using a probe that is situated further downstream, spanning positions 472-634nt (*Clk* probe 2, Figure 4.2A), yielded a protected band in the RPA assay that exhibited the expected daily cycle in intensity, confirming the presence of a *Clk* transcript with a longer 3' UTR (Figure S4.3A). We considered that the short form might arise during the RNAse cleavage step of the RPA assay as a result of non-stable base-pairing due to the long stretch of A residues in this region (Figure 4.2A). To test this idea we generated an *in vitro* transcript that spans the presumed first cleavage site and subjected it to RPA using *Clk* probe 1. The sizes of the protected bands are consistent with a significant portion of the probe being cleaved in the region complementary to the A stretch located just downstream of the first *ban* site on the *Clk* 3' UTR (Figure 4.2C, lane 1, arrowhead). Moreover, we measured polyA tail lengths using primers just upstream to either the predicted short form of long form. Whereas the long form yields polyA tail lengths of about 150-200nt, we were unable to identify a substantial polyA tail from the short form (Figure S4.3B). Together, our results indicate that the sole or major form of the *Clk* 3'UTR in flies is ~1kb long.

We next sought to evaluate whether the putative second *ban* site is functional by generating a *luc-Clk* reporter that contains 1.5kb of the *Clk* 3' region, termed *luc-Clk*3'-*l*. The longer form of the *Clk* 3' UTR exhibits ~ 60% repression when co-expressing *ban* (Figure 4.2E), significantly more than the ~40% observed for the shorter version (Figure 4.1D) and consistent with multiple *ban* sites. Mutating either *ban* site (*Clk*3'-*l*/ban#1 or *Clk*3'-*l*/ban#2) singly resulted in ~40% repression by *ban*, suggesting each site has similar efficacy when present alone. Because these two *ban* sites are greater that 40nt apart, it is not expected that they would function in a cooperative manner [63, 203] and that appears to be the case as repression in the presence of both *ban* sites is less than would be expected by adding the effects of both sites alone. Mutating both sites resulted in Luc activity levels that were ~80-90% of values obtained in the absence of co-expressed *ban* (Figure 4.2E), suggesting that these two sites can account for the majority of *ban*-mediated repression but that other less potent sites might also be present in the *Clk* 3' UTR.

Multiple *ban* sites in the *Clk* 3' UTR function in concert to augment the robustness of behavioral rhythms

To investigate the physiological significance of the *Clk* 3' UTR *ban* sites, we generated mutants that are null for *Clk* in an attempt to better evaluate the function of *Clk*-containing germ-line transformants. To date, the described *Clk* mutants are the dominant negative Clk^{Jrk} allele [202] and a hypomorph termed Clk^{ar} [175]. Using FLP-FRT recombination [204] we generated a deletion mutant, termed Clk^{out}, that is missing ~5kb of *Clk* 5' sequences, including the transcription start site and regulatory sequences that direct spatial and circadian expression ([120]; see materials and methods). The Clk^{out} flies exhibit no evidence of circadian rhythmicity and do not produce detectable levels of CLK protein, indicating they are true *Clk* nulls (Table 4.2, Figure 4.3 and data not shown). We did not detect any gross effects on development or viability for Clk^{out} mutants (data not

Table 4.2: Locomotor activity rhythms for transgenic flies bearing *Clk*-containing transgenes and controls[a]

Genotype[b]	Period (hr ±SEM)	Power[c]	Rhythmicity (%)[d]	Total flies[e]
yw;PBac{y$^+$-attp-9A}VK00018	23.5±0.1	126	96.8	30
yw;P{CaryP}attP40	23.9±0.08	90.8	100	32
w;;*Clk*^{out}	AR	-	-	16
<u>two copies of transgene</u>				
w;p{*Clk*WT(A)};*Clk*^{out}	23.9±0.1	82.2	86.2	29
w;p{*Clk*ban#1(A)};*Clk*^{out}	24.7±0.12	70.7	88	25
w;p{*Clk*ban#2(D)};*Clk*^{out}	24.6±0.13	68.8	80.8	15
w;p{*Clk*ban#1-2(A)};*Clk*^{out}	24.3±0.14	59.8	57.1	7
w;p{*Clk*ban#1-2(C)};*Clk*^{out}	25.5±0.22	26.3	33.3	30
<u>one copy of transgene</u>				
w;p{*Clk*WT(A)}/*cyo*;*Clk*^{out}	25.1±0.19	57.5	71.4	7
w;p{*Clk*ban#1(A)}/*cyo*;*Clk*^{out}	25.7±0.38	28.7	40	15
w;p{*Clk*ban#2(D)}/*cyo;Clk*^{out}	25.1±0.08	28.9	30	20
w;p{*Clk*ban#1-2(A)}/*cyo*;*Clk*^{out}	24.9±0.29	18.6	33.3	15
w;p{*Clk*ban#1-2(C)}/*cyo*;*Clk*^{out}	24.5±0.49	17.2	36.4	22

[a] Young male flies were maintained at 25^{o}C and exposed to 5 days of 12:12 LD cycles followed by 6 days of DD.
[b] Different lines for *Clk* transgenes and variants are designated by the letters in parenthesis.
[c] Power is a measure of the strength or amplitude of the rhythm in arbitrary units.
[d] Percentage of flies showing locomotor rhythms with a power value of ≥10 and a width value of ≥2.
[e] Total number of flies that survived until the end of the experimental period.

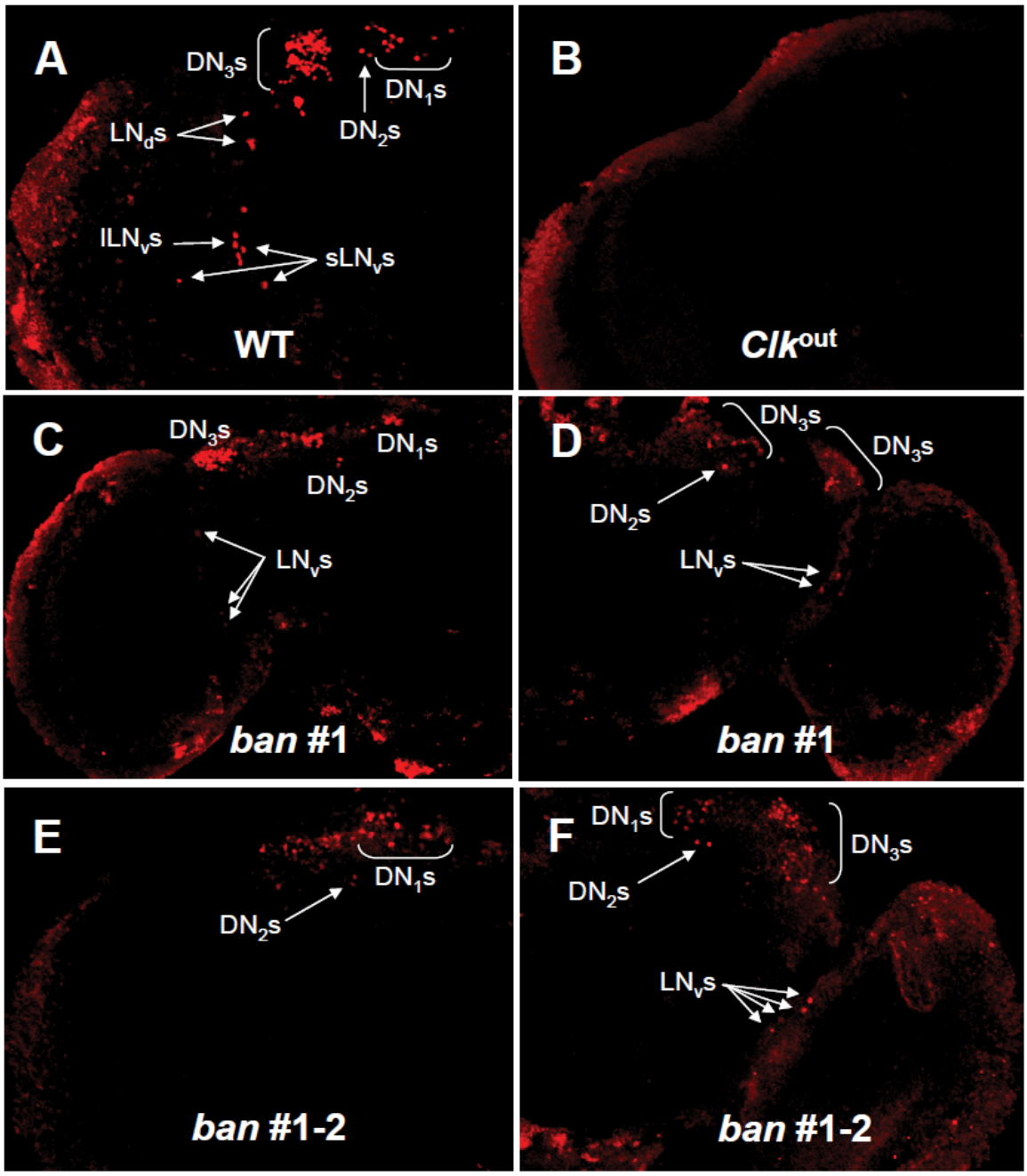

Figure 4.3. CLK levels are reduced in LNs of *ban* #1 and *ban* #1-2 mutant brains. Brains were dissected from adults collected at ZT1, immunostaining with CLK GP50 antiserum, and imaged by confocal microscopy. **A.** A 38μm projected Z-series image of CLK expression (red) from a WT *Clk* rescued *Clk*^{out} fly brain hemisphere (WT), where dorsal is at the top. Arrows and brackets denote CLK immunoreactivity in brain oscillator

Figure legend of figure 4.3 continued

cells: Dorsal Neurons 1 (DN_1s), Dorsal Neurons 2 (DN_2s), Dorsal Neurons 3 (DN_3s), Dorsal Lateral Neurons (LN_ds), large Ventral Lateral Neurons (lLN_vs), small Ventral Lateral Neurons (sLN_vs). **B.** A 46µm projected Z-series image of CLK expression in a *Clk*^{out} fly brain hemisphere, where dorsal is at the top. No specific staining is detected. **C.** A 52µm projected Z-series image of CLK expression in *ban* #1 rescued *Clk*^{out} left fly brain hemisphere (*ban* #1), where dorsal is at the top. **D.** A 64µm projected Z-series image of CLK expression in a *ban* #1 mutant brain hemisphere, where dorsal is at the top. CLK immunofluorescence was either undetectable in LNs (**C**) or detected in only a subset of LNs (**D**). **E, F.** 40µm projected Z-series images of CLK expression in *ban* #1-2 rescued *Clk*^{out} fly brain hemispheres (*ban* #1-2), where dorsal is at the top. CLK immunofluorescence was either undetectable in LNs (**E**) or detected in only a subset of LNs (**F**). All images are representative of 4 brains. CLK staining in LNs was undetectable in 3 of 4 *ban* #1 and *ban* #1-2 mutant brains.

shown). Transformation vectors were generated that contain *Clk* genomic sequences beginning ~2.5kb upstream of the start of transcription and ending with the same ~1.5kb 3' region that we assayed in cultured cells (Figure 4.2). In addition to a wildtype *Clk* construct, we generated versions that contain mutations in either a single *ban* site or both. We used transformation vectors that contain attB integration sites to enable site-directed chromosomal insertion, which reduces concerns associated with possible variations due to positional effects on transgene expression [182]. Stable germ-line transformants bearing the different *Clk*-containing transgenes were crossed into a homozygous Clk^{out} genetic background.

When present in two copies, transgenic flies carrying the wild-type *Clk* transgene (p{*Clk*WT}) resulted in highly robust activity rhythms (~90% of flies exhibit rhythmic behavior) with normal periods of ~23.5-24.0 hr (Table 4.2), indicating that this transgene contains all the relevant sequences required for *Clk* function in the circadian system. Also, with regards to circadian rhythms, the essentially wild-type rescue indicates that the Clk^{out} flies are only defective in *Clk* function. Intriguingly, although period lengths sometimes varied slightly between genotypes, there was a strong effect on the amplitudes of behavioral rhythms that highly correlated with the number of *Clk* 3' UTR *ban* binding sites. Whereas mutating either *ban* site alone (p{*Clk*ban#1} or p{*Clk*ban#2}) modestly reduced the strength of the rhythm to about the same extent (i.e., see power values, Table 4.2), the proportion of flies that were weakly rhythmic or arrhythmic was higher when assaying flies where both *ban* sites were mutated (p{*Clk*ban #1-2}; Table 4.2). This was the case even though we noted variability between different independent lines of the same transgene. For example, although the proportion of rhythmic flies varied between ~35-55% for the double *ban* site mutants, they were more arrhythmic compared to any of the single *ban* site mutants (Table 4.2).

To further investigate why mutating *ban* sites in the *Clk* 3' UTR is associated with reductions in circadian amplitude, we measured behavioral rhythms of Clk^{out} flies carrying only one copy of the transgene. For flies with a single copy of wildtype p{*Clk*WT}, the strength of the rhythm was reduced ~30% compared to two copies but the majority of flies were rhythmic (Table 4.2). These results are consistent with earlier work showing that CLK is likely the limiting component in the clockworks and that reducing its levels/activity compromises the ability of the circadian system to drive robust behavioral rhythms [19, 23, 175]. Remarkably, rhythm strength was potently reduced for all the *ban* mutants when comparing flies carrying one copy of the transgene to those with double the dosage. For example, even though the majority of single *ban* site mutants exhibited rhythmic behavior with two copies of the transgene, they were largely arrhythmic with significantly reduced strengths when only one copy was present (Table 4.2). Thus, when present in two copies the single *ban* binding site mutants behave as if they are slightly above the threshold levels of CLK required to sustain robust overt rhythms and further reductions of approximately two-fold begin to mimic the more dampened circadian system observed with two copies of the double *ban* site mutants. In general, the results indicate that circadian amplitude is highly sensitive to the number of *ban* sites on *Clk* and that mutating these sites compromises the robustness of the circadian system making it more susceptible to reductions in CLK levels.

Mutating *ban* binding sites in the *Clk* 3' UTR decreases CLK protein levels specifically in the key PDF-expressing pacemaker neurons

Our behavioral studies clearly indicate that the two *ban* sites we identified have physiologically relevant and significant effects on the robustness of circadian rhythms in *Drosophila*. However, the gene dosage results suggest that eliminating *ban* sites functions in a similar direction as lowering the dosage of *Clk* (Table 4.2). Although *Clk*

mRNA levels undergo daily changes in abundance [22], CLK protein abundance is essentially constant throughout a daily cycle [10, 124, 174]. When probing extracts prepared from whole heads we noted that the levels of CLK protein were generally lower in the *ban* site mutants compared to that observed in p{*Clk*WT} flies, but the differences were modest and somewhat variable (data not shown). Nonetheless, much of the clock protein staining in head extracts is derived from the compound eyes [205], which have little to no effect on driving activity rhythms. To better evaluate CLK staining in pacemaker cells we performed immunohistochemical staining of CLK in isolated brains. The ~150 circadian clock neurons in the adult brain can be sub-divided into several anatomically and functionally distinct groups of cells, which include the s-LNvs, l-LNvs, dorsal lateral neurons (LNds) and three sub-groups of dorsal neurons (DN1, DN2 and DN3) [53]. As expected, there was no detectable CLK-immunoreactive signal in the Clk^{out} flies and p{*Clk*WT} flies showed a similar spatial pattern as that observed for wildtype flies [206] (Figure 4.3, compare panels A and B).

Remarkably, the staining intensity of CLK in the small and large LNvs (and possibly LNds) was strongly reduced in single and double *ban* site mutants, whereas other groups of pacemaker neurons in the brain (e.g., DNs) were less affected (Figure 4.3C-F). Although CLK staining in the LNvs showed some fly-to-fly variation (panels C-F), the overall intensity in this sub-group of pacemakers was clearly less compared to wild-type transgenics. As the s-LNvs are the key pacemaker cells in the circadian neural network required for driving robust activity rhythms [56, 178, 196], these results provide a compelling explanation for the weak rhythms manifested by mutants in *ban* binding sites on the *Clk* 3' UTR. We did not observe obvious differences in overall staining intensity of CLK in the LNvs between single and doubly *ban* site mutants, although we cannot rule out small but important differences. Together, our findings indicate that mutating *ban* sites in the *Clk* 3' UTR leads to dramatic reductions in CLK protein levels, particularly in the LNvs,

strongly suggesting a non-conventional stimulation of CLK protein production by the *ban* miRNA.

DISCUSSION

As a means to understand the role of miRNAs in circadian timing systems we used several popular prediction programs to identify predicted miRNA binding sites on core clock genes in *D. melanogaster*. In this study we focused on the *Clk* gene as a possible target of *ban*. Expression of *ban* in pacemaker cells significantly lengthens free-running periods. Analysis of the *Clk* 3' UTR revealed that it is much longer than the currently annotated entry and that it contains at least two *ban* binding sites that can account for most of the *ban*-mediated repression as assayed in cultured *Drosophila* S2 cells using a Luc-based reporter (Figures 4.1 and 4.2). To determine the physiological significance of these results we generated a *Clk* loss-of-function mutant and evaluated the circadian function of transgenes with mutations in *Clk ban* binding sites. Mutating either *ban* site -#1 or -#2 in the *Clk* 3' UTR reduced the strength of behavioural rhythms, whereas flies with both sites mutated manifested either very weak behavioural rhythms or were arrhythmic (Table 4.2). Gene dosage studies indicated that mutating *ban* binding sites in the *Clk* 3' UTR function in the same manner as lowering the levels of *Clk* expression (Table 4.2). Intriguingly, the single and double *ban* binding site mutants strongly reduce CLK staining intensity specifically in the LNv sub-group of pacemaker cells (Figure 4.3). Together, our results raise the strong possibility that the *ban* binding sites on the *Clk* 3' UTR function in a concerted and graded manner as key modulators of circadian amplitude by ensuring that the levels of the rate-liming CLK protein are maintained at high enough values in the s-LNvs to drive robust behavioural rhythms.

While this paper was in the process of being submitted, similar findings were reported by Kadener and co-workers [73]. For example, they also show that ectopic

expression of *ban* in pacemaker neurons lengthens behavioural periods by about 3-4 hr. In addition, they demonstrate that the *Clk* 3' UTR is ~700 bp downstream of the currently annotated version and contains multiple *ban* binding sites, very similar to our findings. To address physiological significance they analyzed the rescue capabilities of *Clk*-containing transgenes in the Clk^{ar} hypomorphic allele. Mutating the same two *ban* sites we studied (*ban* sites #1 and #2) in addition to the third conserved site (*ban* site #3), significantly lowered the strengths of activity rhythms. They also suggested a fourth putative *ban* binding site that does not appear to be conserved, which we did not identify or analyze. Transgenic flies carrying all four sites mutated exhibited similarly weak activity rhythms compared to those with three sites inactivated, suggesting minimal if any contribution from the fourth putative *ban* site.

Our findings are not only in excellent agreement with their results but also add novel and unanticipated insights into the mechanism underlying how *ban* binding sites on the *Clk* 3' UTR contribute to the robustness of the circadian system. Having realized that the *Clk* 3' UTR is extended and contains the possibility for multiple *ban* binding sites, we compared the relative contributions of *ban* sites #1 and #2, individually and as a unit. Results in cultured cells indicated that each site likely functions independently and to a similar degree in mediating *ban*-dependent repression. These findings are consistent with the current view that individual miRNA binding sites can have modest effects on gene expression and that cooperative interaction is restricted to nearby sites [203], which would not be expected for the *ban* sites in the 3' UTR of *Clk* (Figure 4.2).

Although all the determinants governing how miRNAs recognize target sites are not clear, the strongest interactions are for those miRNAs that base-pair across the entire seed region (8mer) [63]. *Ban* site #1 has the signature of a '7mer-A1' motif that has contiguous complementarity to the seed region (positions 2-7 of the miRNA) in addition to an A residue at the 3' end of the site, which is known to increase the efficacy of target

regulation by miRNAs [63]. We also noted the possibility for 3' 'supplementary' base-pairing involving positions 16-19 of the *ban* miRNA that are conserved in the 3' UTRs of *Clk* from other *Drosophila* species. *Ban* site #2 is more reminiscent of a so-called '3'-compensatory site', whereby base-pairing to the 3' portion of the miRNA can not only supplement a 7-8mer match, but it can also compensate for a single nucleotide bulge or mismatch in the seed [63, 207]. In addition, the stretch of A residues (Figure 4.2) could improve miRNA accessibility, enhancing the local effectiveness of this site [203, 208]. The observation that *ban* sites #1 and #2 might be suboptimal suggested that they function in a combinatorial manner to regulate *Clk* expression.

To examine the contributions of *ban* binding sites on the *Clk* 3' UTR we generated a novel *Clk*-null, which we term Clk^{out}, using the FLP/FRT recombination strategy. Rescue experiments indicated that the strength of behavioral rhythms is causally linked to the number of *ban* binding sites in the *Clk* 3' UTR (Table 4.2). Mutations in either *ban* site #1 or #2 led to similar decreases in circadian rhythm amplitude, suggesting they provide roughly equivalent contributions to *Clk* gene expression, consistent with results obtained in cultured cells (Figure 4.1). Inactivating both sites severely dampens circadian rhythms, rendering the majority of flies either arryhythmic or weakly rhythmic. While differences in period length were observed for the different genotypes, the significance of these results is difficult to ascertain as *ban* site mutant flies that were rhythmic showed a larger spread in period length (Table 4.2 and data not shown). Thus, the *ban* sites on the *Clk* 3' UTR also help maintain the precision of the clockworks, which is likely interwoven with pacemaker amplitude. In this regard we believe that the period-lengthening effects of overexpressing *ban* in pacemaker neurons (Table 4.1 and Figure S4.2) is likely minimally linked, if at all, to *Clk* gene regulation and might involve other targets in the clockworks, a conclusion also favoured by Kadener et al. (2009). Together, the findings are in agreement with prior work suggesting that regulation of *Clk* expression is a major element

modulating the amplitude of the circadian system but has a less potent effect on the pace of the clock [19, 23, 139, 175], which is mainly governed by the daily phosphorylation cycle governing PER protein stability [34].

Prior results indicated that reductions in *Clk* levels/activity are associated with decreases in circadian rhythm amplitude [175] and that 3-5 fold increases in the overall levels of CLK have little effect on circadian rhythms [19]. We were curious as to why increasing the number of *ban* sites inactivated in the *Clk* 3' UTR, which would be predicted to steadily increase CLK protein levels, resulted in weaker behavioral rhythms. To further investigate this apparent conundrum, we measured activity rhythms in Clk^{out} flies that carried either one or two copies of the different *Clk*-containing transgenes. Modulating gene dosage of the wildtype p{*Clk*WT} transgene showed that reducing from two to one copy led to modest decreases in the strength of the rhythm (Table 4.2). This trend was not only observed for the *ban* site mutants but exaggerated, indicating that inactivating *ban* sites in the *Clk* 3' UTR renders the circadian system extremely vulnerable to decreases in CLK protein levels. This was very apparent for the single *ban* site mutants, which manifested largely rhythmic behavior at two copies but suffered a dramatic impairment in circadian amplitude when only one copy of the transgene was present. The results suggest that one copy of the single *ban* site mutant is roughly similar to two copies of the double *ban* site mutant, in striking agreement with prior work showing that a single miRNA binding site appears to contribute on the order of two-fold to gene regulation [201, 209, 210]. We suspect that the Clk^{out} genetic background provided a very sensitized system to assay more subtle effects from single *ban* site mutants and alterations in gene dosage.

Our molecular studies provide an unexpected yet solid mechanism for the link between *ban* sites on the *Clk* 3' UTR and the robustness of the circadian system in *Drosophila*. Removing *ban* binding sites leads to decreases in CLK protein levels, most

notably in the LNvs (Figure 4.3 and data not shown). These results nicely dovetail with our gene dosage studies indicating that mutating *ban* sites function in the same direction as lowering *Clk* gene dosage and fit well within the known framework of the *Drosophila* circadian neural network wherein the s-LNvs are the critical pacemaker neurons required for driving robust behavioral rhythms under free-running conditions. The loss of CLK expression preferentially in the LNs of *ban* binding site mutants is intriguing, but the cause of this phenotype is currently not known. One possibility is that *Clk* expression in the LNvs is more dependent on *ban* miRNA compared to other clock cells. The effect of *ban* miRNA need not be direct and could involve displacing inhibitory factors that bind the *Clk* 3' UTR and repress translation. Alternatively, *ban* may function through *Clk* during LN development, thus loss of *ban* target sites may impair the development of LNs. Additional studies will be needed to test these possibilities. That miRNAs can up-regulate translation of target genes is not unprecedented. A recent study suggested that miRNAs can switch from repression to activation in non-proliferating cells [211]. This might offer an explanation as to why the *ban* sites on the *Clk* 3' UTR act to inhibit gene expression when assayed in cultured S2 cells.

In summary, we show that multiple ban binding sites in the 3' UTR of *Clk* function in a combinatorial manner to maintain CLK protein levels above threshold values required to drive robust and precise behavioral rhythms. The mechanism by which *ban* sites up-regulate CLK production seems particularly important in the LNvs, which are critical for sustaining the circadian neural network that underlies circadian behavior. Previously we suggested that a post-translational phosphorylation/de-phosphorylation program is central to regulating CLK protein stability and might act to stabilize the limiting levels of CLK against stochastic fluctuations, minimizing the propagation of 'molecular noise' in the feedback circuitry [10]. Findings in this manuscript suggest that miRNAs might have general roles in providing resistance to perturbation in gene regulatory networks by

ensuring limiting components are maintained at appropriate levels, thereby imparting robustness and precision to the highly dynamic circadian systems. Indeed, accumulating evidence indicates that miRNAs function as fine-tuning regulators that add robustness to gene expression networks and biological systems [171-173]. Our results also show that in key brain pacemaker neurons the *ban* binding sites in the *Clk* 3' UTR function to up-regulate CLK protein levels, raising the interesting speculation that depending on the cellular context miRNAs might function to boost the expression of target genes.

Acknowledgments

We thank Richard Padgett and Ying Li for the pAc-*luc* construct used to generate the *Clk* 3' UTR fusions used in this study and pAc-*bantam*, *bantam* sensor and the *renilla luciferase* construct. We thank Ken Irvine for access to a plate reader and Yongqiang Feng for advice on recombineering strategies.

Contributions: Liu, Ng, Yu, Mahesh in Paul Hardin's lab created the Clk^{out} flies. Houl did the ICC experiments for figure 3. All the other experiments are performed by Evrim Yildirim.

SUPPLEMENTARY TABLES AND FIGURES FOR CHAPTER 4

Table S4.1: Locomotor activity rhythms for *bantam* overexpressing lines at different temperature and photoperiods[a]

Genotype[b]	Period (hr ±SEM)	Power[c]	Rhythmicity (%)[d]	Total flies[e]	Photo-period[f]	Tempe-rature(°C)
yw;;UAS-*bantam*	23.5±0.05	75.5	77.4	31	12:12	18
yw;*pdfGAL4*	24.4±0.11	93.3	87.5	32	12:12	18
pdfGAL4> UAS-*bantam*	26.1±0.28*	62.6	71.9	32	12:12	18
w;*tim*(UAS)*GAL4*	24.2±0.21	43.2	68.8	32	12:12	18
tim(UAS)*GAL4*> UAS-*bantam*	26.5±0.11*	114.7	93.8	32	12:12	18
yw;*timGAL4/cyo*	24.1±0.19	99	89.3	28	12:12	18
timGAL4>UAS-*bantam*	27.4±0.07*	124	96.9	32	12:12	18
w;*gmrGAL4*	23±0.06	133.8	93.8	32	12:12	18
gmrGAL4>UAS-*bantam*	23.3±0.1	129.2	90.3	31	12:12	18
yw;;UAS-*bantam*	23.9±0.32	59	61.5	26	9:15	25
yw;*pdfGAL4*	24.7±0.09	101.4	53.3	15	9:15	25
pdfGAL4> UAS-*bantam*	25.1±0.08*	136.7	93.5	31	9:15	25
w;*tim*(UAS)*GAL4*	24.4±0.26	84.2	75	16	9:15	25
tim(UAS)*GAL4*> UAS-*bantam*	25.6±0.09*	95.1	71	31	9:15	25
yw;*timGAL4/cyo*	23.9±0.15	124	94.1	17	9:15	25
timGAL4> UAS-*bantam*	26.7±0.09*	129.1	96.9	32	9:15	25
gmrGAL4> UAS-*bantam*	23.2±0.06	136	96.7	30	9:15	25

[a] Young male flies were maintained at indicated photoperiod and temperature.
[b] Independent transgenic lines are designated by the numbers in parenthesis.
[c] Power is a measure of the strength or amplitude of the rhythm in arbitrary units.
[d] Percentage of flies showing locomotor rhythms with a power value of ≥10 and a width value of ≥2.
[e] Total number of flies that survived until the end of the experimental period.
[f] Flies are entrained at indicated light:dark cycles for 5 days and then exposed to 6 days darkness.
* The periods of these crosses are statistically different (p-values<0.01) than both parent's periods.

Table S4.2 Sequences of primers used in this study

Primers used in clk rescue construct:	
ClkLA-f	atgtggcgcgccGCCCCAAAAATCCATAAATGCT
ClkLA-r	gtgttggatccAGGGGTGTTATAGAGAGGGACA
ClkRA-f	gtgtggatccGCAGAGTGAAACCTGTGCAA
ClkRA-r	atatatgtgcggccgcTCCCGGTTATGAGTTTTTCG
ClkLAseq-f	gcggctggaactctaagaca
Clk5'check-r	gacaaagatgtgccgactga
RAseq-r	ACAACCACGTCTTTCCCTTG
Clk3'check-f	gagcaaagagccacttacGG
MCS-F	TTTAAACCTCGAGCGGTCCGTTATC
MCS-R	CTAAAGGGAACAAAAGCTGGGTAC
Primers used in cloning:	
Clk2719	gactcgctgttgtcctgcat
FseI-Clk3'-241-r	gtgtggccggccagacctttctatagtacacctatg
FseI-Clk3'-f	ggtggccggcccgtatacccactgtatataacactct
FseI-Clk3'-1580-r	attaggccggccggtacccactgttgagtacggcgtgt
AscI-Clk3'-f	ggcgcgcccgtatacccactgtatataacactct
Primers used for site-directed mutagenesis:	
ban(UU)-f1	gatttggtttgactgtttttcatacaagtttgatcattttgaaagctgattttgtcaatg
ban(UU)-r1	Cattgacaaaatcagctttcaaaatgatcaaacttgtatgaaaaacagtcaaac caaatc
ban(UU)-f2	actacgaaaccggttttcgatttggttatactgtttttcatacaagtttgat
ban(UU)-r2	atcaaacttgtatgaaaaacagtataaccaaatcgaaaaccggtttcgtagt
ban1-f	cccagagctagttgtagatcaaaacagactgagtattgtccc
ban1-r	gggacaatactcagtctgttttgatctacaactagctctggg
ban2-f	Ataacataaacataggtgtactatagaaaaggaatcaaaaaaaaaaaatccatt gtaagtagg
ban2-r	cctacttacaatggatttttttttttttgattccttttctatagtacacctatgtttatgttat
V5-f	Gccccaggcagtagtcaaggtaagcctatccctaaccctctcctcggtctcgattcta cgtagggccggc
V5-r	Gccggccctacgtagaatcgagaccgaggagagggttagggataggcttaccttga ctactgcctggggc

Table S4.2 continued

Primers used in cloning for RPA probes and poly(A) tail length assay:

Clk3'-133-f	atcggaagcccagagctagttgta
Clk3'-962-f	gtaattgaacatgctaaccaaacc
Clk3'-100-f	aattgaattcttggcctctggctctcttta
Clk3'-345-r	cctcgatggcacttactgga
Clk3'-472-f	aattgaattcttttcaagactgggcttcgt
Clk3'-634-r	tcagaaaagatcgggcctaa

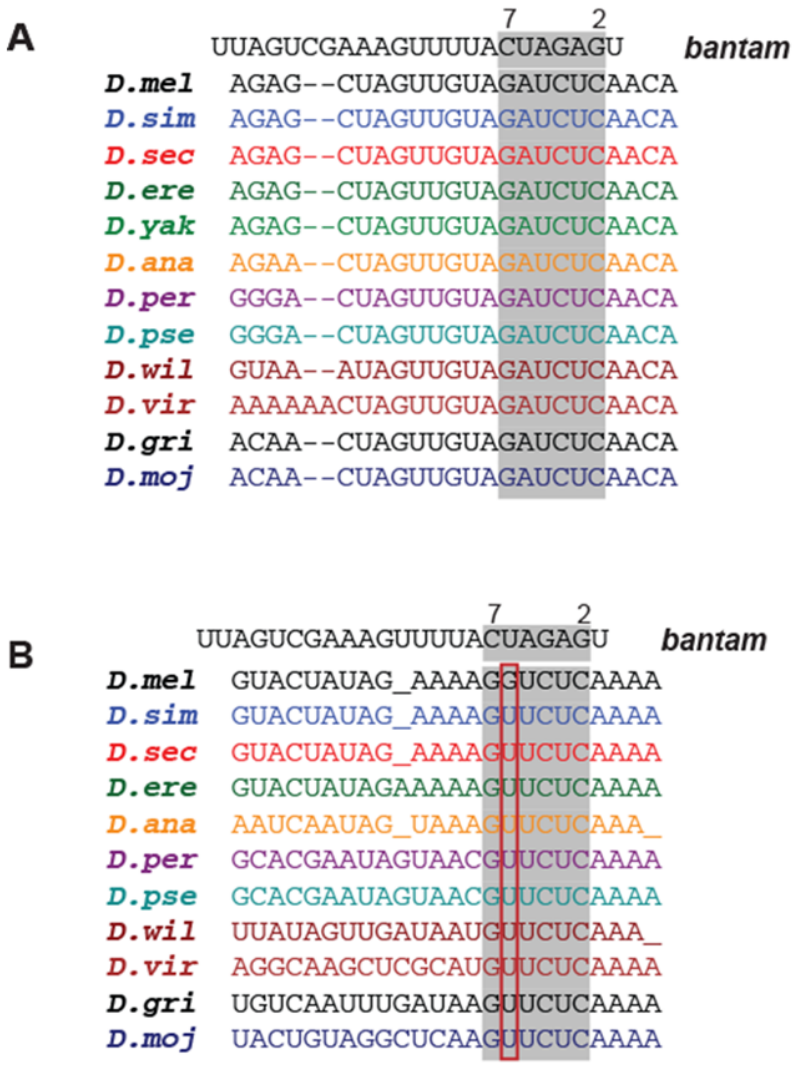

Figure S4.1. Evolutionary conservation of *Clk* ban sites #1 (A) and #2 (B).

Above group alignments for each *ban* site is shown the *ban* miRNA sequence with the seed region shaded. A potential mis-match/wobble in the seed region for *ban* site #2 is identified by a red box (B).

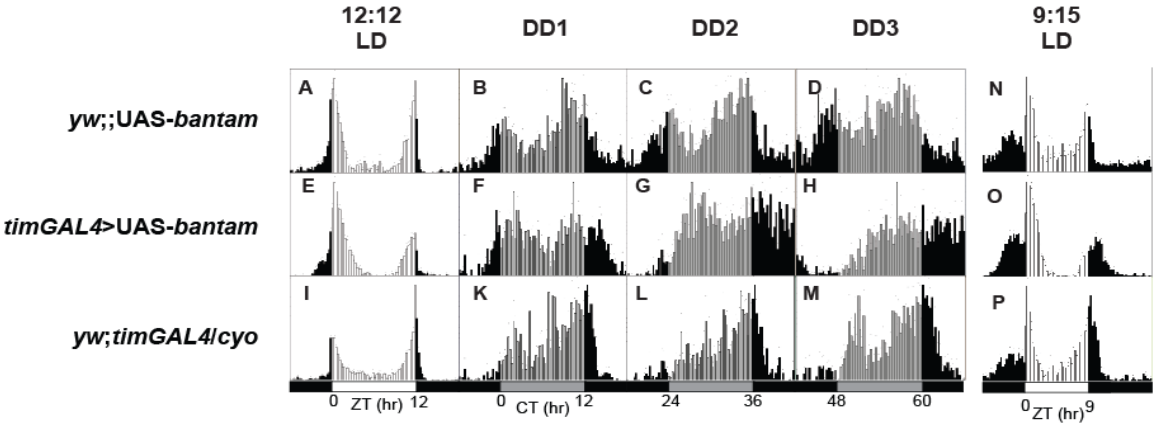

Figure S4.2. Daily activity patterns for *tim*-GAL4>UAS-*bantam* flies and parental controls.

Flies were either entrained by 5 days of 12:12LD (A-M) or 9:15LD (N-P), followed by constant darkness (DD). Histograms represent the daily distribution of activity (eductions) for the indicated genotypes (left) during either the light/dark cycle (A, E, I, N, O and P) or during constant darkness (B-D, F-H and K-M). For the eductions during LD, data from the last three days of LD were pooled from individual flies to generate a group average. For activity records during DD, successive days are shown from DD1 to DD3. Vertical bars indicate activity (15-min bins) during lights-on (white), lights-off (black) or subjective day (grey).

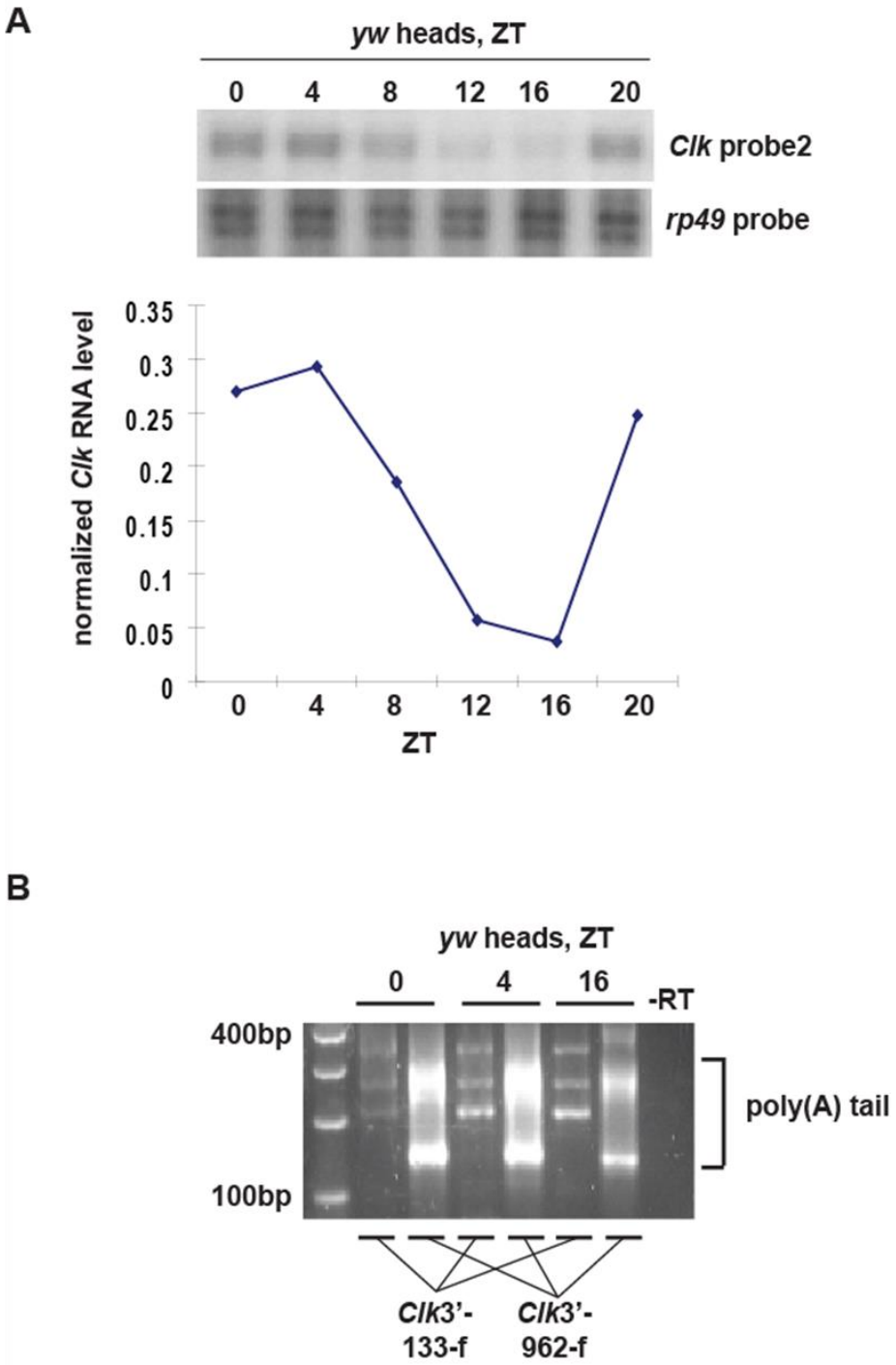

Figure S4.3. The *Clk* 3' UTR is significantly longer than the currently annotated version.

Figure legend of figure S4.3 continued

A. Results of RPA using Clk probe2. Flies were collected at the indicated time points in 12:12LD and RNA extracted from fly heads. Top, image of autoradiograph showing the signals from the *Clk* and rp49 protected probes. Bottom, graph shows relative abundance of *Clk* transcripts. **B.** RNA was isolated from heads of flies collected at the indicated times during 12:12LD and processed for poly(A) tail length analysis. We used two different primers that are ~100bp upstream of either the annotated 3' (*Clk*3'-133-f) or the more downstream suspected 3' cleavage site (*Clk*3'-962-f). A control experiment in the absence of RT (-RT) showed no bands. Note that only the 'long primer' yielded products with extensive poly(A) tails.

Chapter 5: Additional studies showing that mutations in *bantam* miRNA sites on *Clk* lead to lower levels of CLK protein in key pacemaker cells

(with findings in Chapter 4, manuscript in preparation)

INTRODUCTION

A previous report [73] and results described in Chapter 4 of my thesis, identified the *Clk* 3' UTR as an *in vivo* target for regulation by the *bantam (ban)* miRNA. In both studies, transgenic flies carrying mutations in *ban* binding sites found on the *Clk* 3' UTR displayed lower amplitude circadian behavioral rhythms. My studies were based on transgenic flies whereby I mutated two *ban* sites in the *Clk* 3' UTR, termed p{*Clk*ban#1-2}. Using the p{*Clk*ban#1-2} flies I additionally showed that the *Clk ban* site mutants have lower CLK protein levels in key pacemaker neurons in the brain, consistent with the weak behavioral rhythms. Because miRNAs are thought to function by specifically repressing target gene expression (either via mRNA stability and/or protein synthesis), our results suggested that *ban* works in a non-conventional manner leading to increases in CLK levels. However, the p{*Clk*ban#1-2} flies displayed some variability in the strength of behavioral rhythms and CLK staining in brains. We considered that the variability might be the result of not abolishing all the *ban* binding sites in the *Clk* 3' UTR as during the course of our studies we identified a third *ban* site, which was later confirmed in the published work [73]. Although some of the results shown in Chapter 4 were published while our manuscript was under review, the effects of *ban* on CLK levels have not been published. To enhance our studies we decided to evaluate behavioral rhythms and CLK levels in the more complete triple *ban* site knock out, herein termed p{*Clk*ban#1-2-3}. We show that CLK levels are indeed lower in key pacemaker neurons when *ban* sites are

eliminated from the *Clk* 3' UTR, raising the intriguing possibility that *ban* miRNA increases CLK levels.

Furthermore, we sought to verify if *ban* is active in the s-LNvs, the key brain pacemaker neurons required for driving circadian behaviors. However, the *ban* expression pattern in the adult brain has not been determined. Because the previously generated sensors for *ban* activity [80] or expression [212] did not give any signal in adult brain even for control constructs, we created a new *ban* sensor using miRNA-sponge strategy. By overexpressing this *ban* sponge we show that *ban* is expressed in s-LNvs. Together our results presented here and Chapter 4, show that *ban* is expressed in key clock neurons and regulates CLK levels in an unconventional manner, leading to increases in the robustness of circadian cycling.

MATERIALS AND METHODS

Many of the experiments performed in this chapter, such as luciferase based reporter assays, behavioral analysis of transgenic flies, generation of tissue culture or transformation constructs, have already been discussed in Chapter 4. I will briefly mention the different experimental procedures specific to this chapter.

Transgenic flies

The same *attB*-P[acman]-*Clk*V5 vector as in Chapter 4 was used to generate transgenic flies harboring the two original *ban* site mutations on *Clk* 3' UTR (Chapter 4) and the third site (see Figure 5.1). All final constructs were confirmed by DNA sequencing. *Clk*-containing transformation vectors were injected into *yw*;PBac{y^{+}-attp-9A}VK00018 embryos by BestGene Inc. (Chino Hills, CA,USA). In addition, P-element insertion lines were created using the same construct by Genetics Services Inc. (Sudbury, MA, USA).

To create an *in vivo ban* sensor we used miRNA-sponge strategy ([213]). A 23 base long near complementary sequence to *ban* (AATCAGCTTTCA**TC-**TGATCTCA, where bold part forms a 3 base bulge when paired with *ban*) was chosen as the basis for the *ban*-sponge. A long DNA sequence containing 4 copies of this base sequence separated by CGAT was cloned into a pGEM7 vector (Promega). Two copies of this unit (thus 8 copies of *ban* bulged sequence) were then cloned into the 3' end of a pUAST-eGFP vector, leading to the construct termed, pUAST-eGFP-*ban* sponge. As a control construct, reverse sequence of the unit in pGEM7 vector was cloned in the 3' UTR of the pUAST-eGFP vector, generating pUAST-eGFP control. Transgenic flies carrying these constructs were generated by Genetics Services Inc. (Sudbury, MA, USA) using standard P-element insertion methods.

Immunoblotting

Fly head extracts were prepared as previously described ([10]). Briefly, fly heads were homogenized with RIPA buffer (25mM Tris-HCl, pH 8.0, 50 mM NaCl, 0.5% deoxycholate, 0.5% NP-40 and 0.1% SDS) supplemented protease inhibitor tablet and PhosStop (Roche) and incubated for 15 min on ice. The contents were briefly sonicated, and supernatant was removed following centrifugation. Extracts were resolved by 4-15% gradient SDS-PAGE and immunoblotted in the presence of goat anti-CLK (dC-17) (Santa Cruz biotech.) at 1:2000 dilution. HRP-conjugated anti-goat antibody (GE Healthcare) was used at 1:200 dilution.

Phase Response Curve (PRC)

Anchored PRC was generated using standard protocols as previously described [98] [97]. Briefly, adult flies were entrained for 4 days by exposure to 12hr:12hr light:dark (LD) cycles at 18^{o}C. At the beginning of the last dark phase of the fourth LD cycle, the

lights were kept off for the remainder of the experiment. On the last LD cycle in the night phase beginning from ZT13, every 2 hr a group of flies was exposed to 10 min saturating (2000lux) light-pulses followed by 7 days in constant darkness (DD). A separate group of flies was not treated and served as non-pulsed controls. The phases of the locomoter activity on the 2nd and 3rd day in DD were calculated for each group using evening peak off-set (defined as 75% of the evening peak) as a phase marker by Brandeis Rhythm Package software. The phase shifts were determined by the difference of phases between pulsed and non-pulsed controls.

Confocal imaging of adult brains

Whole mounts of adult brains were prepared and imaged as described previously [51]. Briefly, adult flies were collected on DD3 at CT1 and fixed for 3 hr in 4% paraformaldehyde with 0.1% Triton X-100 at room temperature (RT) in darkness. After fixation, brains were dissected in cold PBS and washed twice with PBT solution (PBS containing 0.5% Triton X-100). Brains were incubated in blocking solution (PBT with 10% donkey serum) for 1 hr at RT, and then overnight at 4°C with the addition of primary antibodies at the following final dilutions: anti-PDF (C7) [101], 1:200 and if necessary anti-CLK (dC-17) (Santa Cruz Biotech.). Subsequently, brains were washed three times with PBT and then incubated overnight in blocking solution with the secondary antibodies Alexa Fluor 488-conjugated anti-goat IgG (Invitrogen) or Alexa Fluor 594-conjugated anti-mouse IgG (Invitrogen), both at a final dilution of 1:200 dilution. After several washes with PBT, brains were transferred onto slides and mounted with Vectashield (Vector Laboratories) on a coverslip. Confocal images were obtained with a Leica SP2 confocal microscope and processed with LCS Lite software. Quantification of the staining or GFP intensity was performed using the Image J software (NIH) from both average and maximum projections.

RESULTS

The *Clk* 3' UTR contains a third functional *ban* target site

The *Clk* 3' UTR harbors multiple computationally predicted *ban* target sites in addition to the two sites described in Chapter 4, most of them being 6mers. Initially, we did not think that the additional sites were functional because the presence of ectopic *ban* did not reduce the expression of a *luciferase* reporter construct flanked at the 3' end by the *Clk* 3' UTR harboring mutant *ban* binding sites 1 and 2 (Chapter 4). While expression from this construct in the presence of ectopic *ban* was not statistically significant compared to no additional *ban*, its levels were still less than that of the control in the absence of ectopic *ban*. This prompted us to examine the rest of the *Clk* 3' UTR closer for additional *ban* sites. Using the same reporter assays as in Chapter 4 with the truncated versions of *Clk* 3' UTR, we pinpointed another *ban* target seed in the 3' UTR of *Clk* at position 356-361 bp downstream from the translation stop signal (Figure 5.1A). Mutating two bases in this putative *ban* site (herein named as *Clk*3'ban#3) relieved the repression of *Clk* 3' UTR by 20%, which is similar to the other two sites when altered alone. Altering all three *ban* seeds on *Clk* 3' UTR (*Clk*3'ban#1-2-3) removed any inhibition by *ban* (Figure 5.1 B). While we cannot rule out that there might be additional *ban* sites on the *Clk* 3' UTR, our data clearly shows that the three *ban* sites we identified are responsible for most of the repression by *ban* in our luciferase based reporter assay, which is consistent with a previous report [73].

Mutating three *ban* target sites on the *Clk* 3' UTR strongly attenuates the strength of behavioral rhythms

To test the physiological significance of the newly identified third *ban* target site on behavioral rhythms, we created transgenic flies harboring mutations in this site alone or in combination with the two other previously identified sites in the *Clk* 3' UTR. We used the

A

Clk3' CGAGGCGCAAACAAGGAUCUCU
*Clk3'*ban#3 CGAGGCGCAAACAAGGAUCΔΔU

B

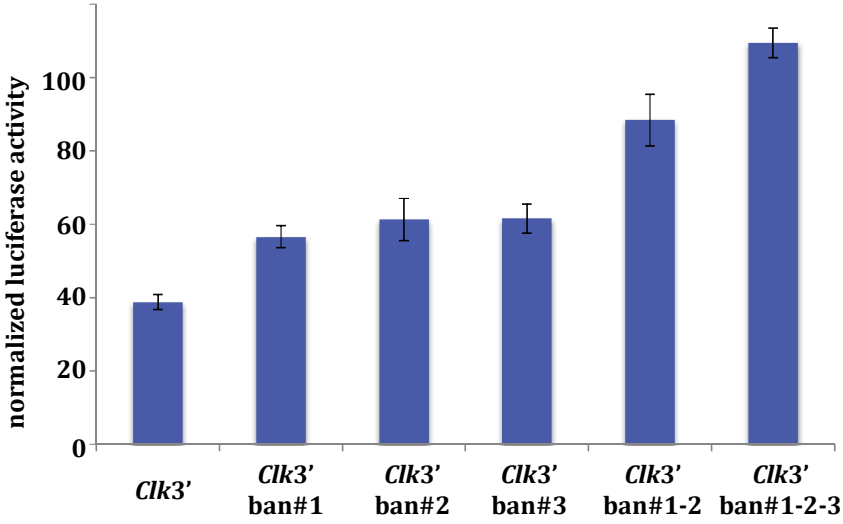

Figure 5.1. Identification of a third *ban* site on the *Clk* 3' UTR.

A, Sequence of the *Clk* 3' UTR between bases 341-362 after the translation stop codon. The predicted *ban* target 6mer seed is shaded. Also shown are the sequences mutated in the *Clk* 3'ban#3 mutant. **B,** Luc reporter activity levels of constructs with the wild type of mutant versions of the *Clk* 3' UTR in the presence of ectopic *ban*. Value for the wild type *Clk* version in the absence of ectopic *ban* was set to 100 and all other values normalized. Averages from at least three independent experiments are shown.

same site directed insertion strategy as in Chapter 4. The transgenes were crossed into the *Clk* knockout (*Clk*^{out}) background, and the behavioral experiments were performed at 18^{o}C.

Abolishing the 3rd *ban* site reduced the number of rhythmic flies and the rhythm strength, in a similar way as was found by mutating the other two *ban* sites (Table 5.1). The biggest effect on circadian rhythmicity and amplitude was observed when abrogating binding of *ban* to all three *ban* seeds on the *Clk* 3' UTR. These results suggest that the *ban* sites in *Clk* are not redundant but function in an additive manner. We still observed some variability in the proportion of rhythmic flies for the p{*Clk*ban#1-2-3} line (~25-50%) between independent experiments, however the power of their rhythm was always significantly lower when compared to p{*Clk*WT} (Table 5.1 and data not shown). Despite the very weak rhythms in constant dark conditions, p{*Clk*ban#1-2-3} flies did not display any entrainment defect in LD cycles; they showed well-defined activity peaks centered on light/dark transitions similar to p{*Clk*WT} flies under LD; and in stark contrast to *Clk*^{out} flies, which only abruptly responded to lights-on without any anticipation of the dark-to-light transition (Figure 5.2A). However, in constant darkness, p{*Clk*ban#1-2-3} flies progressively lost their rhythms. Because weak circadian rhythms can be augmented in light/dark cycles, our results suggest that mutating the *ban* sites on *Clk* does not abolish clock function but it severely dampens its amplitude.

We also generated wild type *Clk* or triple *ban* site mutant *Clk* transgenic lines using P-element mediated insertion [herein named as p{*Clk*WT(P)} and p{*Clk*ban#1-2-3(P)}]. Flies containing only a single WT copy of *Clk* in the *Clk*^{out} background were about 55% rhythmic, whereas the rhythmicity of *ban* mutant flies was very low (0-25%), consistent with the earlier published report using P-element insertion lines (Table 5.1) [73]. The reasons underlying the lower behavioral rhythmicity observed in both WT and *ban* mutant transgenics based on P-element transformation compared to site-directed insertion lines

Table 5.1: Locomotor activity rhythms for transgenic flies bearing *Clk*-containing transgenes and controls[a]

Genotype[b]	Period (hr ±SEM)	Power[c]	Rhythmicity (%)[d]	Total flies[e]
w;;*Clk*^{out}	AR	-	-	16
w;p{*Clk*WT};*Clk*^{out}	24.4±0.09	92.5	100	29
w;p{*Clk*ban#1};*Clk*^{out}	24.7±0.12	70.7	88	25
w;p{*Clk*ban#2};*Clk*^{out}	24.6±0.13	68.8	80.8	15
w;p{*Clk*ban#3};*Clk*^{out}	24.5±0.	57.8	64	25
w;p{*Clk*ban#1-2};*Clk*^{out}	24.6±0.12	57.4	54.5	25
w;p{*Clk*ban#1-2-3};*Clk*^{out}	24±0.22	49.1	41.2	17
P-element insertion lines[f]:				
w;p{*Clk*WT(P)}/-;*Clk*^{out}	25.5±0.67	41.7	55.6	18
w;p{*Clk*ban#1-2-3(P1)}/-; *Clk*^{out}	25.3±2.25	49.8	14.3	14
w;p{*Clk*ban#1-2-3(P2)}/-; *Clk*^{out}	26±0	42.9	14.3	21
w;p{*Clk*ban#1-2-3(P3)}/-; *Clk*^{out}	26.5±0	18.9	25	10

[a] Young male flies were maintained at 18^{o}C and exposed to 5 days of 12:12 LD cycles followed by 6 days of DD.
[b] Different lines for *Clock* transgenes and variants are designated by the letters in parenthesis.
[c] Power is a measure of the strength or amplitude of the rhythm in arbitrary units.
[d] Percentage of flies showing locomotor rhythms with a power value of ≥10 and a width value of ≥2.
[e] Total number of flies that survived until the end of the experimental period.
[f] This set of transgenic lines carry only one copy of the *Clk* containing transgene

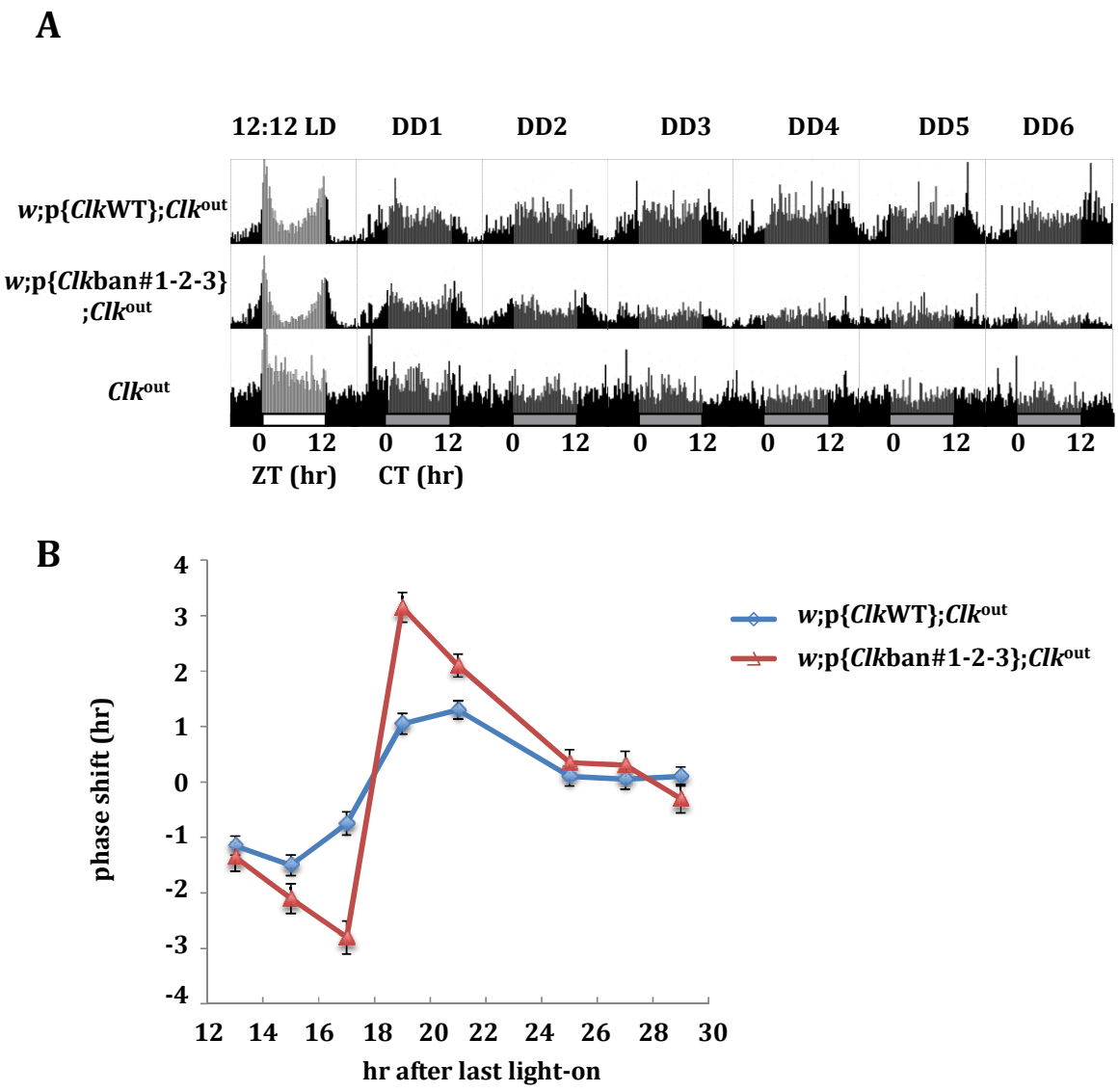

Figure 5.2. Abolishing the three *ban* sites in the *Clk* 3' UTR leads to flies with low amplitude circadian clocks.

A, Adult flies of the indicated genotypes (left of panels) were exposed to 5 days of 12:12 LD cycles followed by 6 days in DD. Activity histograms are shown for the last day in LD and the following 6 days in DD. **B,** Adult flies were exposed to 4 days of 12:12 LD cycles followed by 6 days DD. Beginning from the night phase of the last LD cycle, short light pulses were given to a group of flies at the indicated times.; another group of flies were not pulsed and served as controls. The resulting phase shifts in the locomoter activity

Figure legend of figure 5.2 continued

rhythm of pulsed flies compared to unpulsed controls for each genotype are shown. Note the larger magnitude phase shifts for p{*Clk*ban#1-2-3} flies.

are not clear, but possibly involve an expression difference between the VK00018 genomic insertion site and insertions at other sites. In any case, using two different strategies to generate transgenic flies, our results indicate that the *ban* sites on *Clk* increase the strength of circadian behavioral rhythms.

To further explore the difference in the rhythm strength between p{*Clk*WT} and p{*Clk*ban#1-2-3}, we performed a phase response curve experiment (PRC). PRCs can be used to gauge oscillator strength; based on theoretical considerations and experimentation, weak amplitude oscillators show greater phase shifts after a perturbation, such as light pulses. Exposure to short light pulses in the early night lead to phase delays, whereas the same treatment during the late night leads to phase advances. By plotting the phase shifts as a function of when the light pulse was given, yields a PRC. This is a classic method to infer the amplitude of circadian timing systems. Flies were entrained to standard LD cycles and then kept in total darkness (DD). Beginning on the dark phase of the last LD cycle, flies were exposed to short light pulses and returned to dark. We then measured the shift in evening activity peaks two days later. The p{*Clk*ban#1-2-3} flies showed increases in the magnitude of phase shifts during both the delay and advance zones (Figure 5.2B) compared to p{*Clk*WT}; whereas in the subjective day (time, 25-29 hr), the so called 'dead zone', no to very little shift was observed for both lines, as expected (Figure 5.2B). This result further supports the idea that *ban* sites on the *Clk* 3' UTR confer robustness to circadian rhythms.

Ban **site mutations lead to decreases in the levels of CLK in the key s-LNvs pacemaker neurons but not all clock neurons**

Once we established that the p{*Clk*ban#1-2-3} flies manifest severely dampened behavioral rhythms, we sought to determine the levels of CLK in pacemaker neurons. There are about 150 pacemaker neurons in the adult *Drosophila* brain, driving activity

rhythms (reviewed in [53]). Those neurons are further classified according to their function and anatomical location. The pigment dispersing factor (PDF) expressing small ventro-lateral neurons (s-LNvs) were shown to be the main pacemaker driving molecular and behavioral rhythms in constant darkness; and the ablation of those cells or null mutations in PDF results in arrhythmicity in free-running conditions (reviewed in [53]). Because p{*Clk*ban#1-2-3} flies cannot sustain rhythms in free-running conditions (Fig, 5.2, Table 5.1), we specifically investigated CLK expression in the s-LNvs. To this end, flies were collected at CT1 in DD3 and brains analyzed by immunohistochemistry. CLK staining intensity was significantly reduced in the small and large LNvs of p{*Clk*ban#1-2-3} flies (Figure 5.3 A, B). Another group of clock neurons in the brain, the so-called lateral dorsal neurons (LNds), however did not show any observable difference in CLK staining between wild type and mutant transgenic lines. Thus, there is specificity in the clock cells wherein *ban* regulates CLK expression. Reinforcing this idea, CLK levels were comparable in total head extracts between wild type and *ban* site mutant flies through the last LD and DD3 (Figure 5.3C), suggesting that *Clk* is a target of *ban* in only a small fraction of the clock cells in the head. We also stained the brains from P-element insertion lines. While transgenic flies carrying the wild type construct had strong CLK staining in the s-LNv pacemaker neurons, the p{*Clk*ban#1-2-3(P)} brains did not show any CLK staining (data not shown). Our findings show that *ban* regulates *Clk* expression in key pacemaker neurons that are important in the persistence of rhythms in free-running conditions. Although reductions in CLK levels in the s-LNvs of *ban* mutants are consistent with the weak behavioral rhythms, they are surprising because miRNAs repress gene expression. Thus, our results raise the intriguing possibility that *ban* miRNA increases *Clk* expression in the s-LNvs, suggesting a novel action for miRNAs.

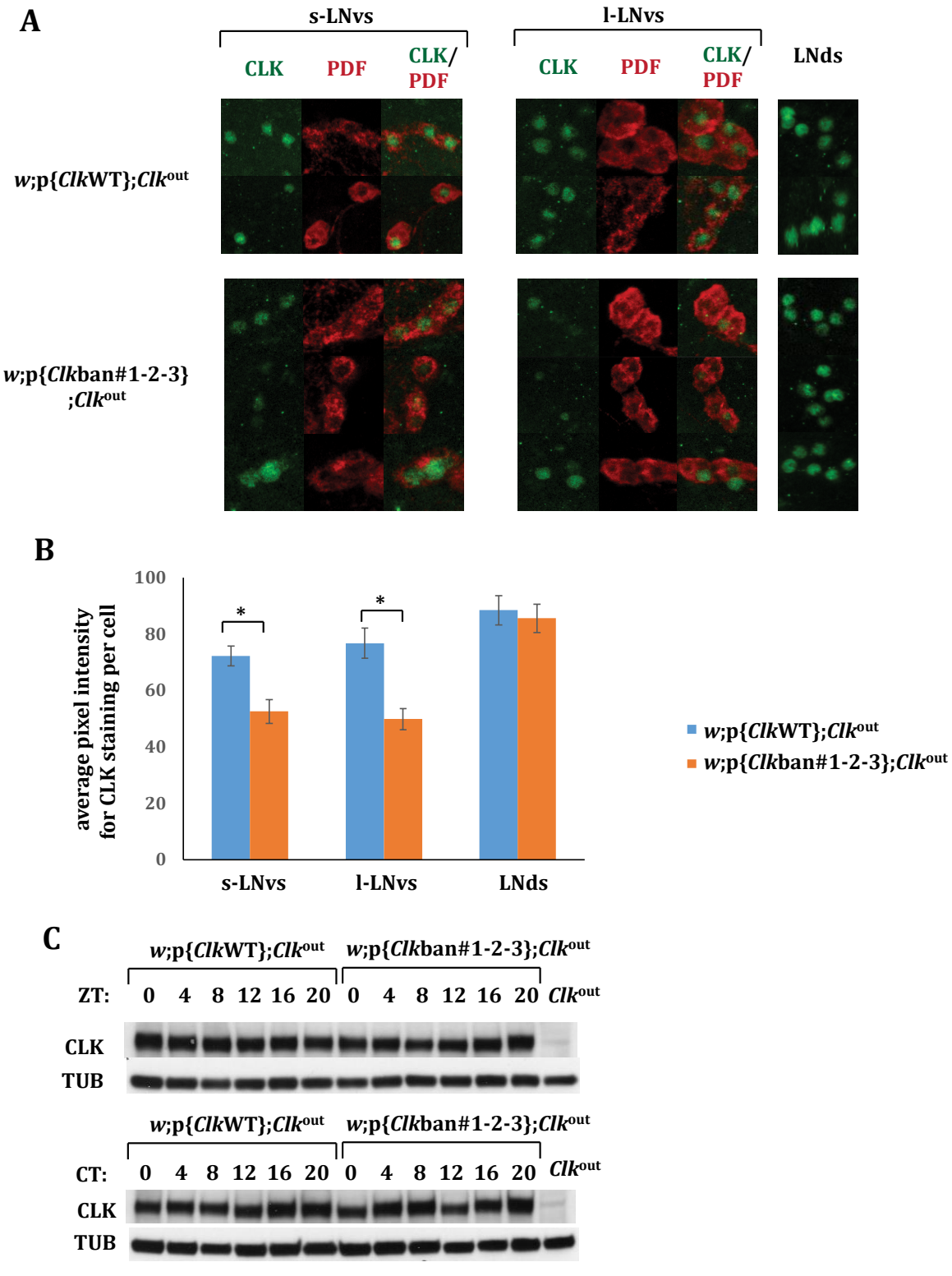

Figure 5.3. CLK protein levels are lower in LNv clock cells in p{*Clk*ban#1-2-3} flies.

Figure legend of figure 5.3 continued

A, Adult flies were entrained to 12:12 LD cycles followed by 3 days of DD. At CT1 of the last DD flies were collected, dissected and the brains were subjected to immonuhistochemistry in the presence of anti-CLK (dC-17) (shown in green) or anti-PDF (shown in red) antibodies. Representative images are shown for the indicated genotypes for different subgroups of circadian brain pacemaker neurons; s-LNvs, l-LNvs and LNds. **B,** CLK staining in s-LNvs, l-LNvs and LNds was quantified for the indicated transgenics. Average values of ~30 cells from 10 brains processed in two independent experiments were shown. * indicates statistical significance (Student t-test $p<0.05$) between genotypes. **C,** Adult flies of the indicated genotype were exposed to 12:12 LD cycles, followed by three days in DD. Shown are the CLK levels from whole head extracts prepared at the indicated time points during the last LD cycle (ZT; top panle) or third day in DD (CT; bottom panel). Extracts from *Clk*^{out} flies served as a negative control for the anti-CLK (dC-17) antibody.

miRNA *ban* is expressed in LNvs

We next checked if *ban* is expressed in the s-LNv pacemaker neurons. To date, the *ban* expression pattern in the *Drosophila* adult brain has not been reported. We used a well-characterized *ban* sensor [80] and *lacZ* enhancer trap [212]; however we could not detect significant signals in adult brains (data not shown). Therefore, we created a new *ban* sensor based on a GFP '*bantam* sponge' that contains a 3' UTR with multiple units of 23bp imperfect complimentary sequences against the whole length of *ban*. The *ban* reporter was put under the UAS-promoter to enable the overexpression in desired cells using GAL4-drivers. As a control we used a similar GFP construct with inverted repeats of the same 23bp unit in its 3' UTR. This type of strategy has been used to soak or deplete a specific miRNA, which is indicated by the relief of repression of target genes [213]. The repression mode of these sponges are thought to be more on the translational level due to imperfect base pairing with the miRNA, which prevents the cleavage of the transcript by RNA-induced silencing complex, prolonging its half-life, and enabling long term repression. If *ban* is endogenously expressed in a cell and functioning normally we should observe a reduction in GFP intensity in flies expressing the *ban* sponge (termed p{GFP-*ban* sponge} compared to flies expressing the GFP-control (termed p{GFP-control}).

GFP-*ban* sponge and GFP-control were expressed with a strong *tim* promoter (timUASgal4), and brains were subjected to immunohistochemistry. The GFP intensity of the construct containing the *ban* sponge was clearly reduced in s-LNvs compared to the controls. The reduction in expression levels is consistent with endogenous *ban* expression in these cells (Figure 5.4 A, B). We did not extensively examine other pacemaker neurons due to weak signals from both construct, however strong and relatively similar levels of GFP in medulla/glial cells suggests specificity for *ban* expression in the s-LNvs. Overexpression of either construct did not impair circadian rhythmicity

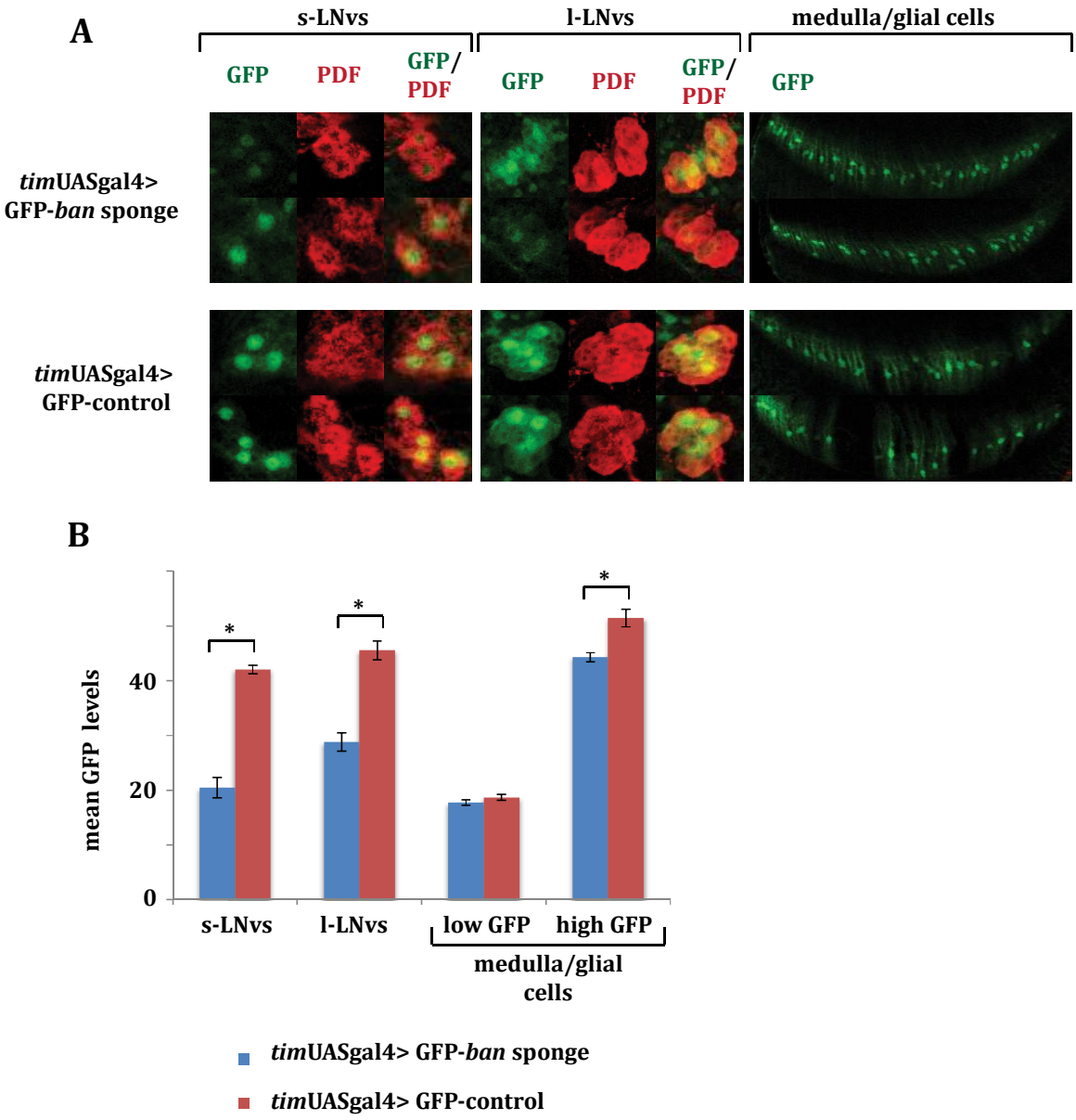

Figure 5.4. *Ban* is expressed in the s-LNvs

A, Flies containing the indicated UAS-driven GFP constructs and the timUASgal4 driver were entrained to 12:12LD cycles followed by 3 days in DD. On the third day in DD at CT1 flies were collected, the brains dissected and stained with anti-PDF antibody (red) as a marker for LNvs. Representative images of LNvs, and medulla/glial cells are displayed. **B,** Average values of GFP signal from ~40 LNvs and medulla/glial cells are shown for the

Figure legend of figure 5.4 continued

respective genotypes. * indicates statistically significant difference (Student t-test $p<0.05$) between genotypes.

(Table S5.1). Together, these findings show that *ban* is expressed in the s-LNvs and, at least with a *ban* sponge reporter, can function to inhibit gene expression, suggesting an unusual functional interaction between *ban* and *ban* sites on the 3' UTR of *Clk*.

DISCUSSION

Micro RNAs are implicated in various biological processes including circadian rhythms ([72] [71] [70]). That *ban* targets *Clk* has already been published [73] and also described Chapter 4. However, an aspect of our work that has not been reported is the effect of *ban* regulation on CLK levels (Chapter 4). In this study we sought to extend our knowledge about the role of *ban* in regulating *Clk* expression and circadian behavior. *Ban* acts on the *Clk* 3' UTR though at least three *ban* target sites, consistent with the prior study [73]. Mutating all three *ban* sites on the *Clk* 3' UTR resulted in very weak behavioral rhythms, which is very nicely explained by lower levels of CLK in key pacemaker neurons (Figure 5.3). Finally, we show that *ban* is expressed in s-LNvs (Figure 5.4), consolidating the importance of *ban*-*Clk* interactions in these cells.

Using luciferase-based reporters in S2 cell culture we found that the *Clk* 3' UTR contains at least 3 functional *ban* target sites (Figure 5.1B). Abolishing each site alone or especially in combination in flies increased the incidence of arrhythmicity and reduced the amplitude of the behavioral rhythms (Table 5.1, Figure 5.2A). We performed all experiments at 18^{o}C, because some p{*Clk*ban#1-2-3} flies did not survive to the end of the experiment at higher temperatures (data not shown). The life-span and metabolic abnormalities of p{*Clk*ban#1-2-3} flies will be discussed in more detail in addendum 1 of this thesis. However, it is unlikely that the weaker behavioral rhythms in DD manifested by p{*Clk*ban#1-2-3} flies is due to health issues. For example, in LD the flies are strongly rhythmic. Also, the PRC experiments were performed with young flies (Figure 5.2B) and

the magnitude of phase shifts in p{*Clk*ban#1-2-3} flies was significantly increased (Figure 5.2B).

We also tested transgenic flies that were generated using P-element mediated insertion strategy to test if the results we obtained were peculiar to a particular insertion site. p{*Clk*ban#1-2-3(P)} lines were nearly completely arrhythmic (Table 5.1), and did not display any anticipation of the lights-on transition in LD (data not shown), very similar to Clk^{out}. Thus, the circadian phenotype for these mutants was more severe than those evaluated at the VK insertion site. However, even the wild type line of the P element generated lines showed a higher rate of arrhythmicity, consistent with an earlier report [73]. It is known that insertion sites are prone to local positional effects on the chromatin altering the levels or pattern of the transgene expression [214]. It is possible that the VK00018 insertion site enables higher expression of our *Clk* containing constructs compared to other sites that were targeted by P-element insertion.

Prior work showed that *Clk* mutations that cause a decrease in CLK levels reduce the strength of behavioral rhythms [215]. Because miRNAs function by repressing gene expression, but the p{*Clk*ban#1-2-3} flies have reduced rhythm strength, this prompted us to investigate CLK expression in the s-LNv pacemaker neurons responsible for driving circadian rhythms. Indeed, mutating the three *ban* sites in the *Clk* 3' UTR leads to significant reductions in CLK staining, especially in s-LNvs (Figure 5.3), further supporting our earlier results described in Chapter 4. Despite the fact that lower CLK levels explain the weak behavioral rhythms in p{*Clk*ban#1-2-3} flies, our results raise the intriguing possibility that the binding of *ban* to the 3' UTR of *Clk* actually increases its expression in LNvs. However, the inhibition of the constructs containing *Clk* 3' UTR by ectopic *ban* in S2 cells (Chapter 4 and Figure 5.1B); and the repression of a GFP based sensor by endogenous *ban* in s-LNvs (Figure 5.4), implies that there are other unknown factors and/or mechanisms involved in the modulation of *Clk* by *ban* in s-LNvs.

Using a new GFP-*ban* sponge we showed that *ban* is expressed in LNvs (Figure 5.4), further supporting the role of *ban* in modulating CLK levels specifically in these pacemaker neurons. miRNA *ban** derived from the other side of the stem-loop might also be expressed in neurons, and might regulate our GFP-control, which has partial complementary sites to it. However according to miRBase (mirbase.org), *ban** is expressed at least an order of magnitude less than miRNA *ban*. Also, a previous study did not find any detectable *ban** [80] in developing tissues. Still, to reinforce of our results, additional experiments will be performed by co-expressing our *ban* sensor and *ban*. The GFP-*ban* sponge should be further down-regulated when expressed with ectopic *ban* in the pacemaker neurons. If *ban* is necessary to maintain sufficient CLK levels in the s-LNvs, why do flies overexpressing the GFP-*ban* sponge in the pacemaker neurons, mimicking a *ban*–null environment (Table S5.1) or *ban* hypomorphs (Chapter 4-Table 4.1) do not have weaker circadian rhythms? One possible answer to this question is that there are other targets of *ban* in the circadian network regulating *Clk* levels. That might not be surprising because miRNAs as network stabilizers might modulate multiple genes in the same feedback loops. Therefore it is intriguing to note that *Par domain protein 1* (*pdp1*), the transcriptional activator of *Clk*, contains computationally predicted *ban* target sites. Further studies are needed to show the significance of these sites and the direction of regulation. In summary, our results here and those described in Chapter 4 strongly suggest that the regulation of *Clk* expression by *ban* might represent a novel mode-of-action for miRNAs.

Contributions: All the experiments in this chapter were performed by Evrim Yildirim.

SUPPLEMENTARY TABLE FOR CHAPTER 5

Table S5.1: Locomotor activity rhythms for transgenic flies bearing *ban* sponge and control[a]

Genotype[b]	Period (hr ±SEM)	Power[c]	Rhythmicity (%)[d]	Total flies[e]
GFP-*ban* sponge	23.4±0.08	114.4	92.3	26
GFP-control	23.7±0.09	84.2	87.5	24
*tim*UASgal4	24.7±0.18	70.7	64	25
*tim*UASgal4> GFP-*ban* sponge	24.4±0.06	117.5	100	26
*tim*UASgal4> GFP-control	24±0.9	96.7	94.1	24

[a] Young male flies were maintained at 25^{o}C and exposed to 5 days of 12:12 LD cycles followed by 6 days of DD.
[b] Transgenic flies bearing GFP based constructs alone or driven by timUASgal4 driver.
[c] Power is a measure of the strength or amplitude of the rhythm in arbitrary units.
[d] Percentage of flies showing locomotor rhythms with a power value of ≥10 and a width value of ≥2.
[e] Total number of flies that survived until the end of the experimental period.

Addendum 1: *Bantam* miRNA sites on the circadian *Clock* gene modulate longevity and metabolism in *Drosophila*

(Yildirim and Edery, manuscript in preparation)

While examining the effects of *ban* target sites in the *Clk* 3' UTR on locomoter activity rhythms (see Chapters 4 and 5), we noted that some of the the p{*Clk*ban#1-2-3} and Clk^{out} flies did not survive the entire test period (usually 7-10 days) when the behavior assays were performed at 25^{o} and 29^{o}C, whereas flies containing the wild type *Clk* transgene did not show an increased mortality rate at these temperatures (data not shown). At all test temperatures (18^{o}, 25^{o} and 29^{o}C), the p{*Clk*ban#1-2-3} flies showed weak activity rhythms and the Clk^{out} flies were arrhythmic (data not shown). Several lines of evidence indicate that the rhythm defects in the p{*Clk*ban#1-2-3} and Clk^{out} flies are not health related. Most notably, at 18^{o}C the *Clk* mutants and the wild type *Clk* control have normal life spans but the same rhythm defects are still observed in the *Clk* mutants (Chapter 4 and 5). However we were very intrigued by the unexpected possible connection between *ban* sites in the *Clk* 3' UTR and life-span in *Drosophila*.

To test if eliminating the *ban* sites on the *Clk* 3' UTR might also have an effect on longevity, we performed standard survival experiments at the different temperatures (18^{o}, 25^{o}, 29^{o}C), using isogenized p{*Clk*WT} and p{*Clk*ban#1-2-3} lines, in addition to Clk^{out} flies. At each temperature tested, Clk^{out} flies had the shortest life-span followed by p{*Clk*ban#1-2-3} flies (Figure 6.1A for 29^{o}C, and data not shown), when reared under a standard food recipe. It is not surprising that the Clk^{out} mutation reduces life-span, because a null-mutation of *cyc*, the partner of *dClk*, was shown to decrease life span [216]. More interesting is the reduced longevity of p{*Clk*ban#1-2-3} flies as compared to p{*Clk*WT}. As noted earlier (Chapters 4 and 5), CLK levels are indistinguishable in fly head extracts

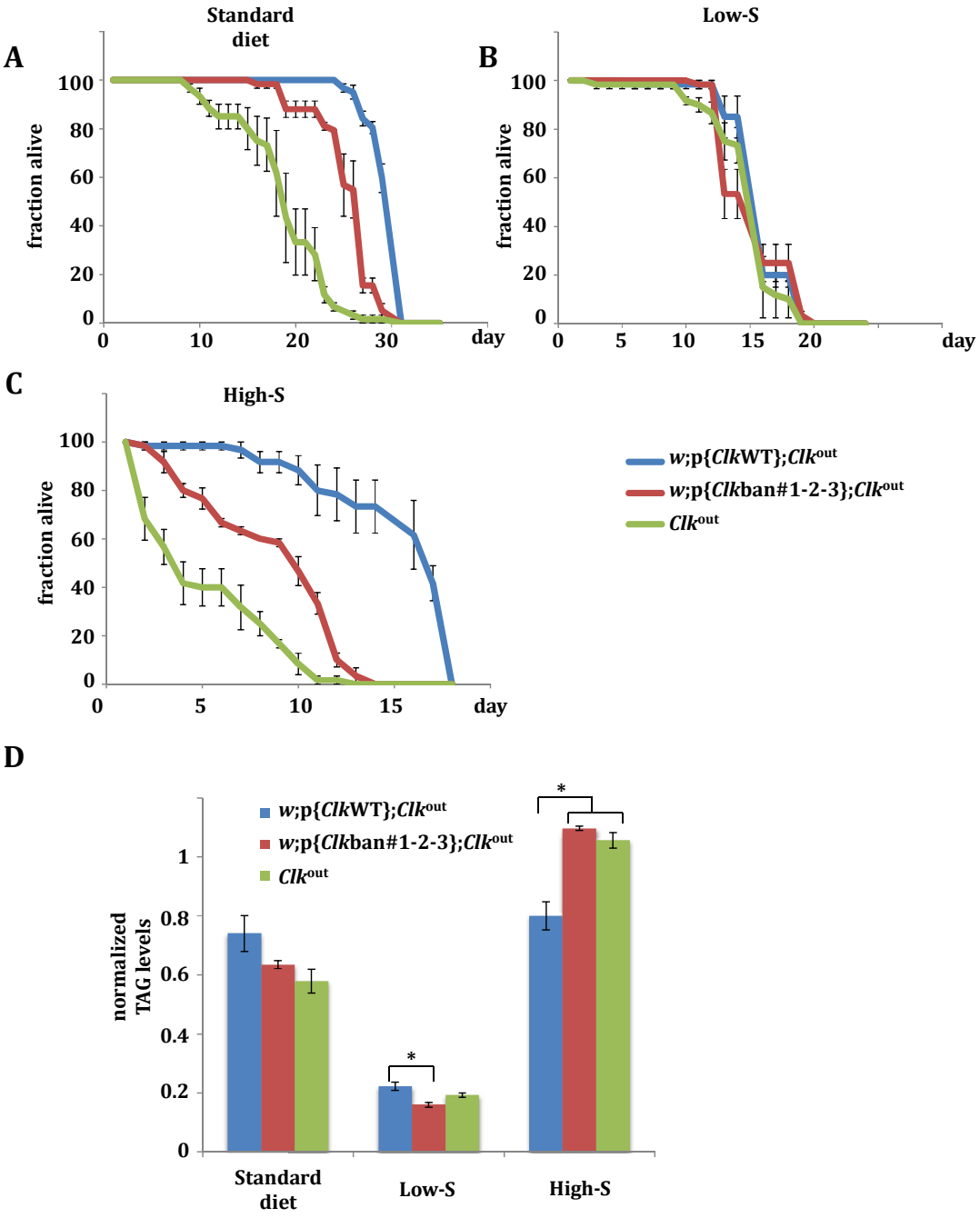

Figure 6.1. *Ban* sites on *Clk* modulate life span and energy metabolism.

The survival curves of male flies of indicated genotypes at 29ºC under different diet (**A**, standard Bloomington fly food; **B**, Low-S diet: 2.5% sugar + 10%yeast; **C**, High-S diet: 40% sugar + 10% yeast). The difference in survivalship between all genotypes were statistically significant (log rank test, $p<0.05$) in **A** and **C**, but not **B**. **D**, Age-matched male

Figure legend of figure 6.1 continued

adult flies were reared on indicated diet for 7 days at 18ºC. On the last day at ZT1 flies were collected; triaclygleceride (TAG) and protein levels measured using whole body extracts. TAG levels shown, were normalized to protein content.

between p{*Clk*WT} and p{*Clk*ban#1-2-3} flies (Chapters 4 and 5). The main difference is that p{*Clk*ban#1-2-3} flies have reduced CLK staining in the key ventro-lateral pacemaker neurons (Chapters 4 and 5). Because p{*Clk*ban#1-2-3} flies have reduced survival, similar to Clk^{out} flies, this further supports the notion that mutating the *ban* sites on the *dClk* 3' UTR reduces CLK levels. Our results suggest that similar to its effect in the s-LNvs and circadian behavior, *ban* might up-regulate *Clk* in other adult tissues important for survival.

We further tested survival with different food recipes mainly by changing the sugar concentration, because calorie restriction is a well established method of extending life-span in a wide variety of organism ([217], reviewed in [218]), including *D. melanogaster* [219]. The nutritional content of the fly diet derives primarily from two ingredients: sucrose (carbohydrate) and brewer's yeast (protein). We based our studies on prior work showing that flies survive longer on a low sugar diet (i.e., 2.5% sugar; Low-S) compared to a higher sugar diet (40% sugar; High-S) [220] (Figure 6.1B, C). In our experiments the yeast content was kept the same (10%). When survival was assayed using Low-S at 29^{o}C and other temperatures, all three genotypes had similar survival (Figure 6.1B, data not shown). However, flies had increased mortality when fed the low sugar diet compared to the standard food (Figure 6.1, panels A and B), which might be because the standard food also contains soy flour and corn meal and constitutes a fuller diet. Intriguingly, when assayed on 40% sugar, the life span of both p{*Clk*ban#1-2-3} and Clk^{out} flies were dramatically reduced compare to the wild type control (Figure 6.1C). Thus, there is a clear mortality trend that follows the severity of the *Clk* mutation (i.e., Clk^{out} $>$ triple *ban* mutant $>$ WT control), and the increased mortality of the *Clk* mutant flies compared to the *Clk* wild type control is augmented with increasing sugar in the diet.

We next asked if the reduction in life span in the presence of high sugar food could be tied to altered energy metabolism. Excess glucose is converted to glycogen and

triacylglycerides (TAG) for long-term storage and to this end, we measured the TAG levels from flies reared under different food compositions at 18^{o}C, where all flies from three genotypes survived during the test period (data not shown). When reared on low sugar diet there was no or small differences of TAG content between all three genotypes (Figure 6.1D). A previous study also did not find any difference in TAG levels among circadian clock mutants [221]. However, in the presence of 40% sugar, p{*Clk*ban#1-2-3} and *Clk*^{out} accumulated significantly more TAG, similar to the case of mice carrying the mammalian *Clk* mutation [222]. This difference in TAG levels was observed only in the presence of high sugar diet, which might be the reason that the other study missed it [221]. The decrease in the life span can not be explained only by the altered lipid metabolism, because mutant flies still lived shorter when reared on standard food even though they have similar TAG levels compared to wild type flies. However higher TAG levels could have contributed to the early demise of p{*Clk*ban#1-2-3} and *Clk*^{out} flies when fed high sugar diet, possibly leading to hearth dysfunction [223]. Although more studies will have to be done to better understand the physiological reasons for why the risk of mortality in p{*Clk*ban#1-2-3} and *Clk*^{out} flies increases with sugar levels in the diet, mutations in the mammalian *Clk* gene are associated with metabolic syndromes, such as diabetes [224], [225], suggesting that the our p{*Clk*ban#1-2-3} flies might offer a more physiologically relevant model (compared to a null mutant) to study the link between circadian rhythms and metabolism.

Addendeum 2: Preliminary studies on a phospho-cluster near the *per^{Clk}* mutation that contributes to clock speed

(Yildirim, Chiu and Edery, manuscript in preparation)

We previously identified several phospho-clusters in the dPER circadian clock inhibitory domain (CCID) using mass spectroscopy [34]. One of these phospho-clusters (T978/S981/T983) was found near the classical *per* mutation *per^{Clk}* (A975V) in a not very well conserved region across *Drosophila* species (Figure 7.1 A, B). Both T978 and S981 are flanked on the C-terminus by a proline residue, suggesting they are phosphorylated by a pro-directed kinase. In prior we showed that NEMO, a pro-directed kinase, phosphorylates S596 on dPER ([38]).

To check if the *per^{Clk}* mutation affects the phosphorylation of the T978/S981/T983 phospho-module, we created transgenic flies where we altered all three identified residues of this cluster alone or in combination with the *per^{Clk}* mutation. While mutating T978/S981/T983 to Alanine significantly shortens the period (about 1 hr when present in double copies), changing these residues to the potentially phospho-mimic Aspartic acid only had modest effects on the period (Table 7.1). We therefore focused our studies on the alanine mutants that abrogate phosphorylation.

Flies carrying a *per^{Clk}* variant of the *per* transgene displayed faster clocks as previously reported [226]. Blocking the phosphorylation of T978/S981/T983 (T978A/S981A/T983A) in combination with the *per^{Clk}* mutation did not increase the speed of the clock further, which suggests that phosphorylation of this cluster is downstream of the *per^{Clk}* mutation (Table 7.2). We also tested transgenic flies carrying only single Ala replacements in this phospho-cluster. The largest effect on the period was observed with S981A; while T983A did not lead any differences in clock speed (Table 7.2). The increase

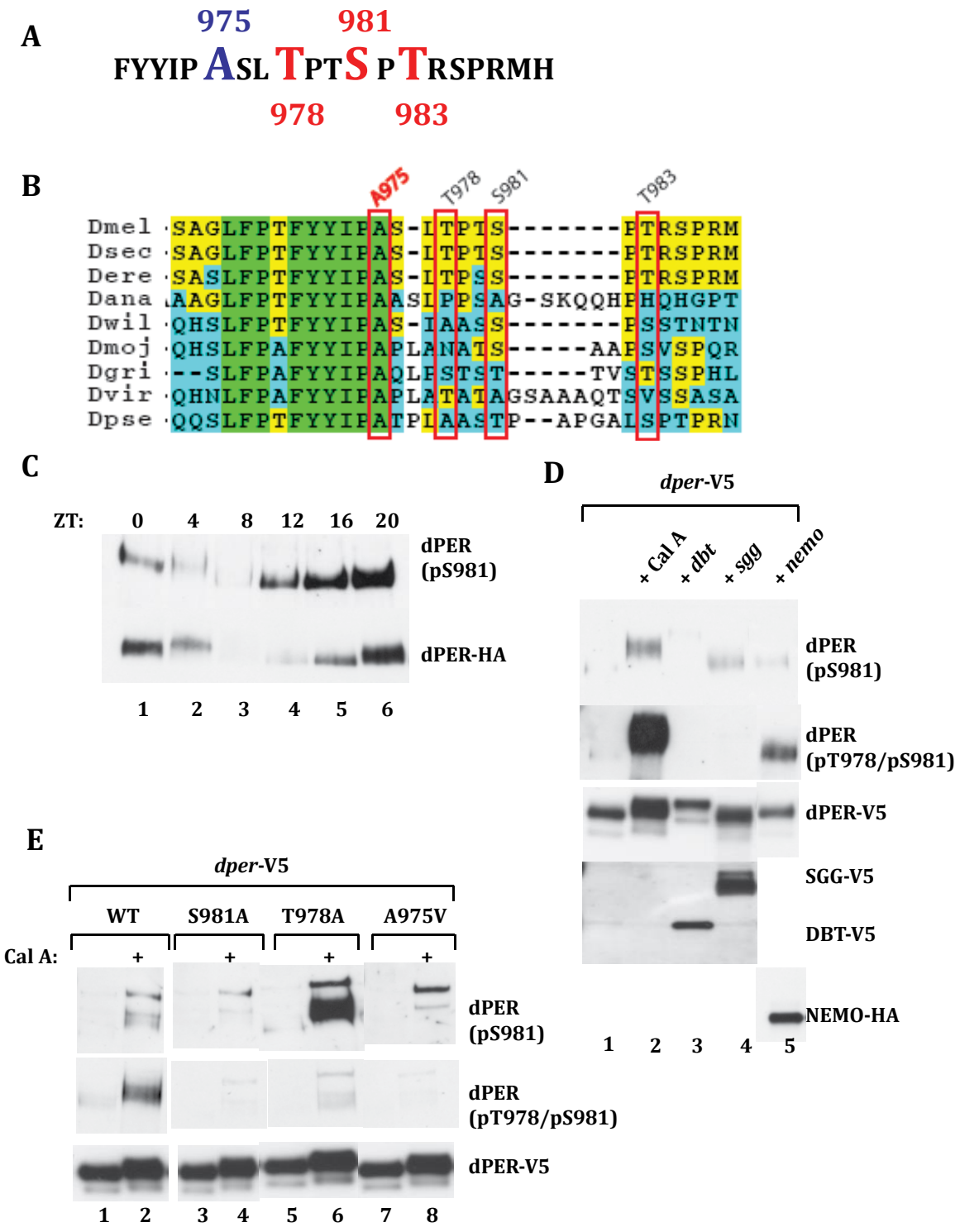

Figure 7.1. Characterization of a new phospho-cluster near the *per*^{Clk} mutation.

A, The sequence of PER protein between residues 970-989. Phospho-residues are marked in red and the residue altered in *per*^{Clk} mutation is shown in blue. **B,** The region of

Figure legend of figure 7.1 continued

PER containing phospho-sites T978/S981/T983 is not very well conserved in *Drosophila*. **C,** Adult flies were collected at the indicated times (ZT) and prepared head extracts were subjected to immunoprecipitation with anti-HA beads. Recovered immune complexes were resolved by 6% SDS-PAGE and blotted in the presence of anti-HA to measure total dPER levels or dPER phospho-specific anti-pS981 antibody. **D**, S2 were transiently transfected with pAc-per-V5 alone (lane 1, 2) or in the presence of pMT driven kinases (lane 3, 4, 5). Cells were treated 4 hours with the proteasome inhibitor MG132 and the protein synthesis inhibitor cycloheximide after 18 hours of kinase induction, or were treatead with Calyculin A for 1.5 hr in the presence of MG312 and cyclohexamide (lane 2). Extract were prepared and dPER containing complexes were immunoprecipitated with anti-V5 beads. Recovered complexes were resolved using 4-15% gels in the presence of indicated antibodies on the right panel. **E,** Wild type or mutant variants of pAc-*per*-V5 plasmids were transected into S2 cells. 1.5 hr before the collection cells were treated with Calyculin A in the presence of MG312 and cyclohexamide, or as a mock treatment just with MG312 and cyclohexamide. dPER complexes were immunoprecipitated with anti-V5 beads. Recovered complexes were resolved using 6% gel for phospho-specific antibodies or 4-15% gels for anti-V5 antibody.

Table 7.1: Locomotor activity rhythms for mutant PER transgenics and controls[a]

Genotype[b]	Period (hr ±SEM)	Power[c]	Rhythmicity (%)[d]	Total flies[e]
wper^0; *per*$^+$-HA (T978A/S981A/T983A) (3F)	22.4±0.06	124.1	92.3	26
wper^0; *per*$^+$-HA (T978D/S981D/T983D) (1M)	24±0.15	98.7	60	21
wper^0; *per*$^+$-HA (T978D/S981D/T983D) (3M)	23.9±0.1	90.8	92.3	32
wper^0; *per*$^+$-HA (1M)	23.5±0.05	139.3	100	30
wper^0; *per*$^+$-HA (2M)	23.4±0.07	125.2	100	32
Single copy transgenics[f]:				
wper^0; *per*$^+$-HA (T978A/S981A/T983A)/- (3F)	23.4±0.04	98.3	100	32
wper^0; *per*$^+$-HA (T978A/S981A/T983A)/- (1M)	22.8±0.04	90	100	32
wper^0; *per*$^+$-HA (T978A/S981A/T983A)/- (2M)	23.2±0.04	108	100	32
wper^0; *per*$^+$-HA (T978D/S981D/T983D)/- (1M)	24.7±0.08	96.2	100	32
wper^0; *per*$^+$-HA (T978D/S981D/T983D)/- (2M)	24.3±0.06	77.2	100	31
wper^0; *per*$^+$-HA (T978D/S981D/T983D) (3M)	24.8±0.05	91	100	32
wper^0; *per*$^+$-HA (A975V)/- (2F)	22.9±0.06	99.3	100	31
wper^0; *per*$^+$-HA (A975V)/- (1M)	22.6±0.05	103.4	100	31
wper^0; *per*$^+$-HA (A975V)/- (1F)	22.6±0.07	99	96.9	32
wper^0; *per*$^+$-HA (A975V/ T978A/S981A/T983A)/- (1F)	22.7±0.05	98.6	100	30
wper^0; *per*$^+$-HA (A975V/ T978A/S981A/T983A)/- (2F)	22.3±0.05	102.7	100	32
wper^0; *per*$^+$-HA (A975V/ T978A/S981A/T983A)/- (5F)	22.8±0.06	97.3	100	32
wper^0; *per*$^+$-HA (A975V/ T978D/S981D/T983D)/- (1F)	23.3±0.05	90.7	100	31
wper^0; *per*$^+$-HA (T978D/S981D/T983D)/- (2F)	23.9±0.08	83.5	100	32
wper^0; *per*$^+$-HA (T978D/S981D/T983D)/- (3F)	23.4±0.06	103.8	100	31
wper^0; *per*$^+$-HA/- (1M)	24.4±0.07	150.9	100	30

[a] Young male flies were maintained at 25°C and exposed to 5 days of 12:12 LD cycles followed by 6 days of DD

[b] Independent transgenic lines are designated by the numbers in parenthesis

[c] Power is a measure of the strength or amplitude of the rhythm in arbitrary units

[d] Percentage of flies showing locomotor rhythms with a power value of ≥10 and a width value of ≥2

[e] Total number of flies that survived until the end of the experimental period

[f] These lines contains only a single wild type or mutant *per* transgene

Table 7.2: Behavioral rhythms for mutant PER transgenics and controls[a]

Genotype[b]	Period (hr ±SEM)	Power[c]	Rhythmicity (%)[d]	Total flies[e]
wper^{0}; *per*$^{+}$-HA (T978A)/- (1M)	24.4±0.12	113.5	83.3	14
wper^{0}; *per*$^{+}$-HA (T978A)/- (2M)	24.4±0.07	151.7	100	17
wper^{0}; *per*$^{+}$-HA (T978A)/- (3M)	24±0.14	146.3	100	15
wper^{0}; *per*$^{+}$-HA (T978D)/- (2M)	25.3±0.05	138.9	100	25
wper^{0}; *per*$^{+}$-HA (T978D)/- (4M)	24.7±0.13	139.6	100	24
wper^{0}; *per*$^{+}$-HA (T978D)/- (5M)	26.2±0.13	137.4	100	31
wper^{0}; *per*$^{+}$-HA (S981A)/- (1M)	23.1±0.05	145	96.7	30
wper^{0}; *per*$^{+}$-HA (S981A)/- (2F)	23.3±0.04	161.1	100	32
wper^{0}; *per*$^{+}$-HA (S981A)/- (3F)	23.6±0.06	161.8	100	26
wper^{0}; *per*$^{+}$-HA (S981D)/- (1M)	23.4±0.04	165	100	26
wper^{0}; *per*$^{+}$-HA (S981D)/- (2M)	23.6±0.04	147.9	100	22
wper^{0}; *per*$^{+}$-HA (S981D)/- (3M)	23.7±0.07	135.7	100	31
wper^{0}; *per*$^{+}$-HA (T983A)/- (2M)	23.9±0.09	135.7	96.8	31
wper^{0}; *per*$^{+}$-HA (T983A)/- (3M)	24.3±0.11	146.5	100	17
wper^{0}; *per*$^{+}$-HA (T983A)/- (4M)	24.4±0.31	56.2	90.6	32
wper^{0}; *per*$^{+}$-HA (T983D)/- (1M)	24±0.13	127.4	95.2	21
wper^{0}; *per*$^{+}$-HA/- (1M)	24.4±0.07	150.9	100	30

[a] Young male flies were maintained at 25^{o}C and exposed to 5 days of 12:12 LD cycles followed by 6 days of DD

[b] Independent transgenic lines containing only a single copy of *per* wild type or mutant variant transgenes are designated by the numbers in parenthesis

[c] Power is a measure of the strength or amplitude of the rhythm in arbitrary units

[d] Percentage of flies showing locomotor rhythms with a power value of ≥10 and a width value of ≥2

[e] Total number of flies that survived until the end of the experimental period

in the period length of T978D mutation suggests that the phospho-occupancy of this residue might be involved in the period setting.

To better study the phosphorylation of this module, we created phospho-specific antibodies against single or doubly phosphorylated peptides, pS981 and pT978/pS981. The specificity of these antibodies was tested as before (e.g., Chapter 2). Essentially, recombinant *dper* was expressed in S2 cells in the presence of the protein phosphatase inhibitor (Cal A) to induce hyper-phosphorylation of dPER. Subsequently, extracts were subjected to immunoprecipitation followed by immunoblotting in the presence of the phospho-specific antibody. Whereas wild type dPER is recognized by both the pS981 and pT978/pS981 phospho-specific antibodies (Figure 7.1E, lanes 1 and 2), the anti-pS981 signal is strongly diminished when probing the dPER(S981A) but not dPER(T978A) (Figure 7.1E, compare lanes 4 and 6). Moreover, mutating either S981 or T978 abolished recognition of dPER by the anti-pT978/pS981 antibody (Figure 7.1E, lanes 4 and 6). Other studies using phosphatase treatment further confirmed the phospho-specificity of the antibodies (data not shown).

As an initial attempt to identify the kinase phosphorylating this cluster we used the S2 cell system to express a *dper* containing plasmid in the presence of several circadian relevant kinases (Figure 7.1D). Both *sgg* and *nemo* were able to phosphorylate S981 to some extent, however the anti-pT978/pS981 antibody recognized a clear signal only in the presence of *nemo*, suggesting that *nemo* might also be involved in the regulation of these proline-directed sites.

To find if there is any hierarchy between T978 and S981 phosphorylation and if per^{Clk} mutation abolishes phosphorylation of T978/S981, we expressed wild type and mutant versions of *dper* in the presence of the phosphatase inhibitor Calyculin A. In agreement with the behavior data, per^{Clk} (A975V) mutation blocked the phosphorylation of this cluster (Figure 7.1E, compare lanes 2 and 8). Preventing the phosphorylation of T978

enhanced the phosphorylation of S981 (Figure 7.1E, compare lanes 2 and 6). Even though it is tempting to speculate that phosphorylation of T978 blocks that of S981; T978D mutation in fly lengthened the period as opposed to the S981A mutation which caused a shortening in the period. The increase in signal of anti-pS981 antibody in the presence of the T978A mutation might be explained by an enhanced affinity of the antibody to that peptide. To solve this problem, further studies involving ELISA tests using different peptides need to be performed, as in Chapter 2.

The temporal phosphorylation pattern of S981 in flies followed the daily cycling of PER levels, suggesting it is constitutively phosphorylated at the same extent throughout a daily cycle (Figure 7.1C). We could not detect good signals from fly extracts using the anti-pT978/pS981 (data not shown). In any case our results provide a possible explanation for the period shortening effect of the classical *per*^{Clk} mutation; i.e., the *per*^{Clk} mutation inhibits further phosphorylation of the T978A/S981A/T983A cluster, which speeds up the pace of the clock. Thus, we have identified another (potentially NEMO-mediated) hierarchical phospho-cluster that regulates circadian period, further suggesting that clock speed is governed by a complex interaction of phosho-clusters. Future work will involve trying to determine the molecular underpinnings for how phosphorylation at the T978A/S981A/T983A phospho-cluster affects the molecular clock (e.g., *dper* mRNA and protein rhythms), which will form the basis of a short manuscript.

Contributions: J. Chiu identified potential phosphor sites on PER in a previous study (Chiu, 2008). All the experiments presented here were performed by Evrim Yildirim.

Chapter 6. Summary

Circadian rhythms are driven by the daily oscillation in the expression of a few core clock genes. While the rhythmic transcription of clock genes forms the basis of cyclic gene expression, posttranscriptional mechanisms contribute to the period and amplitude of the oscillator. In this thesis, I studied how phosphorylation, and miRNAs modulate the key clock genes *per* and *Clk* in the *Drosophila* circadian timing system. I showed that phospho-sites S826/S828 in the NLS-2 region of PER are important in the entrainment to light and temperature cycles, unearthing a previously unknown function for PER that is not related to regulating the pace of the clock (Chapter 2). In related studies, CLK phosphorylation was shown to play a role in thermal entrainment, possibly by regulating the amplitude of the rhythms, as our results from Chapter 3 showed. In addition to the role of phosphorylation in circadian rhythm generation, I examined and characterized the involvement of the miRNA *bantam* in the *Drosophila* circadian system, which revealed a very unusual mode-of-action by up-regulating the level of its target, CLK, in key pacemaker neurons (Chapters 4 and 5). Altogether, the work described in this thesis makes novel contributions to our understanding of how post-transcriptional regulatory pathways contribute to circadian timing. Below I briefly summarize my work, including work not formally presented in this thesis.

dPER, the main circadian repressor in the *Drosophila* clock undergoes a complex phosphorylation program that regulates its levels and function throughout a daily cycle. A network of hierarchical phosphorylation events mediated by multiple kinases build a so called 'phospho-timer' [38]. Distinct phospho-sites enhance or slow down the daily downswing in dPER levels, while in other cases modulate the timing of nuclear translocation time, and so dictate the period of the circadian clock. For example, an earlier downswing in the levels of dPER, as observed in the classic per^{S} mutant, speeds up the

clock by advancing the start of CLK-CYC-mediated transcription. To date, all the characterized phospho-sites on dPER are associated with these two aspects of dPER metabolism, stability and nuclear entry.

In this thesis I present evidence that phosphorylation of two residues in the NLS-2 region of dPER modulates entrainment without affecting the degradation or subcellular localization of dPER (Chapter 2). Even though blocking phosphorylation of S826/S828 changed the period slightly (about an hour), we did not observe an effect on dPER stability, progressive phosphorylation, timing of nuclear entry, or *dper* mRNA/protein curves. The main and largest effect of altering these residues was on the entrainment by daily light-dark and especially temperature cycles. Light information is processed through the circadian photoreceptor CRY increasing its affinity for TIM and targeting both proteins to degradation [12]. Without TIM, dPER becomes unstable. Thus, the light-mediated degradation of TIM and subsequent destabilization of dPER was thought to be the basis of entrainment. For example, light in the early night leads to degradation of TIM in the cytoplasm, delaying the nuclear entry of dPER, thus (seemingly) explaining why light-pulses during this part of the night yield phase delays in circadian rhythms. Our results suggest another mechanism for the role of TIM and dPER in entrainment. TIM might act as a temporal scaffold to protect certain sites on dPER from posttranslational modifications including phosphorylation in a time specific manner. In the absence of TIM, these modules get activated and regulate phase-specific responses (although it is still not clear how dPER phosphorylation can encode phase specific information). A similar role of TIM acting as a scaffold in aiding binding of PER to CLK has been reported [9]. Thus, dPER might be the main entrainment agent and determinant of the phase. This would be similar to the mammalian clock, where light stimulates the expression of *mPer1* and *mPer2* by CREB through a very complex inter-cellular signaling pathway (reviewed in [227]).

We observed the largest effect of mutating the NLS-2 region on entrainment to daily temperature cycles. It is known that both dPER and TIM levels show oscillations in daily abundance during temperature cycles [105]. However, how changes in temperature drive cycles in dPER and TIM has yet to be determined. Very recently it was reported that PDF signals from lateral neurons might lead to degradation of TIM independent of CRY in evening cells, which provides a possible explanation of TIM rhythms in constant darkness [228]; a similar mechanism might exist in temperature cycles. Further studies will be needed to characterize the daily phosphorylation pattern of S826/S828 during temperature entrainment.

Another novel result in our study was that the NLS-2 region did not act as a nuclear translocation signal (NLS) *in vivo*. This region was only tested in S2 tissue culture and with a truncated dPER protein containing only the C-terminal portion [8], which might explain the discrepancy between results in S2 cells and flies. An N-terminal NLS has been reported and might be the main determinant of dPER nuclear entry [86]. Clearly, mutations in NLS-2 do not affect the timing of dPER nuclear entry (Chapter 2). Although the biochemical function of NLS-2 is not clear, flies carrying a *dper* mutant transgene where basic residues of NLS-2 were altered, displayed very little circadian response to short light pulses, very similar to the circadian blind cry^{01} mutant [105]. It will be of interest to determine if NLS-2 mutant flies are more resistant to the arhythmicity induced by exposure to constant light [229]. If so, this would further support the ideas that the NLS-2 region is critical for circadian photosensitivity.

Irrespective of the biochemical function of NLS-2 sequence, our results showed a surprising role for dPER phosphorylation in entrainment. Further studies will be needed to gain insight into how this entrainment module relays time-of-the–day information to downstream players in the circadian system. Our findings might be very relevant to human health; humans experience phase shifts due to jetlag or work shift. If there exists similar

entrainment modules on human PER, the activities of relevant kinases could be modulated using inhibitors to delay or advance the rhythms and align with the local time.

I also tested the function of several other phospho-clusters on dPER, including T978/S981/T983 near the *per*^{Clk} mutation (Addendum 2), S1185/S1187/T1191 and T610 (data not shown). The *per*^{Clk} mutation interacted genetically with the T978/S981/T983 cluster in flies, and blocked phosphorylation of this module in S2 cells. Both T978 and S981 are proline-direted phospho-sites and could be phosphorylated by NEMO in S2 tissue culture. It is intriguing to find the involvement of NEMO in this module, as NEMO has been shown to modulate another proline-directed site S596 near *per*^{s} imposing time-delay for DBT mediated phosphorylation of nearby sites [38]. How the phosphorylation of pro-directed sites affects dPER are not yet clear, but they seem to act in a priming dependent manner to “activate” a phospho-cluster for subsequent phosphorylation, thus acting as important switches in clock speed control. In general, multi-site phosphorylation of dPER is thought to lead to a more open structure, enhancing degradation [38]. Intriguingly, the key phospho-timer in the Neurospora clock FREQUECNY (FRQ) is also thought to undergo phosphorylation dependent changes in conformation leading to degradation [37]. With regards to the T978/S981/T983 cluster in flies, additional studies will examine the dPER protein and RNA rhythms in mutant transgenics and together these results will form the basis of a short manuscript in the near future.

Besides the phospho-clusters I described in my thesis, I also analyzed other phospho-clusters but did not pursue the findings much further. Studying the S1185/S1187/T1191 cluster unveiled another hierarchical phosphorylation cascade, initiated by DBT, which phosphorylates T1191, priming subsequent phosphorylation of S1187 by SGG, at least in tissue culture (data not shown). However altering these residues in flies did not affect the period or entrainment (data not shown), showing that not all phospho-sites on dPER have an obvious function in setting the speed of the clock.

Further work would be needed to identify the aspects of dPER metabolism/function these sites contribute to. Finally, I also examined phosphorylation of T610 on dPER, a site near to the *per*^{S} cluster. Altering T610 mainly affected the stability of dPER in tissue culture cells, and lengthened the period in flies dramatically (data not shown). Furthermore mutating both S596 and T610 to alanine in flies shortened the period to a similar extend as S596A mutation, suggesting that the T610 phosphorylation event is upstream of S596 or that both phospho-sites act in parallel in regulating the stability of dPER. Similar results were recently published by another group [41] and therefore I did not pursue this further.

The major take home lesson from my combined studies on characterizing dPER phospho-sites is that the clusters can have very different effects on dPER metabolism and function. Of special importance is the realization that just because a phospho-site/cluster has little effect on the speed of the clock (the usual way to interpret 'significance') does not mean it has no physiological value. Of course, the case in point for this conclusion is my findings on S826/828 and its unprecedented role in entrainment. Whether or not other clusters, such as S1185/S1187/T1191, will reveal other unchartered aspects of PER function is presently not clear. Certainly, the PER phosphorylation program is very complex and based on the integration of many phospho-sites.

In addition to characterizing dPER phospho-sites I also made an initial attempt at quantitative phosphoproteomics using the Mass Spectrometry Facility that is directed by Dr. Peter Lobel at my home institute. To this end I purified dPER from S2 cells in the presence of protein phosphatase (PP) 1 or 2A inhibitors in combination with a GSK3-β (*sgg* homolog of *Drosophila*) inhibitor, followed by TMT labeling and mass spectroscopy. PP2A and PP1A were suggested to have differential effects on dPER metabolism by probably acting on different phospho-sites [50], [49]. SGG phosphorylates dPER at least on S657 and probably other sites ([40] and data not shown). Thus using different combination of inhibitors, we hoped to see quantifiable difference in the extent of

phosphorylation of distinct sites. If successful with this strategy, we sought to expand our analysis; e.g., kinetics of progressive phosphorylation in the presence of DBT, identify hierarchical phosphorylation events and interdependencies between phospho-sites. Although I did not have the time to fully explore these issues, initial results were encouraging and I feel confident that the overall strategy I helped optimize will lead to further insights into the role of phosphorylation on dPER metabolism/activity and possiblely help identify new clock kinases.

Besides PER, other clock proteins are phosphorylated. I contributed to studies aimed at understanding how phosphorylation affects dCLK function (Chapter 3). We identified at least 15 phospho-sites using mass spectrometry, and blocking phosphorylation at these sites stabilized dCLK in flies and decreased the period length slightly. Most importantly dCLK phospho mutant flies could not entrain to daily temperature cycles but could entrain to light-dark cycles. Thus, similar to my studies on S826/828, phosphorylation of dCLK also affects entrainment. However, unlike phosphorylation of the NLS-2 'entrainment module', the defect in the thermal entrainment of dCLK phospho mutant is likely due to a higher amplitude clock caused by increased expression of dPER. Overexpression of PER renders flies resistant to arrhythmicity in constant light conditions [230]. Similar to this, higher amplitude oscillation in PER levels may override resetting by weaker environmental cues, such as temperature. Thus, it is likely that the entrainment defect in dCLK phospho mutant flies is downstream of the effects on clock amplitude, unlike the case for S826/828 which has no noticeable effect on the clockworks, suggesting a primary role in entrainment.

In the other major focus of my thesis I identified *ban* as a regulator of circadian amplitude and characterized its interaction with *dClk* (Chapter 4 and 5). *ban* imparts robustness to circadian rhythms through its target *dClk,* by maintaining dCLK levels in key pacemaker neurons. However, the direction of this regulation is very surprising and

contrary to the conventional wisdom that miRNAs downregulate the target gene expression. It is not unprecedented that miRNAs enhance the expression of their targets, however the mechanism involved in this type of regulation is usually indirect [231], [232], [233]. At least in one case, but only in cell cycle arrested cells, miRNA 369-3 was shown to increase the translation of its target through the parts of the RNA induced silencing complex and an interaction with AU rich elements (AREs) [211], [234]. In S2 cells ectopic *ban* repressed expression via the *dClk* 3' UTR, but in neurons, mitotically inactive tissues, *ban* might act in the opposite way as in previous example. The mechanism of the regulation of *dClk* by *ban* is yet to be determined. However lower dCLK levels in the ley pacemaker neurons of p{*Clk*ban#1-2-3} flies nicely explains their loss of behavioral rhythms in constant darkness.

Over or under-expression of *ban* does not result in lower amplitude rhythms, implying ban might have other targets in core clock mechanism. I also generated UAS-*ban*(mut) construct expressing a mutant version of *ban* with a seed complementary to the *dClk* 3' mutations. This flies could be used in future studies to test the effect of *ban* directly on *dClk*. Most likely, This construct will behave like a miRNA in flies, because *ban*(mut) can repress the mutant *dClk* 3' in S2 cells (Chapter 4, Figure 4.1). It will be interesting to examine if overexpression of *ban*(mut) in s-LNvs of p{*Clk*ban#1-2-3} can rescue the lower amplitude rhythms. Furthermore, gene-switch drivers could be used to limit the expression of *ban*(mut) only in adult stage to remove any developmental issue. These experiments should give a clearer answer on the direction of this regulation. Although some of my results were not able to be published because of a competing paper that was published while ours was under review (Chapter 4), the unconventional effect of *dClk ban* sites on dCLK levels in specific clock cells should form the basis of an interesting manuscript.

During our studies of *ban* sites on *dClk* we uncovered a novel role of *dClk* in longevity and fat metabolism (Addendum 1). Altering *ban* sites on *dClk* or abolishing dCLK

function as in *Clk*^{out} mutants led to shorter life-spans in various conditions tested. Furthermore at high sugar containing food, p{*Clk*ban#1-2-3} and *Clk*^{out} flies accumulated significantly higher triacylglycerides, which might contributed to their early demise. The connection of *dClk* and metabolism is not surprising; it has already been shown that mammalian CLK is involved in insulin metabolism [222], and disruption of CLK leads to diabetes [224], [225]. Our results suggest, that dCLK plays a similar metabolic role in *Drosophila*.

In conclusion, in my thesis work, I showed several examples of the importance of posttranscriptional regulation in circadian rhythm generation and entrainment. The results presented here will shed new insights on the molecular underpinning of circadian clocks, how they are synchronized and their interaction with other physiological systems.

REFERENCES:

1. Edery, I., *Circadian rhythms in a nutshell.* Physiol Genomics, 2000. **3**(2): p. 59 - 74.
2. Panda, S., J.B. Hogenesch, and S.A. Kay, *Circadian rhythms from flies to human.* Nature, 2002. **417**(6886): p. 329-335.
3. Buhr, E.D., S.-H. Yoo, and J.S. Takahashi, *Temperature as a Universal Resetting Cue for Mammalian Circadian Oscillators.* Science, 2010. **330**(6002): p. 379-385.
4. Dunlap, J., *Molecular bases for circadian clocks.* Cell, 1999. **96**(2): p. 271 - 290.
5. Konopka, R.J. and S. Benzer, *Clock mutants of Drosophila melanogaster.* Proc Natl Acad Sci U S A, 1971. **68**(9): p. 2112-6.
6. Hardin, P.E., *The circadian timekeeping system of Drosophila.* Curr Biol, 2005. **15**(17): p. R714-22.
7. Menet, J.S., et al., *Dynamic PER repression mechanisms in the Drosophila circadian clock: from on-DNA to off-DNA.* Genes & Development, 2010. **24**(4): p. 358-367.
8. Chang, D.C. and S.M. Reppert, *A Novel C-Terminal Domain of Drosophila PERIOD Inhibits dCLOCK:CYCLE-Mediated Transcription.* Current Biology, 2003. **13**(9): p. 758-762.
9. Sun, W.C., et al., *Two Distinct Modes of PERIOD Recruitment onto dCLOCK Reveal a Novel Role for TIMELESS in Circadian Transcription.* The Journal of Neuroscience, 2010. **30**(43): p. 14458-14469.
10. Kim, E. and I. Edery, *Balance between DBT/CKIepsilon kinase and protein phosphatase activities regulate phosphorylation and stability of Drosophila CLOCK protein.* Proc Natl Acad Sci U S A, 2006. **103**(16): p. 6178 - 6183.
11. Emery, P., et al., *CRY, a Drosophila Clock and Light-Regulated Cryptochrome, Is a Major Contributor to Circadian Rhythm Resetting and Photosensitivity.* Cell, 1998. **95**(5): p. 669-679.
12. Busza, A., et al., *Roles of the Two Drosophila CRYPTOCHROME Structural Domains in Circadian Photoreception.* Science, 2004. **304**(5676): p. 1503-1506.
13. Koh, K., X. Zheng, and A. Sehgal, *JETLAG Resets the Drosophila Circadian Clock by Promoting Light-Induced Degradation of TIMELESS.* Science, 2006. **312**(5781): p. 1809-1812.
14. Peschel, N., et al., *Light-Dependent Interactions between the Drosophila Circadian Clock Factors Cryptochrome, Jetlag, and Timeless.* Current Biology, 2009. **19**(3): p. 241-247.
15. Kaushik, R., et al., *PER-TIM Interactions with the Photoreceptor Cryptochrome Mediate Circadian Temperature Responses in Drosophila.* PLoS Biol, 2007. **5**(6): p. e146.
16. Collins, B., et al., *Drosophila CRYPTOCHROME Is a Circadian Transcriptional Repressor.* Current Biology, 2006. **16**(5): p. 441-449.

17. Ko, H.W., J. Jiang, and I. Edery, *Role for Slimb in the degradation of Drosophila Period protein phosphorylated by Doubletime.* Nature, 2002. **420**(6916): p. 673-678.
18. Cyran, S.A., et al., *vrille, Pdp1, and dClock Form a Second Feedback Loop in the Drosophila Circadian Clock.* Cell, 2003. **112**(3): p. 329-341.
19. Kim, E.Y., et al., *Drosophila CLOCK protein is under posttranscriptional control and influences light-induced activity.* Neuron, 2002. **34**(1): p. 69-81.
20. Zheng, X., et al., *An Isoform-Specific Mutant Reveals a Role of PDP1ε in the Circadian Oscillator.* The Journal of Neuroscience, 2009. **29**(35): p. 10920-10927.
21. Rutila, J., et al., *CYCLE is a second bHLH-PAS clock protein essential for circadian rhythmicity and transcription of Drosophila period and timeless.* Cell, 1998. **93**(5): p. 805 - 814.
22. Bae, K., et al., *Circadian regulation of a Drosophila homolog of the mammalian Clock gene: PER and TIM function as positive regulators.* Mol Cell Biol, 1998. **18**(10): p. 6142-51.
23. Bae, K., et al., *dCLOCK is present in limiting amounts and likely mediates daily interactions between the dCLOCK-CYC transcription factor and the PER-TIM complex.* J Neurosci, 2000. **20**(5): p. 1746-53.
24. Kadener, S., et al., *Clockwork Orange is a transcriptional repressor and a new Drosophila circadian pacemaker component.* Genes Dev, 2007. **21**(13): p. 1675 - 1686.
25. Lim, C., et al., *Clockwork orange encodes a transcriptional repressor important for circadian-clock amplitude in Drosophila.* Curr Biol, 2007. **17**(12): p. 1082 - 1089.
26. Nakajima, M., et al., *Reconstitution of Circadian Oscillation of Cyanobacterial KaiC Phosphorylation in Vitro.* Science, 2005. **308**(5720): p. 414-415.
27. O/'Neill, J.S. and A.B. Reddy, *Circadian clocks in human red blood cells.* Nature, 2011. **469**(7331): p. 498-503.
28. O/'Neill, J.S., et al., *Circadian rhythms persist without transcription in a eukaryote.* Nature, 2011. **469**(7331): p. 554-558.
29. Gallego, M. and D. Virshup, *Post-translational modifications regulate the ticking of the circadian clock.* Nat Rev Mol Cell Biol, 2007. **8**(2): p. 139 - 148.
30. Bae, K. and I. Edery, *Regulating a circadian clock's period, phase and amplitude by phosphorylation: insights from Drosophila.* J Biochem (Tokyo), 2006. **140**(5): p. 609 - 617.
31. Lim, C. and R. Allada, *Emerging roles for post-transcriptional regulation in circadian clocks.* Nat Neurosci, 2013. **16**(11): p. 1544-1550.
32. Mehra, A., et al., *Post-translational modifications in circadian rhythms.* Trends in Biochemical Sciences, 2009. **34**(10): p. 483-490.
33. Edery, I., et al., *Temporal phosphorylation of the Drosopila period protein.* Proceedings of the National Academy of Sciences, 1994. **91**(6): p. 5.

34. Chiu, J.C., et al., *The phospho-occupancy of an atypical SLIMB-binding site on PERIOD that is phosphorylated by DOUBLETIME controls the pace of the clock.* Genes & Development, 2008. **22**(13): p. 1758-1772.
35. Baker, C.L., et al., *Quantitative Proteomics Reveals a Dynamic Interactome and Phase-Specific Phosphorylation in the Neurospora Circadian Clock.* Molecular Cell, 2009. **34**(3): p. 354-363.
36. Vanselow, K., et al., *Differential effects of PER2 phosphorylation: molecular basis for the human familial advanced sleep phase syndrome (FASPS).* Genes & Development, 2006. **20**(19): p. 2660-2672.
37. Querfurth, C., et al., *Circadian Conformational Change of the Neurospora Clock Protein FREQUENCY Triggered by Clustered Hyperphosphorylation of a Basic Domain.* Molecular Cell, 2011. **43**(5): p. 713-722.
38. Chiu, Joanna C., Hyuk W. Ko, and I. Edery, *NEMO/NLK Phosphorylates PERIOD to Initiate a Time-Delay Phosphorylation Circuit that Sets Circadian Clock Speed.* Cell, 2011. **145**(3): p. 357-370.
39. Lin, J.-M., A. Schroeder, and R. Allada, *In Vivo Circadian Function of Casein Kinase 2 Phosphorylation Sites in Drosophila PERIOD.* J. Neurosci., 2005. **25**(48): p. 11175-11183.
40. Ko, H.W., et al., *A Hierarchical Phosphorylation Cascade That Regulates the Timing of PERIOD Nuclear Entry Reveals Novel Roles for Proline-Directed Kinases and GSK-3β/SGG in Circadian Clocks.* The Journal of Neuroscience, 2010. **30**(38): p. 12664-12675.
41. Garbe, D.S., et al., *Cooperative Interaction between Phosphorylation Sites on PERIOD Maintains Circadian Period in Drosophila.* PLoS Genet, 2013. **9**(9): p. e1003749.
42. Szabo, A., et al., *The CK2 kinase stabilizes CLOCK and represses its activity in the Drosophila circadian oscillator.* PLoS Biol, 2013. **11**(8): p. e1001645.
43. Akten, B., et al., *A role for CK2 in the Drosophila circadian oscillator.* Nat Neurosci, 2003. **6**(3): p. 251-257.
44. Meissner, R.-A., et al., *TIMELESS Is an Important Mediator of CK2 Effects on Circadian Clock Function In Vivo.* The Journal of Neuroscience, 2008. **28**(39): p. 9732-9740.
45. Akten, B., et al., *Ribosomal S6 Kinase Cooperates with Casein Kinase 2 to Modulate the Drosophila Circadian Molecular Oscillator.* The Journal of Neuroscience, 2009. **29**(2): p. 466-475.
46. Kloss, B., et al., *Phosphorylation of period is influenced by cycling physical associations of double-time, period, and timeless in the Drosophila clock.* Neuron, 2001. **30**(3): p. 699 - 706.
47. Nawathean, P. and M. Rosbash, *The Doubletime and CKII Kinases Collaborate to Potentiate Drosophila PER Transcriptional Repressor Activity.* Molecular Cell, 2004. **13**(2): p. 213-223.
48. Kula-Eversole, E., et al., *Surprising gene expression patterns within and between PDF-containing circadian neurons in Drosophila.* Proceedings of the National Academy of Sciences, 2010. **107**(30): p. 13497-13502.

49. Sathyanarayanan, S., et al., *Posttranslational Regulation of Drosophila PERIOD Protein by Protein Phosphatase 2A.* Cell, 2004. **116**(4): p. 603-615.
50. Fang, Y., S. Sathyanarayanan, and A. Sehgal, *Post-translational regulation of the Drosophila circadian clock requires protein phosphatase 1 (PP1).* Genes & Development, 2007. **21**(12): p. 1506-1518.
51. Kim, E.Y., et al., *A role for O-GlcNAcylation in setting circadian clock speed.* Genes & Development, 2012. **26**(5): p. 490-502.
52. Toh, K.L., et al., *An hPer2 Phosphorylation Site Mutation in Familial Advanced Sleep Phase Syndrome.* Science, 2001. **291**(5506): p. 1040-1043.
53. Nitabach, M.N. and P.H. Taghert, *Organization of the Drosophila Circadian Control Circuit.* Current Biology, 2008. **18**(2): p. R84-R93.
54. Park, J.H., et al., *Differential regulation of circadian pacemaker output by separate clock genes in Drosophila.* Proceedings of the National Academy of Sciences, 2000. **97**(7): p. 3608-3613.
55. Peng, Y., et al., *Drosophila Free-Running Rhythms Require Intercellular Communication.* PLoS Biol, 2003. **1**(1): p. e13.
56. Grima, B., et al., *Morning and evening peaks of activity rely on different clock neurons of the Drosophila brain.* Nature, 2004. **431**(7010): p. 869-873.
57. Shafer, O.T., et al., *Widespread Receptivity to Neuropeptide PDF throughout the Neuronal Circadian Clock Network of Drosophila Revealed by Real-Time Cyclic AMP Imaging.* Neuron, 2008. **58**(2): p. 223-237.
58. Li, Y., et al., *PDF and cAMP enhance PER stability in Drosophila clock neurons.* Proceedings of the National Academy of Sciences, 2014. **111**(13): p. E1284-E1290.
59. Stoleru, D., et al., *The Drosophila Circadian Network Is a Seasonal Timer.* Cell, 2007. **129**(1): p. 207-219.
60. Yao, Z. and O.T. Shafer, *The Drosophila Circadian Clock Is a Variably Coupled Network of Multiple Peptidergic Units.* Science, 2014. **343**(6178): p. 1516-1520.
61. Welsh, D.K., J.S. Takahashi, and S.A. Kay, *Suprachiasmatic Nucleus: Cell Autonomy and Network Properties.* Annual Review of Physiology, 2010. **72**(1): p. 551-577.
62. Fabian, M.R., N. Sonenberg, and W. Filipowicz, *Regulation of mRNA Translation and Stability by microRNAs.* Annual Review of Biochemistry, 2010. **79**(1): p. 351-379.
63. Bartel, D.P., *MicroRNAs: target recognition and regulatory functions.* Cell, 2009. **136**(2): p. 215-33.
64. Miska, E.A., et al., *Caenorhabditis elegans microRNAs Are Individually Not Essential for Development or Viability.* PLoS Genet, 2007. **3**(12): p. e215.
65. Li, Y., et al., *MicroRNA-9a ensures the precise specification of sensory organ precursors in Drosophila.* Genes Dev, 2006. **20**(20): p. 2793-805.

66. Herranz, H. and S.M. Cohen, *MicroRNAs and gene regulatory networks: managing the impact of noise in biological systems.* Genes & Development, 2010. **24**(13): p. 1339-1344.
67. Ebert, Margaret S. and Phillip A. Sharp, *Roles for MicroRNAs in Conferring Robustness to Biological Processes.* Cell, 2012. **149**(3): p. 515-524.
68. Yang, M., et al., *Circadian regulation of a limited set of conserved microRNAs in Drosophila.* BMC Genomics, 2008. **9**: p. 83.
69. Siré, C., et al., *Diurnal oscillation in the accumulation of Arabidopsis microRNAs, miR167, miR168, miR171 and miR398.* FEBS Letters, 2009. **583**(6): p. 1039-1044.
70. Cheng, H., et al., *microRNA modulation of circadian-clock period and entrainment.* Neuron, 2007. **54**(5): p. 813 - 829.
71. Luo, W. and A. Sehgal, *Regulation of Circadian Behavioral Output via a MicroRNA-JAK/STAT Circuit.* Cell, 2012. **148**(4): p. 765-779.
72. Vodala, S., et al., *The Oscillating miRNA 959-964 Cluster Impacts Drosophila Feeding Time and Other Circadian Outputs.* Cell Metabolism, 2012. **16**(5): p. 601-612.
73. Kadener, S., et al., *A role for microRNAs in the Drosophila circadian clock.* Genes & Development, 2009. **23**(18): p. 2179-2191.
74. Huang, Z.J., I. Edery, and M. Rosbash, *PAS is a dimerization domain common to Drosophila Period and several transcription factors.* Nature, 1993. **364**(6434): p. 259-262.
75. Kim, E.Y., et al., *A DOUBLETIME Kinase Binding Domain on the Drosophila PERIOD Protein Is Essential for Its Hyperphosphorylation, Transcriptional Repression, and Circadian Clock Function.* Mol. Cell. Biol., 2007. **27**(13): p. 5014-5028.
76. Nawathean, P., D. Stoleru, and M. Rosbash, *A Small Conserved Domain of Drosophila PERIOD Is Important for Circadian Phosphorylation, Nuclear Localization, and Transcriptional Repressor Activity.* Molecular and Cellular Biology, 2007. **27**(13): p. 5002-5013.
77. Gekakis, N., et al., *Isolation of timeless by PER protein interaction: Defective interaction between timeless protein and long-period mutant PERL.* Science, 1995. **270**(5237): p. 811-815.
78. Saez, L. and M.W. Young, *Regulation of nuclear entry of the Drosophila clock proteins period and timeless.* Neuron, 1996. **17**(5): p. 911-20.
79. Rieger, D., et al., *Functional Analysis of Circadian Pacemaker Neurons in Drosophila melanogaster.* The Journal of Neuroscience, 2006. **26**(9): p. 2531-2543.
80. Brennecke, J., et al., *bantam Encodes a Developmentally Regulated microRNA that Controls Cell Proliferation and Regulates the Proapoptotic Gene hid in Drosophila.* Cell, 2003. **113**(1): p. 25-36.
81. Markson, J.S. and E.K. O'Shea, *The molecular clockwork of a protein-based circadian oscillator.* FEBS Lett, 2009. **583**(24): p. 3938-47.

82. Kloss, B., et al., *The Drosophila clock gene double-time encodes a protein closely related to human casein kinase Iepsilon.* Cell, 1998. **94**(1): p. 97-107.
83. Price, J.L., et al., *double-time Is a Novel Drosophila Clock Gene that Regulates PERIOD Protein Accumulation.* Cell, 1998. **94**(1): p. 83-95.
84. Ashmore, L.J. and A. Sehgal, *A fly's eye view of circadian entrainment.* J Biol Rhythms, 2003. **18**(3): p. 206-16.
85. Curtin, K.D., Z.J. Huang, and M. Rosbash, *Temporally regulated nuclear entry of the Drosophila period protein contributes to the circadian clock.* Neuron, 1995. **14**(2): p. 365-72.
86. Vosshall, L.B., et al., *Block in nuclear localization of period protein by a second clock mutation, timeless.* Science, 1994. **263**(5153): p. 1606-9.
87. Darlington, T.K., et al., *Closing the circadian loop: CLOCK-induced transcription of its own inhibitors per and tim.* Science, 1998. **280**(5369): p. 1599-603.
88. Lee, C., K. Bae, and I. Edery, *PER and TIM inhibit the DNA binding activity of a Drosophila CLOCK-CYC/dBMAL1 heterodimer without disrupting formation of the heterodimer: a basis for circadian transcription.* Mol Cell Biol, 1999. **19**(8): p. 5316-25.
89. Grima, B., et al., *The F-box protein slimb controls the levels of clock proteins period and timeless.* Nature, 2002. **420**(6912): p. 178-82.
90. Lin, J.M., et al., *A role for casein kinase 2alpha in the Drosophila circadian clock.* Nature, 2002. **420**(6917): p. 816-20.
91. Martinek, S., et al., *A role for the segment polarity gene shaggy/GSK-3 in the Drosophila circadian clock.* Cell, 2001. **105**(6): p. 769-79.
92. Yu, W., J.H. Houl, and P.E. Hardin, *NEMO kinase contributes to core period determination by slowing the pace of the Drosophila circadian oscillator.* Curr Biol, 2011. **21**(9): p. 756-61.
93. Kivimae, S., L. Saez, and M.W. Young, *Activating PER repressor through a DBT-directed phosphorylation switch.* PLoS Biol, 2008. **6**(7): p. e183.
94. Lee, C., K. Bae, and I. Edery, *The Drosophila CLOCK protein undergoes daily rhythms in abundance, phosphorylation, and interactions with the PER-TIM complex.* Neuron, 1998. **21**(4): p. 857-67.
95. Dolezelova, E., D. Dolezel, and J.C. Hall, *Rhythm defects caused by newly engineered null mutations in Drosophila's cryptochrome gene.* Genetics, 2007. **177**(1): p. 329-45.
96. Chiu, J.C., et al., *Assaying Locomotor Activity to Study Circadian Rhythms and Sleep Parameters in Drosophila.* 2010(43): p. e2157.
97. Emery, P., et al., *Drosophila CRY is a deep brain circadian photoreceptor.* Neuron, 2000. **26**(2): p. 493-504.
98. Suri, V., et al., *Evidence that the TIM light response is relevant to light-induced phase shifts in Drosophila melanogaster.* Neuron, 1998. **21**(1): p. 225-34.
99. Robins, H., Y. Li, and R.W. Padgett, *Incorporating structure to predict microRNA targets.* Proceedings of the National Academy of Sciences of the United States of America, 2005. **102**(11): p. 4006-4009.

100. Sidote, D., et al., *Differential Effects of Light and Heat on theDrosophila Circadian Clock Proteins PER and TIM.* Molecular and Cellular Biology, 1998. **18**(4): p. 2004-2013.
101. Cyran, S.A., et al., *The Double-Time Protein Kinase Regulates the Subcellular Localization of the Drosophila Clock Protein Period.* The Journal of Neuroscience, 2005. **25**(22): p. 5430-5437.
102. Majercak, J., W. Chen, and I. Edery, *Splicing of the period gene 3'-terminal intron is regulated by light, circadian clock factors, and phospholipase C.* Mol Cell Biol, 2004. **24**(8): p. 3359 - 3372.
103. Ko, H.W., et al., *Cis-combination of the classic per(S) and per(L) mutations results in arrhythmic Drosophila with ectopic accumulation of hyperphosphorylated PERIOD protein.* J Biol Rhythms, 2007. **22**(6): p. 488-501.
104. Shafer, O.T., M. Rosbash, and J.W. Truman, *Sequential Nuclear Accumulation of the Clock Proteins Period and Timeless in the Pacemaker Neurons of Drosophila melanogaster.* J. Neurosci., 2002. **22**(14): p. 5946-5954.
105. Stanewsky, R., et al., *The cryb mutation identifies cryptochrome as a circadian photoreceptor in Drosophila.* Cell, 1998. **95**(5): p. 681-92.
106. Lee, C., et al., *Resetting the Drosophila clock by photic regulation of PER and a PER-TIM complex.* Science, 1996. **271**(5256): p. 1740-4.
107. Rothenfluh, A., M.W. Young, and L. Saez, *A TIMELESS-independent function for PERIOD proteins in the Drosophila clock.* Neuron, 2000. **26**(2): p. 505-14.
108. Rieger, D., R. Stanewsky, and C. Helfrich-Forster, *Cryptochrome, compound eyes, Hofbauer-Buchner eyelets, and ocelli play different roles in the entrainment and masking pathway of the locomotor activity rhythm in the fruit fly Drosophila melanogaster.* J Biol Rhythms, 2003. **18**(5): p. 377-91.
109. Dushay, M.S., et al., *Phenotypic and genetic analysis of Clock, a new circadian rhythm mutant in Drosophila melanogaster.* Genetics, 1990. **125**(3): p. 557-78.
110. Konopka, R.J., et al., *An ultrashort clock mutation at the period locus of Drosophila melanogaster that reveals some new features of the fly's circadian system.* J Biol Rhythms, 1994. **9**(3-4): p. 189-216.
111. Suri, V., J.C. Hall, and M. Rosbash, *Two novel doubletime mutants alter circadian properties and eliminate the delay between RNA and protein in Drosophila.* J Neurosci, 2000. **20**(20): p. 7547-55.
112. Wheeler, D.A., et al., *Behavior in light-dark cycles of Drosophila mutants that are arrhythmic, blind, or both.* J Biol Rhythms, 1993. **8**(1): p. 67-94.
113. Busza, A., A. Murad, and P. Emery, *Interactions between circadian neurons control temperature synchronization of Drosophila behavior.* J Neurosci, 2007. **27**(40): p. 10722-33.
114. Johnson, C.H., *Forty years of PRCs--what have we learned?* Chronobiol Int, 1999. **16**(6): p. 711-43.

115. Allada, R. and B.Y. Chung, *Circadian organization of behavior and physiology in Drosophila.* Annu Rev Physiol, 2010. **72**: p. 605-24.
116. Zhang, E.E. and S.A. Kay, *Clocks not winding down: unravelling circadian networks.* Nat Rev Mol Cell Biol, 2010. **11**(11): p. 764-76.
117. Hastings, J.W., B. Rusak, and Z. Boulos, *Circadian rhythms: the physiology of biological timing*. 4th ed. Neural and integrative animal physiology, ed. P.C. L. 1991, USA: New York : Wiley-Liss, c1991.
118. Yoshii, T., C. Hermann, and C. Helfrich-Forster, *Cryptochrome-positive and -negative clock neurons in Drosophila entrain differentially to light and temperature.* J Biol Rhythms, 2010. **25**(6): p. 387-98.
119. Hardin, P.E., *Molecular genetic analysis of circadian timekeeping in Drosophila.* Adv Genet, 2011. **74**: p. 141-73.
120. Glossop, N.R., et al., *VRILLE feeds back to control circadian transcription of Clock in the Drosophila circadian oscillator.* Neuron, 2003. **37**(2): p. 249-61.
121. Partch, C.L., C.B. Green, and J.S. Takahashi, *Molecular architecture of the mammalian circadian clock.* Trends Cell Biol, 2014. **24**(2): p. 90-9.
122. Diernfellner, A.C. and T. Schafmeier, *Phosphorylations: Making the Neurosporacrassa circadian clock tick.* FEBS Lett, 2011. **585**(10): p. 1461-6.
123. Reischl, S. and A. Kramer, *Kinases and phosphatases in the mammalian circadian clock.* FEBS Lett, 2011. **585**(10): p. 1393-9.
124. Yu, W., et al., *PER-dependent rhythms in CLK phosphorylation and E-box binding regulate circadian transcription.* Genes Dev, 2006. **20**(6): p. 723-33.
125. Yu, W., et al., *DOUBLETIME plays a noncatalytic role to mediate CLOCK phosphorylation and repress CLOCK-dependent transcription within the Drosophila circadian clock.* Mol Cell Biol, 2009. **29**(6): p. 1452-8.
126. Weber, F., et al., *Second messenger and Ras/MAPK signalling pathways regulate CLOCK/CYCLE-dependent transcription.* J Neurochem, 2006. **98**(1): p. 248-57.
127. Lee, C., et al., *Posttranslational mechanisms regulate the mammalian circadian clock.* Cell, 2001. **107**(7): p. 855-67.
128. Kondratov, R.V., et al., *BMAL1-dependent circadian oscillation of nuclear CLOCK: posttranslational events induced by dimerization of transcriptional activators of the mammalian clock system.* Genes Dev, 2003. **17**(15): p. 1921-32.
129. Yoshitane, H., et al., *Roles of CLOCK phosphorylation in suppression of E-box-dependent transcription.* Mol Cell Biol, 2009. **29**(13): p. 3675-86.
130. Spengler, M.L., et al., *A serine cluster mediates BMAL1-dependent CLOCK phosphorylation and degradation.* Cell Cycle, 2009. **8**(24): p. 4138-46.
131. Tischkau, S.A., et al., *Protein kinase G type II is required for night-to-day progression of the mammalian circadian clock.* Neuron, 2004. **43**(4): p. 539-49.

132. Shim, H.S., et al., *Rapid activation of CLOCK by Ca2+-dependent protein kinase C mediates resetting of the mammalian circadian clock.* EMBO Rep, 2007. **8**(4): p. 366-71.
133. Schlosser, A., J.T. Vanselow, and A. Kramer, *Mapping of phosphorylation sites by a multi-protease approach with specific phosphopeptide enrichment and NanoLC-MS/MS analysis.* Anal Chem, 2005. **77**(16): p. 5243-50.
134. Golic, K.G. and M.M. Golic, *Engineering the Drosophila genome: chromosome rearrangements by design.* Genetics, 1996. **144**(4): p. 1693-711.
135. Parks, A.L., et al., *Systematic generation of high-resolution deletion coverage of the Drosophila melanogaster genome.* Nat Genet, 2004. **36**(3): p. 288-92.
136. Thibault, S.T., et al., *A complementary transposon tool kit for Drosophila melanogaster using P and piggyBac.* Nat Genet, 2004. **36**(3): p. 283-7.
137. Venken, K.J., et al., *P[acman]: a BAC transgenic platform for targeted insertion of large DNA fragments in D. melanogaster.* Science, 2006. **314**(5806): p. 1747-51.
138. Groth, A.C., et al., *Construction of transgenic Drosophila by using the site-specific integrase from phage phiC31.* Genetics, 2004. **166**(4): p. 1775-82.
139. Kadener, S., et al., *Circadian transcription contributes to core period determination in Drosophila.* PLoS Biol, 2008. **6**(5): p. e119.
140. Zhao, J., et al., *Drosophila clock can generate ectopic circadian clocks.* Cell, 2003. **113**(6): p. 755-66.
141. Pittendrigh, C.S., *ON TEMPERATURE INDEPENDENCE IN THE CLOCK SYSTEM CONTROLLING EMERGENCE TIME IN DROSOPHILA.* Proc Natl Acad Sci U S A, 1954. **40**(10): p. 1018-29.
142. Chen, Y., et al., *Alterations of per RNA in noncoding regions affect periodicity of circadian behavioral rhythms.* J Biol Rhythms, 1998. **13**(5): p. 364-79.
143. Rensing, L. and P. Ruoff, *Temperature effect on entrainment, phase shifting, and amplitude of circadian clocks and its molecular bases.* Chronobiol Int, 2002. **19**(5): p. 807-64.
144. Glaser, F.T. and R. Stanewsky, *Temperature synchronization of the Drosophila circadian clock.* Curr Biol, 2005. **15**(15): p. 1352-63.
145. Yoshii, T., et al., *Temperature cycles drive Drosophila circadian oscillation in constant light that otherwise induces behavioural arrhythmicity.* Eur J Neurosci, 2005. **22**(5): p. 1176-84.
146. Yoshii, T., M. Sakamoto, and K. Tomioka, *A temperature-dependent timing mechanism is involved in the circadian system that drives locomotor rhythms in the fruit fly Drosophila melanogaster.* Zoolog Sci, 2002. **19**(8): p. 841-50.
147. So, W.V. and M. Rosbash, *Post-transcriptional regulation contributes to Drosophila clock gene mRNA cycling.* EMBO J, 1997. **16**(23): p. 7146-55.
148. Edery, I., *A master CLOCK hard at work brings rhythm to the transcriptome.* Genes Dev, 2011. **25**(22): p. 2321-6.

149. Lamaze, A., et al., *The E3 ubiquitin ligase CTRIP controls CLOCK levels and PERIOD oscillations in Drosophila.* EMBO Rep, 2011. **12**(6): p. 549-57.
150. He, Q., et al., *CKI and CKII mediate the FREQUENCY-dependent phosphorylation of the WHITE COLLAR complex to close the Neurospora circadian negative feedback loop.* Genes Dev, 2006. **20**(18): p. 2552-65.
151. Schafmeier, T., et al., *Transcriptional feedback of Neurospora circadian clock gene by phosphorylation-dependent inactivation of its transcription factor.* Cell, 2005. **122**(2): p. 235-46.
152. Eide, E.J., et al., *The circadian regulatory proteins BMAL1 and cryptochromes are substrates of casein kinase Iepsilon.* J Biol Chem, 2002. **277**(19): p. 17248-54.
153. Sanada, K., T. Okano, and Y. Fukada, *Mitogen-activated protein kinase phosphorylates and negatively regulates basic helix-loop-helix-PAS transcription factor BMAL1.* J Biol Chem, 2002. **277**(1): p. 267-71.
154. Pittendrigh, C., V. Bruce, and P. Kaus, *ON THE SIGNIFICANCE OF TRANSIENTS IN DAILY RHYTHMS.* Proc Natl Acad Sci U S A, 1958. **44**(9): p. 965-73.
155. Liu, Y., et al., *How temperature changes reset a circadian oscillator.* Science, 1998. **281**(5378): p. 825-9.
156. Brown, S.A., et al., *Rhythms of mammalian body temperature can sustain peripheral circadian clocks.* Curr Biol, 2002. **12**(18): p. 1574-83.
157. Lahiri, K., et al., *Temperature regulates transcription in the zebrafish circadian clock.* PLoS Biol, 2005. **3**(11): p. e351.
158. Matsumoto, A., et al., *Light and temperature cooperate to regulate the circadian locomotor rhythm of wild type and period mutants of Drosophila melanogaster.* J Insect Physiol, 1998. **44**(7-8): p. 587-596.
159. Gentile, C., et al., *Cryptochrome antagonizes synchronization of Drosophila's circadian clock to temperature cycles.* Curr Biol, 2013. **23**(3): p. 185-95.
160. Vinayak, P., et al., *Exquisite light sensitivity of Drosophila melanogaster cryptochrome.* PLoS Genet, 2013. **9**(7): p. e1003615.
161. Lakin-Thomas, P.L., S. Brody, and G.G. Cote, *Amplitude model for the effects of mutations and temperature on period and phase resetting of the Neurospora circadian oscillator.* J Biol Rhythms, 1991. **6**(4): p. 281-97.
162. Pittendrigh, C.S., W.T. Kyner, and T. Takamura, *The amplitude of circadian oscillations: temperature dependence, latitudinal clines, and the photoperiodic time measurement.* J Biol Rhythms, 1991. **6**(4): p. 299-313.
163. Abraham, U., et al., *Coupling governs entrainment range of circadian clocks.* Mol Syst Biol, 2010. **6**: p. 438.
164. Vitaterna, M.H., et al., *The mouse Clock mutation reduces circadian pacemaker amplitude and enhances efficacy of resetting stimuli and phase-response curve amplitude.* Proc Natl Acad Sci U S A, 2006. **103**(24): p. 9327-32.

165. Dallmann, R., J.P. DeBruyne, and D.R. Weaver, *Photic resetting and entrainment in CLOCK-deficient mice.* J Biol Rhythms, 2011. **26**(5): p. 390-401.
166. Winfree, A.T., *The Geometry of Biological Time*. Second Edition ed. 2001: Springer.
167. Gatfield, D., et al., *Integration of microRNA miR-122 in hepatic circadian gene expression.* Genes Dev, 2009. **23**(11): p. 1313-26.
168. Na, Y.J., et al., *Comprehensive analysis of microRNA-mRNA co-expression in circadian rhythm.* Exp Mol Med, 2009.
169. Xu, S., et al., *MicroRNA (miRNA) transcriptome of mouse retina and identification of a sensory organ-specific miRNA cluster.* J Biol Chem, 2007. **282**(34): p. 25053-66.
170. Brodersen, P. and O. Voinnet, *Revisiting the principles of microRNA target recognition and mode of action.* Nat Rev Mol Cell Biol, 2009. **10**(2): p. 141-8.
171. Cohen, S.M., J. Brennecke, and A. Stark, *Denoising feedback loops by thresholding--a new role for microRNAs.* Genes Dev, 2006. **20**(20): p. 2769-72.
172. Li, X., et al., *A MicroRNA Imparts Robustness against Environmental Fluctuation during Development.* Cell, 2009. **137**(2): p. 273-282.
173. Stark, A., et al., *Animal MicroRNAs confer robustness to gene expression and have a significant impact on 3'UTR evolution.* Cell, 2005. **123**(6): p. 1133-46.
174. Houl, J.H., et al., *Drosophila CLOCK is constitutively expressed in circadian oscillator and non-oscillator cells.* J Biol Rhythms, 2006. **21**(2): p. 93-103.
175. Allada, R., et al., *A recessive mutant of Drosophila Clock reveals a role in circadian rhythm amplitude.* Embo J, 2003. **22**(13): p. 3367-75.
176. Hipfner, D.R., K. Weigmann, and S.M. Cohen, *The bantam Gene Regulates Drosophila Growth.* Genetics, 2002. **161**(4): p. 1527-1537.
177. Blau, J. and M.W. Young, *Cycling vrille expression is required for a functional Drosophila clock.* Cell, 1999. **99**(6): p. 661-71.
178. Renn, S.C., et al., *A pdf neuropeptide gene mutation and ablation of PDF neurons each cause severe abnormalities of behavioral circadian rhythms in Drosophila.* Cell, 1999. **99**(7): p. 791-802.
179. Klarsfeld, A., et al., *Novel features of cryptochrome-mediated photoreception in the brain circadian clock of Drosophila.* J Neurosci, 2004. **24**(6): p. 1468-77.
180. Taghert, P.H., et al., *Multiple amidated neuropeptides are required for normal circadian locomotor rhythms in Drosophila.* J Neurosci, 2001. **21**(17): p. 6673-86.
181. Li, X. and R.W. Carthew, *A microRNA mediates EGF receptor signaling and promotes photoreceptor differentiation in the Drosophila eye.* Cell, 2005. **123**(7): p. 1267-77.

182. Fish, M.P., et al., *Creating transgenic Drosophila by microinjecting the site-specific phiC31 integrase mRNA and a transgene-containing donor plasmid.* Nat Protoc, 2007. **2**(10): p. 2325-31.
183. Markstein, M., et al., *Exploiting position effects and the gypsy retrovirus insulator to engineer precisely expressed transgenes.* Nat Genet, 2008. **40**(4): p. 476-83.
184. Rosato, E. and C.P. Kyriacou, *Analysis of locomotor activity rhythms in Drosophila.* Nat Protoc, 2006. **1**(2): p. 559-68.
185. Warming, S., et al., *Simple and highly efficient BAC recombineering using galK selection.* Nucleic Acids Res, 2005. **33**(4): p. e36.
186. Hardin, P.E., J.C. Hall, and M. Rosbash, *Feedback of the Drosophila period gene product on circadian cycling of its messenger RNA levels.* Nature, 1990. **343**(6258): p. 536-40.
187. Grun, D., et al., *microRNA target predictions across seven Drosophila species and comparison to mammalian targets.* PLoS Comput Biol, 2005. **1**(1): p. e13.
188. Lewis, B.P., C.B. Burge, and D.P. Bartel, *Conserved Seed Pairing, Often Flanked by Adenosines, Indicates that Thousands of Human Genes are MicroRNA Targets.* Cell, 2005. **120**(1): p. 15-20.
189. Baek, D., et al., *The impact of microRNAs on protein output.* Nature, 2008. **455**(7209): p. 64-71.
190. Nolo, R., et al., *The bantam microRNA is a target of the hippo tumor-suppressor pathway.* Curr Biol, 2006. **16**(19): p. 1895-904.
191. Thompson, B.J. and S.M. Cohen, *The Hippo pathway regulates the bantam microRNA to control cell proliferation and apoptosis in Drosophila.* Cell, 2006. **126**(4): p. 767-74.
192. Bilen, J., et al., *MicroRNA pathways modulate polyglutamine-induced neurodegeneration.* Mol Cell, 2006. **24**(1): p. 157-63.
193. Yang, Y., et al., *The bantam microRNA is associated with drosophila fragile X mental retardation protein and regulates the fate of germline stem cells.* PLoS Genet, 2009. **5**(4): p. e1000444.
194. Herranz, H., et al., *A Wingless and Notch double-repression mechanism regulates G1-S transition in the Drosophila wing.* Embo J, 2008. **27**(11): p. 1633-45.
195. Selbach, M., et al., *Widespread changes in protein synthesis induced by microRNAs.* Nature, 2008. **455**(7209): p. 58-63.
196. Stoleru, D., et al., *Coupled oscillators control morning and evening locomotor behaviour of Drosophila.* Nature, 2004. **431**(7010): p. 862-868.
197. Shang, Y., L.C. Griffith, and M. Rosbash, *Light-arousal and circadian photoreception circuits intersect at the large PDF cells of the Drosophila brain.* Proc Natl Acad Sci U S A, 2008. **105**(50): p. 19587-94.
198. Sheeba, V., et al., *Large ventral lateral neurons modulate arousal and sleep in Drosophila.* Curr Biol, 2008. **18**(20): p. 1537-45.
199. Hall, J.C., *Genetics and molecular biology of rhythms in Drosophila and other insects.* Adv Genet, 2003. **48**: p. 1-280.

200. Shah, C. and K. Forstemann, *Monitoring miRNA-mediated silencing in Drosophila melanogaster S2-cells.* Biochim Biophys Acta, 2008. **1779**(11): p. 766-72.
201. Nahvi, A., C.J. Shoemaker, and R. Green, *An expanded seed sequence definition accounts for full regulation of the hid 3' UTR by bantam miRNA.* Rna, 2009. **15**(5): p. 814-22.
202. Allada, R., et al., *A mutant Drosophila homolog of mammalian Clock disrupts circadian rhythms and transcription of period and timeless.* Cell, 1998. **93**(5): p. 791-804.
203. Grimson, A., et al., *MicroRNA targeting specificity in mammals: determinants beyond seed pairing.* Mol Cell, 2007. **27**(1): p. 91-105.
204. Bischof, J. and K. Basler, *Recombinases and their use in gene activation, gene inactivation, and transgenesis.* Methods Mol Biol, 2008. **420**: p. 175-95.
205. Zeng, H., P.E. Hardin, and M. Rosbash, *Constitutive overexpression of the Drosophila period protein inhibits period mRNA cycling.* Embo J, 1994. **13**(15): p. 3590-8.
206. Houl, J.H., et al., *CLOCK expression identifies developing circadian oscillator neurons in the brains of Drosophila embryos.* BMC Neurosci, 2008. **9**: p. 119.
207. Brennecke, J., et al., *Principles of microRNA-target recognition.* PLoS Biol, 2005. **3**(3): p. e85.
208. Kertesz, M., et al., *The role of site accessibility in microRNA target recognition.* Nat Genet, 2007. **39**(10): p. 1278-84.
209. Doench, J.G., C.P. Petersen, and P.A. Sharp, *siRNAs can function as miRNAs.* Genes Dev, 2003. **17**(4): p. 438-42.
210. Pillai, R.S., et al., *Inhibition of translational initiation by Let-7 MicroRNA in human cells.* Science, 2005. **309**(5740): p. 1573-6.
211. Vasudevan, S., Y. Tong, and J.A. Steitz, *Switching from Repression to Activation: MicroRNAs Can Up-Regulate Translation.* Science, 2007. **318**(5858): p. 1931-1934.
212. Tanaka-Matakatsu, M., et al., *Regulation of apoptosis of rbf mutant cells during Drosophila development.* Developmental Biology, 2009. **326**(2): p. 347-356.
213. Ebert, M.S., J.R. Neilson, and P.A. Sharp, *MicroRNA sponges: competitive inhibitors of small RNAs in mammalian cells.* Nat Meth, 2007. **4**(9): p. 721-726.
214. Levis, R., T. Hazelrigg, and G. Rubin, *Effects of genomic position on the expression of transduced copies of the white gene of Drosophila.* Science, 1985. **229**(4713): p. 558-561.
215. Allada, R., et al., *A recessive mutant of Drosophila Clock reveals a role in circadian rhythm amplitude*. Vol. 22. 2003. 3367-3375.
216. Hendricks, J.C., et al., *Gender Dimorphism in the Role of cycle (BMAL1) in Rest, Rest Regulation, and Longevity in Drosophila melanogaster.* Journal of Biological Rhythms, 2003. **18**(1): p. 12-25.

217. McCay CM, C.M., Maynard LA, *The effect of retarded growth upon the length of life span and upon the ultimate body size.* Journal of Nutrition, 1935. **10**: p. 63-79.
218. Masoro, E.J., *Overview of caloric restriction and ageing.* Mechanisms of Ageing and Development, 2005. **126**(9): p. 913-922.
219. Pletcher, S.D., et al., *Genome-Wide Transcript Profiles in Aging and Calorically Restricted Drosophila melanogaster.* Current Biology, 2002. **12**(9): p. 712-723.
220. Skorupa, D.A., et al., *Dietary composition specifies consumption, obesity, and lifespan in Drosophila melanogaster.* Aging Cell, 2008. **7**(4): p. 478-490.
221. DiAngelo, J.R., et al., *The Central Clock Neurons Regulate Lipid Storage in Drosophila.* PLoS ONE, 2011. **6**(5): p. e19921.
222. Turek, F.W., et al., *Obesity and Metabolic Syndrome in Circadian Clock Mutant Mice.* Science, 2005. **308**(5724): p. 1043-1045.
223. Na, J., et al., *A , Drosophila Model of High Sugar Diet-Induced Cardiomyopathy.* PLoS Genet, 2013. **9**(1): p. e1003175.
224. Marcheva, B., et al., *Disruption of the clock components CLOCK and BMAL1 leads to hypoinsulinaemia and diabetes.* Nature, 2010. **466**(7306): p. 627-631.
225. Sadacca, L.A., et al., *An intrinsic circadian clock of the pancreas is required for normal insulin release and glucose homeostasis in mice.* Diabetologia, 2011. **54**(1): p. 120-124.
226. Hamblen, M.J., et al., *Molecular and Behavioral Analysis of Four period Mutants in Drosophila melanogaster Encompassing Extreme Short, Novel Long, and Unorthodox Arrhythmic Types.* Genetics, 1998. **149**(1): p. 165-178.
227. Golombek, D.A. and R.E. Rosenstein, *Physiology of Circadian Entrainment*. Vol. 90. 2010. 1063-1102.
228. Guo, F., et al., *PDF neuron firing phase-shifts key circadian activity neurons in Drosophila*, ed. L. Ptáček. Vol. 3. 2014.
229. Emery, P., et al., *A unique circadian-rhythm photoreceptor.* Nature, 2000. **404**(6777): p. 456-7.
230. Murad, A., M. Emery-Le, and P. Emery, *A Subset of Dorsal Neurons Modulates Circadian Behavior and Light Responses in Drosophila.* Neuron, 2007. **53**(5): p. 689-701.
231. Bruno, Ivone G., et al., *Identification of a MicroRNA that Activates Gene Expression by Repressing Nonsense-Mediated RNA Decay.* Molecular Cell, 2011. **42**(4): p. 500-510.
232. Li, L.-C., et al., *Small dsRNAs induce transcriptional activation in human cells.* Proceedings of the National Academy of Sciences, 2006. **103**(46): p. 17337-17342.
233. Jopling, C.L., et al., *Modulation of Hepatitis C Virus RNA Abundance by a Liver-Specific MicroRNA.* Science, 2005. **309**(5740): p. 1577-1581.
234. Vasudevan, S., Y. Tong, and J.A. Steitz, *Cell cycle control of microRNA-mediated translation regulation.* Cell Cycle, 2008. **7**(11): p. 1545-1549.